Murine Norovirus 1 productively infects murine macrophages in a dynamin II-, cholesterol-, and USP14- dependent mechanism but is independent of endosome acidification, clathrin, caveolin, flotillin, GRAF1, and phagocytosis.

by

Jeffrey William Perry

A dissertation submitted in partial fulfillment
of the requirements for the degree of
Doctor of Philosophy
(Microbiology and Immunobiology)
in the University of Michigan
2012

Doctoral Committee:

Assistant Professor Christiane E. Wobus, chair
Professor Vern Carruthers
Professor Joel Swanson
Associate Professor Billy Tsai
Assistant Professor Akira Ono

© Jeffrey William Perry

2012

Dedicated to

Patrica Ann Perry

Acknowledgements

Obtaining a doctoral degree is a long difficult process that cannot be accomplished alone. I would like to thank the many people who have mentored me through this process. I give my heartfelt thanks to Dr. Allen Kurta and Dr. Daniel Clemans (Eastern Michigan University) for the opportunity to work in research laboratories during my undergraduate degree where I learned how to critically interpret science. I am also indebted to Dr. Mary O'Riordan (University of Michigan) for the opportunity to work in her laboratory, where I gained a greater appreciation of microbial pathogenesis. Upon beginning my graduate career, I was fortunate in finding an energetic and motivated mentor, Dr. Christiane Wobus. Dr. Wobus challenged me to do better science, to present that science better, and to be a better mentor.

I have also been fortunate to work with a diverse team of scientists. I must thank Dr. Stefan Taube for helping establish the laboratory and putting up with me for the longest of any coworker. I also thank my fellow graduate students, Mariam Gonzalez-Hernandez and Juliana Cunha, who were always ready to make me laugh when needed. I would like to thank the undergraduates and rotating graduate students who I mentored for their patience including: Jason

Houdek, Sagar Patel, Charles Ko, Mohammad Ahmed, David Chapel, Alok Karnik, Hilary Payne, Andy Kocab, Ciara Reyes, and Zach Benet.

I need to thank my extended family for supporting me throughout this process. George Lomas and Jane Lomas are the best parents-in-law anyone could ask for. Without their help, I would have never made it through graduate school. I would also like to thank my brother, Steven Perry, and sister, Barbra Perry, for their love and support. I am indebted to my father, Edwin Perry, for raising me and my siblings under difficult circumstances, and supporting me in my educational pursuits.

In the first two weeks of my graduate career, my wife and I welcomed Patricia Jane into the world. Patty is my beautiful baby girl and I will always love her. A few years later, we brought Theodore Emmett back home from the hospital to his curious but skeptical sister, and then I flew out to a meeting where I gave a talk. Teddy is my handsome little guy, and I love him dearly. From the first few weeks until defending this thesis, I have struggled to balance my work and family life. I hope that my family can understand how hard I have tried and continue to try to do just that.

I cannot thank my wife, Sarah Jane, adequately for her love and support. I do not know how many times I have left her with Patty and Teddy to run to work and continue some experiment. I don’t remember how many times I asked her to fix grammar mistakes, or to listen to me practice a talk, but I do remember her helping me each time I asked without complaint. Words cannot express my gratitude for her patience, support, and love.

Table of Contents

List of Figures

List of Abbreviations

AAV2	adeno-associated virus 2
Amiloride	EIPA or 5-ethyl-*N*-isopropyl amiloride
AP2	clathrin-coated pit adaptor protein 2
ARF6	ADP- ribosylation factor 6
ASK1	apoptosis signal-regulating kinase 1
ATF6	Activating transcription factor 6
ATG12	autophagy- related protein 12
Baf A	Bafilomycin A
Be2-c	human neuroblastoma cell line
BMDMs	Bone marrow- derived macrophages (obtained from Swiss Webster mice)
BMV	brome mosaic virus
Bort	Bortezomib (alternative name Velcade)
CAV-1	Caveolin 1
CaCV	canine Calicivirus
CHC	Clathrin heavy chain
Chl, Chloro	choroquine
CLC	Clathrin ligand- independent compartment
CVB3	Group B coxsackievirus 3
CTb	Cholera toxin subunit B
Cyto D	Cytochalasin D
DAPI	4', 6-diaminidino-2-phenylindole
DCs	Dendritic cells
DMSO	dimethyl sulfoxide
DN	Dominant negative
DRM	detergent- resistant membranes
DRP1	dynamin- related protein 1
DSM	detergent- sensitive membranes
DUB	deubiquitinating enzyme
Dyna	Dynasore
EBHS	European brown hare syndrome virus
EEA1 or EE	early endosome- associated membrane protein 1
EIF2α	eukaryotic translation-initiation factor 2α
EIPA	5-ethyl-*N*-isopropyl amiloride
ELISA	enzyme- linked immunosorbent assay
EMCV	encephalomyocarditis virus
ER	endoplasmic reticulum
ERAD	endoplasmic reticulum- associated degradation
ERSE	endoplasmic reticulum stress response elements

FBS	Fetal bovine serum
Fc	constant domain of the immunoglobin G family
FCV	Feline Calicivirus
fJAM 1	feline junctional adhesion molecule 1
FIPV	Feline infectious peritoneal virus
GEEC	GPI- enrichment endocytic compartment
GFP	Green fluorescent protein
GLS	Golgi-localization sequence
HBGA	histo- blood group antigen
HCV	Hepatitis C virus
HECT	homologous to E6-associated protein C-terminus
HPI	hours post infection
HuNoV	Human norovirus
ICP0	infected cell protein 0
IgG	immunoglobin G
IKK	inhibitor of nuclear factor kappa B inhibitor kinase alpha
IL2	Interleukin 2 receptor
IRES	internal ribosomal entry site
Ires	Irestatin
IRE1	inositol- response element 1
IRF3	interferon- regulatory factor 3
ISG15	interferon- stimulated gene 15
JNK	JUN N-terminal kinase
KSHV	Kaposi's sarcoma- associated herpesvirus
LC3	microtubule- associated protein light chain 3
LE	late endosomes
MAVS	mitochondrial anti-viral signaling protein
MβCD	Methyl beta cyclo dextran
ME	maturing endosomes
MHV 68	murine hepatitis virus 68
MNV-1	Murine norovirus 1 (strain CW3, passage 6)
MTOC	microtubule organizing center
MOI	Multiplicity of infection
NEDD8	neural precursor cell expressed developmentally down-regulated protein 8
Neura	*Vibrio cholerae* neuraminidase
NFKB	nuclear factor kappa B
NR	Neutral red
NS	nonstructural
NS4B	nonstructural protein 4 B of Hepatitis C Virus
NSP1	nonstructural protein 1
NT	non- targeting siRNA
NW	Norwalk virus
OTUB	ovarian tumor- related proteases
OPA1	optic atrophy 1 homologue
ORF	open reading frame

PABP	poly (A)- binding protein
PBS	Phosphate buffered saline
PERK	PKR- like endoplasmic reticulum kinase
PHD	plant homeodomains
PLpro	SARS-Cov papain-like protease
PVR	Poliovirus receptor
qRT-PCR	quantitative real- time polymerase chain reaction
RAW cells	RAW 264.7 cells
RCV	Rabbit Calicivirus
RDRP	RNA- dependent RNA polymerase
RE	recycling endosomes
RHDV	rabbit hemorrhagic disease virus
RIG I	retinoic acid- induced gene I
RING	really interesting new gene
RNA	ribonucleic acid
SARS- Cov	severe acute respiratory syndrome coronavirus
siRNA	small interfering RNA
SMSV	San Miguel Sea Lion virus
SRDCs	Splenic derived-dendritic cell line
SUMO	small ubiquitin-like modifier
SV40	Simian virus 40
T, Thapsi	Thapsigargin
TBK	Tank- binding kinase 1
TLR	Toll- like receptor
TRAF2	tumor-necrosis factor- receptor associated factor 2
TRIMM25	tripartite motif-containing protein 25
U Box	ubiquitin fusion degradation 2 homology domain
Ub	ubiquitin
UCH	ubiquitin C-terminal hydrolases
UPR	unfolded protein response
UPREs	unfolded protein response elements
USP	ubiquitin-specific proteases
USP14	ubiquitin-specific protease 14
Vero	African green monkey kidney cell line
VESV	vesicular exanthema of swine virus
VLP	Virus- like particle
VPg	virus protein, genome linked
VSV	vesicular stomatitis virus
WP	WP1130
XBP 1	X-box binding protein 1

Abstract

Viruses are obligate intracellular parasites that require their hosts for all steps of the viral life cycle. The mechanism of how an inert particle of protein, lipid, and nucleic acid usurps the machinery of the host to infect is critical to elucidating the pathogenesis of a virus. The mechanism by which Murine Norovirus (MNV), a non- enveloped positive- strand RNA virus, productively infects murine macrophages (Macs) and dendritic cells (DCs) was the subject of my thesis work. Using pharmacological inhibitors, dominant- negative constructs, and siRNA knockdowns, I have demonstrated that MNV strain CW3, passage 6 (MNV-1) enters Macs by a cholesterol-, and dynamin II- dependent mechanism. Additionally, after entering into Macs or DCs, I observed that the virus does not require acidification of the endosome as a trigger to initiate infection. Once the viral genome has been released into the host cytoplasm, it traffics to the site of viral replication. For positive- strand RNA viruses, this site of replication requires the recruitment of host- derived membranes. Specifically for MNV-1, membranes derived from the endoplasmic reticulum (ER) are required for viral replication. The unfolded protein response (UPR), a cellular response to the accumulation of unfolded protein in the ER, regulates the synthesis of new ER. Therefore, MNV-1 replication in cells may be regulated by the UPR. We serendipitously discovered a small inhibitor of MNV-1 infection, which inhibited host deubiquitinases (DUBs),

including USP14, the only shown to associate with the UPR, and resulted in the activation of the UPR. We also demonstrated that MNV-1, La Crosse virus, encephalomyocarditis virus, and Sindbis virus infections are inhibited by chemical induction of the UPR. These results suggest that the UPR could be an important target for the development of broad- spectrum antiviral therapies. However, the mechanism by which the UPR inhibits viral infection is unclear. Upon activation, the UPR regulation of ER synthesis may restrict recruitment of ER membranes to the site of viral replication, thereby inhibiting viral infection. Clearly, further investigations are warranted to determine the requirements of norovirus entry and infection, but my research has laid a framework for further investigations.

Chapter 1

Introduction

1.1 *Caliciviridae*

Caliciviruses are taxonomically classified as a family of viruses containing a single- stranded, poly- adenylated, and positive- sense non- segmented ribonucleic acid (RNA) genome in a protein capsid lacking a lipid component (105). The family is further divided into five recognized genera: Lagoviruses, Vesiviruses, Sapoviruses, Noroviruses, and the newest member, Neboviruses (104, 368). Although not presently recognized as a genus, Recovirus, discovered infecting Rhesus monkeys, is the newest proposed genus (79). Infections by *Caliciviruses* are, in general, species specific, and successful culturing of these viruses has been limited to only a few strains. Most notably, the Sapovirus and the Norovirus genus have only a porcine- (109) and murine- restricted virus that grow in culture respectively (157). Further investigation into the distribution and pathogenesis of caliciviruses has been complicated and is considerably hindered due to a lack of basic research tools, including the limitation in culturing these viruses. However, with recent advances in molecular techniques, studies into the

distribution of caliciviruses have revealed a worldwide prevalence, suggesting that these viruses are more common than previously appreciated.

Lagoviruses have the narrowest host range of the caliciviruses, infecting only rabbits and hares. To date, only three species have been identified; rabbit hemorrhagic disease virus (RHDV), European brown hare syndrome virus (EBHS), and rabbit calicivirus (RCV) (55, 83, 178, 190). RHDV and EBHS cause acute systemic viral hemorrhagic disease, with RHDV being more severe, typically, than EBHS. RCV causes an acute infection that is self- limiting, and the host develops an adaptive immunity that does not protect against RHDV (178). Although the worldwide prevalence of this virus has yet to be established, some studies suggest that Lagoviruses are widespread in Europe, Mexico, Australia, and New Zealand (2, 212).

In contrast to Lagoviruses, Vesiviruses have the broadest host range of the caliciviruses. Vesiviruses infect cats (feline calicivirus, FCV), dogs (canine calicivirus, CaCV), sea lions (San Miguel Sea Lion virus, SMSV), and pigs (vesicular exanthema of swine virus, VESV) (104). FCV typically causes an upper respiratory infection but can cause a more severe systemic infection in felines (257, 266). After development of a tissue culture system capable of growing FCV, it was widely adopted as a model for studying caliciviruses and, among other important discoveries for caliciviruses, led to the identification of the first host receptor: feline junctional adhesion molecule 1 (fJAM-1) (197). After identification of CaCV in canine feces, CaCV has been associated with diarrhea in dogs (206, 285). Although little is known about SMSV, it is thought to be

closely related to VESV, which caused an outbreak in the US in the 1960s in swine herds. A current hypothesis suggests that swine were fed contaminated food containing a close relative of SMSV, and that virus spread to 43 states in the United States of America (236). The proposed transmission of SMSV to a pig suggests species barriers to Vesiviruses may not be as restrictive as those of other caliciviruses. Examples for this broader tropism include the following: FCV was recovered from a dog suffering from diarrhea (66), a laboratory worker became infected by SMSV (299), and serological evidence of cattle responding to SMSV antigens has been documented (171). Taken together, Vesiviruses may be the only calicivirus genus that is capable of crossing species barriers.

Neboviruses are a recent addition to the calicivirus family (243). Currently, the genus is thought to be restricted to cattle, with Newbury 1 virus and Newbury 2 virus isolated from calves with diarrheal disease (58, 356). Experimental infection with Newbury 2 virus produced gastroenteritis in calves and resulted in mild pathology in the small intestine (25, 116). Little else is known concerning the pathogenesis of Newbury 1 or Newbury 2 virus, as these viruses are not culturable. Recently, the Newbury 2 virus genome has been published, resulting in its placement into the calicivirus family (58, 243). Future investigations may reveal a widespread presence of Newbury viruses in cattle similar to other caliciviruses.

Although not currently recognized as a genus in the calicivirus family, Recoviruses were recently discovered infecting Rhesus monkeys (78, 79). Only one species has been identified to date, the Tulane virus, which readily infects

macaques and macaque cells in culture. Tulane virus was isolated from Rhesus macaques in a research institution, but the worldwide distribution of this virus is unknown. The Tulane virus causes gastroenteritis in Rhesus monkeys and is being developed as a model system for studying gastroenteritis caused by a calicivirus (79).

Sapoviruses were originally isolated from an outbreak of gastroenteritis at an orphanage in Sapporo, Japan (169). The prevalence and pathogenesis of these viruses are not well understood due to culturing limitations with only one porcine- restricted culturable virus identified to date, called porcine enteric calicivirus (109). However, recent developments in molecular techniques have allowed for sequence analysis and surveillance. Sapoviruses consist of 5 genogroups (denoted by GI – GV). Genogroup III (GIII) exclusively infects swine, while the other genogroups can also infect humans (119, 368). However, recent isolation of human sapoviruses in swine populations has complicated these distinctions. Both porcine and human sapoviruses have worldwide distributions, have caused outbreaks of gastroenteritis, and have been recovered from environmental sources, such as water and shellfish (119). In general, clinical symptoms of human sapovirus infections are less severe than human noroviruses and fewer outbreaks are associated with human sapoviruses than human noroviruses. However, outbreaks caused by human sapoviruses are on the rise, suggesting a need for further research into this relatively unknown human pathogen (80, 119, 222, 249).

Noroviruses were originally isolated from an outbreak of gastroenteritis at an elementary school in Norwalk, Ohio (155). Human noroviruses (HuNoVs) are now recognized as the major cause of non-bacterial associated gastroenteritis worldwide (156). Although HuNoVs are not cultivable, advances in detection using techniques, such as quantitative Real-Time Polymerase Chain Reaction (qRT-PCR) (335), enzyme- linked immunosorbent assay (ELISA) (102, 161), and sequencing, have elucidated their global distribution. Isolation of noroviruses in pigs, cattle, sheep, dogs, a lion cub, and mice suggest that these viruses are widespread pathogens, although most exhibit strict species tropism (157, 203, 204, 242, 298, 343).

With advances in molecular detection, caliciviruses have been discovered from a variety of sites and animals around the world (108, 145, 208, 244, 273, 298, 310, 333, 343). The ability of these viruses to infect at low viral doses, to remain stable in the environment, and to be produced to high levels during infection makes them proficient at causing large, fast- spreading outbreaks. The sources of these outbreaks can be environmental (202), but recent evidence suggests animal reservoirs may contribute to outbreaks (12). Although not documented for every calicivirus genus, some Vesiviruses can cross species barriers to infect a variety of hosts, as mentioned above. The presence of noroviruses closely related to HuNoVs isolated from swine (207, 343) and the replication of HuNoV in gnotobiotic pigs, or a germfree pig, (305) suggests that noroviruses may be able to cross species barriers as well. Although the frequencies of these events are not known, they highlight the potential for

possible zoonotic transmission. The ability of HuNoVs and human sapoviruses to cause outbreaks in humans poses a serious public health threat. Currently there are no effective antiviral treatments or FDA approved vaccines to contain or prevent these outbreaks. HuNoVs are by far the most prevalent cause of human disease within the calicivirus family, and thus merit further investigation into their pathogenesis and ways to prevent it.

1.1.1 Human Noroviruses

Since their discovery, HuNoVs have been increasingly recognized as the major cause of non-bacterial gastroenteritis worldwide. HuNoVs result in an estimated 23 million infections, 50,000 hospitalizations, and 500 deaths annually in the United States alone (214). More recently, HuNoVs have been recognized as the cause of more than 50% of all food-borne outbreaks of gastroenteritis in the United States, even when bacterial and non-bacterial sources are included (350). The sheer number of cases, the extensive decontamination requirements, and the robust infectivity of HuNoVs all contribute to a significant economic impact. In addition, inactivation of HuNoV with viral decontamination protocols established by the World Health Organization to limit the spread of virus epidemics fail to significantly reduce viral titers (224), suggesting environmental contamination after an outbreak is a serious concern. Since HuNoVs have been classified as a class B bio- defense agent by the National Institutes of Health, they may also be a concern of national security (142). Unfortunately, the only effective means of controlling HuNoV outbreaks are strict hygiene and

decontamination measures. Without basic research into the pathogenesis of HuNoV, specific antiviral treatments may not be developed and preventable outbreaks may continue to occur.

For the last forty years, many researchers have tried to grow HuNoV in the laboratory with no success (71). Although development of a gnotobiotic pig model has shown some success, the expense and other limitations of these experiments have restricted this model's broad use (47). The lack of a tissue culture system or small animal model has severely hampered the investigation of norovirus biology. However, even without a culturable virus some developments including sequencing of the Norwalk virus (NV) genome, the prototype HuNoV (149), development of a RT-PCR protocol for identification of virus strains (335), and antibody- based detection methods for HuNoV (102, 161) have allowed characterization of HuNoV epidemiology and its worldwide distribution.

After sequencing NV, researchers have determined the genomic structure of the first norovirus (Figure 1.1). The positive- sense RNA genome is subdivided into three open reading frames (ORF) flanked by small untranslated regions at the 3' and 5' ends. The 5' end of the genome has been shown to be attached to a viral protein, called virus protein, genome- linked (VPg), similar to polioviruses (258). The 3' end of the genome contains a poly- adenine tail, seen in many RNA virus genomes. The first ORF is expressed as a polyprotein containing the nonstructural genes, NS1/2 (or N-Terminal protein), NS3 (or nucleoside triphosphatase- like protein, NTPase), NS4 (or 3A- like protein), NS5 (or VPg), NS6 (or viral protease, Pro), and NS7 (or the RNA- dependent RNA polymerase,

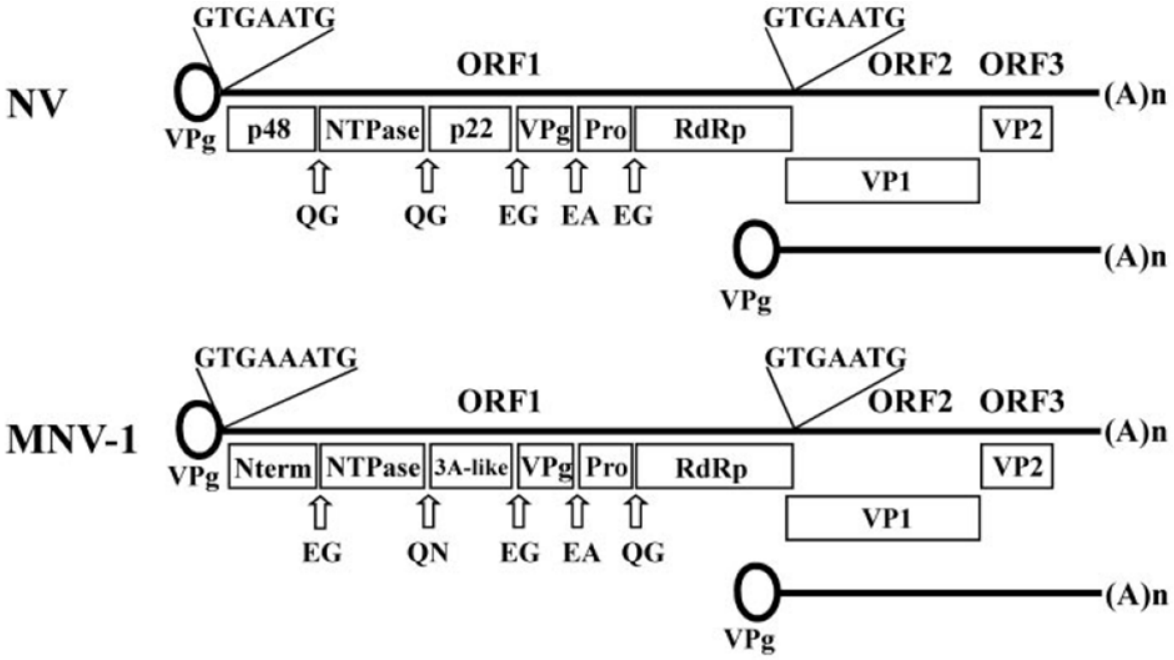

Figure 1.1 Genomic organization of Norwalk Virus and Murine Norovirus. Representations of both Norwalk Virus (NV) and Murine Norovirus (MNV-1) are depicted. Arrows indicate protease cleavage sites, and the amino acids surrounding the cleavage site are also shown. The subgenomic RNA is shown below the genomic RNA. The presence of a viral protein linked to the genomic and subgenomic RNA (VPg) is predicted, but not proven for noroviruses. (Figure adapted from Wobus et. al. 2006)

RdRp).The second ORF consists of the major capsid subunit VP1, 180 copies of which polymerize to form the entire outer shell of the virus particle. The third ORF contains the minor capsid subunit (or VP2), a small highly basic protein that is thought to stabilize the genome inside the virus particle (157, 303).

Noroviruses are divided into five genogroups based on sequence (Figure 1.2). Genogroups I, II, and IV infect humans (104, 368). Genogroup II also infects swine (207), while genogroup IV has also been detected in a dog and a lion cub (203, 204). Genogroup III has been isolated from cattle and sheep (282) and genogroup V is the only group that has been shown to infect mice (157). The signs and symptoms of these infections can range from no outward signs of disease (e.g. MNV infection of mice) to severe acute gastroenteritis (e.g. HuNoV infection of man). Interestingly, in STAT1- deficient mice, MNV causes viremia and eventual death of the animal (157). Noroviruses from all five genogroups are capable of causing fast spreading outbreaks, although mechanisms behind these outbreaks are not well understood.

Examination of HuNoV has determined that one genogroup of the three, specifically genogroup II genotype 4 (GII.4), is the dominant cause of gastroenteritis outbreaks in humans currently (349). The molecular determinants for the greater prevalence of GII.4 are not well understood, but several characteristics of these viruses are thought to contribute to their dominance. In general, GII.4 binds with greater affinity to the host through the viral attachment receptor human histo-blood group antigens (HBGAs), and is more stable in the

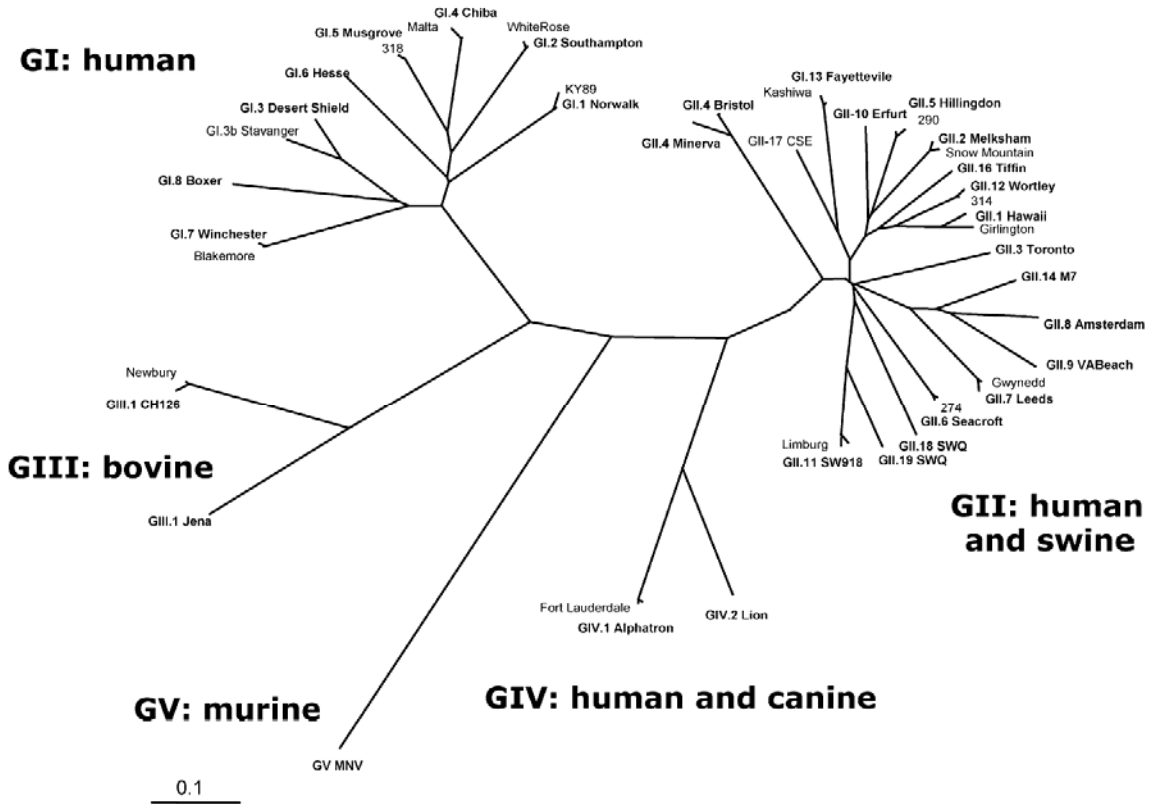

Figure 1.2 Phylogenetic classification of Noroviruses. Using sequence comparison of the major capsid protein, a consensus Bayesian tree was constructed for several Norovirus genotypes. These 32 genotypes can be categorized into five distinct genogroups. (from Patel et al., 2009)

environment compared to other genogroups (27). Although transmission of HuNoVs has not been addressed, these characteristics may explain the prevalence of GII.4 although further investigation into the spread and pathogenesis of HuNoV is necessary to determine the predominant characteristics of these viruses necessary to cause and sustain outbreaks (139).

To date, the only way to study HuNoV pathogenesis is by experiments with human volunteers (152, 186). These studies suggest that as few as 18 virus particles can cause infections (323). After inoculation of the virus, symptom onset can begin within 12 hours (186). Symptoms most commonly include excessive diarrhea and vomiting, although mild fever, malaise, and dizziness have also been associated with the infection. Symptoms typically resolve 24 to 72 hours after infection, but shedding of virus has been shown to persist for weeks to months even in immuno- competent individuals, especially children (152). In individuals with suppressed immune systems, including organ transplant patients, persistence of symptoms and shedding can carry on for years (7, 275). In addition, asymptomatic individuals can shed virus for months and may be sources of new outbreaks (63). The amount of viral shedding has been quantitated and measures up to 10^{10} virus genomes per gram of stool (287). The high viral titers shed and the low infectious dose suggests that one person infected with HuNoV can produce enough virions to infect the world's population. Rampant production of virus during infection, low infectious dose, and stability in the environment, as mentioned previously, all lend themselves to a very high transmission rate. This rate can be measured experimentally and is referred to as

the reproduction number, or the number of people infected from the initially infected individual. One calculated reproduction number for HuNoV is 14 (125). This is one of the highest reproduction numbers and dwarfs the reproduction numbers of 4 and 6 reported for influenza A and poliovirus, respectively (54, 67).

Although human volunteer studies can determine important characteristics of HuNoV pathogenesis, a more reductionist approach is required for understanding how the virus causes disease in humans. Many models have been developed to study HuNoV including, virus- like particles (VLPs), a HuNoV replicon system, and a gnotobiotic pig model. In addition, scientists use surrogate models to study norovirus or calicivirus biology using MNV or FCV infections of cells in culture, or animals. Early adoption of the culturing of FCV was later critiqued as it causes an acute upper respiratory infection in cats, and lacks the characteristic low pH stability of virions observed for noroviruses (8, 35, 262, 283). Bacterial expression of HuNoV capsids without viral genomic material, or VLPs, has been essential in determining the requirements of viral attachment to HBGAs (143, 290, 291, 314, 347, 357). Recently, a NV replicon system has been developed by the expression of the NV complementary DNA (cDNA) lacking the viral capsid from a eukaryotic expression plasmid. A role for host cholesterol during NV genomic replication has been established using the replicon system, as well as sensitivity to the interferon response (43, 44). However, the lack of an infectious cell culture model of noroviruses has seriously hampered norovirus research. Recently, a gnotobiotic pig model of HuNoV infection has been developed and results in a productive infection of pigs (47). Chimpanzees have

also been infected with HuNoV and productive infection occurs in this model, but interestingly these primates do not show signs of infection (20). However, the complications of these model systems, including questions raised about the proper development of an immune system in the gnotobiotic pig model, and the cost of maintaining both models, have limited their adoption. All of these models have contributed to the field of norovirus research. However, a more tractable model of infection was vital to understanding norovirus biology. By discovering MNV, the missing tool to elucidating norovirus biology was uncovered (157, 354).

1.1.2 Murine Norovirus

In 2003, MNV was discovered infecting mice deficient in both recombination activating gene 2 (RAG2) and signal transducers and activators of transcription 1 (STAT 1), an immunocompromised host, in a mouse research colony at Washington University in St. Louis, MO (157). Murine DCs and Macs were quickly identified as the cellular tropism for MNV after its discovery (353). Development of a tissue culture system (353), multiple reverse genetics systems (6, 46, 345, 365), and a small animal model (157), have helped refine MNV as an excellent tool for studying norovirus biology. To date, MNV is the only model for studying productive infection of a norovirus and has helped to crack open the field of norovirus research. MNV has been instrumental in elucidating key mechanisms of norovirus biology including: attachment (319, 320), internalization (93, 255, 256), and replication (303, 353). Further exploration into norovirus pathogenesis can only be accomplished in a model system that infects cells in

culture, infects a small animal, is genetically malleable, and is reproducibly grown by other laboratories.

The manifestation of MNV infection in immuno-competent mice is not outwardly apparent, which can explain why the virus has eluded detection until recently (157). Reports suggest acute infection can cause fecal inconsistency, a form of mild diarrhea, but infection can either resolve itself within seven days or persists for weeks or months depending on virus strain (227). After infection, the adaptive immune response develops a robust and protective immunity against MNV-1, although other strains have yet to be tested (41). In immuno-compromised mice, including RAG2 / STAT1 knockouts, in which the virus was originally isolated, MNV infection is not controlled and can cause viremia, a term referring to a systemic viral infection, and even cause death (157).

MNV shares many important characteristics with HuNoVs, making it an invaluable model system. The three ORFs expressed from both RNA genomes are very similar in structure and sequence, with 65 % nucleotide identity (Figure 1.1) (158). Both viruses also infect via the fecal-oral route, replicate in the gastrointestinal tract to high viral titers, and are shed in the feces. Both viruses cause an acute infection that is self-resolving or can persist with viral shedding observed for months (37, 89, 134, 135, 230, 292). Although signs of disease from MNV infection of immuno-competent mice are not outwardly apparent, mice deficient in STAT 1 or the interferon alpha, beta, and gamma receptors exhibit diarrhea and stomach distension, a medical condition that suggests a delay in the emptying of the stomach (157, 227). Like HuNoV, MNV is more widespread

than previously believed, with “specific pathogen- free” mice in research colonies across the world ranging from 22% to 64% MNV seropositive or PCR positive (3, 136, 162, 166). In one study, 15 genetically distinct strains have been isolated, which form one genogroup and one serogroup but these strains exhibit biological differences (Figure 1.3). The worldwide presence of this viral pathogen in research settings has resulted in complications with interpreting results from MNV- infected animals (162, 179), and requires further investigation to determine other complications of MNV contamination.

One key characteristic that allows both MNVs and HuNoVs to maintain their widespread prevalence is their viral capsids. The virus particle is made from 180 copies of the major structural protein, VP1. The noroviral genome is encased in an environmentally stable protein shell that effectively prevents the viral genome from environmental stresses and delivers the genome into the host at the proper time and place to begin infection. Environmental stability of these virus particles (27, 35, 96) and overall structure of the capsid is very similar between HuNoV and MNV (52, 315, 316, 321). The identification of host carbohydrate binding motifs has been mapped in various strains of both HuNoV (289) and MNV (318). Although they bind different carbohydrate structures, these sites are located in similar regions of the capsid based on x ray crystallography analysis.

Besides differences in carbohydrate binding, there are differences between the model, MNV, and the system being modeled, HuNoV. For example, MNV does not cause the classical hallmarks of severe acute gastroenteritis seen

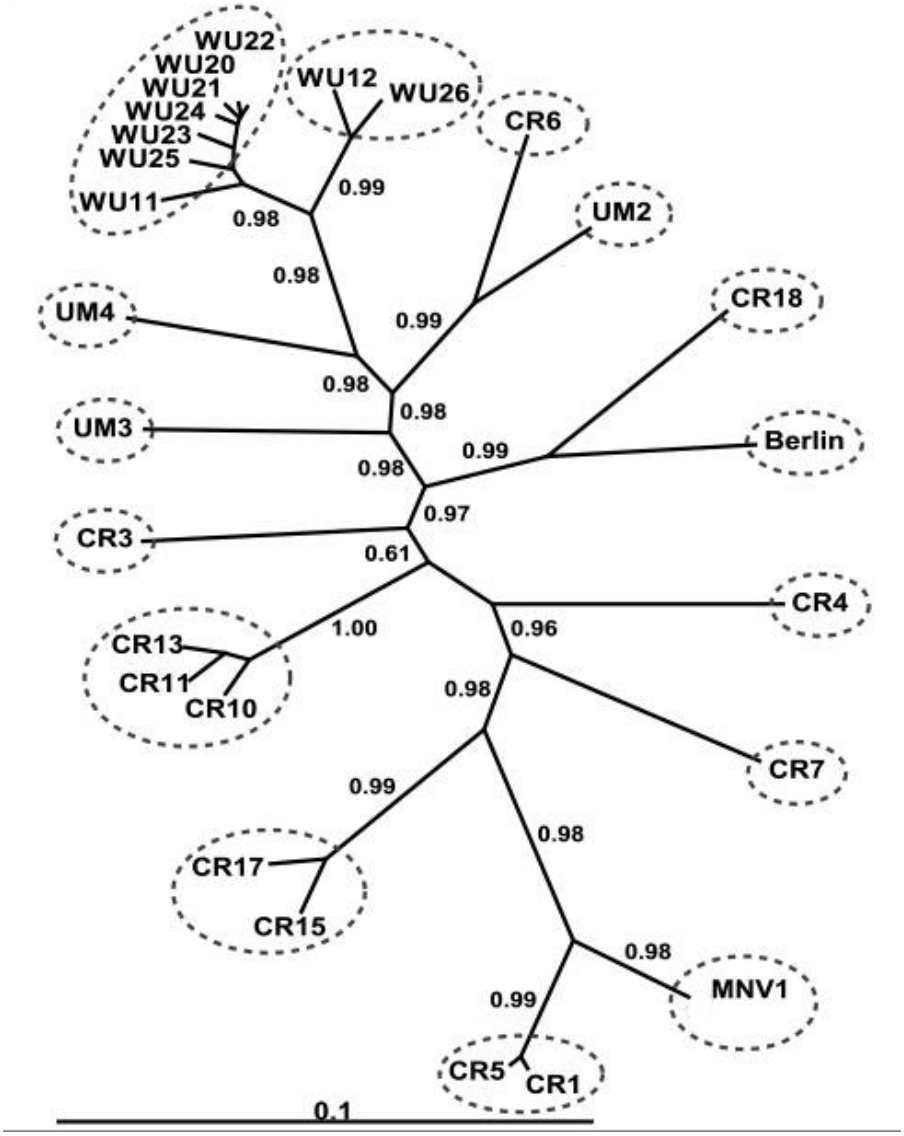

Figure 1.3 Phylogenetic analysis of Murine Noroviruses. 26 sequences of MNV genomes comprise 15 distinct virus strains. A consensus Bayesian phylogenetic tree based on full-length MNV genomes is shown. Genetically distinct MNV strains are circled. (from Thackray et. al. 2009)

with HuNoV infection, including diarrhea or vomiting (157). Although mice lack the emetic reflex required for vomiting (317), diarrhea in mice has been observed in enteric virus infections, including rotavirus infection of infant mice (306). The reasons why mice infected with MNV do not experience diarrhea are unclear. In addition, the cell type(s) that HuNoVs infect has not been determined. Attempts at infecting Macs and DCs differentiated from peripheral blood mononuclear cells have not been successful, yet intestinal subsets of DCs and Macs were not tested (177). Another difference in these viruses is the presence of an ORF 4 in MNV that does not exist in HuNoVs. Although the function of ORF 4 has not been fully elucidated, one study suggests that it may be a virulence factor (211). Defining differences between the system and the model is required for developing a robust model. In the case of MNV, the information gained through testing the model system can also be invaluable as the first observations for noroviruses.

One important reason to use MNV as a model system is the availability of research tools and techniques. Although MNV was only recently discovered, researchers have developed important tools for investigating norovirus biology including a tissue culture system (354), reverse genetics systems to manipulate the viral genome (6, 46, 345, 365), and a small animal model (157). Using these tools, we have begun to understand the progression of norovirus infection in not only immuno-competent (134, 135), but also immuno-compromised hosts (157). Further investigation will elucidate important steps of the norovirus life cycle.

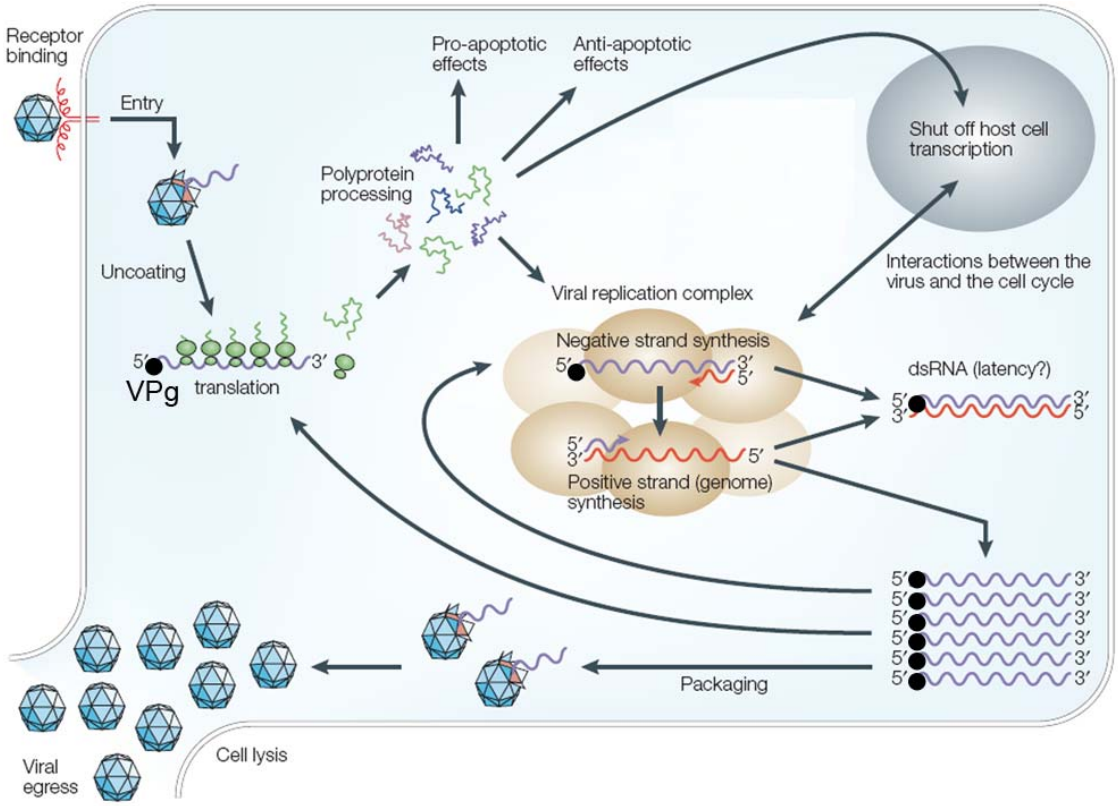

Figure 1.4 Life cycle of a positive- strand RNA genome containing virus. The life cycle of a typical positive- strand RNA virus is illustrated. Positive-sense viral RNA is shown in purple and negative-sense RNA in red. dsRNA, double-stranded RNA, VPg, virus protein, genome-linked. (Figure adapted from Whitton et. al. 2005)

1.2 Positive- Strand Virus Life Cycle

The life cycle of a virus can be divided into the following steps: attachment, internalization, uncoating, genomic replication, progeny assembly, and release (Figure 1.4). In each of these steps, the virus must mimic, disrupt, and/or destroy the machinery of the host for productive viral entry, replication, assembly, and release to occur. The mechanism by which noroviruses executes these steps is poorly understood. However, the themes of the viral life cycle of a positive- strand RNA genome containing virus can be generalized from already elucidated mechanisms of Caliciviruses. For the purpose of this thesis, only the life cycle of non-enveloped viruses will be considered.

1.2.1 Virus Attachment

The first step of any effective viral infection is the physical interaction of the virus particle with the host cell, called attachment or binding. Attachment occurs between the virus and a host component, called a viral receptor. Viral receptors can be host proteins, carbohydrates, lipids, or any combination of these. Viral receptors are categorized into attachment or entry receptors. An attachment receptor, or co-receptor, only allows the virus to attach and does not allow productive infection. Entry receptors are necessary and sufficient for viral entry and infection. For MNV, the requirement for sialic acid during attachment has been discovered including regions of the virus capsid important in attachment (319, 320). However, since sialic acid on a cell does not dictate infectability of that cell, we hypothesize that MNV requires at least one additional unidentified receptor for entry and infection.

1.2.2 Virus Internalization

Once the virus particle has attached to the host, the virion must initiate internalization, which requires interaction of the virus with a viral entry receptor(s). The viral entry receptor is typically internalized into the cell as part of its cellular function. For example, the transferrin receptor internalizes iron into the cell (192), and viruses tag along for the ride, such as mouse mammary tumor virus particle binding to the transferrin receptor for entry (341). For non-enveloped viruses, internalization is a requirement, while direct fusion of the viral membrane with host cellular membranes has only been observed for some enveloped viruses. The mechanisms by which viruses are internalized are variable and depend on the trafficking of the viral entry receptor. Therefore, these mechanisms are as variable as the host receptors themselves. Once the virus particle interacts with the host receptor, it becomes cargo of the endocytic machinery and, therefore, requires the host for internalization.

The process of receptor- mediated endocytosis was once hypothesized to be a simple process by which nutrients, communication molecules, and even toxins, entered the cell. Receptor- mediated endocytosis was contrasted with passive endocytosis, or pinocytosis, which lacked direct interactions between host receptors and cargo, and with phagocytosis, which was restricted to a few immune cells, as described by Elie Metchnikoff in 1882 (322). The true complexity of the internalization processes by a eukaryotic cell has only recently been appreciated. With the discovery of clathrin, a protein that facilitates

endocytosis through a receptor- mediated process, it was hypothesized and widely believed that clathrin could be responsible for all endocytosis into the cell (70). However, this was improbable after inhibition of clathrin- mediated endocytosis, using a dominant negative construct of dynamin II, could not stop all endocytosis into the cell (56). Since then an explosion of additional endocytic processes have been characterized (Figure 1.5). One of the driving forces behind the elucidation of endocytic processes has been the elucidation of how viruses enter a cell. For example, the existence of caveolin as a method of endocytosis was greatly strengthened by the elucidation of the entry process of Simian Virus 40 (253, 254). Further discovery of endocytic processes, with viruses being used as molecular probes, may reveal more complexity into an already diverse field.

1.2.2.1 Clathrin- mediated endocytosis

Clathrin is a collection of proteins, including large chain and small chain proteins that form heterodimers called triskelions (163). Three of these triskelions polymerize to form the basic subunit of the clathrin lattice. Once a receptor is activated through interactions with its cargo, the receptor initiates the process of clathrin polymerization, although evidence suggests spontaneous clathrin polymerization can also occur (74). This process involves over 150 different cellular proteins, including protein adaptors such as epidermal growth factor receptor pathway substrate 15 (EPS15) and adaptor protein 2 (AP2) (217). These proteins bind directly to the receptor and clathrin lattice to stabilize polymerization (363). Polymerization of clathrin continues until an invagination of

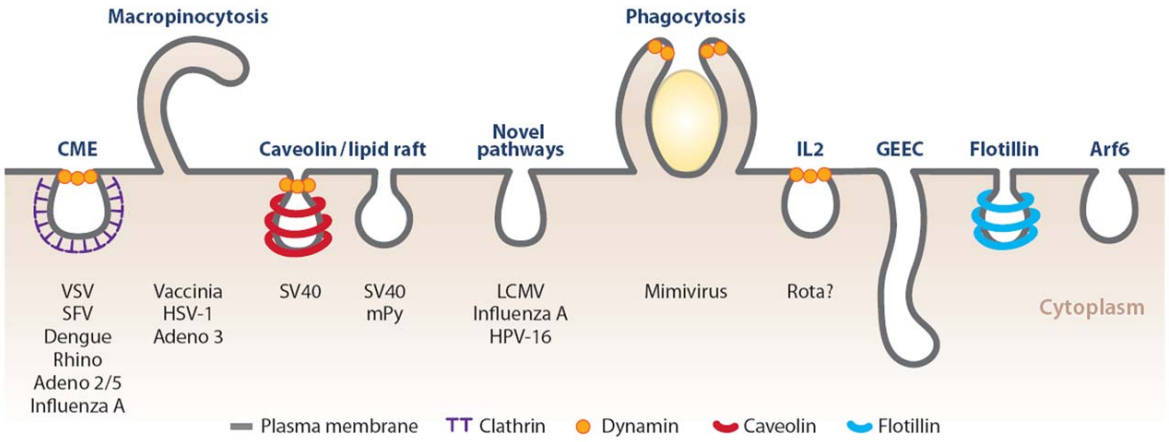

Figure 1.5 Endocytic Mechanisms.
Depicted are the known mechanisms of endocytosis in animal cells. The defined mechanisms of endocytosis include: clathrin- mediated, caveolar/lipid raft mediated, dynamin II- mediated endocytosis as well as macropinocytosis and phagocytosis. Interleukin 2 receptor (IL2), GPI- enriched endocytic compartments, flotillin, and ADP- ribosylation factor 6 (ARF6) are involved in endocytic mechanisms that are poorly defined. Novel pathways are for other processes that are not known to be associated with the other endocytosis mechanisms depicted. Viruses that enter cells through the process are listed underneath. Adeno 2/5, adenovirus 2/5; Adeno 3, adenovirus 3; CME, clathrin-mediated endocytosis; HPV-16, human papillomavirus 16; HSV-1, herpes simplex virus 1; LCMV, lymphocytic choriomeningitis virus; mPy, mouse polyomavirus; SFV, Semliki Forest virus; SV40, simian virus 40; VSV, vesicular stomatitis virus. (Figure adapted from Mercer et. al. 2010)

the cellular membrane creates a depression in the cell membrane, called a clathrin- coated pit. Polymerization of the clathrin coat continues pulling the membrane into a spherical structure that is still attached to the cellular membrane. A small GTPase called dynamin then physically separates the newly formed endosome from the cellular membrane (122, 263, 279, 280). Clathrin-mediated endocytosis is a well studied mechanism by which cargo is brought into the cell, although the kinetics, cellular requirements, and shape of the clathrin lattice may depend on cell type (264, 265, 355).

Besides important cellular cargo including epithelial growth hormone (115), viruses have also usurped this mechanism to gain access to the host. Many viral receptors have been shown to traffic through clathrin- mediated endocytosis, including the receptors for some reoviruses, FCV, and adenovirus (201). Interestingly, the size of the endosomes created by clathrin can vary greatly even to accommodate a bacteria, *Listeria monocytogenes*. This observation suggests that size should not exclude larger viruses, such as vesicular stomatitis virus (311), from using this entry mechanism (334). Once internalized into the cell, clathrin- coated vesicles last only minutes in the cell before the clathrin coat disassembles and the vesicle traffics through the cell becoming an early, then late endosome, and finally a lysosome (Figure 1.6) (118). Soon after formation, these previously clathrin- coated vesicles gain markers of early endosomes. Additional fusion with pre-existing endosomes adds additional markers to these vesicles, including intermediate endosome, late endosome, and finally lysosomal markers (163). Throughout this process,

vacuolar ATPases acidify the lumen of the endosome. Estimates suggest the change of the endosomal lumen's pH from a pH of 7 in newly formed endosomes, to a pH of about 4 in lysosomes (248). However, this "endosome maturation" is not the only trafficking pattern observed for endosomes. Recycling endosomes are endosomes that traffic into the cell, but due to interactions with various recycling signals, including Rab 4, 11, and 22, trafficked back to the plasma membrane where they fuse back with the cellular membrane (330).

1.2.2.2 Lipid Raft- Mediated Endocytosis

The cellular membrane does not consist of an evenly distributed mixture of lipids, glycolipids, carbohydrates, and proteins as originally hypothesized (294). In fact, just as the cell is divided into functionally independent membrane bound regions, called organelles, the cellular membrane consists of heterogenous mixture of various microdomains (293). These microdomains are thought to consolidate signaling proteins so that their signals are amplified, and spatially regulated. One common microdomain in the cellular membrane is the lipid raft, an enrichment of sphingolipids and cholesterol (261). One experimental approach at isolating lipid rafts, or detergent- resistant membranes (DRMs) is through selectable permeabilization and ultracentrifugation. This approach allowed investigators to differentiate these membranes from other microdomains of the cellular membrane called detergent- sensitive membranes (DSMs), and identify lipid raft- associated from non- lipid raft- associated proteins (26). However, this selectable solubilization approach has several drawbacks (228).

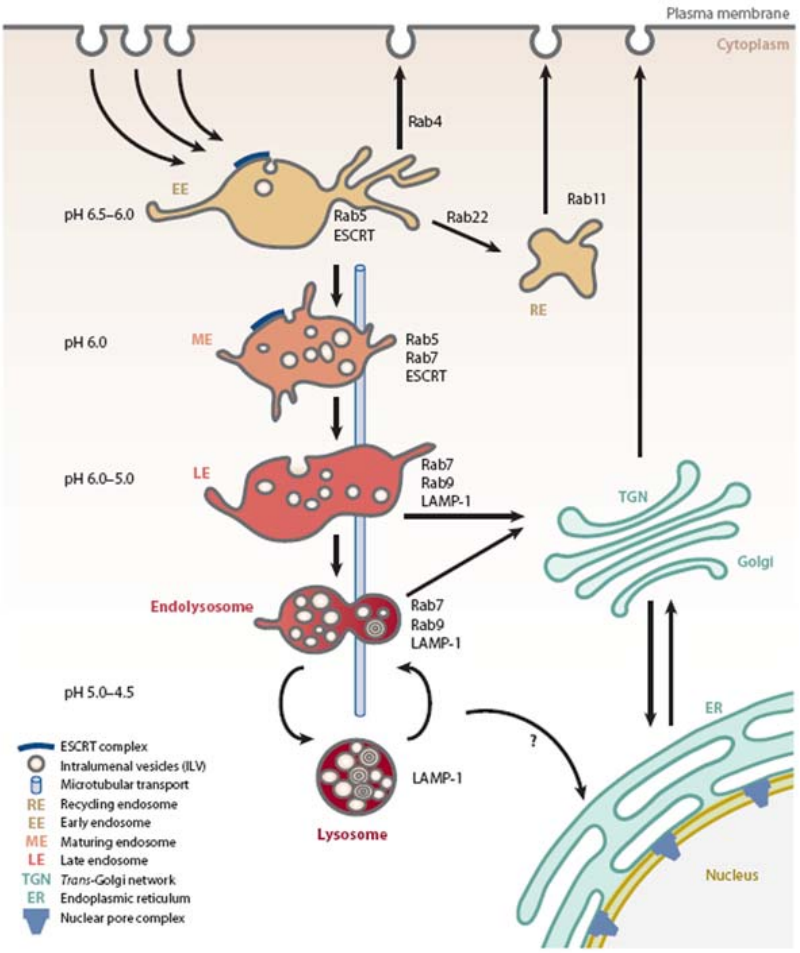

Figure 1.6 Endosome Maturation.
The main organelles of the endocytic pathway are the early endosomes (EEs), maturing endosomes (MEs), late endosomes (LEs), recycling endosomes (REs), and lysosomes. EEs are usually located in the periphery of the cytoplasm and are formed with the help of rab-protein (Rab) 5 after formation from the cellular membrane. Maturation of the endosome occurs as the EE traffics into the cell and obtains additional membrane proteins after fusion with additional endosomes. MEs contain markers of both early and late endosomes, such as Rab 5 and Rab 7. They then undergo further acidification and conversion to mature LEs, which can fuse with each other and eventually with lysosomes, generating endolysosomes in which active degradation takes place. The dense core lysosomes correspond to the end points of such degradation processes; they serve as a depository for lysosomal enzymes and membrane proteins awaiting fusion with incoming LEs. Endosomes can also undergo recycling to the plasma membrane. LAMP-1, lysosomal-associated membrane protein; ESCRT, endosomal sorting complex required for transport; ILV, intralumenal vesicles; TGN, the *trans*-Golgi network (Figure from Mercer et. al. 2010).

Another way to determine the role of lipid rafts is through depleting cholesterol in the cells, using various chemicals, including methyl- beta cyclodextrin (MβCD). Cholesterol depletion inhibits many endocytic processes including caveolin-, flotillin- and GRAF1- mediated endocytosis (174), which suggests these processes are dependent on host cholesterol. Recently, researchers have proposed that DRMs can be further classified into domains containing specific proteins and their complexes, such as tetraspanin- enriched lipid rafts (364).

1.2.2.3 Caveolin- mediated endocytosis

Caveolin- mediated endocytosis requires the caveolin protein family, caveolins 1, 2, and 3 (51). The removal of caveolin 1 resulted in the complete loss of caveolin- mediated endocytosis except in muscle cells. Restoration of caveolin- mediated endocytosis was observed upon reintroduction of caveolin 1 expression (84). This suggests that caveolin 1 is necessary and sufficient for caveolin- mediated endocytosis except in muscle cells were caveolin 3 serves this purpose. Caveolins 1 and 3 can encapsulate membrane from the plasma membrane and internalize endosomes into the cytosol by a cholesterol-dependent mechanism (81, 229, 277). Caveolin 2 is ubiquitously expressed, but is retained in the Golgi apparatus. Although it can be found on the cellular membrane in heterodimers with Caveolin 1, its function is not well understood (24, 182, 188, 251). Caveolin is a monomer that interacts directly with the cellular membrane through a hairpin loop domain in areas enriched in cholesterol. Membrane interaction aids in oligomerization of caveolin and endocytosis.

Although caveolin- coated vesicles were previously shown to traffic to a pH neutral compartment, termed the caveosome (253), this structure has been characterized as an experimental artifact and is actually a multi-vesicular compartment only observed during over- expression of caveolin (76). Currently, caveolin- mediated endocytosis is thought to traffic caveolin- coated vesicles to similar endosomal compartments as clathrin- mediated endocytosis such as early endosomes. However, the mechanism by which caveolin initiates, propagates, and finally pinches off an endosome is not completely understood and requires further investigation. Interestingly, caveolin may also regulate cellular processes independent of traditional endocytic processes, such as serving as protein scaffolding for signal transduction and as a way to traffic proteins from the Golgi apparatus to the cellular membrane (124).

Simian virus 40 (SV40) enters the host through caveolin- mediated endocytosis (5, 253). Later evidence during productive infection of caveolin-knockout cells with SV40 raised questions about independent requirement of caveolin on entry of SV40 (57). However, other viruses besides SV40 require caveolin for infection, and it has been suggested that echovirus 1 enters cells in a caveolin- dependent process (260). Understanding the mechanism by which these viruses enter the cell will help to define the mechanism of caveolin-mediated endocytosis.

1.2.2.4 Dynamin II- dependent endocytosis

Dynamin is a family of GTPases that facilitates the separation of the nascent endosomes from the plasma membrane and also participates in actin remodeling and stabilization (36). The dynamin family consists of three members, dynamin I, II, and III, but is further complicated by splice variants of each of these proteins. Dynamin I is found in neurons, but has recently been discovered in neuroendocrine cells (191, 234). Dynamin II is expressed ubiquitously (331), while dynamin III is restricted to the brain and testes although other cells, such as lung epithelium, may express the protein (36, 271). In addition, there are also dynamin- like proteins including dynamin- related protein 1 (DRP1), optic atrophy 1 homologue (OPA1), atlastin, and mitofusin (75, 107, 133, 137, 245). Dynamin I, II, or III function in many forms of host endocytosis including clathrin- (56, 138, 191, 271), and caveolin- dependent (128, 254), but also clathrin- and caveolin-independent mechanisms (194). The role of dynamin in phagocytosis has been suggested (94, 225). Since endocytosis occurs in cells lacking dynamin (57) or with over-expressed dominant negative dynamin (56), dynamin- independent endocytosis exists but these processes are poorly defined.

The requirement of dynamin during viral infections has been most characterized for clathrin- mediated (130, 150, 151, 250, 300, 342), and caveolin-mediated uptake (254). However, processes independent of clathrin or caveolin may still require a member of the dynamin family, including entry into cells by adeno-associated virus 2 (AAV-2) (241), herpes simplex type 1 (268), and some coxsackieviruses (252). Further investigation into the role of dynamin during

clathrin- and caveolin- independent endocytosis will most likely reveal further requirements of dynamins during virus entry.

1.2.2.5 Phagocytosis and Macropinocytosis

Phagocytosis and macropinocytosis are actin- dependent processes, which take samples of the extracellular matrix into the cell. These processes can produce much larger endosomes than other forms of endocytosis, termed phagosomes, or macropinosomes. Phagocytosis or macropinocytosis may be necessary to facilitate the entry of a few large viruses, including Mimivirus, one of the largest viruses described (94). Although the terms phagocytosis and macropinocytosis have been used to differentiate two distinct processes in the literature, currently these processes cannot be differentiated experimentally. In this thesis, the term phagocytosis will be used to refer to both phagocytosis and macropinocytosis.

For brevity, I will only describe the process of phagocytosis mediated by antibody- coated, or opsonized particles, and the constant domain (Fc) of the immunoglobin G (IgG) family antibody receptor, or Fc- receptor. Particles opsonized by antibodies are coated by the antibody in a uniform manner with the IgG with the Fc region of the antibody pointing away from the particle. Upon interactions of opsonized particles with a phagocytic cell, the Fc region of an IgG interacts with the Fc receptor. As additional Fc receptors bind to the opsonized particle, the receptors begin to cluster and this initiates a signaling cascade that facilitates formation of a phagocytic cup around the particle by an actin- and

myosin- dependent mechanism (106, 180, 313). Additional membrane is recruited to the newly forming phagosome through unknown mechanisms and could include fusion of recycling endosomes or ER- derived membranes (88, 327). Many proteins are required for phagocytosis, including two small GTPases from the rhodopsin (Rho) family, RAS- related C3 botulinum substrate 1 (RAC1) and cell division cycle 42 (CDC42). Rac1 and CDC42 are important regulators of this process. Although CDC42 facilitates actin polymerization upon activation, it is not able to facilitate phagocytosis independently (239). In contrast, RAC1 is sufficient to allow phagocytosis, although the mechanism may differ when functional CDC42 is present. After the phagocytic cup has lengthened enough to encompass the entire opsonized particle, additional proteins, including RAC1 and actin, facilitate fusion of the phagosome, incorporating the newly formed phagosome into the cell (39, 40).

The role of cholesterol during Fc receptor- mediated phagocytosis has not been fully elucidated. Upon Fc receptor clustering by cross- linking or opsonizing particles, the receptor is found in DRMs or lipid rafts. Although the mechanism by which DRMs facilitate phagocytosis is not well understood, it has been suggested that DRM association may facilitate activation of the Fc receptor through the tyrosine kinase v-yes-1 Yamaguchi sarcoma viral related oncogene homolog (Lyn) (173). Since these studies were performed with an artificial stimulus of phagocytosis, the role for cholesterol during natural induction of phagocytosis has yet to be determined.

The role of dynamins during phagocytosis is also unclear. Although in two cell types the role of dynamin II during phagocytosis has been described (98, 233, 328), it may not be a universal requirement for phagocytosis, and may vary between cell types as well as cargoes, including viruses.

Many viruses require phagocytosis to productively infect cells, but the mechanisms behind this entry are poorly understood. These viruses include poxviruses, mimiviruses, cytomegalovirus, Lassa fever virus, HIV, species B human adenovirus serotype 3, echovirus 1, group B Coxsackievirus, herpes simplex virus 1, and Kaposi's sarcoma-associated herpesvirus (34, 94, 215, 216, 267, 301). Large viruses, including mimiviruses (84), may require phagocytosis due to size restrictions. Phagocytosis may also be used as a means of immune evasion. Poxviruses mimic apoptotic blebs, as the virions contain phosphatidyl serine and may resemble cellular apoptotic belbs, the virus can enter cells in a manner that may also evade an immune response (210,211). Whether this mechanism of mimicry is conserved is an open question in the field of virus entry.

1.2.2.6 Other forms of endocytosis

Besides the various forms of endocytosis addressed above, several less characterized forms of uptake have also been documented (51). These mechanisms of extracellular sampling include cholesterol- dependent, Flotillin (or Reggie)- mediated, ADP- ribosylation factor 6 (ARF6)- mediated, GTPase regulator- associated with focal adhesion kinase-1 (GRAF1)- mediated endocytosis, or interleukin 2 receptor (IL2R)- dependent processes (Fig. 1.5).

The classical endocytosis mechanisms requiring clathrin, caveolin, or phagocytosis have been experimentally ruled out for these other forms of endocytosis, thereby categorizing them into independent processes. However, these processes may be interrelated to each other as their independence from each other has not been experimentally ruled out. For example, ARF6- mediated endocytosis might require GRAF1, but the role of GRAF1 in ARF6- dependent endocytosis was not tested. Therefore, further work may consolidate or expand this already complex field.

Cholesterol is critical for caveolin- mediated endocytosis, but cholesterol-dependent endocytosis independent of caveolin has also been documented (57, 165, 209, 238). Cholesterol- dependent endocytosis is further categorized based on the requirement of dynamin II. Both dynamin II- and cholesterol- dependent (231) and dynamin II- independent but cholesterol- dependent processes have been described (57, 165). Interestingly, cholesterol depletion was shown to inhibit SV40 uptake in the presence (253, 260) or absence (57) of caveolin. However, the role of dynamin in SV40 has only been shown for the caveolin-dependent process (252, 260). This suggests that two independent processes can transport SV40 into the cell, or that only cholesterol and not caveolin is sufficient for SV40 uptake. Cellular markers for cholesterol- dependent endocytosis have not been clearly defined. Therefore, only careful elimination of other forms of endocytosis can validate mechanisms such as cholesterol-dependent processes.

Flotillin, also known as Reggie, is a marker of a cholesterol- dependent but clathrin- and caveolin- independent mechanism of internalization although whether flotillin is necessary and sufficient for endocytosis is controversial (97). There are two flotillin proteins, Flotillin 1 and Flotillin 2, or Reggie 2 and 1 respectively, that are highly conserved from fruit fly to human (274). Flotillin 1 associates with DRMs (18), and is thought to be a lipid raft- associated protein. Interestingly, flotillin 1 and 2 do not transverse the cellular membrane, but associate with cellular membranes through palmitoylation (223). It has been suggested that the flotillins most likely associate with unknown transmembrane proteins to facilitate endocytosis due to the lack of a endosomal lumen tail to interact with cargo proteins (15). Flotillin can also heterodimerize with caveolin, although this dimer has an unknown function (337). Flotillin is incorporated into the virus particles of Newcastle disease virus, suggesting flotillins could play a role in the steps of the virus life cycle (175). However, a functional role of flotillin during virus entry has yet to be established.

ARF 6 is a small GTPase that has been associated with the cellular uptake of cholera toxin subunit B (38). Currently, it is thought that ARF6 may facilitate the uptake of cholera toxin subunit B in the absence of clathrin, caveolin, and dynamin II (165). However, whether ARF6 is necessary and/or sufficient to carry out endocytosis has not been experimentally tested. Interestingly, coxsackie virus A9 (126), and even possibly HIV-1 (90), require ARF6 for productive infection. Further elucidation of ARF6- dependent

endocytosis will likely reveal other cellular and viral cargoes and help define how this process is regulated.

GRAF1 is a GTPase activating protein (GAP) that has been shown to facilitate uptake of various clathrin- independent cargoes (194). Although discovered only a few years ago, evidence is mounting that GRAF1 is necessary and sufficient to internalize cargo in a process that is clathrin-, and caveolin-independent. However, the mechanism of GRAF1-mediated endocytosis is still unclear, and the role of cholesterol and dynamin during this process are also unclear (194). It is thought that GRAF1 may regulate the creation and destruction of cell extracellular matrix interactions and cell spread. Indeed, many GRAF1-positive compartments containing various extracellular matrix proteins have recently been described (69). Interestingly, AAV2 infects a human cervical cancer cell line (HeLas) in a process that is independent of clathrin, caveolin, or dynamin II, but dependent on GRAF1 (241). This suggests that other viruses could use GRAF1 as a means to enter cells. However, further research is necessary to determine if GRAF1 is a more widespread requirement of virus entry, and to determine the GTPases that GRAF1 regulates.

The entry process of the interleukin 2 (IL2) receptor requires cholesterol and dynamin II (176). However, a recent study suggests the internalization of the IL2 receptor also requires actin remodeling and RAC1 (101). These results suggest that this process may be a phagocytic manner of uptake, and not an independent endocytic process. Further characterization into the uptake of IL2

receptor is required to categorize it into a phagocytosis- dependent process or into a unique endocytic process.

Differentiation and classification of various endocytic processes will occur with time. If history repeats itself, this process may require the use of viruses as tools to probe the host biology of endocytosis. The afore-mentioned forms of endocytosis are controversial and using viruses as tools could facilitate further characterization of these processes. In fact, viruses have been previously used to dissect the host requirements of endocytosis. For example, the discovery of caveolin- mediated endocytosis was in part dependent on investigations of SV40 infection of human epithelial colorectal adenocarcinoma cells (Caco2 cells) (5).

1.2.3 Virus Uncoating

For non-enveloped viruses, the protein shell that encapsulates the viral genome, or capsid, carries the viral genome from an infected host to a naïve host. The protein shell protects, transports, and releases the genome based on the information preprogrammed into its sequence- dictated structure. To ensure that the virus is in the right place and time to infect, the capsid must initiate this programmed set of instructions only upon activation by specific environmental triggers. Once the trigger is initiated, viral uncoating, or delivery of the viral genome to the site of replication begins.

Non-enveloped viruses must penetrate or disrupt the endosomal or cellular membrane during the entry process to deliver the viral genome to the site of replication, either the cytosol or the nucleus. There are two proposed

mechanisms by which non- enveloped viruses accomplish this feat (127). The first step for both mechanisms requires the virus capsid to undergo a conformational change due to environmental or host interactions. In the first hypothesized uncoating mechanism, conformational changes facilitate direct interaction of the viral capsid with the endosomal or cellular membrane, possibly through post- translational modifications of the capsid such as myristic acid, observed with poliovirus (132). Further conformational changes of the viral capsid are then thought to be sufficient to create a pore in the membrane through which the viral genome is transported. In the second proposed mechanism, peptides released from the virus particle during the conformational change can disrupt the integrity of the endosomal membrane to the point where it no longer surrounds the virus particle. The virus capsid then enters the cytosol where it can further change its conformation to release the genome either into the cytosol or the nucleus. Although these mechanisms of viral uncoating have been suggested for more than fifty years, it is still unclear if these processes are universal for non-enveloped viruses.

Most non-enveloped viruses require internalization into an endosome before uncoating. Upon internalization by endocytosis, the newly pinched off endosome is trafficked into the cell. As mentioned above, endosomes acquire membrane protein markers by fusion with other similar endosomes and “mature” into late endosome or lysosomes, containing very acidic endosomal lumens. Some viral capsids recognize this acidification and use it as a trigger to initiate uncoating. For example, some adenoviruses require endosome acidification to

initiate conformational changes that release capsid subunits and disrupt the early endosome. Once releasing from the endosome, the remaining capsids traffic by microtubules to the nuclear pore, where the viral genome is transported into the nucleus, the site of adenoviral replication (19, 82, 103, 237).

Besides direct interactions of the virus capsid with the acidic endosomal lumen, various host proteases, which may be dependent on an acidic environment for activation, may cleave the virus capsid. Reoviruses require cleavage by cathepsin B and/or L to expose membrane- binding domains that may disrupt the membrane enough to allow the virus to enter the cytosol (9, 73). Interestingly, peptides isolated from cathepsin L cleaved reoviruses allow hemoglobin release from red blood cells, suggesting these peptides could destabilize cellular membranes (42). Once exposed, these peptides may breach the endosome and deliver the virus capsid to the cytosol where further modification may be required to release the viral genome.

Endosome acidification and protease cleavage are not the only mechanisms by which virus particles can undergo uncoating. Direct interactions with the viral entry receptor may be necessary and sufficient to initiate the uncoating program. In particular, poliovirus is well documented to drastically and irreversible change conformation of its protein capsid upon incubation with HeLa cell lysate containing the virus entry receptor Poliovirus receptor (PVR) (61, 62, 85). A defined tunnel structure through the capsid, connecting the virus genome to the extracellular space has been revealed via Cryo electron microscopy, which

may be the initial steps of viral uncoating (28, 29). These observations suggest that proper virus- receptor interactions can be sufficient for viral uncoating.

The mechanism by which MNV uncoats has not been addressed directly. The virus may require endosome acidification, protease cleavage, and/or direct receptor interactions to facilitate uncoating. Some evidence exists that MNV proteins, specifically NS1/2 or N term (303), can be cleaved by host proteases, but the role of protease cleavage on MNV's capsid has not been examined directly. Unfortunately, the entry receptor for MNV is unknown, thus significantly complicating the elucidation of receptor- virus interactions.

1.2.4 Virus Translation

Once delivered to the site of replication, viral genomes must overcome tremendous barriers before the first infectious progeny can emerge from the host. In general, positive- strand RNA virus genomes require protein translation before viral replication can be initiated. For some positive- strand RNA virus genomes, the recruitment of the host's translation machinery is accomplished without the aid of viral proteins, instead they use three- dimensional structures in their genome, called internal ribosome entry site (IRES) (286). However, caliciviruses, including VESV (32), FCV (129), MNV (157), and HuNoVs (59) contain a small viral protein, VPg, covalently linked to the 5' end of the genome. For noroviruses, the VPg may be the only requirement in recruiting the 43S pre-initiation complex, which contains eukaryotic initiation factor 3 (eIF3), the 40S complex, tRNA encoding for methionine, and the viral genome (59, 60). Linkage of the viral VPg

protein at the 5' end of the viral genome properly positions the translation machinery for translation initiation. In addition, the 5' untranslated region of noroviruses is very small, approximately 10 nucleotide base pairs, and most likely is too small to contain an IRES (288, 368). The VPg of various caliviruses, including FCV, HuNoV, and MNV-1 (45, 99, 154) has been shown to directly interact with the host translational machinery (120, 324).

The translated viral genome consists of the nonstructural proteins as a long poly- protein, VP1, and VP2. Although VP1 and VP2 are functional after translation, the nonstructural proteins are cleaved from the poly- protein by the viral protease, NS6 or 3CL-protease. The cleavage sites in the viral polyprotein are highly conserved with the other reported noroviruses, suggesting NS6 function is conserved among Caliciviruses. Host proteases have also been shown to cleave the NS1/2 protein of MNV-1 (303) and FCV, as well as the capsid protein of FCV (1). Cleavage of NS1/2 has been demonstrated by the host protease caspase 3 for MNV-1 (303) and caspase 2 and/or 6 for FCV (1). The role of this cleavage is unknown. However, due to the activation of apoptosis during MNV (21) and FCV (235) infection, this cleavage may have a functional role during viral infection. On the other hand, the role of the viral protease, NS6, in one strain of human norovirus, MD145-12, and FCV has been shown to cleave poly (A)- binding protein (PABP) (172). Host targets of MNV NS6 have yet to be determined, but can clearly lead to greater insight of viral infection and pathogenesis.

1.2.5 Virus Replication

Once the nonstructural genes are translated, the viral proteins traffic to the site of replication of the viral genome. For MNV, it has been demonstrated that the nonstructural proteins traffic to a perinuclear region, which may be near the microtubule organizing center (MTOC) in the host, although the relevance of this trafficking is unknown (144, 303). Early during infection, remodeling of the host membranes creates membranous structures, termed virus replication factories or the membranous web, composed of various organelle membranes, including ER and Golgi apparatus (193, 353, 360). These membranes are enriched for viral proteins, including NS7, or RdRp, as well as host factors required for viral replication and concentrate these proteins for efficient replication. Active replication of the viral genome has been suggested experimentally for MNV at these replication factories by the presence double- stranded RNAs, a replication intermediate (144). Virus particles have also been observed in these regions of membrane reorganization although at later time points, suggesting that these sites may also be used for viral assembly. Interestingly, the membranous structures created during MNV replication contain double- membrane structures and are closely associated with mitochondria (210). These two characteristics are hallmarks of autophagy, a cellular process originally described as a process in which intracellular organelles and cellular structures are degraded as a source of energy for the cell (164). The role of autophagy during viral replication for other viruses, including poliovirus, has been previously suggested (164, 352) but whether autophagy is important during Calicivirus replication is not known. In

general, the mechanism by which noroviruses reorganize and recruit host-derived membranes, which are essential structures for norovirus replication, are not well understood.

A general mechanism of how the Calicivirus genome is replicated has been compiled using studies from MNV (353), FCV (304), and other positive-strand RNA viruses. The viral protein NS7, or the RdRp, associates with the 3' end of the viral genome possibly through interactions with the conserved three-dimensional genomic structure of the 3' untranslated region and/or the VPg (104). Once bound to the 3' end, NS7 polymerizes a complimentary anti-sense viral genome. Then, the NS7 disassociates from the anti- sense genome. This disassociation may be triggered by interactions with the VPg-linked 5' end. Additional positive- strand genomes are produced by the NS7 from the complimentary anti-sense genome. Once these additional positive- strand viral genomes become covalently linked to the viral VPg, these progeny genomes can now undergo translation, or become packaged into new virus particles.

Additionally, sub- genomic transcripts, lacking ORF 1, have been observed during MNV infections (99). These sub- genomic RNAs may be produced by one or both of two proposed mechanisms. A highly conserved three- dimensional structure creates a hairpin loop at the junction between the ORF1 and ORF 2. In the first proposed method, this region may contain an internal promoter and attachment site for NS7 (220). After attachment, NS7 will create a new sub- genomic RNA containing the 3' half of the viral genome, including ORF2, 3, and 4. The promoter region for RHDV, a Calicivirus, has been

isolated and functions as an internal attachment site for NS7 in vitro (221). A second mechanism proposes that this region may result in termination of the synthesis of the complementary anti-sense genome before reaching the ORF 1. Using these truncated anti-sense templates, NS7 could also create sub-genomic RNAs (295). In general, this is supported by observations of truncated anti-sense subgenomic RNAs from brome mosaic virus-infected cells (296, 297, 351). However, evidence for these mechanisms during norovirus infection has not been observed.

1.2.6 Virus Assembly and Release

Upon successful viral replication, the viral genome is packaged into the viral capsid to facilitate progeny production. However, the process of viral assembly is poorly defined in noroviruses. There are two hypotheses to describe the process of virus assembly in general. One theory states that the viral capsid assembles around the viral genome and encapsulates one viral genome. Support for this theory has been observed for tobacco mosaic virus (167) , the bacteriophage R17 (332), HIV (281), SV40 (276) and *Totiviridae* viruses (302). The second theory states that an empty viral capsid is assembled first, and viral genome is transported into the space inside. Again, this process has been shown as the mechanism of packaging by several viruses, including Adenoviruses (246, 247) and herpesviruses (10). Since norovirus assembly has not been examined to date, either of these two mechanisms may be required for assembly. Regardless, the observation that MNV virus particles have been observed near

sites of viral replication (210), suggests that replication and virus assembly are a closely linked process even in a spatial respect.

After viral assembly has completed, the viral particles are then released from the infected cell. The mechanism of how non-enveloped virus particles are released from infected cells is also not well understood, including the release of norovirus particles from infected cells. Due to the lack of a lipid component, non-enveloped viruses in general may require the cellular membrane to become disrupted or destroyed. Recent studies suggest that MNV (21) and FCV (235) infections induce apoptosis late during the viral life cycle. Apoptosis may disrupt the cellular membrane and release viral progeny into the extracellular space. However, there are questions to the exact mechanism of this release since apoptotic cells break down into membrane blebs, and may result in membrane-bound virus particles (284, 309). Disruption of the cellular membrane by cell death to aid release of virus progeny has been suggested for SV40, poliovirus, rotavirus and parvovirus. Interestingly, these viruses have also been detected in the extracellular space before the lysis of infected cells (53, 91, 153, 329). This suggests that viruses have evolved a mechanism to release virus particles before cell death. Further investigation into virus release for noroviruses would help determine which, if any, of these processes facilitate virus release.

1.2.7 Positive- Strand Virus Life Cycle Continuation

Once an infectious particle is released from the cell, it must traffic to a naïve cell to initiate a new infection. This journey can range in time and space

anywhere from traveling to an adjacent cell, such as in a tissue culture setting, to leaving the infected host to find a new susceptible host. After enduring this journey, a virus particle must once again find a permissive host to attach to, internalization into, uncoat within, and replicate inside of. Thus, by accomplishing these steps the virus can repeat the viral life cycle.

1.3 The Ubiquitin Cycle

Viruses usurp the host by regulating various parts of the cellular machinery in order to complete the viral life cycle. Attachment of the virus to the host requires host- derived attachment receptors. Internalization of the virus into the host requires host entry receptors. Viral replication actively redirects the host transcription and/or translation machinery to allow for viral genome and protein production. The event of viral release from the cell requires transport of the virus outside of the cell or through cell death to eject the virus outside the cell. Each of these above mentioned steps of the viral life cycle is intertwined with the host, and, therefore, regulation of host proteins significantly affects the virus life cycle. One recently discovered post-translational modification of proteins, through the direct covalent modification with a small protein called ubiquitin (ub), can drastically affect virus infection (259, 336).

Ub is a small 8 kilodalton protein that is post- translationally conjugated to target proteins through a lysine residue, or in rare cases a histidine, serine, or threonine. Monomers of Ub are activated and covalently linked to Ub- modifying proteins called E1- activating enzymes. E1s then transfer these Ub monomers to

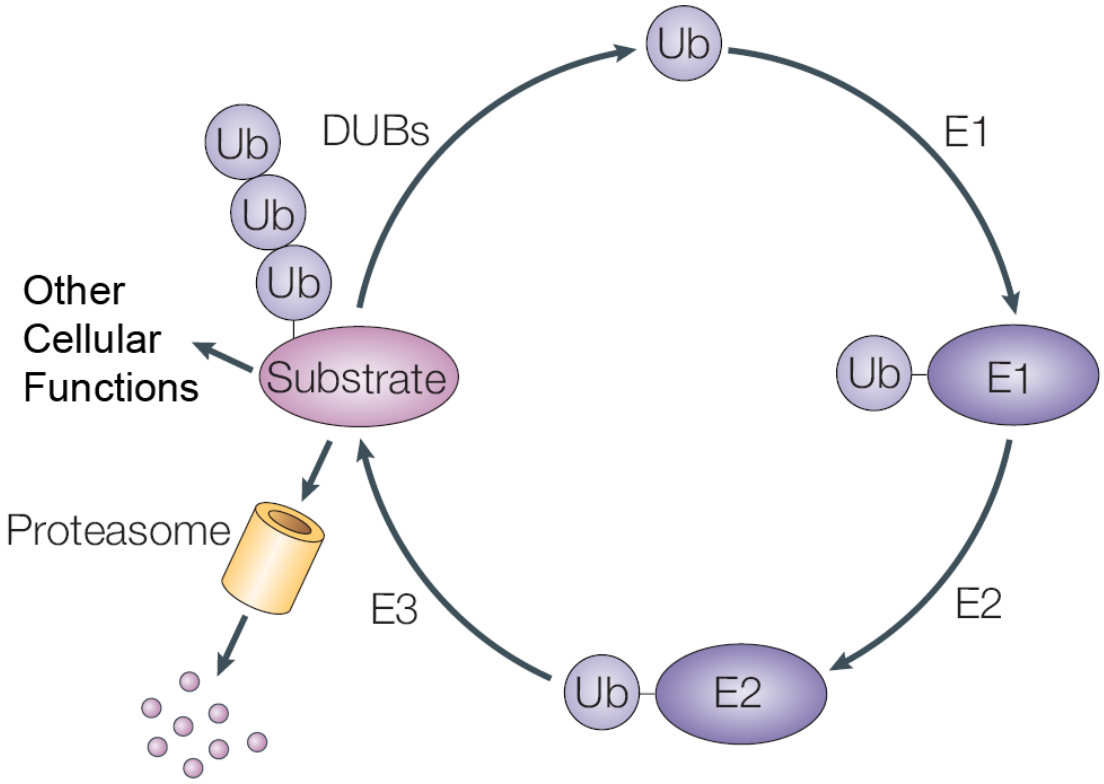

Figure 1.7 The Ubiquitin Cycle
Depicted is the cascade of reactions required to covalently attach an ubiquitin (Ub) to a lysine residue of a target protein through a process called protein ubiquitination. Protein ubiquitination is an ATP- dependent process that requires the sequential actions of three enzymes: an activating enzyme (E1), a conjugating enzyme (E2) and a ligase (E3). Proteins marked with a polymer of Ub (a poly- Ub chain) are selectively targeted to a multisubunit ATP-dependent protease known as the 26S proteasome, resulting in degradation of the substrates and recycling of Ub, although other cellular functions have also been attributed to protein ubiquitination. Ubiquitination is reversible and Ub is removed from substrates by deconjugating enzymes (DUBs). (Adapted from Shuai et. al. 2003)

E2-conjugating enzymes. The Ub is then finally transferred to a target protein through an E3 Ub ligase (Figure 1.7) (259, 336). There are four known domains for E3 ligases, including really interesting new gene (RING) (64), plant homeodomains (PHD)(72, 147), Ub fusion degradation 2 homology domain (U-Box or E4 ligases)(168, 200), and homologous to E6-associated protein C-terminus (HECT) (278). The target protein selectivity most likely occurs at the level of the E3, as these enzymes act directly on the target proteins and there are more members of E3s than E1s or E2s combined (359). Once the target protein has been ubiquitinated, the process of poly- ubiquitination modifies the target protein with a chain of covalently-linked Ubs. Ub has seven lysine residues, which can all be substrates for the ubiquitination machinery as well as the N-terminus of the protein. The length of the Ub chains, as well as the lysines used to conjugate the chains, creates unique signals in the cell. These Ub chains are recognized by over twenty conserved protein domains (68, 141). Proteins with diverse cellular functions have these domains; therefore Ub regulates many cellular processes.

Ub chains linked by the 48th amino acid (K48) as well as linear Ub chains are cellular means to regulate proteins for proteasomal degradation and regulate proteins required for proteasome function (346). In general, Ub chains formed on the 63rd amino acid of Ub (K63) result in activation of the ubiquitinated protein, in general, allowing the protein to signal through transduction pathways (185). The other lysine residues of Ub (K6, K11, K27, K29, K33) have been observed in cells, but their functions have yet to be fully elucidated (358). Recently, some

evidence suggests that K11 may be involved in the regulation of cell division (348). In addition to Ub, other small post-translational modifying proteins have been discovered, including small Ub-like modifier (SUMO), neural precursor cell expressed developmentally down-regulated protein 8 (NEDD8), interferon-stimulated gene 15 (ISG15), autophagy- related protein 12 (ATG12), and microtubule- associated protein light chain 3 (LC3) (160). Although the sequences of these proteins are highly divergent, all the modifications are covalently added to target proteins post-translationally by specific enzymatic reactions, which are usually reversible.

Similar to the antagonistic relationship kinases and phosphatase share, E3 ligases are regulated, in part, by the cysteine proteases that specifically cleave Ub from target proteins, called deubiquitinases (DUBs) (121, 240). Ubiquitinated proteins can be deubiquitinated by DUBs, and it is thought that deubiquitinated protein return to their ubiquitin- free function. DUBs also play a role in poly-Ub chain processing, cleaving free poly Ub chains and newly synthesized Ub, which exist as polyproteins of repeating units. In the human genome, there are 95 putative DUBs that are categorized into five separate families, including Ub-specific proteases (USPs), Ub C-terminal hydrolases (UCHs), Machado-Joseph domain proteases, and ovarian tumor-related proteases (OTUBs), and zinc metalloprotease family members (170, 240). Although the USP family is the most abundant, the Ub cycle is closely regulated through the process of Ub removal and remodeling by DUBs from all five families.

1.3.1 Viruses regulate the Ubiquitin Cycle to facilitate viral infection

Ub regulates many vital cellular processes such as cellular DNA repair (140), endocytosis, vesicle trafficking (131, 269, 270, 307), protein signaling (65, 114), protein degradation (219, 346), and innate immune signaling (14, 199). Recent investigations into immune signaling has revealed that the Ub cycle regulates recognition and clearance of pathogens, antigen presentation, and activation of the adaptive immune response (14, 199). Viruses must interact with the Ub regulatory network to facilitate productive infection or risk the ability of an infected cell to recognize the viral pathogen and initiate the proper immune response, thereby preventing infection.

Viruses alter important signaling pathways in the cell, including signals regulating the innate immune response. Ub regulation of the intracellular sensors of foreign nucleic acid, including retinoic acid- induced gene I (RIG I), has been recently elucidated (196, 205). After binding to 5' triphosphate groups on some viral RNA genomes, RIG I becomes activated and signals through the mitochondrial anti-viral signaling protein (MAVS), also called IPS1, VISA, or CARDIF. This signaling activates downstream kinases, including Tank- binding kinase 1 (TBK1) and inhibitor of nuclear factor kappa B inhibitor kinase alpha (IKK), which in turn activate interferon regulatory factor 3 (IRF3) and nuclear factor kappa B (NF-KB), two known immune- regulatory transcription factors. IRF3 and NF-KB can facilitate the activation of a proper antiviral response in the cell. Inactivation of this signaling, for example, through protease cleavage of

MAVS by the Hepatitis C (HCV) viral protease, inhibits this antiviral response (183, 218). RIG I activation is in part due to the ubiquitination by an E3 ligase, tripartite motif-containing protein 25 (TRIM25) (87). Interestingly, influenza A has been shown to inactivate TRIM25 through its nonstructural protein 1 (86). RIG I is also strongly activated by poly- Ub chains bound through the K63 linkage, but not bound to cellular proteins, called unanchored Ub chains (367). However, the role of these unanchored poly- Ub chains during viral infection is not known. Clearly, the role of intracellular surveillance of viral RNA is highly regulated by the Ub cycle, and some viral pathogens including HCV and influenza A, have evolved mechanisms to disrupt the Ub regulation of this surveillance mechanism.

Besides manipulating various host proteins associated with the Ub system, viruses also encode their own Ub- modifying proteins including E3 ligases. Herpes simplex virus 1 encodes a versatile protein, infected cell protein 0 (ICP0), which is thought to function, at least in part, as an E3 ligase (112). ICP0 facilitates degradation of cell division cycle protein 34 (CDC 34) in a proteasome-dependent process (110, 111, 113). Encoding viral E3 ligases to shuttle important immune signaling proteins to the proteasome for degradation has been observed for many other viruses, including Kaposi's sarcoma- associated herpesvirus (KSHV), murine hepatitis virus 68 (MHV68), and rotaviruses (22, 23, 100, 308). When these virally encoded Ub- modifying proteins are removed, the virus infection is hampered or ablated. This suggests these viral E3 enzymes are required for infection, and without viral regulation of the Ub system viral infection is inhibited.

The discovery of virally- encoded DUBs suggests that both addition and removal of Ub can be implemented in viral strategies for infection. KSHV encodes a viral deubiquitinase, ORF 64, which removes Ub from RIG I, thereby preventing RIG I activation (146). SARS coronavirus (SARS-CoV) encodes a protease, PLpro, which cleaves Ub from poly- Ub chains *in vitro* although the activity of this DUB activity in cells has not been described (13, 49, 187). However, inhibitors of the SARS-CoV protease are also effective inhibitors of SARS infection (48, 95, 272). Adenovirus also encodes a putative DUB, L3 23K proteinase or Avp, like SARS-CoV, its cellular targets have yet to be described (11). Foot and mouth disease virus encodes a papain- like protease that can also cleave Ub, and has been shown to remove Ub from RIG I (340). Interestingly, porcine reproductive and respiratory syndrome virus encodes a DUB that can cleave not only Ub but also the Ub- like protein, ISG15, thereby inhibiting a proper antiviral response in infected cells (312). Although the role of these DUBs during the viral life cycle has yet to be fully elucidated, mutations that inactivate the catalytic activity of the DUB or small molecule inhibitors of the proteolytic function can significantly inhibit viral infection (48, 95, 148, 272, 312, 340). This evidence gives merit to the importance of these virally- encoded DUBs during viral infection.

Clearly there is strong selective pressure on viruses to regulate the Ub cycle, either by subverting the existing signaling pathways or encoding viral versions of Ub modifying enzymes such as E3 ligases and DUBs. However, the understanding of the Ub cycle's regulation of viral replication is in its infancy. For

example, Influenza A encodes a non-structural protein called nucleoprotein (NP), which associates with the viral genomic RNA. When NP is monoubiquitinated, NP associates with the viral replication machinery, and viral replication occurs. When the host DUB, USP11, cleaves the Ub from NP, it no longer associates with the replication machinery and Influenza A replication is significantly inhibited (184). This study was the first to show that Ub regulation directly affects viral replication. The role of the Ub cycle during norovirus biology has yet to be elucidated, and can shed significant insight on how noroviruses manipulate the host cell to facilitate infection.

1.4 The Unfolded Protein Response

The UPR is a cellular response to stress in the ER caused by unfolded proteins, inadequate sources of carbon, including glucose starvation, and/or oxygen deprivation (195, 338, 339). The UPR is regulated by three ER- resident transmembrane proteins called inositol response element 1 (IRE1), PKR- like ER kinase (PERK), and Activating transcription factor 6 (ATF6) (Figure 1.8). Once activated, these proteins up-regulate protein chaperones, disulfide isomerases, and glycosylation machinery to increase the folding and glycosylation capacity of the ER. In addition, the UPR also up- regulates ER- associated degradation (ERAD), increases ER synthesis, and/or inhibits protein translation. Cells unable to return the ER to a balance of folded and unfolded protein may commit themselves to cellular death pathways.

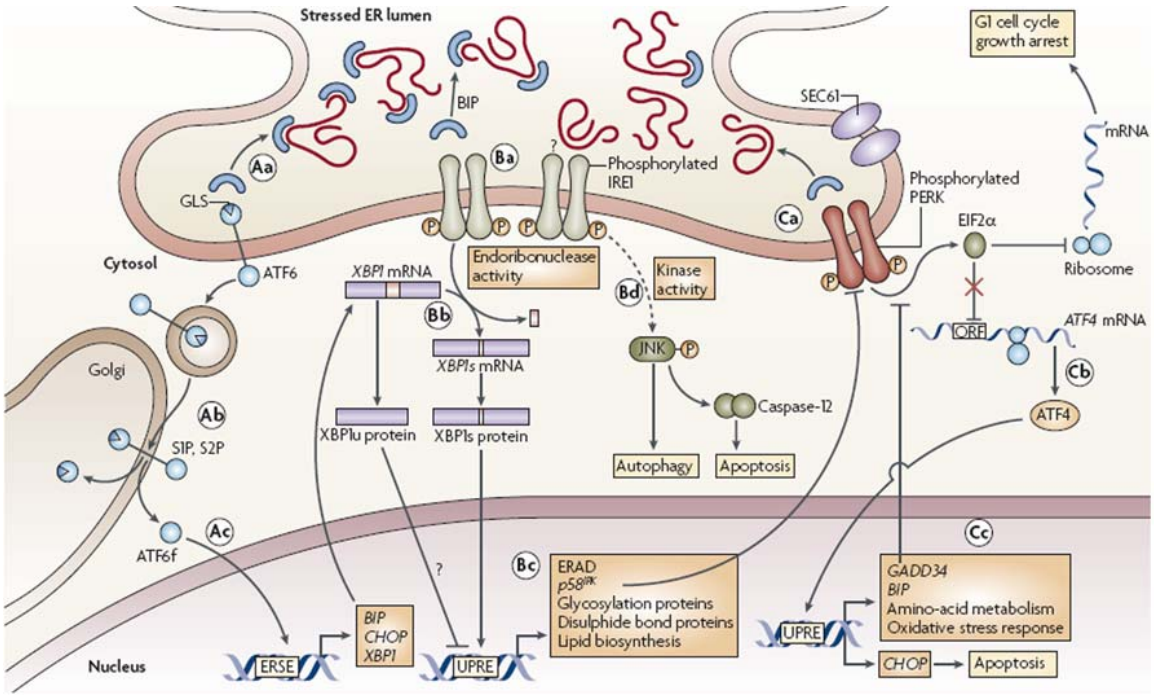

Figure 1.8 The Unfolded Protein Response
During endoplasmic reticulum (ER) stress, BIP is recruited away from activating transcription factor 6 (ATF6), inositol-requiring transmembrane kinase/ endonuclease 1 (IRE1) and PKR- like endoplasmic reticulum kinase (PERK). This activates the unfolded protein response (UPR). The release of BIP exposes a Golgi-localization sequence (GLS) within ATF6 (**Aa**), targeting the molecule to the Golgi. In the Golgi, ATF6 is sequentially cleaved (**Ab**). This releases the ATF6 fragment (ATF6f) transcription factor, which translocates to the nucleus, binds to ER-stress response elements (ERSE) and induces transcription of several genes (**Ac**). The release of BIP from IRE1 allows for homodimerization and activation of IRE1 through autophosphorylation. (**Ba**). Phosphorylated IRE1 possesses endoribonuclease activity that excises a fragment from unspliced *XBP1* mRNA and, following religation by a putative tRNA ligase, forms spliced *XBP1s* mRNA (**Bb**). XBP1s protein translocates to the nucleus, where it binds to UPR elements (UPREs) and up-regulates UPR-associated proteins. Although XBP1u protein is short-lived, it can impair XBP1s transcriptional function (**Bc**). In addition to its endoribonuclease activity, IRE1 activation also leads to activation of JUN N-terminal kinase (JNK), which can promote cell survival by inducing autophagy or can lead to programmed cell death by apoptosis (**Bd**). Much like IRE1, PERK is activated by autophosphorylation following the release of BIP. Phosphorylated PERK also phosphorylates eukaryotic translation-initiation factor 2α (EIF2α), causing translational arrest and subsequent cell cycle growth arrest (**Ca**). ERAD, ER-associated degradation; UPR, unfolded protein response; GLS,Golgi-localization sequence; ATF6f, fragment ATF6; ERSE, ER-stress response elements; UPREs, UPR elements; JNK, JUN N-terminal kinase; TRAF2, tumor-necrosis factor- receptor associated factor 2; EIF2α, eukaryotic translation-initiation factor 2α (Adapted from Todd et al 2008).

One regulator of the UPR is IRE1, which contains both a kinase domain and an endonuclease domain. When bound to heat shock protein 5 (HSPA5 or BiP), a soluble ER- resident protein chaperone, IRE1 is inactive. When BiP is sequestered by unfolded proteins in the ER, IRE1 becomes activated, oligomerizes, autophosphorylates, and activates its RNase activity (16, 325, 361). IRE1 then cleaves the messenger RNA of X-box binding protein 1 (XBP-1) to remove a small inhibitory sequence. The XBP-1 transcript undergoes a novel cytosolic splicing event, and the newly translated XBP-1 protein translocates to the nucleus to begin activation of the UPR by upregulating proteins essential in the UPR (33, 362). IRE1 has also been shown to cleave other transcripts, although the functional consequence of this has not been elucidated. In addition, IRE1 has also been shown to activate JNK signaling, which results in autophagy or cell apoptosis (198).

PERK is a resident ER transmembrane protein that regulates the UPR, through a pathway unique from IRE1. PERK is a kinase, which is regulated through interactions with BiP in a manner similar to IRE1. Upon disassociation of Bip from PERK, PERK dimerizes and the kinase becomes activated (16). Upon activation, PERK phosphorylates a subunit of the translational machinery, eukaryotic initiation factor 2 alpha (EIF2 alpha), and thereby inhibits global protein translation in the cell. Interestingly, PERK is one of four kinases that can phosphorylate EIF2 alpha, although PERK is the only kinase that responds to ER stress. In addition, phosphorylation of EIF2 alpha by PERK leads to a cell cycle arrest in G1 (117). Collectively, PERK activation stops global translation, allowing

cells undergoing ER stress to address this stress before additional cellular translation.

ATF6 is the third transmembrane protein to regulate the UPR. ATF6 is a transcription factor that is retained in the ER due to interactions with BiP, which hides a Golgi apparatus localization sequence (GLS) in ATF6. When BiP no longer binds to ATF-6, the GLS is exposed, and the transcription factor traffics to the Golgi. In the Golgi, two proteases, site 1 protease (S1P) and site 2 protease (S2P), cleave the N-terminal DNA binding domain of ATF6 from the ER. The cleavage product ATF6f is a transcription factor, which then translocates to the nucleus where it up-regulates proteins essential for the UPR. Interestingly, proteins up-regulated by ATF6 are different than those up-regulated by XBP-1 (344).

Two possible outcomes of an activated UPR are the restoration of the ER equilibrium and cell survival or apoptosis. First, the up- regulation of chaperone proteins, synthesis of additional ER, up- regulation of ERAD, and the inhibition of protein translation can result in restoration of the equilibrium in the ER. Once this occurs the cell can return to a normal equilibrium of unfolded proteins in the ER. For example, in plasma cells, recurring stress in the ER can lead to chronic stress instead of cell death suggesting a third outcome to ER stress (92). The second outcome occurs when homeostasis in the ER cannot be established. This causes the cell to commit to an apoptotic pathway.

As mentioned previously, Ub is a key regulatory element to many cellular processes. Although the role of Ub has not been readily established in the UPR,

one study suggests a DUB, USP14, can regulate the activity of IRE1. When USP14 is over- expressed, UPR activation is suppressed. In addition, siRNA knock- down of USP14 causes activation of the UPR. The authors proposed that USP14 interacts with IRE1 and inhibits its activation. Indeed, direct interact between USP14 and IRE1 has been observed in the absence of an active UPR (232). Upon activation of IRE1, USP14 no longer interacts with IRE1. Unfortunately, the role of ubiquitination of IRE1, and/or the role of the deubiquitinase function of USP14 during these interactions have not been elucidated. The mechanism by which the Ub cycle regulates the UPR requires further studies including elucidation of the role of USP14 during the IRE1-dependent arm of the UPR.

1.4.1 The Unfolded Protein Response and viral infection

Viruses have evolved mechanisms to regulate the UPR to ensure infection. Enveloped viruses are dependent on the host secretory organelles, both ER and Golgi apparatus (Golgi), to synthesize, fold, and glycosylate viral membrane glycoproteins required for new virus particle production. The sudden expression of these foreign glycoproteins can induce the UPR, which has been demonstrated during viral infections, including hepatitis B virus (181), HCV (77, 159), West Nile Virus (4), Influenza A (123), and herpesviruses (326). Enveloped viruses also need to regulate the UPR response to limit degradative mechanisms, such as ERAD, PERK-induced translation inhibition, and cellular apoptosis, which would inhibit progeny production.

HCV has evolved multiple mechanisms to regulate the UPR (77, 159). The nonstructural protein 4 B (NS4B) of HCV has been shown to inactivate PERK signaling, thereby allowing virus structural proteins to be produced (369). However, the IRE1- dependent pathway of the UPR is activated during HCV infection. This may be a way to activate beneficial parts of the UPR, such as an increase in protein glycosylation and folding in the ER, and to inactivate degradative parts of the UPR, such as inhibition of protein translation and ERAD. An active UPR may also down- regulate interferon signaling in the cell by degrading interferon alpha/beta receptors and making cells non- responsive to interferons (17, 189, 366). The lack of response to interferons is one complicating factor in chronic infection with HCV (213). However, whether these results obtained in culture translate to processes important in patients chronically infected with HCV, remains unclear. This evidence suggests that regulation of the UPR may contribute to persistent infections by viruses, including RNA viruses. Whether noroviruses can regulate this process to facilitate their own persistence has not been addressed.

Herpesviruses also regulate the UPR to ensure virus infection and progeny production. Early during infection, herpes simplex virus 1 (HSV1) inhibit IRE1 and PERK, but allow ATF6 activation. Interestingly, expression of ICP0, a viral protein with E3 ligase activity, is regulated by host ER stress, and may be a viral sensor of host ER stress (31). In addition, the structural gene glycoprotein B selectively inhibits PERK and ensures continuation of protein translation during infection (226). HSV1 also encodes the protein gamma1 34.5, which keeps

phosphorylated eIF2 alpha to a minimum by maintaining a high level of eIF2 phosphatase activity to ensure protein translation in the cell (50).

The role of the UPR during infections by Caliciviruses has not been tested. However, the requirement of host membranes to form the replication factories upon which the viral genome replicates and the recruitment of ER membranes to these structures by noroviruses suggests that the UPR can be important during norovirus infection (144, 353). Further investigation into the role of the UPR during norovirus infection may lead to novel mechanisms by which noroviruses regulate the UPR.

1.5 Thesis Aims

Noroviruses are a serious public health concern worldwide. The ability of noroviruses to infect at low doses, remain stable in the environment, and replicate to high titers in the host all facilitate large, costly outbreaks. Equally as concerning is the lack of approved antiviral therapies or vaccination strategies to control these pathogens. Instead, only strict hygiene measures can limit the spread of an outbreak. A lack of understanding of norovirus biology has hampered the development of these desperately needed therapies, due to the fact that HuNoV cannot be cultured or grown in a small animal model. With the development of a MNV system to study infection in tissue culture cells and a small animal model, in mice, we have begun elucidating how noroviruses infect their host. The aims of this thesis were able to identify the cellular requirements of virus internalization, the role of pH and endosome acidification on virus

uncoating, and to understand the requirements of the Ub system, specifically deubiquitinases, and the UPR during virus infection.

1.6 References

1. **Al-Molawi, N., V. A. Beardmore, M. J. Carter, G. E. N. Kass, and L. O. Roberts.** 2003. Caspase-mediated cleavage of the feline calicivirus capsid protein. Journal of General Virology **84:**1237-1244.
2. **Alda, F., T. Gaitero, M. Suarez, T. Merchan, G. Rocha, and I. Doadrio.** 2010. Evolutionary history and molecular epidemiology of rabbit haemorrhagic disease virus in the Iberian Peninsula and Western Europe. BMC Evolutionary Biology **10:**347.
3. **Alvarez, L., A. M. Auld, G. M. del Fierro, P. Fung, D. A. Lawrence, E. F. McInnes, M. E. Quinn, L. Rasmussen, R. Stevenson, T. D. Utteridge, and B. A. Vassallo.** 2011. Prevalence of viral, bacterial and parasitological diseases in rats and mice used in research environments in Australasia over a 5-y period. Lab Anim (NY) **40:**341- 351.
4. **Ambrose, R. L., and J. M. Mackenzie.** 2011. West Nile Virus Differentially Modulates the Unfolded Protein Response To Facilitate Replication and Immune Evasion. The Journal of Virology **85:**2723-2732.
5. **Anderson, H. A., Y. Chen, and L. C. Norkin.** 1996. Bound simian virus 40 translocates to caveolin-enriched membrane domains, and its entry is inhibited by drugs that selectively disrupt caveolae. Mol Biol Cell **7:**1825-34.
6. **Arias, A., D. Bailey, Y. Chaudhry, and I. G. Goodfellow.** 2012. Development of a reverse genetics system for murine norovirus 3; long-term persistence occurs in the caecum and colon. Journal of General Virology **doi: 10.1099/vir.0.042176-0**
7. **Atmar, R. L., and M. K. Estes.** 2006. The epidemiologic and clinical importance of norovirus infection. Gastroenterol Clin North Am **35:**275-90, viii.
8. **Bae, J., and K. J. Schwab.** 2008. Evaluation of murine norovirus, feline calicivirus, poliovirus, and MS2 as surrogates for human norovirus in a model of viral persistence in surface water and groundwater. Appl Environ Microbiol **74:**477-84.
9. **Baer, G. S., and T. S. Dermody.** 1997. Mutations in reovirus outer-capsid protein sigma3 selected during persistent infections of L cells confer resistance to protease inhibitor E64. J Virol **71:**4921-8.
10. **Baines, J. D.** 2011. Herpes simplex virus capsid assembly and DNA packaging: a present and future antiviral drug target. Trends Microbiol **19:**606-613.
11. **Balakirev, M. Y., M. Jaquinod, A. L. Haas, and J. Chroboczek.** 2002. Deubiquitinating Function of Adenovirus Proteinase. J Virol **76:**6323-6331.
12. **Bank-Wolf, B. R., M. König, and H.-J. Thiel.** 2010. Zoonotic aspects of infections with noroviruses and sapoviruses. Vet Microbiol **140:**204-212.
13. **Barretto, N., D. Jukneliene, K. Ratia, Z. Chen, A. D. Mesecar, and S. C. Baker.** 2005. The Papain-Like Protease of Severe Acute Respiratory Syndrome Coronavirus Has Deubiquitinating Activity. J Virol **79:**15189-15198.
14. **Baud, V.** 2011. Control of NF-κB activity by proteolysis. Curr Top Microbiol Immunol **349:**97-114.

15. **Bauer, M., and L. Pelkmans.** 2006. A new paradigm for membrane-organizing and -shaping scaffolds. FEBS Lett **580:**5559-5564.
16. **Bertolotti, A., Y. Zhang, L. M. Hendershot, H. P. Harding, and D. Ron.** 2000. Dynamic interaction of BiP and ER stress transducers in the unfolded-protein response. Nat Cell Biol **2:**326-332.
17. **Bhattacharya, S., W.-C. HuangFu, J. Liu, S. Veeranki, D. P. Baker, C. Koumenis, J. A. Diehl, and S. Y. Fuchs.** 2010. Inducible Priming Phosphorylation Promotes Ligand-independent Degradation of the IFNAR1 Chain of Type I Interferon Receptor. Journal of Biological Chemistry **285:**2318-2325.
18. **Bickel, P. E., P. E. Scherer, J. E. Schnitzer, P. Oh, M. P. Lisanti, and H. F. Lodish.** 1997. Flotillin and Epidermal Surface Antigen Define a New Family of Caveolae-associated Integral Membrane Proteins. Journal of Biological Chemistry **272:**13793-13802.
19. **Blumenthal, R., A. Bali-Puri, A. Walter, D. Covell, and O. Eidelman.** 1987. pH-dependent fusion of vesicular stomatitis virus with Vero cells. Measurement by dequenching of octadecyl rhodamine fluorescence. J Biol Chem **262:**13614-9.
20. **Bok, K., G. I. Parra, T. Mitra, E. Abente, C. K. Shaver, D. Boon, R. Engle, C. Yu, A. Z. Kapikian, S. V. Sosnovtsev, R. H. Purcell, and K. Y. Green.** 2011. Chimpanzees as an animal model for human norovirus infection and vaccine development. Proceedings of the National Academy of Sciences **108:**325-330.
21. **Bok, K., V. G. Prikhodko, K. Y. Green, and S. V. Sosnovtsev.** 2009. Apoptosis in Murine Norovirus-Infected RAW264.7 Cells Is Associated with Downregulation of Survivin. J Virol **83:**3647-3656.
22. **Boname, J. M., and P. J. Lehner.** 2011. What Has the Study of the K3 and K5 Viral Ubiquitin E3 Ligases Taught Us about Ubiquitin-Mediated Receptor Regulation? Viruses **3:**118-31.
23. **Boname, J. M., and P. G. Stevenson.** 2001. MHC Class I Ubiquitination by a Viral PHD/LAP Finger Protein. Immunity **15:**627-636.
24. **Breuza, L., S. Corby, J.-P. Arsanto, M.-H. Delgrossi, P. Scheiffele, and A. Le Bivic.** 2002. The scaffolding domain of caveolin 2 is responsible for its Golgi localization in Caco-2 cells. J Cell Sci **115:**4457-4467.
25. **Bridger, J. C., G. A. Hall, and J. F. Brown.** 1984. Characterization of a calici-like virus (Newbury agent) found in association with astrovirus in bovine diarrhea. Infect Immun **43:**133-138.
26. **Brown, D. A., and E. London.** 1998. FUNCTIONS OF LIPID RAFTS IN BIOLOGICAL MEMBRANES. Annual Review of Cell and Developmental Biology **14:**111-136.
27. **Bruggink, L. D., and J. A. Marshall.** 2009. Norovirus epidemics are linked to two distinct sets of controlling factors. International Journal of Infectious Diseases **13:**e125-e126.
28. **Bubeck, D., D. J. Filman, N. Cheng, A. C. Steven, J. M. Hogle, and D. M. Belnap.** 2005. The Structure of the Poliovirus 135S Cell Entry Intermediate at 10-Angstrom Resolution Reveals the Location of an Externalized Polypeptide That Binds to Membranes. J Virol **79:**7745-7755.

29. **Bubeck, D., D. J. Filman, and J. M. Hogle.** 2005. Cryo-electron microscopy reconstruction of a poliovirus-receptor-membrane complex. Nat Struct Mol Biol **12:**615-618.
30. **Burkholder, K. M., J. W. Perry, C. E. Wobus, N. J. Donato, H. D. Showalter, V. Kapuria, and M. X. D. O'Riordan.** 2011. A Small Molecule Deubiquitinase Inhibitor Increases Localization of Inducible Nitric Oxide Synthase to the Macrophage Phagosome and Enhances Bacterial Killing. Infect Immun **79:**4850-4857.
31. **Burnett, H., T. Audas, G. Liang, and R. Lu.** 2012. Herpes simplex virus-1 disarms the unfolded protein response in the early stages of infection. Cell Stress and Chaperones **DOI: 10.1007/s12192-012-0324-8**.
32. **Burroughs, J. N., and F. Brown.** 1978. Presence of a Covalently Linked Protein on Calicivirus RNA. Journal of General Virology **41:**443-446.
33. **Calfon, M., H. Zeng, F. Urano, J. H. Till, S. R. Hubbard, H. P. Harding, S. G. Clark, and D. Ron.** 2002. IRE1 couples endoplasmic reticulum load to secretory capacity by processing the XBP-1 mRNA. Nature **415:**92-96.
34. **Callahan, M. K., P. M. Popernack, S. Tsutsui, L. Truong, R. A. Schlegel, and A. J. Henderson.** 2003. Phosphatidylserine on HIV Envelope Is a Cofactor for Infection of Monocytic Cells. The Journal of Immunology **170:**4840-4845.
35. **Cannon, J. L., E. Papafragkou, G. W. Park, J. Osborne, L. A. Jaykus, and J. Vinje.** 2006. Surrogates for the study of norovirus stability and inactivation in the environment: aA comparison of murine norovirus and feline calicivirus. J Food Prot **69:**2761-5.
36. **Cao, H., F. Garcia, and M. A. McNiven.** 1998. Differential distribution of dynamin isoforms in mammalian cells. Mol Biol Cell **9:**2595-2609.
37. **Capizzi, T., G. Makari-Judson, R. Steingart, and W. Mertens.** 2011. Chronic diarrhea associated with persistent norovirus excretion in patients with chronic lymphocytic leukemia: report of two cases. BMC Infect Dis **11:**131.
38. **Caplan, S., N. Naslavsky, L. M. Hartnell, R. Lodge, R. S. Polishchuk, J. G. Donaldson, and J. S. Bonifacino.** 2002. A tubular EHD1-containing compartment involved in the recycling of major histocompatibility complex class I molecules to the plasma membrane. Embo J **21:**2557-2567.
39. **Castellano, F., C. L. Clainche, D. Patin, M.-F. Carlier, and P. Chavrier.** 2001. A WASp-VASP complex regulates actin polymerization at the plasma membrane. Embo J **20:**5603-5614.
40. **Castellano, F., P. Montcourrier, and P. Chavrier.** 2000. Membrane recruitment of Rac1 triggers phagocytosis. J Cell Sci **113:**2955-2961.
41. **Chachu, K. A., D. W. Strong, A. D. LoBue, C. E. Wobus, R. S. Baric, and H. W. Virgin IV.** 2008. Antibody is critical for the clearance of murine norovirus infection. J Virol **82:**6610-7.
42. **Chandran, K., D. L. Farsetta, and M. L. Nibert.** 2002. Strategy for Nonenveloped Virus Entry: a Hydrophobic Conformer of the Reovirus Membrane Penetration Protein μ1 Mediates Membrane Disruption. J Virol **76:**9920-9933.
43. **Chang, K. O., and D. W. George.** 2007. Interferons and ribavirin effectively inhibit Norwalk virus replication in replicon-bearing cells. J Virol **81:**12111-8.

44. **Chang, K. O., S. V. Sosnovtsev, G. Belliot, A. D. King, and K. Y. Green.** 2006. Stable expression of a Norwalk virus RNA replicon in a human hepatoma cell line. Virology **353:**463-73.
45. **Chaudhry, Y., A. Nayak, M.-E. Bordeleau, J. Tanaka, J. Pelletier, G. J. Belsham, L. O. Roberts, and I. G. Goodfellow.** 2006. Caliciviruses Differ in Their Functional Requirements for eIF4F Components. Journal of Biological Chemistry **281:**25315-25325.
46. **Chaudhry, Y., M. A. Skinner, and I. G. Goodfellow.** 2007. Recovery of genetically defined murine norovirus in tissue culture by using a fowlpox virus expressing T7 RNA polymerase. J Gen Virol **88:**2091-100.
47. **Cheetham, S., M. Souza, T. Meulia, S. Grimes, M. G. Han, and L. J. Saif.** 2006. Pathogenesis of a genogroup II human norovirus in gnotobiotic pigs. J Virol **80:**10372-81.
48. **Chen, X.** 2009. Thiopurine analogue inhibitors of severe acute respiratory syndrome-coronavirus papain-like protease, a deubiquitinating and deISGylating enzyme. Antiviral chemistry & chemotherapy **19:**151-6.
49. **Chen, Z., Y. Wang, K. Ratia, A. D. Mesecar, K. D. Wilkinson, and S. C. Baker.** 2007. Proteolytic Processing and Deubiquitinating Activity of Papain-Like Proteases of Human Coronavirus NL63. J Virol **81:**6007-6018.
50. **Cheng, G., Z. Feng, and B. He.** 2005. Herpes Simplex Virus 1 Infection Activates the Endoplasmic Reticulum Resident Kinase PERK and Mediates eIF-2α Dephosphorylation by the γ134.5 Protein. J Virol **79:**1379-1388.
51. **Cheng, Z. J., R. D. Singh, D. L. Marks, and R. E. Pagano.** 2006. Membrane microdomains, caveolae, and caveolar endocytosis of sphingolipids. Mol Membr Biol **23:**101-10.
52. **Choi, J. M., A. M. Hutson, M. K. Estes, and B. V. Prasad.** 2008. Atomic resolution structural characterization of recognition of histo-blood group antigens by Norwalk virus. Proc Natl Acad Sci U S A **105:**9175-80.
53. **Clayson, E. T., L. V. Brando, and R. W. Compans.** 1989. Release of simian virus 40 virions from epithelial cells is polarized and occurs without cell lysis. J Virol **63:**2278-2288.
54. **Coburn, B., B. Wagner, and S. Blower.** 2009. Modeling influenza epidemics and pandemics: insights into the future of swine flu (H1N1). BMC Medicine **7:**30.
55. **Cooke, B. D.** 2002. Rabbit haemorrhagic disease: field epidemiology and the management of wild rabbit populations. International Office of Epizootics **21:**347-58.
56. **Damke, H., T. Baba, D. E. Warnock, and S. L. Schmid.** 1994. Induction of mutant dynamin specifically blocks endocytic coated vesicle formation. J Cell Biol **127:**915-34.
57. **Damm, E. M., L. Pelkmans, J. Kartenbeck, A. Mezzacasa, T. Kurzchalia, and A. Helenius.** 2005. Clathrin- and caveolin-1-independent endocytosis: entry of simian virus 40 into cells devoid of caveolae. J Cell Biol **168:**477-88.
58. **Dastjerdi, A. M., D. R. Snodgrass, and J. C. Bridger.** 2000. Characterisation of the bovine enteric calici-like virus, Newbury agent 1. FEMS Microbiology Letters **192:**125-131.

59. **Daughenbaugh, K. F., C. S. Fraser, J. W. Hershey, and M. E. Hardy.** 2003. The genome-linked protein VPg of the Norwalk virus binds eIF3, suggesting its role in translation initiation complex recruitment. EMBO J **22:**2852-9.
60. **Daughenbaugh, K. F., C. E. Wobus, and M. E. Hardy.** 2006. VPg of murine norovirus binds translation initiation factors in infected cells. Virol J **3:**33.
61. **de Sena, J., and B. Mandel.** 1977. Studies on the in vitro uncoating of poliovirus II. Characteristics of the membrane-modified particle. Virology **78:**554-566.
62. **De Sena, J., and B. Mandel.** 1976. Studies on the in vitro uncoating of poliovirus: I. Characterization of the modifying factor and the modifying reaction. Virology **70:**470-483.
63. **de Wit, M. A., M. A. Widdowson, H. Vennema, E. de Bruin, T. Fernandes, and M. Koopmans.** 2007. Large outbreak of norovirus: the baker who should have known better. J Infect **55:**188-93.
64. **Deshaies, R. J., and C. A. P. Joazeiro.** 2009. RING Domain E3 Ubiquitin Ligases. Annu Rev Biochem **78:**399-434.
65. **Di Fiore, P. P., S. Polo, and K. Hofmann.** 2003. When ubiquitin meets ubiquitin receptors: a signalling connection. Nat Rev Mol Cell Biol **4:**491-497.
66. **Di Martino, B., C. Di Rocco, C. Ceci, and F. Marsilio.** 2009. Characterization of a strain of feline calicivirus isolated from a dog faecal sample. Vet Microbiol **139:**52-57.
67. **Dietz, V. J.** 1994. Potential impact on vaccination coverage levels by administering vaccines simultaneously and reducing dropout rates. Archives of pediatrics & adolescent medicine **148:**943-9.
68. **Dikic, I., S. Wakatsuki, and K. J. Walters.** 2009. Ubiquitin-binding domains [mdash] from structures to functions. Nat Rev Mol Cell Biol **10:**659-671.
69. **Doherty, G. J., and H. T. McMahon.** 2009. Mechanisms of endocytosis. Annu Rev Biochem **78:**857-902.
70. **Doxsey, S. J., F. M. Brodsky, G. S. Blank, and A. Helenius.** 1987. Inhibition of endocytosis by anti-clathrin antibodies. Cell **50:**453-463.
71. **Duizer, E., K. J. Schwab, F. H. Neill, R. L. Atmar, M. P. Koopmans, and M. K. Estes.** 2004. Laboratory efforts to cultivate noroviruses. J Gen Virol **85:**79-87.
72. **Dul, B. E., and N. C. Walworth.** 2007. The Plant Homeodomain Fingers of Fission Yeast Msc1 Exhibit E3 Ubiquitin Ligase Activity. Journal of Biological Chemistry **282:**18397-18406.
73. **Ebert, D. H., J. Deussing, C. Peters, and T. S. Dermody.** 2002. Cathepsin L and Cathepsin B Mediate Reovirus Disassembly in Murine Fibroblast Cells. Journal of Biological Chemistry **277:**24609-24617.
74. **Ehrlich, M., W. Boll, A. van Oijen, R. Hariharan, K. Chandran, M. L. Nibert, and T. Kirchhausen.** 2004. Endocytosis by Random Initiation and Stabilization of Clathrin-Coated Pits. Cell **118:**591-605.
75. **Ehses, S., I. Raschke, G. Mancuso, A. Bernacchia, S. Geimer, D. Tondera, J.-C. Martinou, B. Westermann, E. I. Rugarli, and T. Langer.** 2009. Regulation of OPA1 processing and mitochondrial fusion by m-AAA protease isoenzymes and OMA1. J Cell Biol **187:**1023-1036.

76. **Engel, S., T. Heger, R. Mancini, F. Herzog, J. Kartenbeck, A. Hayer, and A. Helenius.** 2011. Role of Endosomes in Simian Virus 40 Entry and Infection. J Virol **85:**4198-4211.
77. **Estrabaud, E., S. De Muynck, and T. Asselah.** 2011. Activation of unfolded protein response and autophagy during HCV infection modulates innate immune response. Journal of Hepatology **55:**1150-1153.
78. **Farkas, T., R. W. Cross, E. Hargitt, N. W. Lerche, A. L. Morrow, and K. Sestak.** 2010. Genetic Diversity and Histo-Blood Group Antigen Interactions of Rhesus Enteric Caliciviruses. J Virol **84:**8617-8625.
79. **Farkas, T., K. Sestak, C. Wei, and X. Jiang.** 2008. Characterization of a rhesus monkey calicivirus representing a new genus of Caliciviridae. J Virol **82:**5408-16.
80. **Farkas, T., W. M. Zhong, Y. Jing, P. W. Huang, S. M. Espinosa, N. Martinez, A. L. Morrow, G. M. Ruiz-Palacios, L. K. Pickering, and X. Jiang.** 2004. Genetic diversity among sapoviruses. Arch Virol **149:**1309-1323.
81. **Fielding, P. E., and C. J. Fielding.** 1995. Plasma membrane caveolae mediate the efflux of cellular free cholesterol. Biochemistry **34:**14288-14292.
82. **Fitzgerald, D. J. P., R. Padmanabhan, I. Pastan, and M. C. Willingham.** 1983. Adenovirus-induced release of epidermal growth factor and pseudomonas toxin into the cytosol of KB cells during receptor-mediated endocytosis. Cell **32:**607-617.
83. **Forrester, N. L., M. I. Abubakr, E. M. E. Abu Elzein, A. I. al-Afaleq, F. M. T. Housawi, S. R. Moss, S. L. Turner, and E. A. Gould.** 2006. Phylogenetic analysis of Rabbit haemorrhagic disease virus strains from the Arabian Peninsula: Did RHDV emerge simultaneously in Europe and Asia? Virology **344:**277-282.
84. **Fra, A. M., E. Williamson, K. Simons, and R. G. Parton.** 1994. Detergent-insoluble glycolipid microdomains in lymphocytes in the absence of caveolae. Journal of Biological Chemistry **269:**30745-8.
85. **Fricks, C. E., and J. M. Hogle.** 1990. Cell-induced conformational change in poliovirus: externalization of the amino terminus of VP1 is responsible for liposome binding. J Virol **64:**1934-1945.
86. **Gack, M. U., R. A. Albrecht, T. Urano, K.-S. Inn, I. C. Huang, E. Carnero, M. Farzan, S. Inoue, J. U. Jung, and A. García-Sastre.** 2009. Influenza A Virus NS1 Targets the Ubiquitin Ligase TRIM25 to Evade Recognition by the Host Viral RNA Sensor RIG-I. Cell Host & Microbe **5:**439-449.
87. **Gack, M. U., Y. C. Shin, C.-H. Joo, T. Urano, C. Liang, L. Sun, O. Takeuchi, S. Akira, Z. Chen, S. Inoue, and J. U. Jung.** 2007. TRIM25 RING-finger E3 ubiquitin ligase is essential for RIG-I-mediated antiviral activity. Nature **446:**916-920.
88. **Gagnon, E., S. Duclos, C. Rondeau, E. Chevet, P. H. Cameron, O. Steele-Mortimer, J. Paiement, J. J. M. Bergeron, and M. Desjardins.** 2002. Endoplasmic Reticulum-Mediated Phagocytosis Is a Mechanism of Entry into Macrophages. Cell **110:**119-131.
89. **Gallimore, C. I., D. Lewis, C. Taylor, A. Cant, A. Gennery, and J. J. Gray.** 2004. Chronic excretion of a norovirus in a child with cartilage hair hypoplasia (CHH). J Clin Virol **30:**196-204.

90. **García-Expósito, L., J. Barroso-González, I. Puigdomènech, J.-D. Machado, J. Blanco, and A. Valenzuela-Fernández.** 2011. HIV-1 requires Arf6-mediated membrane dynamics to efficiently enter and infect T lymphocytes. Mol Biol Cell **22:**1148-1166.
91. **Gardet, A., M. Breton, G. Trugnan, and S. Chwetzoff.** 2007. Role for Actin in the Polarized Release of Rotavirus. J Virol **81:**4892-4894.
92. **Gass, J. N., K. E. Gunn, R. Sriburi, and J. W. Brewer.** 2004. Stressed-out B cells? Plasma-cell differentiation and the unfolded protein response. Trends in Immunology **25:**17-24.
93. **Gerondopoulos, A., T. Jackson, P. Monaghan, N. Doyle, and L. O. Roberts.** 2010. Murine norovirus-1 cell entry is mediated through a non-clathrin-, non-caveolae-, dynamin- and cholesterol-dependent pathway. J Gen Virol **91:**1428-38.
94. **Ghigo, E., J. Kartenbeck, P. Lien, L. Pelkmans, C. Capo, J. L. Mege, and D. Raoult.** 2008. Ameobal pathogen mimivirus infects macrophages through phagocytosis. PLoS Pathog **4:**e1000087.
95. **Ghosh, A. K., J. Takayama, K. V. Rao, K. Ratia, R. Chaudhuri, D. C. Mulhearn, H. Lee, D. B. Nichols, S. Baliji, S. C. Baker, M. E. Johnson, and A. D. Mesecar.** 2010. Severe Acute Respiratory Syndrome Coronavirus Papain-like Novel Protease Inhibitors: Design, Synthesis, Protein−Ligand X-ray Structure and Biological Evaluation. J Med Chem **53:**4968-4979.
96. **Girard, M., S. Ngazoa, K. Mattison, and J. Jean.** 2010. Attachment of Noroviruses to Stainless Steel and Their Inactivation, Using Household Disinfectants. Journal of Food Protection **73:**400-404.
97. **Glebov, O. O., N. A. Bright, and B. J. Nichols.** 2006. Flotillin-1 defines a clathrin-independent endocytic pathway in mammalian cells. Nat Cell Biol **8:**46-54.
98. **Gold, E. S., D. M. Underhill, N. S. Morrissette, J. Guo, M. A. McNiven, and A. Aderem.** 1999. Dynamin 2 Is Required for Phagocytosis in Macrophages. The Journal of Experimental Medicine **190:**1849-1856.
99. **Goodfellow, I., Y. Chaudhry, I. Gioldasi, A. Gerondopoulos, A. Natoni, L. Labrie, J. F. Laliberte, and L. Roberts.** 2005. Calicivirus translation initiation requires an interaction between VPg and eIF 4 E. EMBO Rep **6:**968-72.
100. **Graff, J. W., K. Ettayebi, and M. E. Hardy.** 2009. Rotavirus NSP1 Inhibits NFκB Activation by Inducing Proteasome-Dependent Degradation of β-TrCP: A Novel Mechanism of IFN Antagonism. PLoS Pathog **5:**e1000280.
101. **Grassart, A., A. Dujeancourt, P. B. Lazarow, A. Dautry-Varsat, and N. Sauvonnet.** 2008. Clathrin-independent endocytosis used by the IL-2 receptor is regulated by Rac1, Pak1, and Pak2. EMBO reports **9:**356-362.
102. **Gray, J. J., E. Kohli, F. M. Ruggeri, H. Vennema, A. Sánchez-Fauquier, E. Schreier, C. I. Gallimore, M. Iturriza-Gomara, H. Giraudon, P. Pothier, I. Di Bartolo, N. Inglese, E. de Bruin, B. van der Veer, S. Moreno, V. Montero, M. C. de Llano, M. Höhne, and S. M. Diedrich.** 2007. European Multicenter Evaluation of Commercial Enzyme Immunoassays for Detecting Norovirus Antigen in Fecal Samples. Clinical and Vaccine Immunology **14:**1349-1355.
103. **Greber, U. F.** 2002. Signalling in viral entry. Cellular and Molecular Life Sciences **59:**608-626.

104. **Green, K. Y.** 2007. Caliciviridae, p. 949-980. *In* P. M. H. D. M. Knipe (ed.), Fields Virology, 5 ed, vol. 1. Lippincott Williams & Wilkins, Philadelphia.
105. **Green, K. Y., T. Ando, M. S. Balayan, T. Berke, I. N. Clarke, M. K. Estes, D. O. Matson, S. Nakata, J. D. Neill, M. J. Studdert, and H.-J. Thiel.** 2000. Taxonomy of the Caliciviruses. Journal of Infectious Diseases **181:**S322-S330.
106. **Greenberg, S.** 1999. Modular components of phagocytosis. Journal of Leukocyte Biology **66:**712-7.
107. **Griffin, E. E., S. A. Detmer, and D. C. Chan.** 2006. Molecular mechanism of mitochondrial membrane fusion. Biochimica et Biophysica Acta (BBA) - Molecular Cell Research **1763:**482-489.
108. **Guo, C. T., O. Nakagomi, M. Mochizuki, H. Ishida, M. Kiso, Y. Ohta, T. Suzuki, D. Miyamoto, K. I. Hidari, and Y. Suzuki.** 1999. Ganglioside GM(1a) on the cell surface is involved in the infection by human rotavirus KUN and MO strains. J Biochem (Tokyo) **126:**683-8.
109. **Guo, M., K. O. Chang, M. E. Hardy, Q. Zhang, A. V. Parwani, and L. J. Saif.** 1999. Molecular Characterization of a Porcine Enteric Calicivirus Genetically Related to Sapporo-Like Human Caliciviruses. J Virol **73:**9625-9631.
110. **Hagglund, R., and B. Roizman.** 2002. Characterization of the novel E3 ubiquitin ligase encoded in exon 3 of herpes simplex virus-1-infected cell protein 0. Proceedings of the National Academy of Sciences **99:**7889-7894.
111. **Hagglund, R., and B. Roizman.** 2003. Herpes Simplex Virus 1 Mutant in Which the ICP0 HUL-1 E3 Ubiquitin Ligase Site Is Disrupted Stabilizes cdc34 but Degrades D-Type Cyclins and Exhibits Diminished Neurotoxicity. J Virol **77:**13194-13202.
112. **Hagglund, R., and B. Roizman.** 2004. Role of ICP0 in the Strategy of Conquest of the Host Cell by Herpes Simplex Virus 1. J Virol **78:**2169-2178.
113. **Hagglund, R., C. Van Sant, P. Lopez, and B. Roizman.** 2002. Herpes simplex virus 1-infected cell protein 0 contains two E3 ubiquitin ligase sites specific for different E2 ubiquitin-conjugating enzymes. Proceedings of the National Academy of Sciences **99:**631-636.
114. **Haglund, K., P. P. Di Fiore, and I. Dikic.** 2003. Distinct monoubiquitin signals in receptor endocytosis. Trends Biochem Sci **28:**598-604.
115. **Haigler, H. T., J. A. McKanna, and S. Cohen.** 1979. Direct visualization of the binding and internalization of a ferritin conjugate of epidermal growth factor in human carcinoma cells A-431. J Cell Biol **81:**382-395.
116. **Hall, G. A., J. C. Bridger, B. E. Brooker, K. R. Parsons, and E. Ormerod.** 1984. Lesions of Gnotobiotic Calves Experimentally Infected with a Calicivirus-like (Newbury) Agent. Veterinary Pathology Online **21:**208-215.
117. **Hamanaka, R. B., B. S. Bennett, S. B. Cullinan, and J. A. Diehl.** 2005. PERK and GCN2 Contribute to eIF2α Phosphorylation and Cell Cycle Arrest after Activation of the Unfolded Protein Response Pathway. Mol Biol Cell **16:**5493-5501.
118. **Hanover, J. A.** 1985. Transit of receptors for epidermal growth factor and transferrin through clathrin-coated pits. Analysis of the kinetics of receptor entry. J Biol Chem **260:**15938-45.

119. **Hansman, G. S., X. J. Jiang, and K. Y. Green.** 2010. Caliciviruses: Molecular and Cellular Virology, p. 248. Caister Academic Press, Norfolk, UK.
120. **Hardy, M. E., T. J. Crone, J. E. Brower, and K. Ettayebi.** 2002. Substrate specificity of the Norwalk virus 3C-like proteinase. Virus Res **89:**29-39.
121. **Harhaj, E. W., and V. M. Dixit.** 2011. Deubiquitinases in the regulation of NF-[kappa]B signaling. Cell Res **21:**22-39.
122. **Hase, K., K. Kawano, T. Nochi, G. S. Pontes, S. Fukuda, M. Ebisawa, K. Kadokura, T. Tobe, Y. Fujimura, S. Kawano, A. Yabashi, S. Waguri, G. Nakato, S. Kimura, T. Murakami, M. Iimura, K. Hamura, S. I. Fukuoka, A. W. Lowe, K. Itoh, H. Kiyono, and H. Ohno.** 2009. Uptake through glycoprotein 2 of FimH+ bacteria by M cells initiates mucosal immune response. Nature **462:**226-230.
123. **Hassan, I. H., M. S. Zhang, L. S. Powers, J. Q. Shao, J. Baltrusaitis, D. T. Rutkowski, K. Legge, and M. M. Monick.** 2012. Influenza A Viral Replication Is Blocked by Inhibition of the Inositol-requiring Enzyme 1 (IRE1) Stress Pathway. Journal of Biological Chemistry **287:**4679-4689.
124. **Head, B. P., and P. A. Insel.** 2007. Do caveolins regulate cells by actions outside of caveolae? Trends Cell Biol **17:**51-57.
125. **Heijne, J. C. M., P. Teunis, G. Morroy, C. Wijkmans, S. Oostveen, E. Duizer, M. Kretzschmar, and J. Wallinga.** 2009. Enhanced hygiene measures and norovirus transmission during an outbreak. Emerg Infect Dis **DOI: 10.3201/eid1501.080299**.
126. **Heikkilä, O., P. Susi, T. Tevaluoto, H. Härmä, V. Marjomäki, T. Hyypiä, and S. Kiljunen.** 2010. Internalization of Coxsackievirus A9 Is Mediated by β2-Microglobulin, Dynamin, and Arf6 but Not by Caveolin-1 or Clathrin. J Virol **84:**3666-3681.
127. **Helenius, A.** 2007. Virus entry and uncoating, p. 99-118. *In* D. M. Knipe, Howley, P. M. (ed.), Fields Virology, 5 ed, vol. 1. Wolters Kluwer, Philadelphia.
128. **Henley, J. R., E. W. A. Krueger, B. J. Oswald, and M. A. McNiven.** 1998. Dynamin-mediated Internalization of Caveolae. J. Cell Biol. **141:**85-99.
129. **Herbert, T. P., I. Brierley, and T. D. Brown.** 1997. Identification of a protein linked to the genomic and subgenomic mRNAs of feline calicivirus and its role in translation. Journal of General Virology **78:**1033-40.
130. **Hernaez, B., and C. Alonso.** 2010. Dynamin- and Clathrin-Dependent Endocytosis in African Swine Fever Virus Entry. J Virol **84:**2100-2109.
131. **Hicke, L.** 2001. Protein regulation by monoubiquitin. Nat Rev Mol Cell Biol **2:**195-201.
132. **Hogle, J. M.** 2002. POLIOVIRUS CELL ENTRY: Common Structural Themes in Viral Cell Entry Pathways. Annual Review of Microbiology **56:**677-702.
133. **Hoppins, S., L. Lackner, and J. Nunnari.** 2007. The Machines that Divide and Fuse Mitochondria. Annu Rev Biochem **76:**751-780.
134. **Hsu, C. C., L. K. Riley, and R. S. Livingston.** 2007. Molecular characterization of three novel murine noroviruses. Virus Genes **34:**147-55.
135. **Hsu, C. C., L. K. Riley, H. M. Wills, and R. S. Livingston.** 2006. Persistent infection with and serologic cross-reactivity of three novel murine noroviruses. Comp Med **56:**247-51.

136. **Hsu, C. C., C. E. Wobus, E. K. Steffen, L. K. Riley, and R. S. Livingston.** 2005. Development of a microsphere-based serologic multiplexed fluorescent immunoassay and a reverse transcriptase PCR assay to detect murine norovirus 1 infection in mice. Clin Diagn Lab Immunol **12:**1145-51.
137. **Hu, J., Y. Shibata, P.-P. Zhu, C. Voss, N. Rismanchi, W. A. Prinz, T. A. Rapoport, and C. Blackstone.** 2009. A Class of Dynamin-like GTPases Involved in the Generation of the Tubular ER Network. Cell **138:**549-561.
138. **Huang, F., A. Khvorova, W. Marshall, and A. Sorkin.** 2004. Analysis of Clathrin-mediated Endocytosis of Epidermal Growth Factor Receptor by RNA Interference. Journal of Biological Chemistry **279:**16657-16661.
139. **Huang, P., T. Farkas, W. Zhong, M. Tan, S. Thornton, A. L. Morrow, and X. Jiang.** 2005. Norovirus and histo-blood group antigens: demonstration of a wide spectrum of strain specificities and classification of two major binding groups among multiple binding patterns. J Virol **79:**6714-22.
140. **Huang, T. T., and A. D. D'Andrea.** 2006. Regulation of DNA repair by ubiquitylation. Nat Rev Mol Cell Biol **7:**323-334.
141. **Hurley, J. H., S. Lee, and G. Preg.** 2006. Ubiquitin-binding domains. Biochem. J. **399:**361-72.
142. **Hutson, A. M., R. L. Atmar, and M. K. Estes.** 2004. Norovirus disease: changing epidemiology and host susceptibility factors. Trends Microbiol **12:**279-87.
143. **Hutson, A. M., R. L. Atmar, D. M. Marcus, and M. K. Estes.** 2003. Norwalk virus-like particle hemagglutination by binding to h histo-blood group antigens. J Virol **77:**405-15.
144. **Hyde, J. L., S. V. Sosnovtsev, K. Y. Green, C. Wobus, H. W. Virgin, and J. M. Mackenzie.** 2009. Mouse Norovirus Replication Is Associated with Virus-Induced Vesicle Clusters Originating from Membranes Derived from the Secretory Pathway. The Journal of Virology **83:**9709-9719.
145. **Ike, A. C., B. N. Roth, R. Bohm, A. J. Pfitzner, and R. E. Marschang.** 2007. Identification of bovine enteric Caliciviruses (BEC) from cattle in Baden-Wurttemberg. Dtsch Tierarztl Wochenschr **114:**12-5.
146. **Inn, K.-S., S.-H. Lee, J. Y. Rathbun, L.-Y. Wong, Z. Toth, K. Machida, J.-H. J. Ou, and J. U. Jung.** 2011. Inhibition of RIG-I-Mediated Signaling by Kaposi's Sarcoma-Associated Herpesvirus-Encoded Deubiquitinase ORF64. J Virol **85:**10899-10904.
147. **Ivanov, A. V., H. Peng, V. Yurchenko, K. L. Yap, D. G. Negorev, D. C. Schultz, E. Psulkowski, W. J. Fredericks, D. E. White, G. G. Maul, M. J. Sadofsky, M.-M. Zhou, and F. J. Rauscher Iii.** 2007. PHD Domain-Mediated E3 Ligase Activity Directs Intramolecular Sumoylation of an Adjacent Bromodomain Required for Gene Silencing. Molecular Cell **28:**823-837.
148. **Jarosinski, K., L. Kattenhorn, B. Kaufer, H. Ploegh, and N. Osterrieder.** 2007. A Herpesvirus Ubiquitin-Specific Protease Is Critical for Efficient T Cell Lymphoma Formation. Proc Natl Acad Sci U S A **104:**20025-20030.
149. **Jiang, X., M. Wang, K. Wang, and M. K. Estes.** 1993. Sequence and genomic organization of Norwalk virus. Virology **195:**51-61.

150. **Jin, M., J. Park, S. Lee, B. Park, J. Shin, K.-J. Song, T.-I. Ahn, S.-Y. Hwang, B.-Y. Ahn, and K. Ahn.** 2002. Hantaan Virus Enters Cells by Clathrin-Dependent Receptor-Mediated Endocytosis. Virology **294:**60-69.
151. **Johannsdottir, H. K., R. Mancini, J. Kartenbeck, L. Amato, and A. Helenius.** 2009. Host Cell Factors and Functions Involved in Vesicular Stomatitis Virus Entry. J Virol **83:**440-453.
152. **Johnson, P. C., J. J. Mathewson, H. L. DuPont, and H. B. Greenberg.** 1990. Multiple-Challenge Study of Host Susceptibility to Norwalk Gastroenteritis in US Adults. Journal of Infectious Diseases **161:**18-21.
153. **Jourdan, N., M. Maurice, D. Delautier, A. M. Quero, A. L. Servin, and G. Trugnan.** 1997. Rotavirus is released from the apical surface of cultured human intestinal cells through nonconventional vesicular transport that bypasses the Golgi apparatus. J Virol **71:**8268-78.
154. **Kaiser, W. J., Y. Chaudhry, S. V. Sosnovtsev, and I. G. Goodfellow.** 2006. Analysis of protein–protein interactions in the feline calicivirus replication complex. Journal of General Virology **87:**363-368.
155. **Kapikian, A. Z., R. G. Wyatt, R. Dolin, T. S. Thornhill, A. R. Kalica, and R. M. Chanock.** 1972. Visualization by immune electron microscopy of a 27-nm particle associated with acute infectious nonbacterial gastroenteritis. J Virol **10:**1075-81.
156. **Karst, S. M.** 2010. Pathogenesis of Noroviruses, Emerging RNA Viruses. Viruses **2:**748-781.
157. **Karst, S. M., C. E. Wobus, M. Lay, J. Davidson, and H. W. Virgin IV.** 2003. STAT1-dependent innate immunity to a Norwalk-like virus. Science **299:**1575-8.
158. **Katayama, K., H. Shirato-Horikoshi, S. Kojima, T. Kageyama, T. Oka, F. Hoshino, S. Fukushi, M. Shinohara, K. Uchida, Y. Suzuki, T. Gojobori, and N. Takeda.** 2002. Phylogenetic analysis of the complete genome of 18 Norwalk-like viruses. Virology **299:**225-239.
159. **Ke, P.-Y., and S. S. L. Chen.** 2011. Activation of the unfolded protein response and autophagy after hepatitis C virus infection suppresses innate antiviral immunity in vitro. J Clin Invest **121:**37-56.
160. **Kerscher, O., R. Felberbaum, and M. Hochstrasser.** 2006. Modification of Proteins by Ubiquitin and Ubiquitin-Like Proteins. Annual Review of Cell and Developmental Biology **22:**159-180.
161. **Khamrin, P., T. A. Nguyen, T. G. Phan, K. Satou, Y. Masuoka, S. Okitsu, N. Maneekarn, O. Nishio, and H. Ushijima.** 2008. Evaluation of immunochromatography and commercial enzyme-linked immunosorbent assay for rapid detection of norovirus antigen in stool samples. J Virol Methods **147:**360-363.
162. **Kim, J. R., S. H. Seok, D. J. Kim, M.-W. Baek, Y.-R. Na, J.-H. Han, T.-H. Kim, J.-H. Park, P. V. Turner, D. H. Chung, and B.-C. Kang.** 2011. Prevalence of Murine Norovirus Infection in Korean Laboratory Animal Facilities. The Journal of Veterinary Medical Science **73:**687-691.
163. **Kirchhausen, T.** 2000. CLATHRIN. Annu Rev Biochem **69:**699-727.
164. **Kirkegaard, K.** 2009. Subversion of the cellular autophagy pathway by viruses. Curr Top Microbiol Immunol **335:**323-33.

165. **Kirkham, M., A. Fujita, R. Chadda, S. J. Nixon, T. V. Kurzchalia, D. K. Sharma, R. E. Pagano, J. F. Hancock, S. Mayor, and R. G. Parton.** 2005. Ultrastructural identification of uncoated caveolin-independent early endocytic vehicles. J Cell Biol **168:**465-476.
166. **Kitajima, M., T. Oka, Y. Tohya, H. Katayama, N. Takeda, and K. Katayama.** 2009. Development of a broadly reactive nested reverse transcription-PCR assay to detect murine noroviruses, and investigation of the prevalence of murine noroviruses in laboratory mice in Japan. Microbiology and Immunology **53:**531-534.
167. **Klug, A.** 1999. The tobacco mosaic virus particle: structure and assembly. Philosophical Transactions of the Royal Society of London. Series B: Biological Sciences **354:**531-535.
168. **Koegl, M., T. Hoppe, S. Schlenker, H. D. Ulrich, T. U. Mayer, and S. Jentsch.** 1999. A Novel Ubiquitination Factor, E4, Is Involved in Multiubiquitin Chain Assembly. Cell **96:**635-644.
169. **Kogasaka, R., Y. Sakuma, S. Chiba, M. Akihara, K. Horino, and T. Nakao.** 1980. Small round virus-like particles associated with acute gastroenteritis in japanese children. J Med Virol **5:**151-160.
170. **Komander, D.** 2010. Mechanism, Specificity and Structure of the Deubiquitinases Conjugation and Deconjugation of Ubiquitin Family Modifiers, p. 69-87. *In* M. Groettrup (ed.), vol. 54. Springer New York.
171. **Kurth, A., J. F. Evermann, D. E. Skilling, D. O. Matson, and A. W. Smith.** 2006. Prevalence of vesivirus in a laboratory-based set of serum samples obtained from dairy and beef cattle. American Journal of Veterinary Research **67:**114-119.
172. **Kuyumcu-Martinez, M., G. Belliot, S. V. Sosnovtsev, K.-O. Chang, K. Y. Green, and R. E. Lloyd.** 2004. Calicivirus 3C-Like Proteinase Inhibits Cellular Translation by Cleavage of Poly(A)-Binding Protein. J Virol **78:**8172-8182.
173. **Kwiatkowska, K., J. Frey, and A. Sobota.** 2003. Phosphorylation of FcγRIIA is required for the receptor-induced actin rearrangement and capping: the role of membrane rafts. J Cell Sci **116:**537-550.
174. **Lajoie, P., and I. R. Nabi.** 2007. Regulation of raft-dependent endocytosis. J. Cell. Mol. Med. **11:**644-53.
175. **Laliberte, J. P., L. W. McGinnes, M. E. Peeples, and T. G. Morrison.** 2006. Integrity of Membrane Lipid Rafts Is Necessary for the Ordered Assembly and Release of Infectious Newcastle Disease Virus Particles. J Virol **80:**10652-10662.
176. **Lamaze, C., A. Dujeancourt, T. Baba, C. G. Lo, A. Benmerah, and A. Dautry-Varsat.** 2001. Interleukin 2 receptors and detergent-resistant membrane domains define a clathrin-independent endocytic pathway. Mol Cell Biol **7:**661-671.
177. **Lay, M. K., R. L. Atmar, S. Guix, U. Bharadwaj, H. He, F. H. Neill, K. J. Sastry, Q. Yao, and M. K. Estes.** 2010. Norwalk virus does not replicate in human macrophages or dendritic cells derived from the peripheral blood of susceptible humans. Virology **406:**1-11.
178. **Le Gall-Reculé, G., F. Zwingelstein, M.-P. Fages, S. Bertagnoli, J. Gelfi, J. Aubineau, A. Roobrouck, G. Botti, A. Lavazza, and S. Marchandeau.** 2011.

Characterisation of a non-pathogenic and non-protective infectious rabbit lagovirus related to RHDV. Virology **410:**395-402.

179. **Lencioni, K. C., A. Seamons, P. M. Treuting, L. Maggio-Price, and T. Brabb.** 2008. Murine norovirus: an intercurrent variable in a mouse model of bacteria-induced inflammatory bowel disease. Comp Med **58:**522-33.
180. **Leverrier, Y., K. Okkenhaug, C. Sawyer, A. Bilancio, B. Vanhaesebroeck, and A. J. Ridley.** 2003. Class I Phosphoinositide 3-Kinase p110β Is Required for Apoptotic Cell and Fcγ Receptor-mediated Phagocytosis by Macrophages. Journal of Biological Chemistry **278:**38437-38442.
181. **Li, B., B. Gao, L. Ye, X. Han, W. Wang, L. Kong, X. Fang, Y. Zeng, H. Zheng, S. Li, Z. Wu, and L. Ye.** 2007. Hepatitis B virus X protein (HBx) activates ATF6 and IRE1-XBP1 pathways of unfolded protein response. Virus Res **124:**44-49.
182. **Li, S., J. Couet, and M. P. Lisanti.** 1996. Src Tyrosine Kinases, Gα Subunits, and H-Ras Share a Common Membrane-anchored Scaffolding Protein, Caveolin. Journal of Biological Chemistry **271:**29182-29190.
183. **Li, S., L. Ye, X. Yu, B. Xu, K. Li, X. Zhu, H. Liu, X. Wu, and L. Kong.** 2009. Hepatitis C virus NS4B induces unfolded protein response and endoplasmic reticulum overload response-dependent NF-[kappa]B activation. Virology **391:**257-264.
184. **Liao, T.-L., C.-Y. Wu, W.-C. Su, K.-S. Jeng, and M. M. C. Lai.** 2010. Ubiquitination and deubiquitination of NP protein regulates influenza A virus RNA replication. Embo J **29:**3879-3890.
185. **Lim, K.-L., and G. G. Y. Lim.** 2011. K63-linked ubiquitination and neurodegeneration. Neurobiology of Disease **43:**9-16.
186. **Lindesmith, L., C. Moe, S. Marionneau, N. Ruvoen, X. Jiang, L. Lindblad, P. Stewart, J. LePendu, and R. Baric.** 2003. Human susceptibility and resistance to Norwalk virus infection. Nat Med **9:**548-53.
187. **Lindner, H. A., N. Fotouhi-Ardakani, V. Lytvyn, P. Lachance, T. Sulea, and R. Ménard.** 2005. The Papain-Like Protease from the Severe Acute Respiratory Syndrome Coronavirus Is a Deubiquitinating Enzyme. J Virol **79:**15199-15208.
188. **Lipardi, C., R. Mora, V. Colomer, S. Paladino, L. Nitsch, E. Rodriguez-Boulan, and C. Zurzolo.** 1998. Caveolin Transfection Results in Caveolae Formation but Not Apical Sorting of Glycosylphosphatidylinositol (GPI)-anchored Proteins in Epithelial Cells. J Cell Biol **140:**617-626.
189. **Liu, J., W.-C. HuangFu, K. G. S. Kumar, J. Qian, J. P. Casey, R. B. Hamanaka, C. Grigoriadou, R. Aldabe, J. A. Diehl, and S. Y. Fuchs.** 2009. Virus-Induced Unfolded Protein Response Attenuates Antiviral Defenses via Phosphorylation-Dependent Degradation of the Type I Interferon Receptor. Cell Host & Microbe **5:**72-83.
190. **Liu, S. J., X. H.P., P. B.Q., and Q. N.H.** 1984. A new viral disease in rabbits. Anim Husb Vet Med **16:**253-5.
191. **Liu, Y.-W., M. C. Surka, T. Schroeter, V. Lukiyanchuk, and S. L. Schmid.** 2008. Isoform and Splice-Variant Specific Functions of Dynamin-2 Revealed by Analysis of Conditional Knock-Out Cells. Mol Biol Cell **19:**5347-5359.

192. **Lok, C. N.** 1998. Regulation of transferrin function and expression: review and update. Biological signals and receptors **7:**157-78.
193. **Love, D. N., and M. Sabine.** 1975. Electron microscopic observation of feline kidney cells infected with a feline calicivirus. Arch Virol **48:**213-228.
194. **Lundmark, R., G. J. Doherty, M. T. Howes, K. Cortese, Y. Vallis, R. G. Parton, and H. T. McMahon.** 2008. The GTPase-Activating Protein GRAF1 Regulates the CLIC/GEEC Endocytic Pathway. Current Biology **18:**1802-1808.
195. **Ma, Y., and L. M. Hendershot.** 2004. The role of the unfolded protein response in tumour development: friend or foe? Nat Rev Cancer **4:**966-977.
196. **Maelfait, J., and R. Beyaert.** 2012. Emerging Role of Ubiquitination in Antiviral RIG-I Signaling. Microbiology and Molecular Biology Reviews **76:**33-45.
197. **Makino, A., M. Shimojima, T. Miyazawa, K. Kato, Y. Tohya, and H. Akashi.** 2006. Junctional adhesion molecule 1 is a functional receptor for feline calicivirus. J Virol **80:**4482-90.
198. **Malhi, H., and R. J. Kaufman.** 2011. Endoplasmic reticulum stress in liver disease. Journal of Hepatology **54:**795-809.
199. **Malynn, B. A., and A. Ma.** 2010. Ubiquitin Makes Its Mark on Immune Regulation. Immunity **33:**843-852.
200. **Marín, I.** 2004. Parkin and relatives: the RBR family of ubiquitin ligases. Physiological genomics **17:**253-63.
201. **Marsh, M., and A. Helenius.** 2006. Virus entry: open sesame. Cell **124:**729-40.
202. **Marshall, J. A., and L. D. Bruggink.** 2011. The Dynamins of Norovirus Outbreak Epidemics: Recent Insights. Int. J. Environ. Res. Publich Health **8:**1141-49.
203. **Martella, V., Campolo, M., Lorusso, E., Cavicchio, P., Camero, M., Bellacicco, A. L., Decaro, N., Elia, G., Greco, G., Corrente, M., Desario, C., Arista S., Banyai, K., Koopmans, M., Buonavoglia, C.** 2007. Norovirus in captive lion (Panthera leo). Emerg Infect Dis **13:**1071-1073.
204. **Martella, V., E. Lorusso, N. Decaro, G. Elia, A. Radogna, M. D'Abramo, C. Desario, A. Cavalli, M. Corrente, M. Camero, C. A. Germinario, K. Banyai, B. Di Martino, F. Marsilio, L. E. Carmichael, and C. Buonavoglia.** 2008. Detection and molecular characterization of a canine norovirus. Emerg Infect Dis **14:**1306-8.
205. **Matsumiya, T.** 2010. Function and regulation of retinoic acid-inducible gene-I. Critical reviews in immunology **30:**489-513.
206. **Matsuura, Y., Y. Tohya, K. Nakamura, M. Shimojima, F. Roerink, M. Mochizuki, K. Takase, H. Akashi, and T. Sugimura.** 2002. Complete Nucleotide Sequence, Genome Organization and Phylogenic Analysis of the Canine Calicivirus. Virus Genes **25:**67-73.
207. **Mattison, K., A. Shukla, A. Cook, F. Pollari, R. Friendship, D. Kelton, S. Bidawid, and J. M. Farber.** 2007. Human noroviruses in swine and cattle. Emerg Infect Dis **13:**1184-8.
208. **Mauroy, A., A. Scipioni, E. Mathijs, C. Miry, D. Ziant, C. Thys, and E. Thiry.** 2008. Noroviruses and sapoviruses in pigs in Belgium. Arch Virol.
209. **Mayor, S., S. Sabharanjak, and F. R. Maxfield.** 1998. Cholesterol-dependent retention of GPI-anchored proteins in endosomes. Embo J **17:**4626-4638.

210. **McCartney, S. A., L. B. Thackray, L. Gitlin, S. Gilfillan, H. W. Virgin IV, and M. Colonna.** 2008. MDA-5 recognition of a murine norovirus. PLoS Pathog **4:**e1000108.
211. **McFadden, N., D. Bailey, G. Carrara, A. Benson, Y. Chaudhry, A. Shortland, J. Heeney, F. Yarovinsky, P. Simmonds, A. Macdonald, and I. Goodfellow.** 2011. Norovirus Regulation of the Innate Immune Response and Apoptosis Occurs via the Product of the Alternative Open Reading Frame 4. PLoS Pathog **7:**e1002413.
212. **McIntosh, M., S. Behan, F. Mohamed, Z. Lu, K. Moran, T. Burrage, J. Neilan, G. Ward, G. Botti, L. Capucci, and S. Metwally.** 2007. A pandemic strain of calicivirus threatens rabbit industries in the Americas. Virol J **4:**96.
213. **McPherson, S., E. E. Powell, H. D. Barrie, A. D. Clouston, M. McGuckin, and J. R. Jonsson.** 2011. No evidence of the unfolded protein response in patients with chronic hepatitis C virus infection. Journal of Gastroenterology and Hepatology **26:**319-327.
214. **Mead, P. S., L. Slutsker, V. Dietz, L. F. McCaig, J. S. Bresee, C. Shapiro, P. M. Griffin, and R. V. Tauxe.** 1999. Food-related illness and death in the United States. Emerg Infect Dis **5:**607-25.
215. **Mercer, J., and A. Helenius.** 2008. Vaccinia Virus Uses Macropinocytosis and Apoptotic Mimicry to Enter Host Cells. Science **320:**531-535.
216. **Mercer, J., and A. Helenius.** 2009. Virus entry by macropinocytosis. Nat Cell Biol **11:**510-520.
217. **Merrifield, C. J., D. Perrais, and D. Zenisek.** 2005. Coupling between Clathrin-Coated-Pit Invagination, Cortactin Recruitment, and Membrane Scission Observed in Live Cells. Cell **121:**593-606.
218. **Meylan, E., J. Curran, K. Hofmann, D. Moradpour, M. Binder, R. Bartenschlager, and J. Tschopp.** 2005. Cardif is an adaptor protein in the RIG-I antiviral pathway and is targeted by hepatitis C virus. Nature **437:**1167-1172.
219. **Miller, J., and C. Gordon.** 2005. The regulation of proteasome degradation by multi-ubiquitin chain binding proteins. FEBS Lett **579:**3224-3230.
220. **Miller, W. A., T. W. Dreher, and T. C. Hall.** 1985. Synthesis of brome mosaic virus subgenomic RNA in vitro by internal initiation on (-)-sense genomic RNA. Nature **313:**68-70.
221. **Morales, M., J. Bárcena, M. A. Ramírez, J. A. Boga, F. Parra, and J. M. Torres.** 2004. Synthesis in Vitro of Rabbit Hemorrhagic Disease Virus Subgenomic RNA by Internal Initiation on (–)Sense Genomic RNA. Journal of Biological Chemistry **279:**17013-17018.
222. **Moreno-Espinosa, S., T. Farkas, and X. Jiang.** 2004. Human caliciviruses and pediatric gastroenteritis. Semin Pediatr Infect Dis **15:**237-45.
223. **Morrow, I. C., S. Rea, S. Martin, I. A. Prior, R. Prohaska, J. F. Hancock, D. E. James, and R. G. Parton.** 2002. Flotillin-1/Reggie-2 Traffics to Surface Raft Domains via a Novel Golgi-independent Pathway. Journal of Biological Chemistry **277:**48834-48841.
224. **Mouchtouri, V. A.** 2010. State of the art: public health and passenger ships. Int Marit Health **61:**49-98.

225. **Mulherkar, N., M. Raaben, J. C. de la Torre, S. P. Whelan, and K. Chandran.** 2011. The Ebola virus glycoprotein mediates entry via a non-classical dynamin-dependent macropinocytic pathway. Virology **419:**72-83.
226. **Mulvey, M., C. Arias, and I. Mohr.** 2007. Maintenance of Endoplasmic Reticulum (ER) Homeostasis in Herpes Simplex Virus Type 1-Infected Cells through the Association of a Viral Glycoprotein with PERK, a Cellular ER Stress Sensor. J Virol **81:**3377-3390.
227. **Mumphrey, S. M., H. Changotra, T. N. Moore, E. R. Heimann-Nichols, C. E. Wobus, M. J. Reilly, M. Moghadamfalahi, D. Shukla, and S. M. Karst.** 2007. Murine norovirus 1 infection is associated with histopathological changes in immunocompetent hosts, but clinical disease is prevented by STAT1-dependent interferon responses. J Virol **81:**3251-63.
228. **Munro, S.** 2003. Lipid Rafts: Elusive or Illusive? Cell **115:**377-388.
229. **Murata, M., J. Peränen, R. Schreiner, F. Wieland, T. V. Kurzchalia, and K. Simons.** 1995. VIP21/caveolin is a cholesterol-binding protein. Proceedings of the National Academy of Sciences **92:**10339-10343.
230. **Murata, T., N. Katsushima, K. Mizuta, Y. Muraki, S. Hongo, and Y. Matsuzaki.** 2007. Prolonged norovirus shedding in infants <or=6 months of age with gastroenteritis. Pediatr Infect Dis J **26:**46-9.
231. **Nabi, I. R., and P. U. Le.** 2003. Caveolae/raft-dependent endocytosis. J Cell Biol **161:**673-677.
232. **Nagai, A., H. Kadowaki, T. Maruyama, K. Takeda, H. Nishitoh, and H. Ichijo.** 2009. USP14 inhibits ER-associated degradation via interaction with IRE1[alpha]. Biochem Biophys Res Commun **379:**995-1000.
233. **Nakanishi, A., T. Abe, M. Watanabe, K. Takei, and H. Yamada.** 2008. Dynamin 2 cooperates with amphiphysin 1 in phagocytosis in sertoli cells. Acta Med Okayama **62:**385-91.
234. **Nakatax, T., A. Iwamoto, Y. Noda, R. Takemura, H. Yoshikura, and N. Hirokawa.** 1991. Predominant and developmentally regulated expression of dynamin in neurons. Neuron **7:**461-469.
235. **Natoni, A., G. E. N. Kass, M. J. Carter, and L. O. Roberts.** 2006. The mitochondrial pathway of apoptosis is triggered during feline calicivirus infection. Journal of General Virology **87:**357-361.
236. **Neill, J. D., R. F. Meyer, and B. S. Seal.** 1995. Genetic relatedness of the caliciviruses: San Miguel sea lion and vesicular exanthema of swine viruses constitute a single genotype within the Caliciviridae. J Virol **69:**4484-4488.
237. **Nemerow, G. R.** 2000. Cell Receptors Involved in Adenovirus Entry. Virology **274:**1-4.
238. **Nichols, B.** 2003. Caveosomes and endocytosis of lipid rafts. J Cell Sci **116:**4707-4714.
239. **Niedergang, F., and P. Chavrier.** 2005. Regulation of phagocytosis by Rho GTPases. Curr Top Microbiol Immunol **291:**43-60.
240. **Nijman, S. M. B., M. P. A. Luna-Vargas, A. Velds, T. R. Brummelkamp, A. M. G. Dirac, T. K. Sixma, and R. Bernards.** 2005. A Genomic and Functional Inventory of Deubiquitinating Enzymes. Cell **123:**773-786.

241. **Nonnenmacher, M., and T. Weber.** 2011. Adeno-Associated Virus 2 Infection Requires Endocytosis through the CLIC/GEEC Pathway. Cell Host & Microbe **10:**563-576.
242. **Oliver, S. L., E. Asobayire, A. Charpilienne, J. Cohen, and J. C. Bridger.** 2007. Complete genomic characterization and antigenic relatedness of genogroup III, genotype 2 bovine noroviruses. Arch Virol **152:**257-72.
243. **Oliver, S. L., E. Asobayire, A. M. Dastjerdi, and J. C. Bridger.** 2006. Genomic characterization of the unclassified bovine enteric virus Newbury agent-1 (Newbury1) endorses a new genus in the family Caliciviridae. Virology **350:**240-50.
244. **Oliver, S. L., E. Wood, E. Asobayire, D. C. Wathes, J. S. Brickell, M. Elschner, P. Otto, P. R. Lambden, I. N. Clarke, and J. C. Bridger.** 2007. Serotype 1 and 2 bovine noroviruses are endemic in cattle in the United kingdom and Germany. J Clin Microbiol **45:**3050-2.
245. **Orso, G., D. Pendin, S. Liu, J. Tosetto, T. J. Moss, J. E. Faust, M. Micaroni, A. Egorova, A. Martinuzzi, J. A. McNew, and A. Daga.** 2009. Homotypic fusion of ER membranes requires the dynamin-like GTPase Atlastin. Nature **460:**978-983.
246. **Ostapchuk, P., M. Almond, and P. Hearing.** 2011. Characterization of Empty Adenovirus Particles Assembled in the Absence of a Functional Adenovirus IVa2 Protein. J Virol **85:**5524-5531.
247. **Ostapchuk, P., and P. Hearing.** 2003. Minimal cis-Acting Elements Required for Adenovirus Genome Packaging. J Virol **77:**5127-5135.
248. **Owen, D. J., and J. P. Luzio.** 2000. Structural insights into clathrin-mediated endocytosis. Curr Opin Cell Biol **12:**467-474.
249. **Pang, X. L., B. E. Lee, G. J. Tyrrell, and J. K. Preiksaitis.** 2009. Epidemiology and genotype analysis of sapovirus associated with gastroenteritis outbreaks in Alberta, Canada: 2004–2007. Journal of Infectious Diseases **199:**547-551.
250. **Parker, J. S. L., and C. R. Parrish.** 2000. Cellular Uptake and Infection by Canine Parvovirus Involves Rapid Dynamin-Regulated Clathrin-Mediated Endocytosis, Followed by Slower Intracellular Trafficking. J Virol **74:**1919-1930.
251. **Parolini, I., M. Sargiacomo, F. Galbiati, G. Rizzo, F. Grignani, J. A. Engelman, T. Okamoto, T. Ikezu, P. E. Scherer, R. Mora, E. Rodriguez-Boulan, C. Peschle, and M. P. Lisanti.** 1999. Expression of Caveolin-1 Is Required for the Transport of Caveolin-2 to the Plasma Membrane. Journal of Biological Chemistry **274:**25718-25725.
252. **Patel, K. P., C. B. Coyne, and J. M. Bergelson.** 2009. Dynamin- and Lipid Raft-Dependent Entry of Decay-Accelerating Factor (DAF)- Binding and Non-DAF-Binding Coxsackieviruses into Nonpolarized Cells. Journal of Virology **83:**11064-11077.
253. **Pelkmans, L., J. Kartenbeck, and A. Helenius.** 2001. Caveolar endocytosis of simian virus 40 reveals a new two-step vesicular-transport pathway to the ER. Nat Cell Biol **3:**473-83.
254. **Pelkmans, L., D. Püntener, and A. Helenius.** 2002. Local Actin Polymerization and Dynamin Recruitment in SV40-Induced Internalization of Caveolae. Science **296:**535-539.

255. **Perry, J. W., Taube, S., Wobus, C. E.** 2009. Murine Norovirus-1 entry into permissive macrophages and dendritic cells is pH-independent Virus Res **143:**125-129.
256. **Perry, J. W., and C. E. Wobus.** 2010. Endocytosis of Murine Norovirus 1 into Murine Macrophages Is Dependent on Dynamin II and Cholesterol. Journal of Virology **84:**6163 - 6176.
257. **Pesavento, P. A., N. J. Maclachlan, L. Dillard-Telm, C. K. Grant, and K. F. Hurley.** 2004. Pathologic, Immunohistochemical, and Electron Microscopic Findings in Naturally Occurring Virulent Systemic Feline Calicivirus Infection in Cats. Veterinary Pathology Online **41:**257-263.
258. **Pettersson, R. F., V. Ambros, and D. Baltimore.** 1978. Identification of a protein linked to nascent poliovirus RNA and to the polyuridylic acid of negative-strand RNA. J Virol **27:**357-365.
259. **Pickart, C. M.** 2001. Mechanisms Underlying Ubiquitination. Annu Rev Biochem **70:**503-533.
260. **Pietiäinen, V., V. Marjomäki, P. Upla, L. Pelkmans, A. Helenius, and T. Hyypiä.** 2004. Echovirus 1 Endocytosis into Caveosomes Requires Lipid Rafts, Dynamin II, and Signaling Events. Mol Biol Cell **15:**4911-4925.
261. **Pike, L. J.** 2006. Rafts defined: a report on the Keystone symposium on lipid rafts and cell function. Journal of Lipid Research **47:**1597-1598.
262. **Poschetto, L. F., A. Ike, T. Papp, U. Mohn, R. Böhm, and R. E. Marschang.** 2007. Comparison of the Sensitivities of Noroviruses and Feline Calicivirus to Chemical Disinfection under Field-Like Conditions. Appl Environ Microbiol **73:**5494-5500.
263. **Pucadyil, T. J., and S. L. Schmid.** 2008. Real-Time Visualization of Dynamin-Catalyzed Membrane Fission and Vesicle Release. Cell **135:**1263-1275.
264. **Puthenveedu, M. A., and M. von Zastrow.** 2006. Cargo Regulates Clathrin-Coated Pit Dynamics. Cell **127:**113-124.
265. **Puthenveedu, M. A., G. A. Yudowski, and M. von Zastrow.** 2007. Endocytosis of Neurotransmitter Receptors: Location Matters. Cell **130:**988-989.
266. **Radford, A. D.** 2002. Haemorrhagic fever, oedema and high mortality associated with FCV infection. Veterinary record **151:**155.
267. **Raghu, H., N. Sharma-Walia, M. V. Veettil, S. Sadagopan, and B. Chandran.** 2009. Kaposi's Sarcoma-Associated Herpesvirus Utilizes an Actin Polymerization-Dependent Macropinocytic Pathway To Enter Human Dermal Microvascular Endothelial and Human Umbilical Vein Endothelial Cells. J Virol **83:**4895-4911.
268. **Rahn, E., P. Petermann, M.-J. Hsu, F. J. Rixon, and D. Knebel-Mörsdorf.** 2011. Entry Pathways of Herpes Simplex Virus Type 1 into Human Keratinocytes Are Dynamin- and Cholesterol-Dependent. PLoS ONE **6:**e25464.
269. **Raiborg, C., T. E. Rusten, and H. Stenmark.** 2003. Protein sorting into multivesicular endosomes. Curr Opin Cell Biol **15:**446-455.
270. **Raiborg, C., and H. Stenmark.** 2002. Hrs and Endocytic Sorting of Ubiquitinated Membrane Proteins. Cell Structure and Function **27:**403-408.
271. **Raimondi, A., Shawn M. Ferguson, X. Lou, M. Armbruster, S. Paradise, S. Giovedi, M. Messa, N. Kono, J. Takasaki, V. Cappello, E. O'Toole,**

Timothy A. Ryan, and P. De Camilli. 2011. Overlapping Role of Dynamin Isoforms in Synaptic Vesicle Endocytosis. Neuron **70:**1100-1114.
272. **Ratia, K., S. Pegan, J. Takayama, K. Sleeman, M. Coughlin, S. Baliji, R. Chaudhuri, W. Fu, B. S. Prabhakar, M. E. Johnson, S. C. Baker, A. K. Ghosh, and A. D. Mesecar.** 2008. A noncovalent class of papain-like protease/deubiquitinase inhibitors blocks SARS virus replication. Proceedings of the National Academy of Sciences **105:**16119-16124.
273. **Reuter, G., H. Biro, and G. Szucs.** 2007. Enteric caliciviruses in domestic pigs in Hungary. Arch Virol **152:**611-4.
274. **Rivera-Milla, E., C. Stuermer, and E. Málaga-Trillo.** 2006. Ancient origin of reggie (flotillin), reggie-like, and other lipid-raft proteins: convergent evolution of the SPFH domain. Cellular and Molecular Life Sciences **63:**343-357.
275. **Rockx, B., M. de Wit, H. Vennema, J. Vinjé, E. de Bruin, Y. van Duynhoven, and M. Koopmans.** 2002. Natural History of Human Calicivirus Infection: A Prospective Cohort Study. Clinical Infectious Diseases **35:**246-253.
276. **Roitman-Shemer, V., J. Stokrova, J. Forstova, and A. Oppenheim.** 2007. Assemblages of simian virus 40 capsid proteins and viral DNA visualized by electron microscopy. Biochem Biophys Res Commun **353:**424-430.
277. **Rothberg, K. G., J. E. Heuser, W. C. Donzell, Y.-S. Ying, J. R. Glenney, and R. G. W. Anderson.** 1992. Caveolin, a protein component of caveolae membrane coats. Cell **68:**673-682.
278. **Rotin, D., and S. Kumar.** 2009. Physiological functions of the HECT family of ubiquitin ligases. Nat Rev Mol Cell Biol **10:**398-409.
279. **Roux, A., and B. Antonny.** 2008. The Long and Short of Membrane Fission. Cell **135:**1163-1165.
280. **Roux, A., G. Koster, M. Lenz, B. Sorre, J.-B. Manneville, P. Nassoy, and P. Bassereau.** 2010. Membrane curvature controls dynamin polymerization. Proceedings of the National Academy of Sciences **107:**4141-4146.
281. **Russell, R., C. Liang, and M. Wainberg.** 2004. Is HIV-1 RNA dimerization a prerequisite for packaging? Yes, no, probably? Retrovirology **1:**23.
282. **S., W., W. Williamson, J. Hewitt, S. Lin, M. Rivera-Aban, A. Ball, P. Scholes, M. Savill, and G. E. Greening.** 2009. Molecular detection of norovirus in sheep and pigs in New Zealand farms. Vet Microbiol **133:**184-9.
283. **Sattar, S. A., M. Ali, and J. A. Tetro.** 2011. In Vivo Comparison of Two Human Norovirus Surrogates for Testing Ethanol-Based Handrubs: The Mouse Chasing the Cat! PLoS ONE **6:**e17340.
284. **Savill, J., I. Dransfield, C. Gregory, and C. Haslett.** 2002. A blast from the past: clearance of apoptotic cells regulates immune responses. Nat Rev Immunol **2:**965-975.
285. **Schaffer, F. L., M. E. Soergel, J. W. Black, D. E. Skilling, A. W. Smith, and W. D. Cubitt.** 1985. Characterization of a new calicivirus isolated from feces of a dog. Arch Virol **84:**181-195.
286. **Schmid, M.** 1994. IRES-controlled protein synthesis and genome replication of poliovirus. Archives of virology. Supplementum **9:**279-89.
287. **Scipioni, A., I. Bourgot, A. Mauroy, D. Ziant, C. Saegerman, G. Daube, and E. Thiry.** 2008. Detection and quantification of human and bovine noroviruses by

a TaqMan RT-PCR assay with a control for inhibition. Molecular and Cellular Probes **22:**215-222.

288. **Scipioni, A., A. Mauroy, J. Vinje, and E. Thiry.** 2008. Animal noroviruses. Vet J **178:**32-45.
289. **Shanker, S., J.-M. Choi, B. Sankaran, R. L. Atmar, M. K. Estes, and B. V. V. Prasad.** 2011. Structural Analysis of Histo-Blood Group Antigen Binding Specificity in a Norovirus GII.4 Epidemic Variant: Implications for Epochal Evolution. J Virol **85:**8635-8645.
290. **Shirato-Horikoshi, H., S. Ogawa, T. Wakita, N. Takeda, and G. S. Hansman.** 2007. Binding activity of norovirus and sapovirus to histo-blood group antigens. Arch Virol **152:**457-61.
291. **Shirato, H., S. Ogawa, H. Ito, T. Sato, A. Kameyama, H. Narimatsu, Z. Xiaofan, T. Miyamura, T. Wakita, K. Ishii, and N. Takeda.** 2008. Noroviruses distinguish between type 1 and type 2 histo-blood group antigens for binding. J Virol.
292. **Siebenga, J. J., M. F. Beersma, H. Vennema, P. van Biezen, N. J. Hartwig, and M. Koopmans.** 2008. High Prevalence of Prolonged Norovirus Shedding and Illness among Hospitalized Patients: A Model for In Vivo Molecular Evolution. J Infect Dis **198:**994-1001.
293. **Simons, K., and G. van Meer.** 1988. Lipid sorting in epithelial cells. Biochemistry **27:**6197-202.
294. **Singer, S. J., and G. L. Nicolson.** 1971. The structure and chemistry of mammalian cell membranes. Am J Pathol **65:**427-437.
295. **Sit, T. L., A. A. Vaewhongs, and S. A. Lommel.** 1998. RNA-Mediated Trans-Activation of Transcription from a Viral RNA. Science **281:**829-832.
296. **Sivakumaran, K., S.-K. Choi, M. Hema, and C. C. Kao.** 2004. Requirements for Brome Mosaic Virus Subgenomic RNA Synthesis In Vivo and Replicase-Core Promoter Interactions In Vitro. J Virol **78:**6091-6101.
297. **Skov, J., M. Gaudin, P. Podbevšek, R. C. L. Olsthoorn, and M. Petersen.** 2012. The subgenomic promoter of brome mosaic virus folds into a stem–loop structure capped by a pseudo-triloop that is structurally similar to the triloop of the genomic promoter. RNA.
298. **Smiley, J. R., A. E. Hoet, M. Tråvén, H. Tsunemitsu, and L. J. Saif.** 2003. Reverse Transcription-PCR Assays for Detection of Bovine Enteric Caliciviruses (BEC) and Analysis of the Genetic Relationships among BEC and Human Caliciviruses. J Clin Microbiol **41:**3089-3099.
299. **Smith, A. W., E. S. Berry, D. E. Skilling, J. E. Barlough, S. E. Poet, T. Berke, J. Mead, and D. O. Matson.** 1998. In Vitro Isolation and Characterization of a Calicivirus Causing a Vesicular Disease of the Hands and Feet. Clinical Infectious Diseases **26:**434-439.
300. **Snyers, L., H. Zwickl, and D. Blaas.** 2003. Human Rhinovirus Type 2 Is Internalized by Clathrin-Mediated Endocytosis. J Virol **77:**5360-5369.
301. **Soares, J. A. P., F. G. G. Leite, L. G. Andrade, A. A. Torres, L. P. De Sousa, L. S. Barcelos, M. M. Teixeira, P. C. P. Ferreira, E. G. Kroon, T. Souto-Padrón, and C. A. Bonjardim.** 2009. Activation of the PI3K/Akt Pathway Early

during Vaccinia and Cowpox Virus Infections Is Required for both Host Survival and Viral Replication. J Virol **83:**6883-6899.

302. **Soldevila, A. I., S. Huang, and S. A. Ghabrial.** 1998. Assembly of the Hv190S Totivirus Capsid Is Independent of Posttranslational Modification of the Capsid Protein. Virology **251:**327-333.
303. **Sosnovtsev, S. V., G. Belliot, K. O. Chang, V. G. Prikhodko, L. B. Thackray, C. E. Wobus, S. M. Karst, H. W. Virgin, and K. Y. Green.** 2006. Cleavage map and proteolytic processing of the murine norovirus nonstructural polyprotein in infected cells. J Virol **80:**7816-31.
304. **Sosnovtsev, S. V., and K. Y. Green.** 2000. Identification and genomic mapping of the ORF3 and VPg proteins in feline calicivirus virions. Virology **277:**193-203.
305. **Souza, M., M. S. Azevedo, K. Jung, S. Cheetham, and L. J. Saif.** 2008. Pathogenesis and immune responses in gnotobiotic calves after infection with the genogroup II.4-HS66 strain of human norovirus. J Virol **82:**1777-86.
306. **Starkey, W. G., J. Collins, T. S. Wallis, G. J. Clarke, A. J. Spencer, S. J. Haddon, M. P. Osborne, D. C. A. Candy, and J. Stephen.** 1986. Kinetics, tissue specificity and pathological changes in murine rotavirus infection of mice. Journal of General Virology **67 (Pt 12):**2625-34.
307. **Staub, O., and D. Rotin.** 2006. Role of Ubiquitylation in Cellular Membrane Transport. Physiological Reviews **86:**669-707.
308. **Stevenson, P. G., S. Efstathiou, P. C. Doherty, and P. J. Lehner.** 2000. Inhibition of MHC class I-restricted antigen presentation by γ2-herpesviruses. Proceedings of the National Academy of Sciences **97:**8455-8460.
309. **Strasser, A., L. O'Connor, and V. M. Dixit.** 2000. Apoptosis Signaling Annu Rev Biochem **69:**217-245.
310. **Sugieda, M., and S. Nakajima.** 2002. Viruses detected in the caecum contents of healthy pigs representing a new genetic cluster in genogroup II of the genus "Norwalk-like viruses". Virus Res **87:**165-72.
311. **Sun, X., V. K. Yau, B. J. Briggs, and G. R. Whittaker.** 2005. Role of clathrin-mediated endocytosis during vesicular stomatitis virus entry into host cells. Virology **338:**53-60.
312. **Sun, Z., Y. Li, R. Ransburgh, E. J. Snijder, and Y. Fang.** 2012. Nonstructural Protein 2 of Porcine Reproductive and Respiratory Syndrome Virus Inhibits the Antiviral Function of Interferon-Stimulated Gene 15. J Virol **86:**3839-3850.
313. **Suzuki, T., H. Kono, N. Hirose, M. Okada, T. Yamamoto, K. Yamamoto, and Z.-i. Honda.** 2000. Differential Involvement of Src Family Kinases in Fcγ Receptor-Mediated Phagocytosis. The Journal of Immunology **165:**473-482.
314. **Tamura, M., K. Natori, M. Kobayashi, T. Miyamura, and N. Takeda.** 2004. Genogroup II noroviruses efficiently bind to heparan sulfate proteoglycan associated with the cellular membrane. J Virol **78:**3817-26.
315. **Tan, M., P. Fang, T. Chachiyo, M. Xia, P. Huang, Z. Fang, W. Jiang, and X. Jiang.** 2008. Noroviral P particle: Structure, function and applications in virus-host interaction. Virology.
316. **Tan, M., R. S. Hegde, and X. Jiang.** 2004. The P domain of norovirus capsid protein forms dimer and binds to histo-blood group antigen receptors. J Virol **78:**6233-42.

317. **Tatsuo, F., and Y. Katsushi.** 1980. The α-naphthoxyacetic acid-elicited retching involves dopaminergic inhibition in mice. Pharmacology Biochemistry and Behavior **12:**735-738.
318. **Taube, S., J. W. Perry, E. McGreevy, K. Yetming, C. Perkins, K. Henderson, and C. E. Wobus.** 2012. Murine Noroviruses (MNV) bind glycolipid and glycoprotein attachment receptors in a strain- dependent manner. Journal of Virology **doi:10.1128/JVI.06854-11**.
319. **Taube, S., J. W. Perry, E. McGreevy, K. Yetming, C. Perkins, K. Henderson, and C. E. Wobus.** 2012. Murine noroviruses (MNV) bind glycolipid and glycoprotein attachment receptors in a strain-dependent manner. J Virol.
320. **Taube, S., J. W. Perry, K. Yetming, S. P. Patel, H. Auble, L. Shu, H. F. Nawar, C. H. Lee, T. D. Connell, J. A. Shayman, and C. E. Wobus.** 2009. Ganglioside-linked terminal sialic acid moieties on murine macrophages function as attachment receptors for Murine Noroviruses (MNV). J Virol **83:**4092-4101.
321. **Taube, S., J. R. Rubin, U. Katpally, T. J. Smith, A. Kendall, J. A. Stuckey, and C. E. Wobus.** 2010. High-resolution x-ray structure and functional analysis of the murine norovirus 1 capsid protein protruding domain. J Virol **84:**5695-705.
322. **Tauber, A. I.** 2003. Metchnikoff and the phagocytosis theory. Nat Rev Mol Cell Biol **4:**897-901.
323. **Teunis, P. F., C. L. Moe, P. Liu, S. E. Miller, L. Lindesmith, R. S. Baric, J. Le Pendu, and R. L. Calderon.** 2008. Norwalk virus: how infectious is it? J Med Virol **80:**1468-76.
324. **Thackray, L. B., C. E. Wobus, K. A. Chachu, B. Liu, E. R. Alegre, K. S. Henderson, S. T. Kelley, and H. W. Virgin IV.** 2007. Murine noroviruses comprising a single genogroup exhibit biological diversity despite limited sequence divergence. J Virol **81:**10460-73.
325. **Tirasophon, W., K. Lee, B. Callaghan, A. Welihinda, and R. J. Kaufman.** 2000. The endoribonuclease activity of mammalian IRE1 autoregulates its mRNA and is required for the unfolded protein response. Genes & Development **14:**2725-2736.
326. **Tirosh, B., N. N. Iwakoshi, B. N. Lilley, A.-H. Lee, L. H. Glimcher, and H. L. Ploegh.** 2005. Human Cytomegalovirus Protein US11 Provokes an Unfolded Protein Response That May Facilitate the Degradation of Class I Major Histocompatibility Complex Products. J Virol **79:**2768-2779.
327. **Touret, N., P. Paroutis, and S. Grinstein.** 2005. The nature of the phagosomal membrane: endoplasmic reticulum versus plasmalemma. Journal of Leukocyte Biology **77:**878-885.
328. **Tse, S. M. L., W. Furuya, E. Gold, A. D. Schreiber, K. Sandvig, R. D. Inman, and S. Grinstein.** 2003. Differential Role of Actin, Clathrin, and Dynamin in Fcγ Receptor-mediated Endocytosis and Phagocytosis. Journal of Biological Chemistry **278:**3331-3338.
329. **Tucker, S. P., C. L. Thornton, E. Wimmer, and R. W. Compans.** 1993. Vectorial release of poliovirus from polarized human intestinal epithelial cells. J Virol **67:**4274-4282.

330. **Ullrich, O., S. Reinsch, S. Urbé, M. Zerial, and R. G. Parton.** 1996. Rab11 regulates recycling through the pericentriolar recycling endosome. J Cell Biol **135:**913-924.
331. **Urrutia, R., J. R. Henley, T. Cook, and M. A. McNiven.** 1997. The dynamins: Redundant or distinct functions for an expanding family of related GTPases? Proc Natl Acad Sci U S A **94:**377-384.
332. **Valegard, K., J. B. Murray, P. G. Stockley, N. J. Stonehouse, and L. Liljas.** 1994. Crystal structure of an RNA bacteriophage coat protein–operator complex. Nature **371:**623-626.
333. **van Der Poel, W. H., J. Vinje, R. van Der Heide, M. I. Herrera, A. Vivo, and M. P. Koopmans.** 2000. Norwalk-like calicivirus genes in farm animals. Emerg Infect Dis **6:**36-41.
334. **Veiga, E., and P. Cossart.** 2005. Listeria hijacks the clathrin-dependent endocytic machinery to invade mammalian cells. Nat Cell Biol **7:**894-900.
335. **Vinjé, J., R. A. Hamidjaja, and M. D. Sobsey.** 2004. Development and application of a capsid VP1 (region D) based reverse transcription PCR assay for genotyping of genogroup I and II noroviruses. J Virol Methods **116:**109-117.
336. **Viswanathan, K., K. Früh, and V. DeFilippis.** 2010. Viral hijacking of the host ubiquitin system to evade interferon responses. Curr Opin Microbiol **13:**517-523.
337. **Volonté, D., F. Galbiati, S. Li, K. Nishiyama, T. Okamoto, and M. P. Lisanti.** 1999. Flotillins/Cavatellins Are Differentially Expressed in Cells and Tissues and Form a Hetero-oligomeric Complex with Caveolins in Vivo. Journal of Biological Chemistry **274:**12702-12709.
338. **Wagner, M., and D. D. Moore.** 2011. Endoplasmic reticulum stress and glucose homeostasis. Current Opinion in Clinical Nutrition & Metabolic Care **14:**367-373.
339. **Walter, P., and D. Ron.** 2011. The Unfolded Protein Response: From Stress Pathway to Homeostatic Regulation. Science **334:**1081-1086.
340. **Wang, D., L. Fang, P. Li, L. Sun, J. Fan, Q. Zhang, R. Luo, X. Liu, K. Li, H. Chen, Z. Chen, and S. Xiao.** 2011. The Leader Proteinase of Foot-and-Mouth Disease Virus Negatively Regulates the Type I Interferon Pathway by Acting as a Viral Deubiquitinase. The Journal of Virology **85:**3758-3766.
341. **Wang, E., N. Obeng-Adjei, Q. Ying, L. Meertens, T. Dragic, R. A. Davey, and S. R. Ross.** 2008. Mouse mammary tumor virus uses mouse but not human transferrin receptor 1 to reach a low pH compartment and infect cells. Virology **381:**230-240.
342. **Wang, K., S. Huang, A. Kapoor-Munshi, and G. Nemerow.** 1998. Adenovirus Internalization and Infection Require Dynamin. J Virol **72:**3455-3458.
343. **Wang, Q. H., M. G. Han, S. Cheetham, M. Souza, J. A. Funk, and L. J. Saif.** 2005. Porcine noroviruses related to human noroviruses. Emerg Infect Dis **11:**1874-81.
344. **Wang, Y., J. Shen, N. Arenzana, W. Tirasophon, R. J. Kaufman, and R. Prywes.** 2000. Activation of ATF6 and an ATF6 DNA Binding Site by the Endoplasmic Reticulum Stress Response. Journal of Biological Chemistry **275:**27013-27020.
345. **Ward, V. K., C. J. McCormick, I. N. Clarke, O. Salim, C. E. Wobus, L. B. Thackray, H. W. Virgin IV, and P. R. Lambden.** 2007. Recovery of infectious

murine norovirus using pol II-driven expression of full-length cDNA. Proc Natl Acad Sci U S A **104:**11050-5.

346. **Weissman, A. M., N. Shabek, and A. Ciechanover.** 2011. The predator becomes the prey: regulating the ubiquitin system by ubiquitylation and degradation. Nat Rev Mol Cell Biol **12:**605-620.
347. **White, L. J., J. M. Ball, M. E. Hardy, T. N. Tanaka, N. Kitamoto, and M. K. Estes.** 1996. Attachment and entry of recombinant Norwalk virus capsids to cultured human and animal cell lines. J Virol **70:**6589-97.
348. **Wickliffe, K. E., A. Williamson, H.-J. Meyer, A. Kelly, and M. Rape.** 2011. K11-linked ubiquitin chains as novel regulators of cell division. Trends Cell Biol **21:**656-663.
349. **Widdowson, M. A., S. S. Monroe, and R. I. Glass.** 2005. Are noroviruses emerging? Emerg Infect Dis **11:**735-7.
350. **Widdowson, M. A., A. Sulka, S. N. Bulens, R. S. Beard, S. S. Chaves, R. Hammond, E. D. Salehi, E. Swanson, J. Totaro, R. Woron, P. S. Mead, J. S. Bresee, S. S. Monroe, and R. I. Glass.** 2005. Norovirus and foodborne disease, United States, 1991-2000. Emerg Infect Dis **11:**95-102.
351. **Wierzchoslawski, R., A. Dzianott, and J. Bujarski.** 2004. Dissecting the Requirement for Subgenomic Promoter Sequences by RNA Recombination of Brome Mosaic Virus In Vivo: Evidence for Functional Separation of Transcription and Recombination. J Virol **78:**8552-8564.
352. **Wileman, T.** 2006. Aggresomes and Autophagy Generate Sites for Virus Replication. Science **312:**875-878.
353. **Wobus, C. E., S. M. Karst, L. B. Thackray, K. O. Chang, S. V. Sosnovtsev, G. Belliot, A. Krug, J. M. Mackenzie, K. Y. Green, and H. W. Virgin.** 2004. Replication of Norovirus in cell culture reveals a tropism for dendritic cells and macrophages. PLoS Biol **2:**e432.
354. **Wobus, C. E., L. B. Thackray, and H. W. Virgin IV.** 2006. Murine norovirus: a model system to study norovirus biology and pathogenesis. J Virol **80:**5104-12.
355. **Wolfe, B. L., and J. Trejo.** 2007. Clathrin-Dependent Mechanisms of G Protein-coupled Receptor Endocytosis. Traffic **8:**462-470.
356. **Woode, G. N., and J. C. Bridger.** 1978. Isolation of Small Viruses Resembling Astroviruses and Caliciviruses from Acute Enteritis Of Calves. J Med Microbiol **11:**441-452.
357. **Xia, M., T. Farkas, and X. Jiang.** 2007. Norovirus capsid protein expressed in yeast forms virus-like particles and stimulates systemic and mucosal immunity in mice following an oral administration of raw yeast extracts. J Med Virol **79:**74-83.
358. **Xu, P., D. M. Duong, N. T. Seyfried, D. Cheng, Y. Xie, J. Robert, J. Rush, M. Hochstrasser, D. Finley, and J. Peng.** 2009. Quantitative Proteomics Reveals the Function of Unconventional Ubiquitin Chains in Proteasomal Degradation. Cell **137:**133-145.
359. **Ye, Y., and M. Rape.** 2009. Building ubiquitin chains: E2 enzymes at work. Nat Rev Mol Cell Biol **10:**755-764.

360. **Yokota, A., H. Takeuchi, N. Maeda, Y. Ohoka, C. Kato, S. Y. Song, and M. Iwata.** 2009. GM-CSF and IL-4 synergistically trigger dendritic cells to acquire retinoic acid-producing capacity. Int Immunol **21:**361-77.
361. **Yoshida, H., K. Haze, H. Yanagi, T. Yura, and K. Mori.** 1998. Identification of the cis-Acting Endoplasmic Reticulum Stress Response Element Responsible for Transcriptional Induction of Mammalian Glucose-regulated Proteins. Journal of Biological Chemistry **273:**33741-33749.
362. **Yoshida, H., T. Matsui, A. Yamamoto, T. Okada, and K. Mori.** 2001. XBP1 mRNA Is Induced by ATF6 and Spliced by IRE1 in Response to ER Stress to Produce a Highly Active Transcription Factor. Cell **107:**881-891.
363. **Young, A.** 2007. Structural insights into the clathrin coat. Seminars in Cell & Developmental Biology **18:**448-458.
364. **Yunta, M., and P. A. Lazo.** 2003. Tetraspanin proteins as organisers of membrane microdomains and signalling complexes. Cellular Signalling **15:**559-564.
365. **Yunus, M. A., C. L.M.W., Y. Chaudhry, B. Dalan, and I. Goodfellow.** 2010. Development of an optimized RNA-based murine norovirus reverse genetics system. Journal of Virological Methods **169:**112-8.
366. **Zeng, L., Y.-P. Liu, H. Sha, H. Chen, L. Qi, and J. A. Smith.** 2010. XBP-1 Couples Endoplasmic Reticulum Stress to Augmented IFN-β Induction via a cis-Acting Enhancer in Macrophages. The Journal of Immunology **185:**2324-2330.
367. **Zeng, W., L. Sun, X. Jiang, X. Chen, F. Hou, A. Adhikari, M. Xu, and Z. J. Chen.** 2010. Reconstitution of the RIG-I Pathway Reveals a Signaling Role of Unanchored Polyubiquitin Chains in Innate Immunity. Cell **141:**315-330.
368. **Zheng, D. P., T. Ando, R. L. Fankhauser, R. S. Beard, R. I. Glass, and S. S. Monroe.** 2006. Norovirus classification and proposed strain nomenclature. Virology **346:**312-23.
369. **Zheng, Y.** 2005. Hepatitis C virus non-structural protein NS4B can modulate an unfolded protein response. The journal of microbiology **43:**529-36.

Chapter 2

Endocytosis of murine norovirus 1 into murine macrophages is dependent on dynamin II and cholesterol

(This chapter was published in the Journal of Virology.

Jeffrey W. Perry and Christiane E. Wobus. Endocytosis of Murine Norovirus 1 into murine macrophages is dependent on dynamin II and cholesterol. Journal of Virology. 2010; 84(12): 6163-76)

(J.W. Perry designed and performed experiments, analysed data and prepared the manuscript. C. E. Wobus designed experiments, analysed data, and prepared the manuscript.)

2.1 Abstract

Although noroviruses cause the vast majority of nonbacterial gastroenteritis in humans, little is known about their life cycle, including viral entry. Murine norovirus (MNV) is the only norovirus to date that efficiently infects cells in culture. To elucidate the productive route of infection for MNV-1 into

murine macrophages, we used a neutral red (NR) infectious center assay and pharmacological inhibitors in combination with dominant-negative (DN) and small interfering RNA (siRNA) constructs to show that clathrin- and caveolin-mediated endocytosis did not play a role in entry. In addition, we showed that phagocytosis or macropinocytosis, flotillin-1, and GRAF1 are not required for the major route of MNV-1 uptake. However, MNV-1 genome release occurred within 1 h, and endocytosis was significantly inhibited by the cholesterol-sequestering drugs nystatin and methyl-β-cyclodextrin, the dynamin-specific inhibitor dynasore, and the dominant-negative dynamin II mutant K44A. Therefore, we conclude that the productive route of MNV-1 entry into murine macrophages is rapid and requires host cholesterol and dynamin II.

2.2 Introduction

Murine noroviruses (MNV) are closely related to human noroviruses (HuNoV), the causative agent of most outbreaks of infectious nonbacterial gastroenteritis worldwide in people of all ages (4, 8, 19, 31, 43, 46, 83). Although a major public health concern, noroviruses have been an understudied group of viruses due to the lack of a tissue culture system and small animal model. Since the discovery of MNV-1 in 2003 (27), reverse genetics systems (10, 81), a cell culture model (84), and a small animal model (27) have provided the tools necessary for detailed study of noroviruses.

One largely unexplored aspect of norovirus biology is the early events during viral infection that are essential during viral pathogenesis. One of these

early events is the attachment of the virus particle to the host. Attachment is mediated by the protruding domain of the MNV-1 capsid (29, 30, 73). For at least three strains (MNV-1, WU-11, and S99), the attachment receptor on the cell surface of murine macrophages is terminal sialic acids, including those found on the ganglioside GD1a (72). The use of carbohydrate receptors for cell attachment is shared with HuNoV, which utilize mostly histo-blood group antigens (HBGA) (18, 34, 70, 71). These carbohydrates are present in body fluids (saliva, breast milk, and intestinal contents) and on the surface of red blood cells and intestinal epithelial cells (33). Some HuNoV strains also bind to sialic acid or heparan sulfate (60, 69). However, despite evidence that for HuNoV HBGA are a genetic susceptibility marker (35), the presence of attachment receptors is not sufficient for a productive infection for either HuNoV (24) or MNV-1 (72). Although the cellular tropism of HuNoV is unknown, MNV infects murine macrophages and dendritic cells *in vitro* and *in vivo* (80, 84). Following attachment, MNV-1 infection of murine macrophages and dendritic cells can proceed in the presence of the endosome acidification inhibitor chloroquine or bafilomycin A1, suggesting that MNV-1 entry occurs independently of endosomal pH (56). However, the cellular pathway(s) utilized by MNV-1 during entry remains unclear.

Viruses are obligate intracellular pathogens that hijack cellular processes to deliver their genome into cells. The most commonly used endocytic pathway during virus entry is clathrin-mediated endocytosis (41). Clathrin-coated vesicles form at the plasma membrane, pinch off by the action of the small GTPase dynamin II, and deliver their contents to early endosomes (12). For example,

vesicular stomatitis virus (VSV) enters cells in this manner (66). However, viruses can also use several clathrin-independent pathways to enter cells, some of which require cholesterol-rich microdomains (i.e., lipid rafts) in the plasma membrane (56). The best studied of these is mediated by caveolin and was initially elucidated through studies of simian virus 40 (SV40) entry (1). SV40 uptake occurs via caveolin-containing vesicles that are released from the plasma membrane in a dynamin II-dependent manner and later fuse with pH-neutral caveosomes (28, 48, 53). However, recent evidence suggest that caveosomes are an artifact of over expression of caveolin 1. Although caveolin-mediated endocytosis is a well-characterized form of cholesterol-dependent endocytosis, other entry mechanisms exist that are clathrin and caveolin independent (5, 14, 55, 57-59, 64, 78). In addition, macropinocytosis and/or phagocytosis can also play a role in viral entry (11, 13, 21, 36, 40, 42, 44, 45). However, the requirement for dynamin II in these processes is not fully understood.

Viral entry has been addressed primarily by pharmacologic inhibitor studies, immunofluorescence and electron microscopy, transfections of dominant-negative (DN) constructs, and more recently by small interfering RNA (siRNA) knockdown. Each of these approaches has some limitations; thus, a combination of approaches is needed to elucidate the mechanism of viral entry into host cells. For example, using electron and fluorescence microscopy, which require a high particle number, does not allow the differentiation of infectious and noninfectious particles. Alternatively, the use of pharmacological inhibitors can result in off-target effects, including cytotoxicity. A recent approach used the

photoreactive dye neutral red (NR) in an infectious focus assay to determine the mechanism of poliovirus entry (6). Cells were infected in the dark in the presence of neutral red, and virus particles passively incorporated the dye. Upon exposure to light, the neutral red dye cross-linked the viral genome to the viral capsid, thus inactivating the virus. Infectious foci were counted several days later. This assay was performed in the presence of various pharmacologic inhibitors of endocytosis. When an inhibitor blocked a productive route of infection, the number of infectious foci was significantly less than that for an untreated control. Major advantages of this technique over traditional assays are the ability to treat cells with pharmacologic inhibitors only during the viral entry process, the reduction of cytotoxicity, and the ability to infect with a low multiplicity of infection (MOI). Furthermore, infectious virus that is prohibited from uncoating is inactivated by illumination. Therefore, only virus particles leading to a productive infection in the presence or absence of the various inhibitors are measured. We successfully adapted this assay for use with MNV-1. Together with the use of pharmacological inhibitors, DN constructs, and siRNA knockdown, we demonstrate that the major MNV-1 entry pathway into murine macrophages resulting in a productive infection occurred by endocytosis and not phagocytosis or macropinocytosis in a manner that was clathrin and caveolin 1, flotillin 1, and GRAF1 independent but required dynamin II and cholesterol.

2.3 Materials and Methods

Cell culture and mice. RAW 264.7 cells were purchased from ATCC (Manassas, VA) and maintained as previously described (84). Swiss Webster mice were purchased from Charles River. Caveolin-1 knockout mice (number 004585) and matched control mice (B6129SF2/J, number 101045) were purchased from Jackson Laboratories. Bone marrow-derived macrophages (BMDMs) were isolated as previously described (84).

Virus stocks. The plaque-purified MNV-1 clone (GV/MNV1/2002/USA) MNV-1.CW3 was used at passage 6 for all experiments (74). To generate NR-containing viral stocks, all activities were carried out in the dark. RAW 264.7 cells were infected with MNV-1 at an MOI of 0.05 and incubated for 40 h in the presence of 10 μg/ml neutral red (Sigma-Aldrich, MO; N2880). Cells were freeze-thawed twice to release virus, and single-use aliquots were stored at –80°C. All NR virus preparations exhibited a minimum two-log reduction in viral titers upon light exposure as determined by plaque assay compared to a control virus not exposed to light. Vesicular stomatitis virus (Indiana strain) was propagated in Vero cells, and single-use aliquots were stored at –80°C.

Growth curves (dynasore inhibition). RAW 264.7 cells or BMDMs were plated at 2 x 10^5 cells/ml in 12-well plates and allowed to attach overnight. Cells were then incubated with the indicated concentrations of dynasore (Sigma-Aldrich, MO) in dimethyl sulfoxide (DMSO) or vehicle control for 30 min. Cells were infected with MNV-1 or VSV at the indicated MOI in the presence of dynasore or vehicle control for 60 min on ice. The cells were washed and fresh media

containing inhibitor added. Infection was allowed to proceed until the indicated time point, when the cells were freeze-thawed twice, and viral titers were determined by plaque assay as previously described (84).

Immunofluorescence assay. RAW 264.7 cells or BMDMs were plated at 2 x 10^5 cells/ml in 6-well plates containing sterile glass coverslips (Fisher Scientific) and allowed to attach overnight. Cells were then incubated with the indicated concentrations of methyl-β-cyclodextrin (MβCD) (Sigma-Aldrich, MO), fetal bovine serum (FBS) and MβCD, or vehicle control (DMSO) for 60 min. Cells were infected with MNV-1 or VSV at the indicated MOI in the presence of inhibitor or vehicle control for 60 min on ice. Cells were washed and fresh media containing inhibitor added. Infection proceeded until the indicated time point when the cells were fixed with 4% paraformaldehyde in phosphate-buffered saline (PBS) for 10 min, washed once with PBS, and stained for the viral nonstructural protein VPg (81) or VSV matrix (38) as previously described (54). Briefly, cells were incubated with a monoclonal mouse antibody raised against MNV-1 VPg (81) diluted 1:5,000 or VSV matrix (38) diluted 1:10,000 in wash buffer (PBS, 1% bovine serum, 1% goat serum, 0.1% Triton X-100) for 1 h. Cells were then washed three times with wash buffer before incubation with an Alexa 594-conjugated goat anti-mouse antibody diluted 1:5,000 (Invitrogen, CA) for 1 h. Cells were washed three times as described above and mounted using Prolong Gold Antifade with DAPI (4', 6-diaminidino-2-phenylindole) (Invitrogen, CA). A total of 500 DAPI-stained cells were examined using the Olympus IX70 inverted microscope at the Center for Live Cell Imaging at the University of Michigan. Cells that had an average

fluorescence intensity of at least three times the average background fluorescence intensity as determined by the Metamorph Premier version 6.3 image analysis software (Molecular Devices, Downington, PA) were counted as infected cells. The number of infected cells was then normalized to the no-treatment control.

NR assay. RAW 264.7 cells were plated at 1 x 10^6 cells/ml in 6-well plates and allowed to attach overnight. For pretreatments, cells were incubated with the indicated concentrations of chloroquine, neuraminidase, dynasore, chlorpromazine, sucrose, nystatin, cytochalasin D, amiloride (EIPA [5-ethyl-*N*-isopropyl amiloride]) (all purchased from Sigma-Aldrich, MO), or vehicle control for 30 min, or 60 min for MβCD. Cells were infected with MNV-1 at an MOI of 0.001 in the presence of inhibitor or vehicle control. After 60 min, the cells were illuminated, and a plaque assay was performed by adding an agarose overlay and staining cells with neutral red after 48 to 72 h. In the case of chlorpromazine and sucrose treatments, cells were infected only for 30 min to maintain cell viability. To assess the nonspecific effects of drugs on later stages of the viral life cycle (posttreatment), cells were infected for 60 min at an MOI of 0.001 in the absence of inhibitors, the infection was stopped by illumination, and inhibitors were added back at the same concentration and length of time as the pretreatments. To determine the dynamic range of the experiment, untreated cells were infected at an MOI of 0.001 and illuminated immediately after addition of virus (0 min) or 60 min after addition of virus.

WST-1 cell viability assay. RAW 264.7 cells and BMDMs were plated at 2 x 10^5 cells/ml in a 96-well plate. Cells were pretreated with chloroquine, neuraminidase, dynasore, chlorpromazine, sucrose, nystatin, cytochalasin D, amiloride (EIPA) (all purchased from Sigma-Aldrich, MO), or vehicle control for 30 min, or 60 min for MβCD. Cells were then treated in the presence of inhibitor or vehicle control for the length of time indicated (Table 1). MβCD combination treatments were performed by 1-h treatment of MβCD followed by 60-min treatment of the other drug in media lacking FBS. At that time, media were removed, and media containing 10% WST-1 reagent (Roche) were added to cells. Cell viability was determined following the manufacturer's recommendations at 120 min after addition of reagent.

Transfection of RAW 264.7 cells. Cells were plated at a density of 4.0 x 10^5 cells/ml in 6-well plates and allowed to attach overnight. The following day, cells were transfected using Lipofectamine 2000 (Invitrogen) following the manufacturer's protocol. Briefly, media were replaced with Optimem media (Invitrogen), and a transfection solution containing 5 μg of plasmid DNA and 8 μl of Lipofectamine 2000 (Invitrogen) was prepared. Cells were incubated with the transfection reagent for 8 h and washed with media. Cells were infected 48 h after transfection with MNV-1 as described above. At 12 h postinfection (hpi), infected cells were processed for immunofluorescence analysis as described above. However, instead of quantitating 500 DAPI-stained cells, 500 DAPI-stained and green fluorescent protein (GFP)-expressing cells with an average fluorescence intensity at least three times the background's average fluorescence

intensity were quantitated as infected cells. The dynamin II wild-type (wt) and DN (K44A) constructs, both containing proteins fused to GFP, were kindly provided by Mark McNiven (Mayo Institute, Rochester, MN) (7). The EPS 15 wt and DN (Δ 95/295) constructs, both containing proteins fused to GFP, were kindly provided by A. Benmerah (INSERM, Paris, France) (3). The RAC 1 wt and DN (T17N) constructs, both containing proteins fused to GFP, as well as the GFP-only construct, were kindly provided by J. Swanson (University of Michigan, Ann Arbor, MI) (26). The caveolin 1 DN construct (GFP fused to the C terminus of wt Cav1) was provided by B. Tsai (University of Michigan, Ann Arbor, MI) (53).

siRNA knockdown. RAW 264.7 cells were plated at a density of 2 x 10^5 cells/ml in a 6-well plate and allowed to attach overnight. The next day, cells were washed once with Accell siRNA delivery media (Dharmacon) before incubation with Accell siRNA delivery media containing 1 μM the indicated Accell siRNA. The cells were incubated for 72 h, washed once with DMEM media, and infected as described above. At 12 h postinfection, virus-infected cells were analyzed by an immunofluorescence assay as described above. Cells treated in parallel were analyzed by SDS-PAGE and then by Western blot analysis to ensure effective knockdown of protein levels. The following sequences were used: clathrin heavy chain (CHC) (GUGUUAUGGAGUAUAUUAA), caveolin 1 (CAV-1) (CCACCAUUCUCAUAUAUAC), flotillin-1 (CUAUUUAACUUCCUGAUUA), and GRAF1 (UUAUCUCCCAUUCAGCACAGAUAUC).

Western blot analysis. Whole-cell lysates from siRNA-transfected RAW 264.7 cells were generated by adding 2x SDS-PAGE sample buffer to cells. Samples were boiled for 5 min and separated by SDS-PAGE. Proteins were then transferred to nitrocellulose (Bio-Rad). Membranes were blocked in 5% nonfat dry milk and incubated with primary antibodies and then with horseradish peroxidase in 5% nonfat dry milk. The following antibodies were used: clathrin heavy chain (no. 610500; BD Transduction Laboratories), caveolin 1 (no. 610406; BD Transduction Laboratories), flotillin-1 (no. sc-25506; Santa Cruz Biotech), and GRAF1 (kindly provided by R. Lundmark, Umea University, Sweden) (37). Band densities were determined using Adobe Photoshop (CA). Briefly, a selection box was created around the band of interest, and the mean pixel intensity determined. The same selection box was used for other bands, and also a region without a signal was used as a background control. The mean pixel intensity of the background control was subtracted from all other mean pixel intensities. The background-subtracted mean pixel intensities were normalized to the value for the nontargeting (NT) siRNA sample, which was set to 100%.

Fluorescent transferrin and cholera toxin subunit B internalization assay. RAW 264.7 cells or BMDMs were plated at 2 x 10^5 cells/ml in 6-well plates containing sterile glass coverslips (Fisher Scientific) and allowed to attach overnight. Cells were pretreated with increasing concentrations of chlorpromazine, sucrose, nystatin, or vehicle control for 30 min, or 60 min for MβCD. Cells were then incubated in 10 μg/ml fluorescently labeled cholera toxin subunit B (Invitrogen) or 50 μg/ml transferrin (Invitrogen, CA) in the presence of

inhibitor. Cells were washed, and media containing inhibitor or vehicle control were added back for 5 min for transferrin or 60 min for cholera toxin subunit B. Cells were fixed in 4% paraformaldehyde and mounted with Prolong Gold Antifade with DAPI (Invitrogen, CA). Cells were examined using the Olympus IX70 inverted microscope at the Center for Live Cell Imaging at the University of Michigan, and images were acquired using the Metamorph Premier version 6.3 image analysis software (Molecular Devices, Downington, PA).

***Listeria monocytogenes* infection of RAW 264.7 cells.** RAW 264.7 cells were plated at 2 x 10^5 cells/ml in 6-well plates containing sterile glass coverslips (Fisher Scientific) and allowed to attach overnight. Cells were pretreated with increasing concentrations of cytochalasin D, amiloride (EIPA), or vehicle control. *Listeria monocytogenes* strain 10403S (a kind gift from M. O'Riordan, University of Michigan, Ann Arbor, MI) was grown overnight to an optical density at 600 nm (OD_{600}) of 1.2 in brain heart infusion (BHI; Sigma Aldrich). Bacteria were pelleted and resuspended in PBS. Cells were infected at an MOI of 1 for 30 min at 37°C. Cells were washed with PBS and 50 μg/ml gentamicin (Fisher Scientific) added to inhibit replication of noninternalized bacteria. After 1 h postinfection, cells were lysed in sterile water and plated onto LB plates. CFU were quantitated 24 h after incubation at 37°C and normalized to the vehicle control.

Statistics. Error bars in the figures represent the standard error between independent experiments. Statistical analysis was performed using Prism

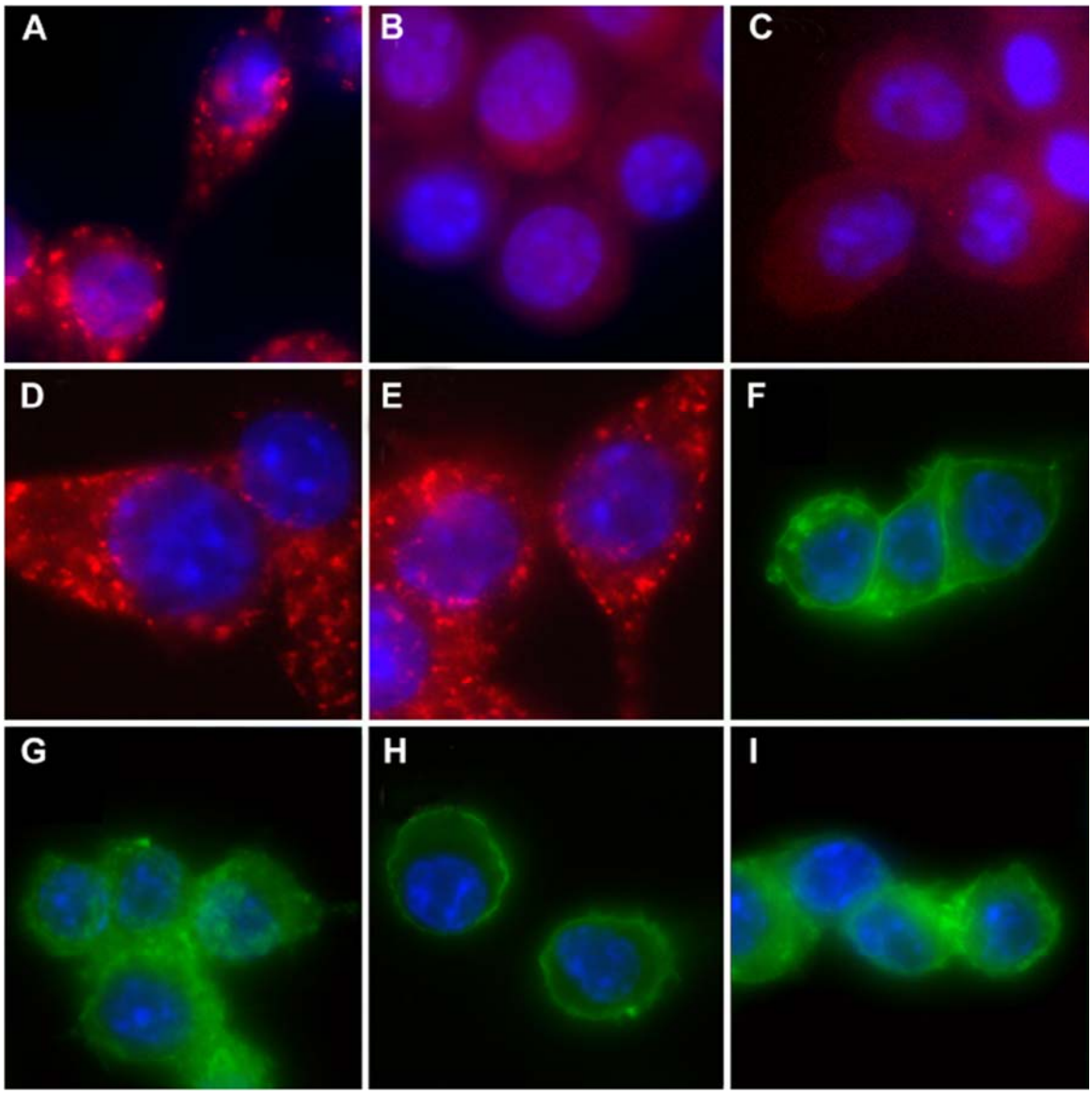

Figure 2.1. Uptake of fluorescently labeled transferrin is inhibited by a hypotonic solution of sucrose or chlorpromazine. RAW 264.7 cells were incubated with vehicle control (A, D, and G), chlorpromazine (B), a hypotonic solution of sucrose (C), or nystatin (F) for 30 min or MβCD (E and H) or MβCD and 10% FBS (I) for 60 min before incubation with 50 µg/ml fluorescently labeled transferrin (A to E) or 10 µg/ml fluorescently labeled cholera toxin subunit B (F to I). Cells were washed and media containing inhibitor or vehicle control added back for 5 min for transferrin or 60 min for cholera toxin subunit B. Cells were fixed in 4% paraformaldehyde and mounted with Prolong Gold Antifade with DAPI (Invitrogen, CA). Cells were examined using an Olympus IX70 inverted microscope and images acquired using the Metamorph Premier version 6.3 image analysis software (Molecular Devices, Downington, PA).

software version 5.01 (GraphPad Software, CA). The two-tailed Student *t* test was used to determine statistical significance.

2.4 Results

Development of a neutral red infectious center assay to study MNV-1 entry.

Viral entry is studied by a combination of different methods, one of which is the inhibition of proteins critical for specific endocytic pathways with pharmacologic inhibitors. However, these inhibitors often have off-target effects, including cytotoxicity for the cell type analyzed. To address this, we empirically determined minimal effective concentrations for RAW 264.7 cells or BMDMs that inhibited uptake of fluorescently labeled transferrin and cholera toxin subunit B (Fig. 2.1) and measured cell viability (Table 1) at these concentrations by WST-1 (Roche), which measures mitochondrial dehydrogenase activity, for all inhibitors used. Cell viability was mostly unaffected at the concentrations used and typically remained above 80% of that of untreated controls. A significant reduction in the signal intensity of fluorescently labeled transferrin was observed for both chlorpromazine- and sucrose-treated cells but not after MβCD treatment compared to untreated cells (Fig. 2.1A and E), indicating a block in transferrin uptake. Although the intensity of the fluorescently labeled cholera toxin subunit B signal did not significantly change, the localization of the signal shifted from a mainly punctate cytoplasmic signal to a predominantly plasma membrane

TABLE 1. Inhibitor treatments do not significantly affect viability of RAW 264.7 cells and BMDMs[a]

Inhibitor	Cell viability (%) (SD)		
	1 h	8 h	12 h
RAW 264.7 cells			
No-treatment control	100 (±18)	100 (±16)	100 (±14)
40 μM chlorpromazine	99 (±10)	ND	ND
200 μM chloroquine	125 (±9)	ND	ND
20 μM cytochalasin D	91.9 (±8)	ND	ND
40 μM dynasore	ND	125 (±39)	ND
80 μM dynasore	117 (±25)	116 (±30)	ND
200 μM EIPA	80.3 (±8)	ND	ND
2 mM MβCD	120 (±16)	ND	122 (±24)
2 mM MβCD + FBS	88 (±14)	ND	102 (±22)
2.5 mU neuraminidase	123 (±6)	ND	ND
50 μM nystatin	125 (±18)	ND	ND
300 mM Sucrose	101 (±16)	ND	ND
2 mM MβCD + 40 μM chlorpromazine	58 (±3)	ND	ND
2 mM MβCD + 20 μM cytochalasin D	92 (±13)	ND	ND
2 mM MβCD + 80 μM dynasore	93 (±8)	ND	ND
2 mM MβCD + 200 μM EIPA	97 (±14)	ND	ND
Primary bone marrow-derived macrophages			
No-treatment control	ND	ND	100 (±10)
80 μM dynasore	ND	ND	76.3 (±7)
160 μM dynasore	ND	ND	79.3 (±12)
2 mM MBCD	ND	ND	96 (±7)
2 mM MBCD + FBS	ND	ND	113 (±8)

Table 2.1 Inhibitor treatments do not significantly affect viability of RAW 264.7 cells and bone marrow derived macrophages.

location after treatment of cells with MβCD or nystatin compared to untreated cells or cells treated with MβCD with FBS that had reconstituted cholesterol levels (Fig. 2.1F to I). This suggests that cholera toxin subunit B was no longer efficiently internalized in the presence of these concentrations of MβCD or nystatin.

In addition, we adapted an assay to study the productive entry of MNV-1 using abbreviated treatments of pharmacological inhibitors as another way to limit off-target effects, including cytotoxicity. We modified the neutral red infectious center assay published for poliovirus, which quantitatively determines the number of viral entry events leading to a productive infection (6). MNV-1 stocks were generated in the presence of the vital dye neutral red. The neutral red dye passively incorporates into the virus particle. Upon illumination, the dye activates and cross-links proteins and nucleic acids. Since the dye and viral genome are trapped in the virion, viral genome that has not been uncoated will be cross-linked irreversibly to the protein capsid, thus inactivating the virus particle. However, the process of viral uncoating allows the neutral red and viral genome to disassociate and thereby become light insensitive. Using MNV-1 particles containing neutral red, we infected RAW 264.7 cells at room temperature for 0, 15, 30, 45, 60, or 75 min before exposure to light for 10 min to determine the entry kinetics for MNV-1 (Fig. 2.2A). This revealed that approximately 100% of NR-containing MNV-1 becomes light insensitive 60 min after addition to RAW 264.7 cells (Fig. 2.2B). This indicated that the kinetics of RNA release (i.e.,

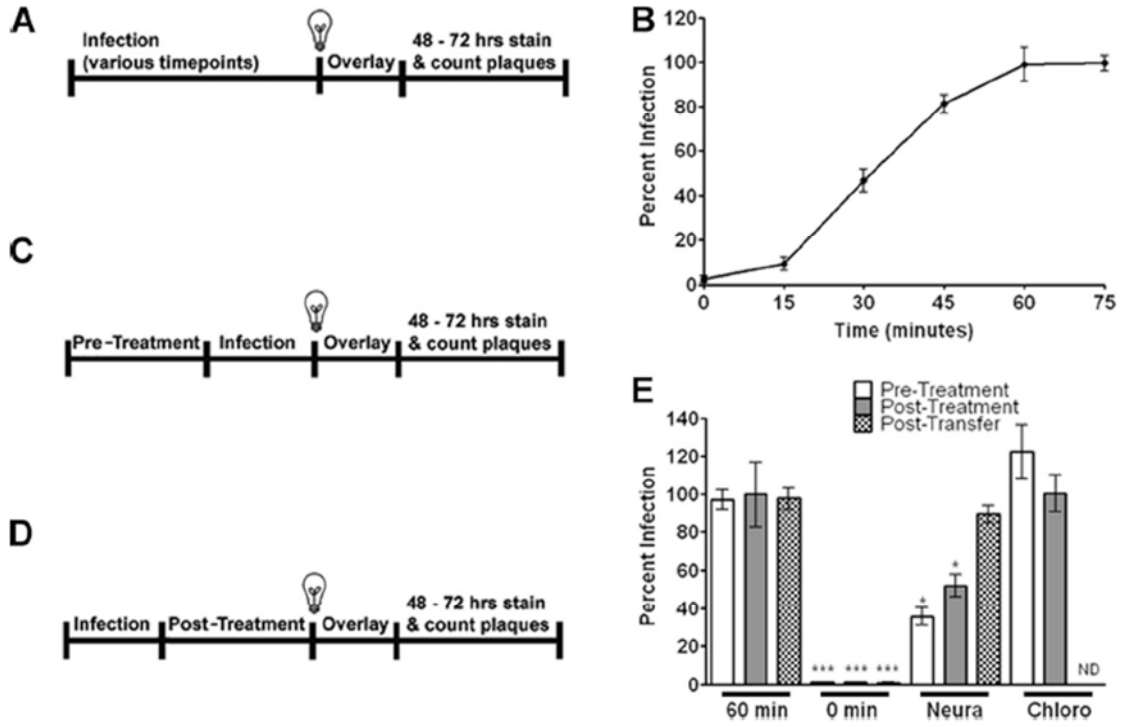

Figure 2.2. Neutral red (NR) infectious center assay confirms a pH-independent and sialic acid-dependent entry mechanism for MNV-1. (A, C, and D) Flow charts of the NR assay describing different treatment conditions. (A and B) MNV-1 rapidly becomes insensitive to light exposure. RAW 264.7 cells were infected with NR-containing virus at an MOI of 0.001, rocked at room temperature, exposed to light at 0, 15, 30, 45, 60, and 75 min postinfection (pi), and overlaid with agarose, and plaques were counted 48 to 72 h pi. (C, D, and E) MNV-1 entry is sialic acid dependent and pH independent. (C and E, pretreatment) RAW 264.7 cells were pretreated with 2.5 mU/ml *Vibrio cholerae* neuraminidase (Neura) or 200 μM chloroquine (Chloro) for 30 min, infected by rocking for 60 min, and overlaid with media containing agarose, and plaques were counted 48 to 72 h pi. (D and E, posttreatment) Alternatively, RAW 264.7 cells were infected with an MOI of 0.001 for 60 min and then posttreated with 2.5 mU/ml *Vibrio cholerae* neuraminidase (Neura) or 200 μM chloroquine (Chloro) for a total of 90 min before performing the NR assay. (E, posttransfer) In case of *Vibrio cholerae* neuraminidase treatment, RAW 264.7 cells were posttreated as described, scraped, and transferred to an untreated monolayer before a plaque assay was performed and viral titers were determined. *****, $P < 0.05$.

uncoating) as measured by this assay had a half-life ($t_{1/2}$) of 33 ± 2 min. This is similar to data from poliovirus genome release in HeLa cells ($t_{1/2}$ = 22 ± 3 min) (6)

To verify the applicability of the NR assay for studying MNV-1 entry, we determined the effect of two known inhibitors: chloroquine, an endosomal acidification inhibitor, and *Vibrio cholerae* neuraminidase, an enzyme that hydrolyzes terminal sialic acids on the host cell surface (54, 72). These inhibitors have either no effect on MNV-1 entry (chloroquine) (54) or significantly decrease MNV-1 infection in murine macrophages (*Vibrio cholerae* neuraminidase) (72). RAW 264.7 cells were pretreated with 200 μM chloroquine or 2.5 mU/ml *Vibrio cholerae* neuraminidase for 30 min prior to infection with NR-containing MNV-1 in the dark for 60 min at an MOI of 0.001. RAW 264.7 cells were then exposed to light for 10 min, washed, and incubated for 48 to 72 h with an agarose media overlay, and virus plaques were quantitated (Fig. 2.2C). To ensure that the inhibitors did not exhibit off-target effects on stages of the viral life cycle other than entry, a posttreatment (Fig. 2.2D) was performed for each inhibitor. These treatments were performed for each inhibitor assayed and equaled the length of the pretreatment. Consistent with our published results (54, 72), MNV-1 entry as measured by the NR assay was not inhibited by pretreatment of cells with 200 μM chloroquine but was inhibited by pretreatment with *Vibrio cholerae* neuraminidase, validating the NR assay (Fig. 2.2E). Posttreatment of cells with 200 μM chloroquine did not inhibit MNV-1 infection, confirming it has no effect on other stages of the viral life cycle (Fig. 2.2E). However, posttreatment of *Vibrio*

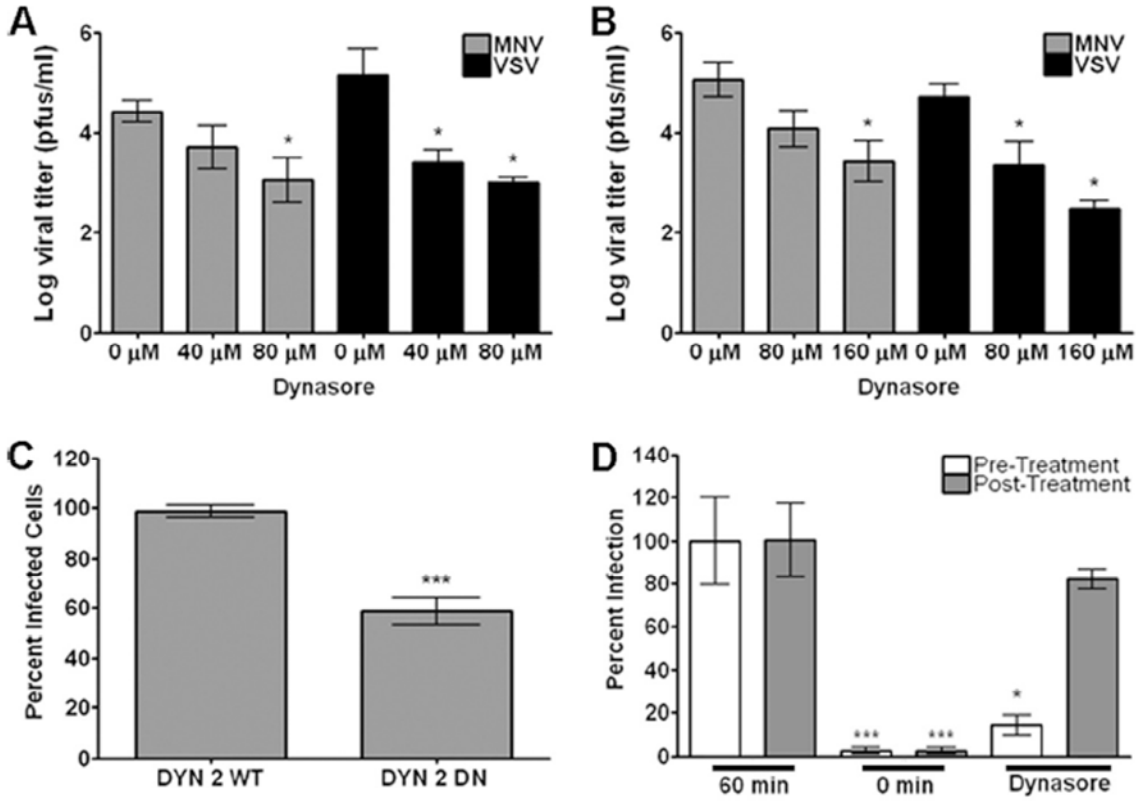

Figure 2.3. MNV-1 infection requires dynamin II. RAW 264.7 cells (A) and BMDMs (B) were pretreated with dynasore at the indicated concentration for 30 min, infected with MNV-1 or VSV on ice for 1 h, and washed with PBS. At 8 h (RAW 264.7 cells) or 10 h (BMDMs) postinfection, cells were freeze-thawed two times and viral titers determined by plaque assay. (C) RAW 264.7 cells were transfected with a wt and DN construct of GFP-tagged dynamin II and then infected with MNV-1 (MOI of 10) for 12 h. The number of VPg-expressing cells was determined by immunofluorescence and normalized to the wt control. (D) RAW 264.7 cells were infected with NR-containing virus at an MOI of 0.001, with rocking at room temperature for 60 min. RAW 264.7 cells were either pretreated (pretreatment) or treated for 60 min postinfection (posttreatment) with 80 μM dynasore before performing a plaque assay and determining viral titers. *****, $P < 0.05$; *******, $P < 0.001$.

cholerae neuraminidase led to a significant decrease in viral infection (Fig. 2.2E). We reasoned that this was due to the dependence of viral infection and spread on sialic acid (i.e., development of plaques). Therefore, we transferred cells to an untreated monolayer of RAW 264.7 cells to circumvent this potential problem. RAW 264.7 cells were infected for 60 min with MNV-1 and illuminated to inactivate virus. Cells were then treated with *Vibrio cholerae* neuraminidase for 90 min, washed, scraped from the plate, and added to an untreated monolayer of RAW 264.7 cells (posttransfer). No significant reduction in MNV-1 infection was observed (Fig. 2.2E). This demonstrated that MNV-1 entry but not later steps of the viral life cycle were inhibited by *Vibrio cholerae* neuraminidase. Taken together, these results confirm studies from our laboratory (54, 72) that MNV-1 enters RAW 264.7 cells in a sialic acid-dependent but pH-independent manner and validate the use of the NR assay for studying the infectious entry pathway of MNV-1.

MNV-1 entry into murine macrophages requires dynamin II.

Dynamin II is a small GTPase that functions by pinching off endosomes from the cell's plasma membrane (68). Its function is required for clathrin-, caveolin-, and cholesterol-dependent endocytosis pathways but not clathrin- and caveolin-independent processes (17, 41). The activity of dynamin II in phagocytosis has been suggested, but various mechanisms of viral entry through phagocytosis do not require it (12). To determine the role of dynamin II during MNV-1 infection, we obtained the small molecule inhibitor dynasore, which

specifically inhibits dynamin I, dynamin II, and Drp 1 (39). Dynamin I is activated only in neuronal cells, and Drp 1 is confined to the mitochondria (49, 67). Therefore, we reason that dynasore affects dynamin II in murine macrophages. RAW 264.7 cells were pretreated and infected at an MOI of 5 with MNV-1 or VSV in the presence of increasing amounts of dynasore or DMSO, and viral titers were determined 8 h postinfection (Fig. 2.3A). MNV-1 viral titers were significantly inhibited by dynasore pretreatment in a dose-dependent manner with an approximately 1.5-log inhibition in viral titers at 80 μM dynasore (Fig. 2.3A). VSV, a virus that requires dynamin II for its uptake via clathrin-mediated endocytosis (66), was used as a positive control and showed a significant decrease in viral titers at both concentrations of dynasore. Similar results were observed when BMDMs were infected, although higher effective concentrations of dynasore were needed in primary cells (Fig. 2.3B). Cell viability of treated cultured and primary macrophages was not significantly affected at these concentrations of inhibitor (Table 2.1). These results demonstrated that dynamin II plays a role in MNV-1 infection.

To further validate these results and look at earlier stages in the viral life cycle, the effect of the dynamin II DN construct K44A (7) on MNV-1 nonstructural gene expression was tested. Due to the poor transfection efficiency of primary macrophages, these experiments were performed only with RAW 264.7 cells. Cells were transfected with GFP-tagged wt and DN constructs. After 48 h, RAW 264.7 cells were infected with MNV-1 and VPg expression was measured by

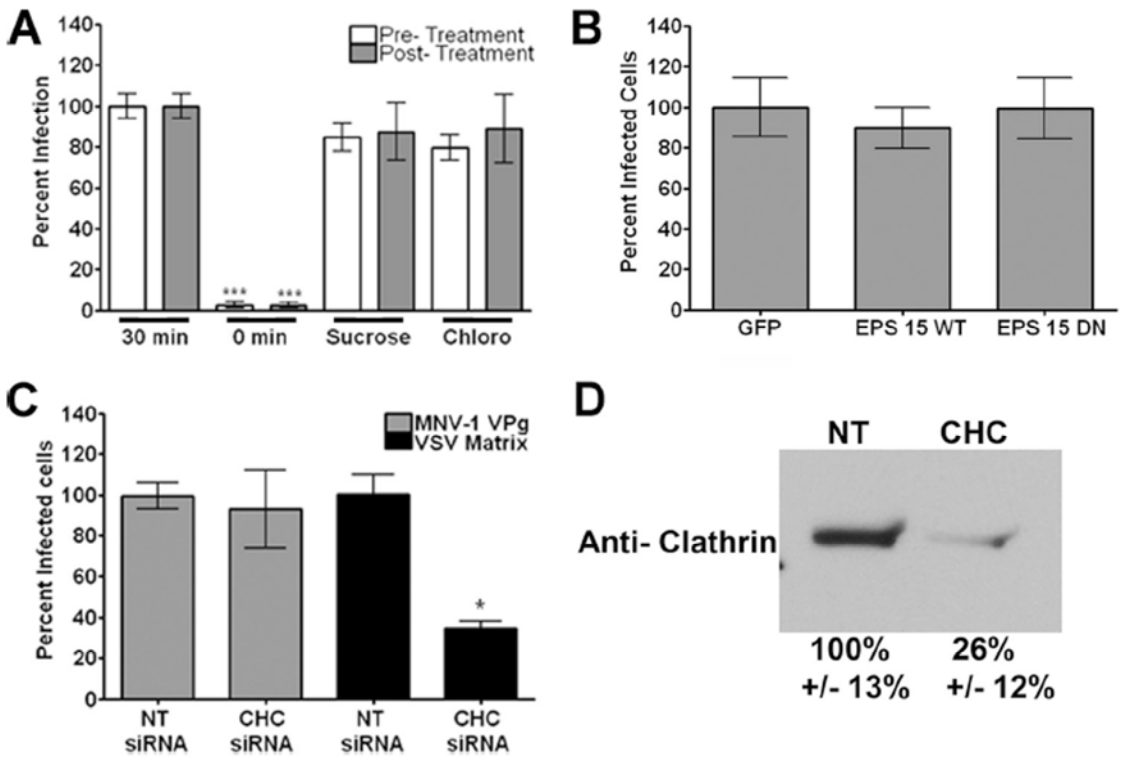

Figure 2.4. MNV-1 infection is clathrin independent. (A) RAW 264.7 cells were infected with NR-containing virus at an MOI of 0.001 and rocked at room temperature for 60 min. RAW 264.7 cells were either pretreated (pretreatment) or treated for 60 min pi (posttreatment) with 40 μM chlorpromazine (Chloro) or 300 mM sucrose. (B) RAW 264.7 cells were transfected with a GFP-only (GFP), GFP-tagged wt (EPS 15 wt), or DN construct (EPS 15 DN) of EPS 15 and then infected with MNV-1 at an MOI of 10 for 12 h. The number of VPg-expressing cells was determined by immunofluorescence and normalized to the value for the GFP-only control. (C) RAW 264.7 cells were incubated with an Accell siRNA clathrin heavy-chain construct (CHC siRNA) or a nontargeting construct (NT siRNA) (Dharmacon) for 72 h. Cells were then infected with MNV-1 or VSV at an MOI of 10. The number of VPg-expressing cells was determined by immunofluorescence 12 h after infection and normalized to the value for the NT control. (D) To verify clathrin heavy-chain protein knockdown, protein samples from cells expressing each siRNA construct were analyzed by immunoblotting for clathrin heavy chain, and protein levels were quantitated as described in the text. *****, $P < 0.05$; *******, $P < 0.001$.

immunofluorescence assay as previously described (54). The number of cells expressing VPg was quantitated and normalized to GFP-tagged wt dynamin II-expressing cells. A significant decrease in cells expressing VPg was observed with the DN construct compared to the wt control (Fig. 2.3C). These results demonstrated that MNV-1 gene expression requires dynamin II.

To determine the role of dynamin II during MNV-1 entry, we tested the effect of dynasore in the NR assay (Fig. 2.3D). Cell viability of treated cells was unaffected at these concentrations (Table 2.1). RAW 264.7 cells were pretreated with dynasore or vehicle control for 30 min and infected with NR-containing MNV-1, and the NR assay was performed as described above. A significant decrease in the number of plaques was observed for the pretreatment but not posttreatment samples, indicating MNV-1 entry required dynamin II. Together, these results demonstrated that dynamin II plays a role during MNV-1 entry into murine macrophages. However, the inability to completely block viral entry suggested a dynamin II-independent form(s) of endocytosis may also play a role during MNV-1 entry.

MNV-1 entry into murine macrophages is clathrin independent.

Clathrin-mediated endocytosis requires dynamin II (16). In addition, feline calicivirus (FCV), a member of the calicivirus family, like MNV-1, has been shown to enter cells through this process (65). Therefore, we determined the role of clathrin during MNV-1 entry. To test this, we first used two pharmacologic inhibitors of clathrin-mediated endocytosis, chlorpromazine and a hypotonic

solution of sucrose, in the NR assay. Chlorpromazine is an inhibitor of clathrin lattice polymerization (79), while a hypotonic solution of sucrose inhibits clathrin-coated pit formation in the plasma membrane (26). However, both inhibitors have known off-target effects (26, 63). Furthermore, these inhibitors are relatively cytotoxic to RAW 264.7 cells. To maintain cell viability above 80% and minimize side effects, RAW 264.7 cells were pretreated for 30 min with 40 μg/ml chlorpromazine or 300 mM sucrose, and the infection (performed in the presence of inhibitor) was reduced to 30 min. At these concentrations, we observed a significant decrease in the uptake of fluorescently labeled transferrin, a known clathrin-mediated endocytosis cargo protein (15), but not of fluorescently labeled cholera toxin B subunit (Fig. 2.1B and C and data not shown). We saw no significant reduction in MNV-1 entry with either chlorpromazine or sucrose treatment (Fig. 2.4A). Furthermore, posttreatment with these inhibitors did not affect MNV-1 infection (Fig. 2.4A). These results suggested MNV-1 entry is clathrin independent.

To confirm this finding, we tested wt and DN constructs of EPS 15, a required adaptor protein for clathrin-mediated endocytosis, for their effect on MNV-1 gene expression (Fig. 2.4B). EPS 15 directly links cargo proteins with the clathrin-coated pit adaptor protein 2 (AP-2) (3). Overexpression of the DN construct of EPS 15 selectively inhibits this process. RAW 264.7 were transfected with plasmids expressing GFP alone, GFP-tagged wt EPS 15, or GFP-tagged DN EPS 15 prior to infection, and virus-infected cells were quantitated by staining for VPg (Fig. 2.4B). We observed no significant change in the number of VPg-

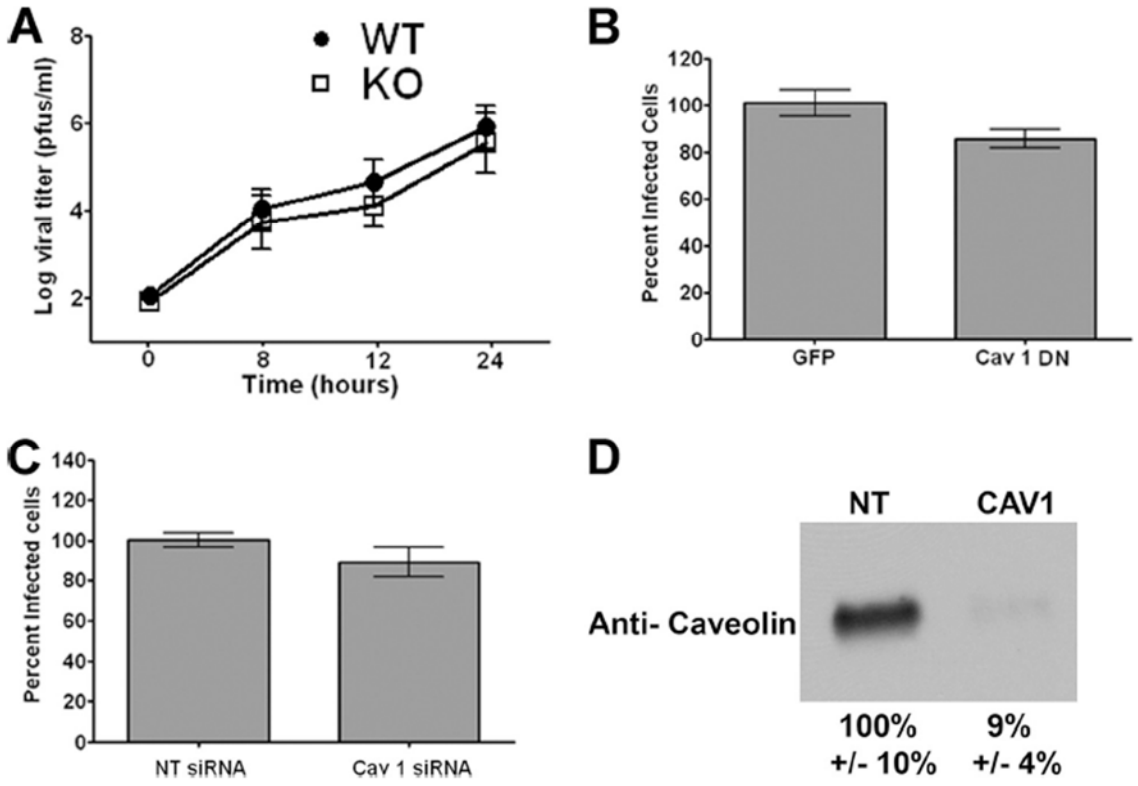

Figure 2.5. MNV-1 infection is caveolin independent. (A) BMDMs were isolated from caveolin 1 knockout mice and wt controls and infected with MNV-1 at an MOI of 2. Viral titers were determined at times indicated. (B) RAW 264.7 cells were transfected with a DN GFP-tagged caveolin 1 (CAV 1 DN) and a GFP-only control (GFP) construct and infected with MNV-1 at an MOI of 10 for 12 h. VPg-expressing cells were determined by immunofluorescence and normalized to the value for the GFP-only control. (C) RAW 264.7 cells were incubated with an Accell siRNA caveolin 1 construct (CAV 1 siRNA) or a nontargeting construct (NT siRNA) (Dharmacon) for 72 h. Cells were then infected with MNV-1 or VSV at an MOI of 10, and VPg expression was determined by immunofluorescence 12 h after infection. The number of VPg-expressing cells was normalized to the value for the NT control. (D) To verify caveolin 1 protein knockdown, protein samples from cells expressing each siRNA construct were analyzed by immunoblotting for caveolin 1 and quantitated as described in the text.

expressing cells in DN EPS 15 compared to those of wt-transfected or GFP-alone controls. These results further support the idea that clathrin played no role during MNV-1 infection.

However, not all clathrin-mediated endocytosis cargo requires EPS 15 (62). Therefore, we tested the role of clathrin during MNV-1 infection by siRNA knockdown of clathrin heavy chain (CHC). We obtained siRNA transfection efficiencies of over 93% for RAW 264.7 cells as determined by fluorescence-activated cell sorter analysis using a fluorescently labeled Accell siRNA construct from Dharmacon (data not shown). RAW 264.7 cells were transfected with an Accell siRNA for the CHC or an NT siRNA and infected with MNV-1 or VSV for 12h at an MOI of 10. Infected cells were quantified by immunofluorescence as described above and stained for MNV-1 VPg or the VSV matrix protein (Fig. 2.4C). No significant decrease of VPg-expressing cells was observed with CHC- compared to NT-transfected cells after MNV-1 infection (Fig. 2.4C). In contrast, a significant decrease of matrix-expressing cells was observed in CHC- compared to NT-transfected cells after VSV infection (Fig. 2.4C). This is consistent with a previous study in which CHC knockdown significantly reduced VSV infection (66). In addition, depletion of CHC was confirmed by analyzing protein levels of CHC by immunoblotting (Fig. 2.4D). CHC protein levels in CHC siRNA-expressing cells were reduced to 26% ± 12% of wt levels in NT siRNA-expressing cells. Taken together, these data demonstrated that clathrin plays no role in MNV-1 entry or infection.

MNV-1 entry into murine macrophages is caveolin 1 independent.

Another pathway dependent on dynamin II is caveolin-mediated endocytosis (25,50). Caveolin 1-associated vesicles can traffic to acidic early endosomes (52) or neutral pH caveosomes (53). Furthermore, previous data from our laboratory have shown that MNV-1 infection of murine macrophages and dendritic cells is not inhibited by the endosome acidification inhibitor bafilomycin A or chloroquine (54). Trafficking of MNV-1 to a pH-neutral compartment, such as the caveosome, would be consistent with this observation. Therefore, we next tested the hypothesis that MNV-1 enters cells in a caveolin 1-dependent manner. BMDMs were isolated from caveolin 1 knockout and matched wt control mice. Both wt and knockout BMDMs were infected with MNV-1 at an MOI of 2 and viral titers determined by plaque assay (Fig. 2.5A). No statistically significant decrease in viral titers was observed with the knockout BMDMs compared to the wt control cells over the examined time course (Fig. 2.5A), although knockout cells consistently produced slightly less MNV-1 than wt cells. Infections using MOIs of 0.5 and 0.05 also showed no significant decrease between the caveolin 1 knockout and wt macrophages (data not shown). These findings suggested that caveolin 1 does not play a significant role during MNV-1 infection.

To confirm these results, a caveolin 1 DN construct was also tested for its effect on MNV-1 viral gene expression. Fusion of GFP to the amino terminus of caveolin 1 prevents caveolin dimerization, and overexpression of this construct

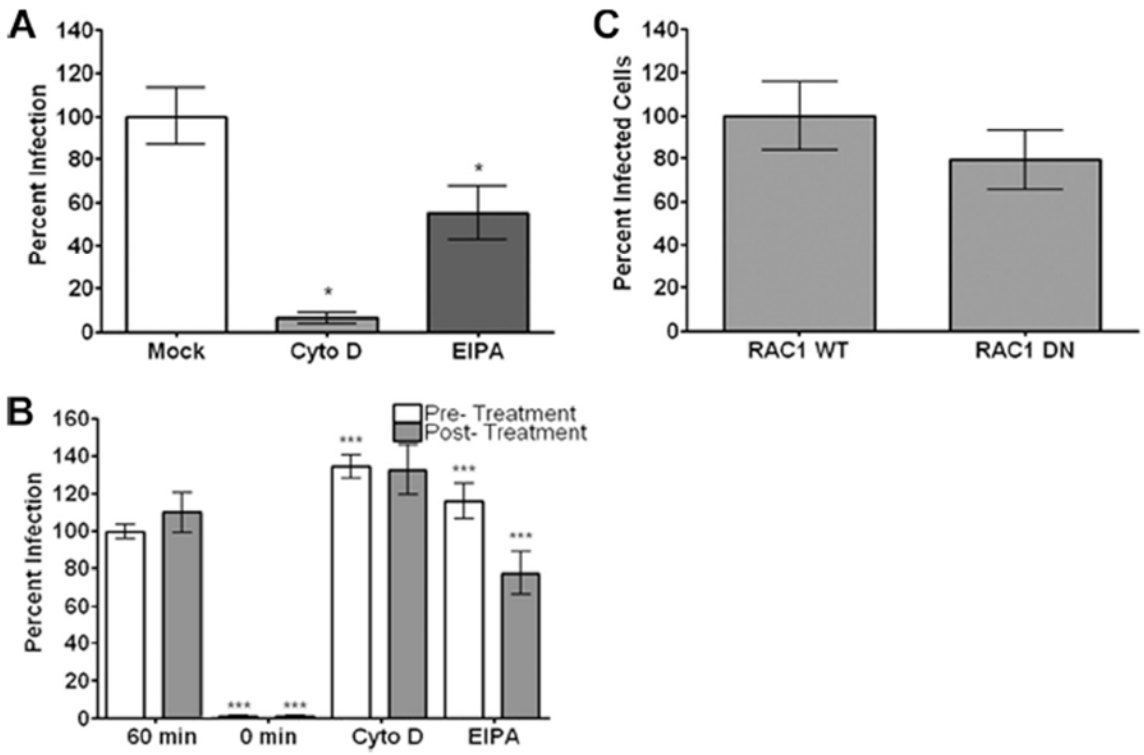

Figure 2.6. MNV-1 infection is independent of phagocytosis and/or macropinocytosis. (A) RAW 264.7 cells were pretreated with 10 μM cytochalasin D (Cyto D), 200 μM amiloride (EIPA), or mock control before infection with *Listeria monocytogenes* strain 10403S at an MOI of 1 for 30 min at 37°C. Replication of noninternalized bacteria was inhibited with 50 μg/ml gentamicin. After 1 h postinfection, cells were lysed and internalized bacteria plated onto LB plates. A total of 24 h after incubation at 37°C, CFU were quantitated and normalized to the value for the mock control. (B) RAW 264.7 cells were infected with NR-containing virus at an MOI of 0.001 and rocked at room temperature for 60 min. RAW 264.7 cells were either pretreated (pretreatment) or treated for 60 min pi (posttreatment) with 10 μM cytochalasin D (cyto D), 200 μM amiloride (EIPA), or mock control. (C) RAW 264.7 cells were transfected with a wt (RAC 1 wt) and a DN (RAC 1 DN) GFP-tagged Rac 1 and infected with MNV-1 at an MOI of 10 for 12 h. The number of VPg-expressing cells was determined by immunofluorescence and normalized to the value for the wt control. *****, $P < 0.05$; *******, $P < 0.001$.

functions as a DN inhibitor (53). RAW 264.7 cells were transfected with the GFP-tagged DN construct of caveolin 1 and a control plasmid expressing only GFP and infected with MNV-1. No significant decrease in the number of VPg-expressing cells was observed in cells transfected with the DN caveolin 1 construct compared to the GFP control-transfected cells (Fig. 2.5B). A trend toward a slightly decreased amount of infected cells was observed with RAW 264.7 cells, as was observed with BMDMs.

These results were also confirmed by siRNA knockdown of caveolin 1. An Accell siRNA (Dharmacon) targeted to caveolin 1 or an NT control siRNA was transfected into RAW 264.7 cells. Cells were infected with MNV-1 as described above and VPg-expressing cells enumerated. No significant decrease in the number of VPg-expressing cells was observed in the caveolin 1 siRNA-transfected cells compared to the NT control siRNA- transfected cells (Fig. 2.5C). Again, a slight but not statistically significant decrease in MNV-1 gene expression in caveolin 1 siRNA-transfected cells was observed, suggesting a potentially minor role for caveolin 1 during MNV-1 infection. Depletion of caveolin 1 in cells was confirmed by analyzing protein samples by immunoblotting (Fig. 2.5D). The relative knockdown of caveolin 1 was at 9% ± 4% of wt levels. Together, these data demonstrate that caveolin 1 did not play a major role in MNV-1 infection of murine macrophages.

MNV-1 entry into murine macrophages is independent of phagocytosis and/or macropinocytosis.

MNV-1 has a tropism for macrophages and dendritic cells (80, 84). These antigen-presenting cells are professional phagocytes (23), raising the possibility that MNV-1 entry occurs via phagocytosis. Furthermore, there is increasing evidence for the importance of macropinocytosis and/or phagocytosis as a mechanism for viral entry (45). Interestingly, although not a requirement, dynamin II can play a role in this process (reviewed in reference 45). Experimentally, however, it is difficult to separate the mechanisms of macropinocytosis and phagocytosis due to the similarities of these processes (reviewed in reference 45). Therefore, we are unable to distinguish an individual requirement of MNV-1 entry for either macropinocytosis or phagocytosis.

To address the importance of phagocytosis/macropinocytosis as an entry mechanism for MNV-1, we examined the effect of cytochalasin D, an inhibitor of actin polymerization, and 5-ethyl-*N*-isopropyl amiloride (EIPA), an inhibitor of macropinocytosis that blocks Na^+/H^+ exchange (82), on MNV-1 entry using the NR assay. Effective concentrations of these inhibitors in RAW 264.7 cells were determined by testing the internalization of the bacterium *L. monocytogenes* into RAW 264.7 cells in the presence of 10 μM cytochalasin D and 200 μM EIPA (Fig. 2.6A). *Listeria monocytogenes* entry into macrophages is dependent on phagocytosis, and uptake is inhibited by cytochalasin D (75). Cell viability of treated cells was unaffected at these concentrations of inhibitors (Table 2.1).

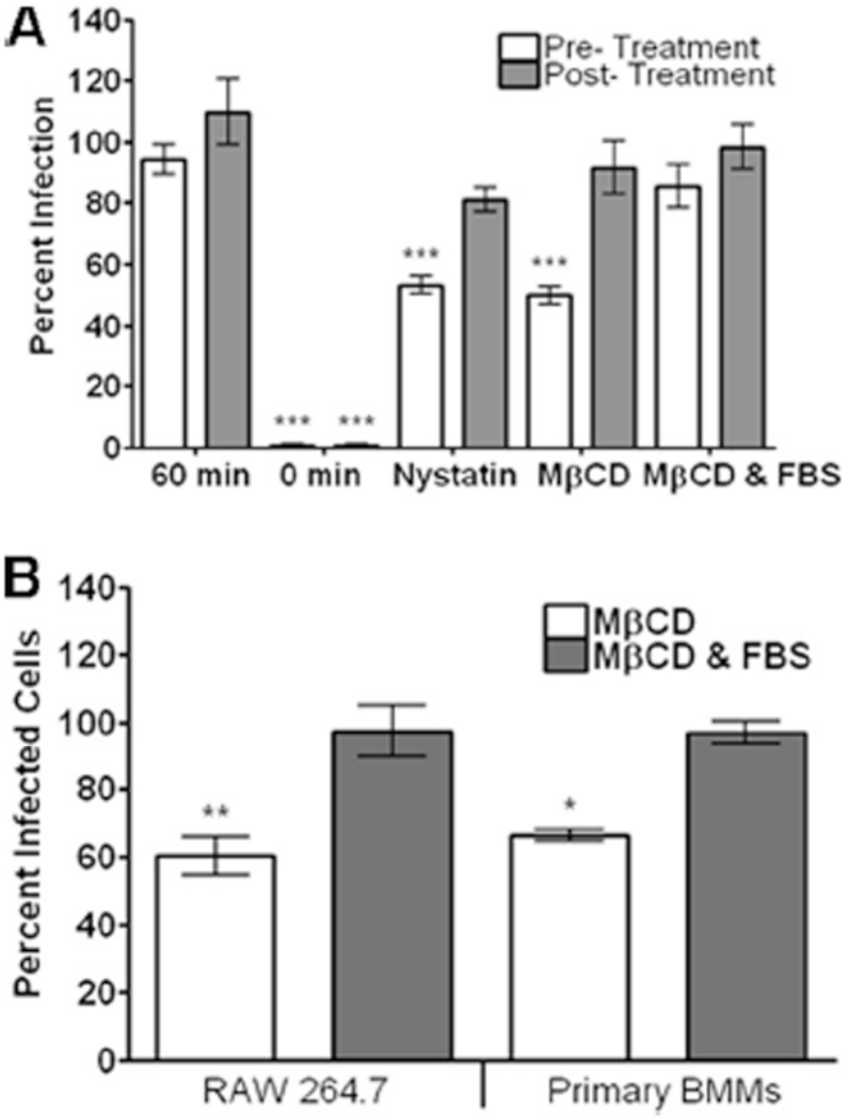

Figure 2.7. MNV-1 infection is cholesterol dependent. (A) RAW 264.7 cells were infected with NR-containing virus at an MOI of 0.001 and rocked at room temperature for 60 min. RAW 264.7 cells were either pretreated (pretreatment) or treated for 60 min pi (posttreatment) with 50 μM nystatin, 2 mM MβCD, or 2 mM MβCD with 10% fetal bovine serum (MβCD & FBS). (B) RAW 264.7 cells or BMDMs were infected with MNV-1 for 12 h after pretreatment with 2 mM MβCD or 2 mM MβCD with 10% fetal bovine serum (MβCD & FBS). The number of VPg-expressing cells was determined by immunofluorescence and normalized to the value for a no-treatment control. *****, $P < 0.05$; ******, $P < 0.01$; *******, $P < 0.001$.

Pretreatment of cells with cytochalasin D or EIPA did not lead to a decrease in MNV-1 infection in the NR assay (Fig. 2.6B). Instead, we observed a significant increase in the amount of MNV-1 entry in the presence of both inhibitors (Fig. 2.6B). This may be because of the upregulation of a productive route of infection by the inhibitors. Alternatively, phagocytosis/macropinocytosis may be a degradative pathway for MNV-1, and blocking this pathway leads to more viruses entering productive routes of infection. Posttreatment of cells with cytochalasin D had no significant effect on MNV-1 infection. Interestingly, posttreatment with EIPA showed a modest but significant decrease in the amount of MNV-1 infection (Fig. 2.6B), suggesting that later stages of the MNV-1 life cycle after entry are partially dependent on Na^+/H^+ exchange. Together, these data suggested that phagocytosis and/or macropinocytosis do not play a significant role in productive MNV-1 entry.

To validate this finding, we tested the requirement of Rac 1 during MNV-1 infection of RAW 264.7 cells. Rac 1 is a small GTPase required during remodeling of the cell's actin cytoskeleton to facilitate the massive membrane rearrangements necessary for phagocytosis (47). A GFP-tagged wt or DN Rac1 construct was transfected into RAW 264.7 cells and then infected with MNV-1. VPg expression was analyzed by immunofluorescence as described above (Fig. 2.6C). The number of VPg-expressing cells showed no significant decrease in the DN-transfected cells compared to the wt Rac 1-transfected cells (Fig. 2.6C). Taken together, these data demonstrated that Rac 1, which is required for phagocytosis/macropinocytosis, is not essential during MNV-1 infection.

However, it is possible that phagocytic mechanisms may play a minor role during later stages in MNV-1 infection, since we observed a decrease in viral infection after EIPA posttreatment and a slight (although not statistically significant) decrease in gene expression in the presence of DN Rac1.

MNV-1 entry into murine macrophages requires cholesterol.

Another form of endocytosis that requires dynamin II is cholesterol-dependent/dynamin II-dependent endocytosis, currently an ill-defined process. Interleukin 2 receptor, the original marker protein for this endocytic pathway, was recently proposed to enter cells by a phagocytic process (22). Some viruses also enter cells in a cholesterol-dependent/dynamin II-dependent manner (51, 61, 77). To address the role of cholesterol in MNV-1 entry, we performed entry and infection assays in the presence of the cholesterol-sequestering drugs MβCD or nystatin. To determine the effect of these drugs on viral entry, RAW 264.7 cells were pretreated with 2 mM MβCD for 1 h or 50 μM nystatin for 30 min to maintain cell viability above 80% (Table 2.1) and infected with NR-containing MNV-1 (Fig. 2.7A). We observed a significant decrease in the amount of virus entry in MβCD- or nystatin-pretreated cells but not in cells with reconstituted cholesterol levels (i.e., MβCD with FBS) (Fig. 2.7A). No effect on MNV-1 titers was observed when

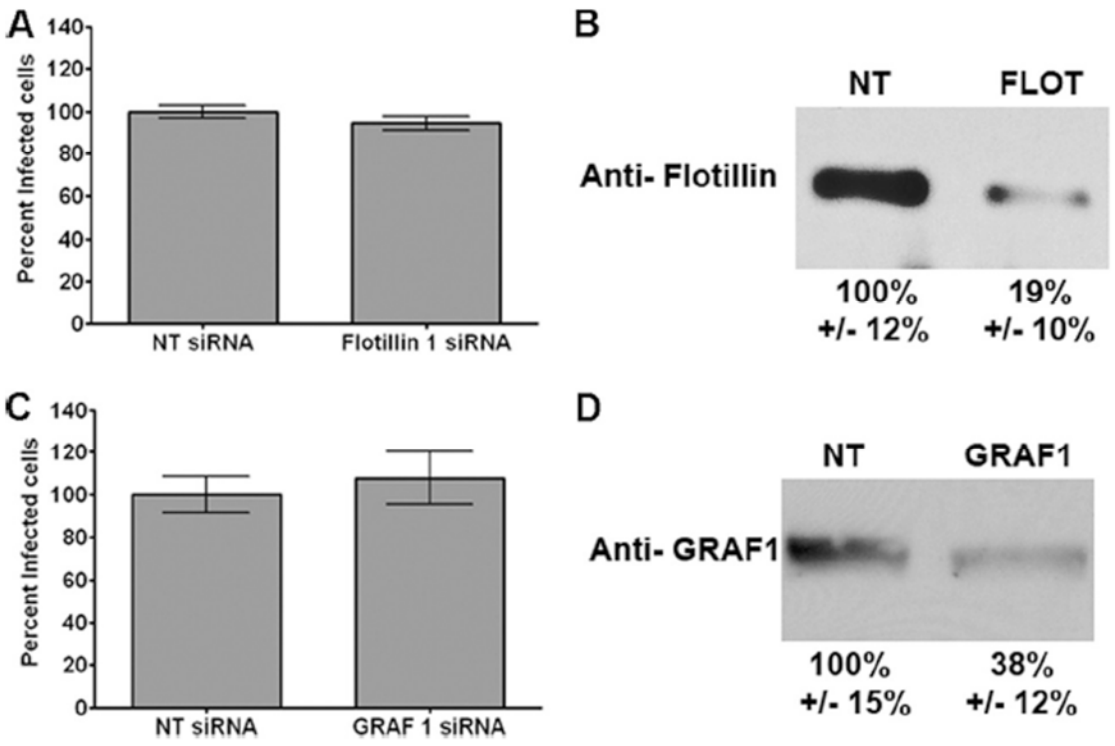

Figure 2.8. The major infectious route for MNV-1 is independent of flotillin-1 and GRAF1. RAW 264.7 cells were incubated with an Accell siRNA against flotillin-1 (A), GRAF1 (C), or a nontargeting (NT) construct (A and C) (Dharmacon) for 72 h. Cells were then infected with MNV-1 at an MOI of 10, and VPg expression was determined by immunofluorescence 12 h after infection. To verify flotillin-1 (FLOT) (B) or GRAF1 (D) protein knockdown, protein samples of cells transfected with the respective siRNA construct were analyzed by immunoblotting for flotillin-1 or GRAF1 and quantitated as described in the text.

cells were treated with these drugs after infection (posttreatment) (Fig. 2.7A). This suggests cholesterol plays an important role during MNV-1 entry.

To verify these results for productive infection of primary macrophages, MNV-1 VPg gene expression was measured by immunofluorescence microscopy. Both RAW 264.7 cells and BMDMs were infected with MNV-1 for 12 h after pretreatment with MβCD or MβCD with FBS. Treatment with MβCD but not MβCD with FBS significantly decreased the number of infected cells in cultured and primary macrophages (Fig. 7.7B), confirming the importance of cholesterol during MNV-1 infection in primary cells.

High concentrations of MβCD not only inhibit cholesterol-dependent mechanisms but can also affect clathrin-mediated endocytosis (76). Therefore, we infected RAW 264.7 cells and BMDMs with VSV after pretreatment with 2 mM MβCD and analyzed matrix protein expression by immunofluorescence. We observed no significant decrease in VSV matrix-expressing cells (data not shown). In addition, the uptake of fluorescently labeled transferrin as a marker of clathrin-mediated endocytosis was not affected by MβCD pretreatment, while internalized fluorescently labeled cholera toxin subunit B was significantly decreased (Fig. 2.1E, 2.1H). Hence, the levels of MβCD used herein are specific for cholesterol-dependent mechanisms. In summary, these results demonstrated an important role for cholesterol during MNV-1 entry in murine macrophages.

Flotillin-1 or GRAF1 plays no major role during MNV-1 infection of murine macrophages.

To identify further markers of MNV-1 entry, we focused on two proteins, flotillin-1 and GRAF1. Although no role during virus entry has been published to date for these proteins, flotillin-1 is a ubiquitous protein that associates with noncaveolar membrane microdomains and plays a role in some cholesterol-dependent methods of endocytosis (2). The small GTPase GRAF1 is required for another cholesterol-dependent pathway called CLIC (clathrin-independent carriers)/GEEC (GPI-enriched endocytic compartments) (37). We first tested whether MNV-1 entry requires flotillin-1. An Accell siRNA from Dharmacon targeting flotillin-1 or an NT control siRNA was transfected into RAW 264.7 cells prior to MNV-1 infection, and the number of virus-infected cells was determined by staining for VPg (Fig. 2.8A). No significant decrease in the number of VPg-expressing cells was observed with cells transfected with the flotillin-1 siRNA compared to those transfected with the NT control siRNA. This was despite the efficient knockdown of flotillin-1, which was confirmed by immunoblotting (Fig. 2.8B). The flotillin-1 protein level in flotillin-1 siRNA-transfected cells was reduced to 19% ± 10% of the protein level in cells transfected with NT siRNA (Fig. 2.8B). These data suggest that flotillin-1 does not play a major role during MNV-1 infection.

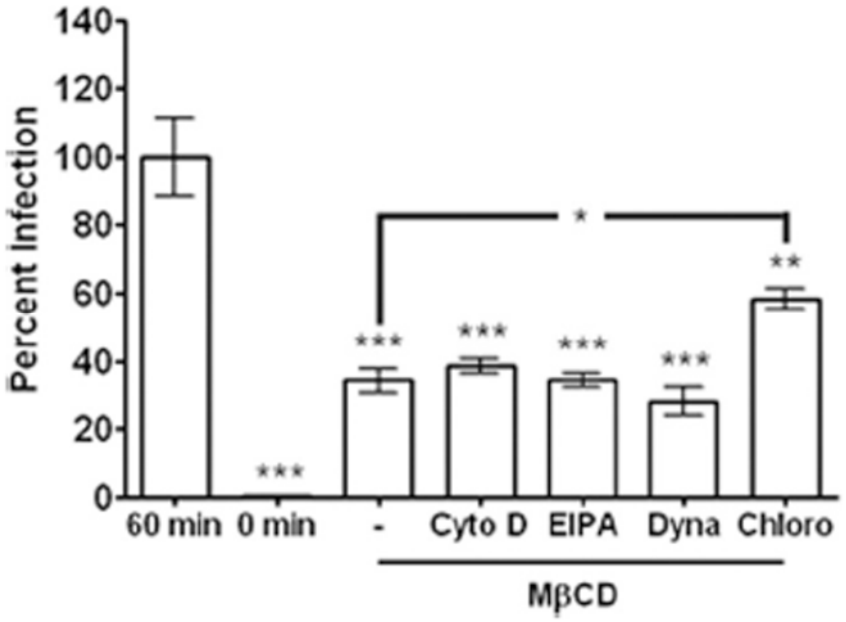

Figure 2.9. Clathrin- and caveolin-dependent endocytosis or phagocytosis/ macropinocytosis are not a minor route of entry for MNV-1. RAW 264.7 cells were pretreated with 2 mM MβCD alone (-), 2 mM MβCD and 10 μM cytochalasin D (cyto D), 2 mM MβCD and 200 μM amiloride (EIPA), 2 mM MβCD and 80 μM dynasore (Dyna), or 2 mM MβCD and 40 μM chlorpromazine (Chloro). RAW 264.7 cells were infected with NR-containing virus at an MOI of 0.001 and rocked at room temperature for 60 min before performing the NR assay and determining viral titers. *****, $P < 0.05$; ******, $P < 0.01$; *******, $P < 0.001$.

The requirement for cholesterol and a direct interaction between GRAF1 and dynamin II prompted us to determine whether GRAF1 is required for MNV-1 infection. RAW 264.7 cells were transfected with a GRAF1 and an NT siRNA, infected with MNV-1, and analyzed for VPg expression. No significant decrease in VPg-expressing cells was observed in GRAF1 siRNA-treated cells compared to the NT control (Fig. 2.8C). This was despite the successful knockdown of GRAF1 (protein levels were reduced to 38% ± 12% of the wt protein level) (Fig. 2.8D). This demonstrated that GRAF1 does not play a major role in MNV-1 uptake into macrophages, but, due to the level of GRAF1 knockdown, a requirement of GRAF1 in a minor route(s) of entry cannot be ruled out. Taken together, these data suggest that the major route of entry for MNV-1 is independent of flotillin-1 and GRAF1.

MNV-1 entry does not use clathrin-mediated endocytosis, caveolin-mediated endocytosis, and/or phagocytosis as a minor route of productive infection.

Overall, our data demonstrate a role for both dynamin II and cholesterol during MNV-1 entry. However, no pharmacologic treatment or expression of DN construct was able to decrease MNV-1 entry or VPg expression below 20% (Fig. 2.3, dynasore treatment). Under most conditions, we observed a decrease of about 50% in RAW 264.7 cells and slightly less in BMDMs. This suggested that either these inhibitors or DN constructs are unable to fully inhibit these processes or that the virus can productively enter the cell by more than one pathway. Virus

entering cells via multiple routes has previously been reported, e.g., influenza A virus (32) and SV40 (14). To test the hypothesis that MNV-1 enters cells by more than one productive pathway, we tested combinations of inhibitors in the NR assay (Fig. 2.9). We pretreated RAW 264.7 cells with combinations of MβCD and other inhibitors (nystatin, chlorpromazine, dynasore, cytochalasin D, and EIPA), infected the cells with NR-containing MNV-1, and performed the NR assay. No significant decrease in MNV-1 entry was observed in the combination treatments compared to the MβCD-only treatment. Inhibition of dynamin II by addition of dynasore and MβCD did not significantly decrease viral entry further compared to addition of MβCD alone, suggesting that clathrin-mediated and caveolin-mediated endocytosis did not play a role in MNV-1 infection. Similar results were obtained with EIPA or cytochalasin D and MβCD, suggesting that phagocytosis/macropinocytosis did not play a role during MNV-1 entry. Interestingly, a significant increase in viral entry was observed in MβCD- and chlorpromazine-treated cells (Fig. 2.9), despite a decrease of cell viability to approximately 60% of untreated controls (Table 2.1). Taken together, these data suggest that clathrin-mediated endocytosis, caveolin-mediated endocytosis, and phagocytosis/macropinocytosis did not play minor roles during MNV-1 infection in RAW 264.7 cells.

2.4 Discussion

Many viruses require the cellular mechanism of endocytosis to productively infect their host. The mechanism of entry during the productive route

of infection for noroviruses has not been addressed previously due to the lack of an efficient cell culture system. However, it has been suggested that the early steps of infection, including entry, are the determinants of cell tropism for this understudied group of viruses (24). Herein, we used a combination of pharmacologic inhibitor studies, dominant-negative mutants, and siRNA knockdowns, with a newly adapted neutral red assay to study the infectious route of entry of MNV-1. These data demonstrate that MNV-1 uptake occurs rapidly (within 1 h) and that the productive route of entry of MNV-1 into murine macrophages requires both host cholesterol and dynamin II. We also showed that the major route of MNV-1 infection of murine macrophages neither is clathrin, caveolin, flotillin-1, or GRAF1 dependent nor involves phagocytosis and/or macropinocytosis. During submission of this article, Gerondopoulos et al. published a report (20) demonstrating that MNV-1 entry into RAW 264.7 cells is mediated by dynamin and cholesterol but independent of clathrin, caveolin, flotillin-1, and macropinocytosis, confirming our findings with those cells.

While little is known about calicivirus entry, FCV enters cells via clathrin-mediated endocytosis (65). Our data clearly demonstrated that clathrin does not play a role during the productive route of infection of murine macrophages by MNV-1 (Fig. 2.4). This further highlights the differences during virus entry between these two viruses, as FCV (65), in contrast to MNV-1 (54), enters cells in a pH-dependent manner. Whether these entry differences reflect differences in the pathogenesis of a respiratory (FCV) versus an enteric (MNV-1) virus and/or differences in the examined cell types (epithelial cells versus macrophages)

remains unknown. In addition, a requirement for host cholesterol during HuNoV replication is known. Inhibitors of cholesterol synthesis significantly reduced HuNoV replication in a HuNoV replicon system (9). Although the direct role of cholesterol during MNV-1 replication was not addressed here, the common requirement for host cholesterol during MNV-1 and HuNoV infection suggests a conservation of cellular constituents during norovirus infection.

The mechanism of cholesterol-and dynamin II-dependent endocytosis is not well defined. Few viruses are reported to enter cells in this manner. Feline infectious peritonitis virus (FIPV) infection of monocytes, a macrophage precursor, is sensitive to the cholesterol-sequestering drug nystatin (but not MβCD) and dynasore (77). Group B coxsackievirus 3 (CVB3) infection of HeLa cells is inhibited by the dynamin II DN construct, K44A, dynasore, MβCD, and filipin treatment (51). Furthermore, rotavirus entry into MA104 cells is inhibited by the K44A DN mutant of dynamin II and by depletion of cholesterol with MβCD but not the other cholesterol-sequestering drugs nystatin and filipin (61). Similar to our results with MNV-1 (Fig. 2.3 and 2.7), inhibition of dynamin II or cholesterol depletion only partially reduced entry of FIPV, CVB3, and rotavirus. Whether this reflects an inherent ability of cells to compensate for blocked endocytic pathways and/or an ability of viruses to use more than one entry pathway remains unknown.

We investigated the role of alternative or minor routes of MNV-1 entry by treatments with combinations of inhibitors in the NR assay. Although no

combination of inhibitors showed a significant decrease in the amount of MNV-1 entry over MβCD treatment alone, we observed a significant increase in the amount of viral entry occurring in the presence of both MβCD and chlorpromazine. This increase was observed despite a decrease in the cell viability to approximately 60% of the untreated control. Although the biological significance of this finding is unclear, this result suggested that MNV-1 can enter RAW 264.7 cells by a clathrin- and cholesterol-independent pathway that is upregulated by treatment with chlorpromazine and MβCD.

In this report, we identified a requirement for cholesterol and dynamin II during MNV-1 entry. However, specific cellular targets of the host endocytic machinery interacting with MNV-1 during this stage in the viral life cycle remain elusive. Further definition of the mechanism of MNV-1 entry will not only better describe a poorly defined endocytic pathway but may also lead to the identification of cellular targets with antinoroviral potential.

2. 5 References

1. **Anderson, H. A., Y. Chen, and L. C. Norkin.** 1996. Bound simian virus 40 translocates to caveolin-enriched membrane domains, and its entry is inhibited by drugs that selectively disrupt caveolae. Mol. Biol. Cell 7:1825-1834.
2. **Babuke, T., and R. Tikkanen.** 2007. Dissecting the molecular function of reggie/flotillin proteins. Eur. J. Cell Biol. 86:525-532.
3. **Belleudi, F., V. Visco, M. Ceridono, L. Leone, R. Muraro, L. Frati, and M. R. Torrisi.** 2003. Ligand-induced clathrin-mediated endocytosis of the keratinocyte growth factor receptor occurs independently of either phosphorylation or recruitment of eps15. FEBS Lett. 553:262-270.
4. **Benmerah, A., M. Bayrou, N. Cerf-Bensussan, and A. Dautry-Varsat.** 1999. Inhibition of clathrin-coated pit assembly by an Eps15 mutant. J. Cell Sci. 112:1303-1311.
5. **Blanton, L. H., S. M. Adams, R. S. Beard, G. Wei, S. N. Bulens, M. A. Widdowson, R. I. Glass, and S. S. Monroe.** 2006. Molecular and epidemiologic trends of caliciviruses associated with outbreaks of acute gastroenteritis in the United States, 2000-2004. J. Infect. Dis. 193:413-421.
6. **Borrow, P., and M. B. Oldstone.** 1994. Mechanism of lymphocytic choriomeningitis virus entry into cells. Virology 198:1-9.
7. **Brandenburg, B., L. Y. Lee, M. Lakadamyali, M. J. Rust, X. Zhuang, and J. M. Hogle.** 2007. Imaging poliovirus entry in live cells. PLoS Biol. 5:e183.
8. **Cao, H., H. M. Thompson, E. W. Krueger, and M. A. McNiven.** 2000. Disruption of Golgi structure and function in mammalian cells expressing a mutant dynamin. J. Cell Sci. 113:1993-2002.
9. CDC. 2007. Norovirus activity—United States, 2006-2007. MMWR Morb. Mortal. Wkly. Rep. 56:842-846.
10. **Chang, K. O.** 2009. Role of cholesterol pathways in norovirus replication. J. Virol. 83:8587-8595.
11. **Chaudhry, Y., M. A. Skinner, and I. G. Goodfellow.** 2007. Recovery of genetically defined murine norovirus in tissue culture by using a fowlpox virus expressing T7 RNA polymerase. J. Gen. Virol. 88:2091-2100.
12. **Clement, C., V. Tiwari, P. M. Scanlan, T. Valyi-Nagy, B. Y. Yue, and D. Shukla.** 2006. A novel role for phagocytosis-like uptake in herpes simplex virus entry. J. Cell Biol. 174:1009-1021.
13. **Conner, S. D., and S. L. Schmid.** 2003. Regulated portals of entry into the cell. Nature 422:37-44.
14. **Coyne, C. B., L. Shen, J. R. Turner, and J. M. Bergelson.** 2007. Coxsackievirus entry across epithelial tight junctions requires occludin and the small GTPases Rab34 and Rab5. Cell Host Microbe 2:181-192.
15. **Damm, E. M., L. Pelkmans, J. Kartenbeck, A. Mezzacasa, T. Kurzchalia, and A. Helenius.** 2005. Clathrin- and caveolin-1-independent

endocytosis: entry of simian virus 40 into cells devoid of caveolae. J. Cell Biol. 168:477-488.
16. **Dautry-Varsat, A.** 1986. Receptor-mediated endocytosis: the intracellular journey of transferrin and its receptor. Biochimie 68:375-38.
17. **De Camilli, P., K. Takei, and P. S. McPherson.** 1995. The function of dynamin in endocytosis. Curr. Opin. Neurobiol. 5:559-565.
18. **Doherty, G. J., and H. T. McMahon.** 2009. Mechanisms of endocytosis. Annu. Rev. Biochem. 78:857-902.
19. **Estes, M. K., B. V. Prasad, and R. L. Atmar.** 2006. Noroviruses everywhere: has something changed? Curr. Opin. Infect. Dis. 19:467-474.
20. **Fankhauser, R. L., S. S. Monroe, J. S. Noel, C. D. Humphrey, J. S. Bresee, U. D. Parashar, T. Ando, and R. I. Glass.** 2002. Epidemiologic and molecular trends of "Norwalk-like viruses" associated with outbreaks of gastroenteritis in the United States. J. Infect. Dis. 186:1-7.
21. **Gerondopoulos, A., T. Jackson, P. Monaghan, N. Doyle, and L. O. Roberts.** 2010. Murine norovirus-1 cell entry is mediated through a non-clathrin, non-caveolae, dynamin and cholesterol dependent pathway. J. Gen. Virol. [Epub ahead of print] doi:10.1099/vir.0.016717-0.
22. **Ghigo, E., J. Kartenbeck, P. Lien, L. Pelkmans, C. Capo, J. L. Mege, and D. Raoult.** 2008. Ameobal pathogen mimivirus infects macrophages through phagocytosis. PLoS Pathog. 4:e1000087.
23. **Grassart, A., A. Dujeancourt, P. B. Lazarow, A. Dautry-Varsat, and N. Sauvonnet.** 2008. Clathrin-independent endocytosis used by the IL-2 receptor is regulated by Rac1, Pak1 and Pak2. EMBO Rep. 9:356-362.
24. **Groves, E., A. E. Dart, V. Covarelli, and E. Caron.** 2008. Molecular mechanisms of phagocytic uptake in mammalian cells. Cell. Mol. Life Sci. 65:1957-1976.
25. **Guix, S., M. Asanaka, K. Katayama, S. E. Crawford, F. H. Neill, R. L. Atmar, and M. K. Estes.** 2007. Norwalk virus RNA is infectious in mammalian cells. J. Virol. 81:12238-12248.
26. **Henley, J. R., E. W. Krueger, B. J. Oswald, and M. A. McNiven.** 1998. Dynamin-mediated internalization of caveolae. J. Cell Biol. 141:85-99.
27. **Heuser, J. E., and R. G. Anderson.** 1989. Hypertonic media inhibit receptor-mediated endocytosis by blocking clathrin-coated pit formation. J. Cell Biol. 108:389-400.
28. **Hoppe, A. D., and J. A. Swanson.** 2004. Cdc42, Rac1, and Rac2 display distinct patterns of activation during phagocytosis. Mol. Biol. Cell 15:3509-3519.
29. **Karst, S. M., C. E. Wobus, M. Lay, J. Davidson, and H. W. Virgin IV.** 2003. STAT1-dependent innate immunity to a Norwalk-like virus. Science 299:1575-1578.
30. **Kartenbeck, J., H. Stukenbrok, and A. Helenius**. 1989. Endocytosis of simian virus 40 into the endoplasmic reticulum. J. Cell Biol. 109:2721-2729.
31. **Katpally, U., N. R. Voss, T. Cavazza, S. Taube, J. R. Rubin, V. L. Young, J. Stuckey, V. K. Ward, H. W. Virgin IV, C. E. Wobus, and T. J.**

Smith. 24 March 2010. High-resolution cryo-electron microscopy structures of MNV-1 and RHDV reveals marked flexibility in the receptor binding domains. J. Virol. doi:10.1128/JVI.00314-10.

32. **Katpally, U., C. E. Wobus, K. Dryden, H. W. Virgin IV, and T. J. Smith.** 2008. Structure of antibody-neutralized murine norovirus and unexpected differences from viruslike particles. J. Virol. 82:2079-2088.
33. **Koopmans, M., J. Vinje, M. de Wit, I. Leenen, W. van der Poel, and Y. van Duynhoven.** 2000. Molecular epidemiology of human enteric caliciviruses in The Netherlands. J. Infect. Dis. 181(Suppl. 2):S262-S269.
34. **Lakadamyali, M., M. J. Rust, H. P. Babcock, and X. Zhuang.** 2003. Visualizing infection of individual influenza viruses. Proc. Natl. Acad. Sci. U. S. A. 100:9280-9285.
35. **Le Pendu, J.** 2004. Histo-blood group antigen and human milk oligosaccharides: genetic polymorphism and risk of infectious diseases. Adv. Exp. Med. Biol. 554:135-143.
36. **Le Pendu, J., N. Ruvoen-Clouet, E. Kindberg, and L. Svensson.** 2006. Mendelian resistance to human norovirus infections. Semin. Immunol. 18:375-386.
37. **Lindesmith, L., C. Moe, S. Marionneau, N. Ruvoen, X. Jiang, L. Lindblad, P. Stewart, J. LePendu, and R. Baric.** 2003. Human susceptibility and resistance to Norwalk virus infection. Nat. Med. 9:548-553.
38. **Liu, N. Q., A. S. Lossinsky, W. Popik, X. Li, C. Gujuluva, B. Kriederman, J. Roberts, T. Pushkarsky, M. Bukrinsky, M. Witte, M. Weinand, and M. Fiala.** 2002. Human immunodeficiency virus type 1 enters brain microvascular endothelia by macropinocytosis dependent on lipid rafts and the mitogen-activated protein kinase signaling pathway. J. Virol. 76:6689-6700.
39. **Lundmark, R., G. J. Doherty, M. T. Howes, K. Cortese, Y. Vallis, R. G. Parton, and H. T. McMahon.** 2008. The GTPase-activating protein GRAF1 regulates the CLIC/GEEC endocytic pathway. Curr. Biol. 18:1802-1808.
40. **Lyles, D. S., L. Puddington, and B. J. McCreedy, Jr.** 1988. Vesicular stomatitis virus M protein in the nuclei of infected cells. J. Virol. 62:4387-4392.
41. **Macia, E., M. Ehrlich, R. Massol, E. Boucrot, C. Brunner, and T. Kirchhausen.** 2006. Dynasore, a cell-permeable inhibitor of dynamin. Dev. Cell 10:839-850.
42. **Maréchal, V., M. C. Prevost, C. Petit, E. Perret, J. M. Heard, and O. Schwartz.** 2001. Human immunodeficiency virus type 1 entry into macrophages mediated by macropinocytosis. J. Virol. 75:11166-11177.
43. **Marsh, M., and A. Helenius.** 2006. Virus entry: open sesame. Cell 124:729-740.
44. **Matilainen, H., J. Rinne, L. Gilbert, V. Marjomaki, H. Reunanen, and C. Oker-Blom.** 2005. Baculovirus entry into human hepatoma cells. J. Virol. 79:15452-15459.

45. **Mead, P. S., L. Slutsker, V. Dietz, L. F. McCaig, J. S. Bresee, C. Shapiro, P. M. Griffin, and R. V. Tauxe.** 1999. Food-related illness and death in the United States. Emerg. Infect. Dis. 5:607-625.
46. **Meier, O., K. Boucke, S. V. Hammer, S. Keller, R. P. Stidwill, S. Hemmi, and U. F. Greber.** 2002. Adenovirus triggers macropinocytosis and endosomal leakage together with its clathrin-mediated uptake. J. Cell Biol. 158:1119-1131.
47. **Mercer, J., and A. Helenius.** 2009. Virus entry by macropinocytosis. Nat. Cell Biol. 11:510-520.
48. **Moreno-Espinosa, S., T. Farkas, and X. Jiang.** 2004. Human caliciviruses and pediatric gastroenteritis. Semin. Pediatr. Infect. Dis. 15:237-245.
49. **Niedergang, F., and P. Chavrier.** 2005. Regulation of phagocytosis by Rho GTPases. Curr. Top. Microbiol. Immunol. 291:43-60.
50. **Norkin, L. C., H. A. Anderson, S. A. Wolfrom, and A. Oppenheim.** 2002. Caveolar endocytosis of simian virus 40 is followed by brefeldin A-sensitive transport to the endoplasmic reticulum, where the virus disassembles. J. Virol. 76:5156-5166.
51. **Obar, R. A., C. A. Collins, J. A. Hammarback, H. S. Shpetner, and R. B. Vallee.** 1990. Molecular cloning of the microtubule-associated mechanochemical enzyme dynamin reveals homology with a new family of GTP-binding proteins. Nature 347:256-261.
52. **Oh, P., D. P. McIntosh, and J. E. Schnitzer.** 1998. Dynamin at the neck of caveolae mediates their budding to form transport vesicles by GTP-driven fission from the plasma membrane of endothelium. J. Cell Biol. 141:101-114.
53. **Patel, K. P., C. B. Coyne, and J. M. Bergelson.** 2009. Dynamin- and lipid raft-dependent entry of decay-accelerating factor (DAF)-binding and non-DAF-binding coxsackieviruses into nonpolarized cells. J. Virol. 83:11064-11077.
54. **Pelkmans, L., T. Burli, M. Zerial, and A. Helenius.** 2004. Caveolin-stabilized membrane domains as multifunctional transport and sorting devices in endocytic membrane traffic. Cell 118:767-780.
55. **Pelkmans, L., J. Kartenbeck, and A. Helenius.** 2001. Caveolar endocytosis of simian virus 40 reveals a new two-step vesicular-transport pathway to the ER. Nat. Cell Biol. 3:473-483.
56. **Perry, J. W., S. Taube, and C. E. Wobus.** 2009. Murine norovirus-1 entry into permissive macrophages and dendritic cells is pH-independent. Virus Res. 143:125-129.
57. **Pietiäinen, V., V. Marjomaki, P. Upla, L. Pelkmans, A. Helenius, and T. Hyypia.** 2004. Echovirus 1 endocytosis into caveosomes requires lipid rafts, dynamin II, and signaling events. Mol. Biol. Cell 15:4911-4925.
58. **Pietiäinen, V. M., V. Marjomaki, J. Heino, and T. Hyypia.** 2005. Viral entry, lipid rafts and caveosomes. Ann. Med. 37:394-403.
59. **Quirin, K., B. Eschli, I. Scheu, L. Poort, J. Kartenbeck, and A. Helenius.** 2008. Lymphocytic choriomeningitis virus uses a novel

endocytic pathway for infectious entry via late endosomes. Virology 378:21-33.
60. **Rojek, J. M., M. Perez, and S. Kunz.** 2008. Cellular entry of lymphocytic choriomeningitis virus. J. Virol. 82:1505-1517.
61. **Rust, M. J., M. Lakadamyali, F. Zhang, and X. Zhuang.** 2004. Assembly of endocytic machinery around individual influenza viruses during viral entry. Nat. Struct. Mol. Biol. 11:567-573.
62. **Rydell, G. E., J. Nilsson, J. Rodriguez-Diaz, N. Ruvoen-Clouet, L. Svensson, J. Le Pendu, and G. Larson.** 2009. Human noroviruses recognize sialyl Lewis x neoglycoprotein. Glycobiology 19:309-320.
63. **Sánchez-San Martín, C., T. Lopez, C. F. Arias, and S. Lopez.** 2004. Characterization of rotavirus cell entry. J. Virol. 78:2310-2318.
64. **Sieczkarski, S. B., and G. R. Whittaker.** 2002. Dissecting virus entry via endocytosis. J. Gen. Virol. 83:1535-1545.
65. **Spoden, G., K. Freitag, M. Husmann, K. Boller, M. Sapp, C. Lambert, and L. Florin.** 2008. Clathrin- and caveolin-independent entry of human papillomavirus type 16—involvement of tetraspanin-enriched microdomains (TEMs). PLoS One 3:e3313.
66. **Stuart, A. D., and T. D. Brown.** 2006. Entry of feline calicivirus is dependent on clathrin-mediated endocytosis and acidification in endosomes. J. Virol. 80:7500-7509.
67. **Sun, X., V. K. Yau, B. J. Briggs, and G. R. Whittaker.** 2005. Role of clathrin-mediated endocytosis during vesicular stomatitis virus entry into host cells. Virology 338:53-60.
68. **Taguchi, N., N. Ishihara, A. Jofuku, T. Oka, and K. Mihara.** 2007. Mitotic phosphorylation of dynamin-related GTPase Drp1 participates in mitochondrial fission. J. Biol. Chem. 282:11521-11529.
69. **Takei, K., P. S. McPherson, S. L. Schmid, and P. De Camilli.** 1995. Tubular membrane invaginations coated by dynamin rings are induced by GTP-gamma S in nerve terminals. Nature 374:186-190.
70. **Tamura, M., K. Natori, M. Kobayashi, T. Miyamura, and N. Takeda.** 2004. Genogroup II noroviruses efficiently bind to heparan sulfate proteoglycan associated with the cellular membrane. J. Virol. 78:3817-3826.
71. **Tan, M., and X. Jiang. 2007.** Norovirus-host interaction: implications for disease control and prevention. Expert Rev. Mol. Med. 9:1-22.
72. **Tan, M., and X. Jiang. 2005.** Norovirus and its histo-blood group antigen receptors: an answer to a historical puzzle. Trends Microbiol. 13:285-293.
73. **Taube, S., J. W. Perry, K. Yetming, S. P. Patel, H. Auble, L. Shu, H. F. Nawar, C. H. Lee, T. D. Connell, J. A. Shayman, and C. E. Wobus.** 2009. Ganglioside-linked terminal sialic acid moieties on murine macrophages function as attachment receptors for murine noroviruses. J. Virol. 83:4092-4101.
74. **Taube, S., J. R. Rubin, U. Katpally, T. J. Smith, A. Kendall, J. A. Stuckey, and C. E. Wobus.** 24 March 2010. High resolution x-ray structure and functional analysis of the murine norovirus (MNV)-1 capsid

protein protruding (P) domain. J. Virol. [Epub ahead of print]. doi:10.1128/JVI.00316-10.

75. **Thackray, L. B., C. E. Wobus, K. A. Chachu, B. Liu, E. R. Alegre, K. S. Henderson, S. T. Kelley, and H. W. Virgin IV.** 2007. Murine noroviruses comprising a single genogroup exhibit biological diversity despite limited sequence divergence. J. Virol. 81:10460-10473.
76. **Tilney, L. G., and D. A. Portnoy.** 1989. Actin filaments and the growth, movement, and spread of the intracellular bacterial parasite, Listeria monocytogenes. J. Cell Biol. 109:1597-1608.
77. **Urs, N. M., K. T. Jones, P. D. Salo, J. E. Severin, J. Trejo, and H. Radhakrishna.** 2005. A requirement for membrane cholesterol in the beta-arrestin- and clathrin-dependent endocytosis of LPA1 lysophosphatidic acid receptors. J. Cell Sci. 118:5291-5304.
78. **Van Hamme, E., H. L. Dewerchin, E. Cornelissen, B. Verhasselt, and H. J. Nauwynck.** 2008. Clathrin- and caveolae-independent entry of feline infectious peritonitis virus in monocytes depends on dynamin. J. Gen. Virol. 89:2147-2156.
79. **Vidricaire, G., and M. J. Tremblay.** 2007. A clathrin, caveolae, and dynamin-independent endocytic pathway requiring free membrane cholesterol drives HIV-1 internalization and infection in polarized trophoblastic cells. J. Mol. Biol. 368:1267-1283.
80. **Wang, L. H., K. G. Rothberg, and R. G. Anderson.** 1993. Mis-assembly of clathrin lattices on endosomes reveals a regulatory switch for coated pit formation. J. Cell Biol. 123:1107-1117.
81. **Ward, J. M., C. E. Wobus, L. B. Thackray, C. R. Erexson, L. J. Faucette, G. Belliot, E. L. Barron, S. V. Sosnovtsev, and K. Y. Green.** 2006. Pathology of immunodeficient mice with naturally occurring murine norovirus infection. Toxicol. Pathol. 34:708-715.
82. **Ward, V. K., C. J. McCormick, I. N. Clarke, O. Salim, C. E. Wobus, L. B. Thackray, H. W. Virgin IV, and P. R. Lambden.** 2007. Recovery of infectious murine norovirus using pol II-driven expression of full-length cDNA. Proc. Natl. Acad. Sci. U. S. A. 104:11050-11055.
83. **West, M. A., M. S. Bretscher, and C. Watts.** 1989. Distinct endocytotic pathways in epidermal growth factor-stimulated human carcinoma A431 cells. J. Cell Biol. 109:2731-2739.
84. **Widdowson, M. A., S. S. Monroe, and R. I. Glass.** 2005. Are noroviruses emerging? Emerg. Infect. Dis. 11:735-737.
85. **Wobus, C. E., S. M. Karst, L. B. Thackray, K. O. Chang, S. V. Sosnovtsev, G. Belliot, A. Krug, J. M. Mackenzie, K. Y. Green, and H. W. Virgin.** 2004. Replication of norovirus in cell culture reveals a tropism for dendritic cells and macrophages. PLoS Biol. 2:e432

Chapter 3

Murine norovirus 1 entry into permissive macrophages and dendritic cells is pH-independent

(This chapter was published in Virus Research.
Jeffrey W. Perry, Stefan Taube and Christiane E. Wobus. Murine Norovirus-1 entry into permissive macrophages and Dendritic cells is pH-independent.Virus Research. 2009 Jul; 143(1):125-129)

(J.W. Perry designed and performed experiments, analysed data and prepared the manuscript. M. S. Taube designed experiments and analysed data. C. E. Wobus designed experiments, analysed data, and prepared the manuscript.)

3.1 Abstract

Murine norovirus (MNV) is a recently discovered mouse pathogen. Unlike the fastidious human noroviruses that cause the overwhelming majority of non-bacterial gastroenteritis worldwide, MNV readily infects cells in culture. Its replication in primary murine macrophages and dendritic cells and their derived

cell lines allows the study of norovirus cell entry for the first time. In this study we determined the role of pH during MNV-1 infection since the low pH environment of endosomes often triggers uncoating of viruses. We demonstrated that MNV-1 viral titers by plaque assay and expression of the non-structural protein VPg by immunofluorescence were not affected by pH in cultured and primary macrophages and dendritic cells in the presence of two known endosome acidification inhibitors, bafilomycin A1 and chloroquine. These data indicate that MNV-1 enters permissive cells in a pH-independent manner.

3.2 Introduction

Noroviruses are an understudied group of non-enveloped positive strand RNA viruses that belong to the *Caliciviridae* family (12). Despite the significant impact of human noroviruses (HuNoV) on public health worldwide as the major agent of non-bacterial gastroenteritis (12), no drug or vaccine exists to treat norovirus infections. This is partially due to the absence of a robust tissue culture system (9, 28). In contrast, murine norovirus (MNV), a highly prevalent agent in research mouse colonies (13,19), readily infects murine macrophages and dendritic cells (DC) in culture and in vivo (34, 35, 36). Similar to HuNoV, MNV replicates in the gastrointestinal tract of its wild type or immunocompromised host, is shed in the feces, and is transmitted by the fecal–oral route (reviewed in 35). The ability to culture a norovirus has already led to insights into norovirus biology (6, 7, 25, 26) and inactivation (for example 1, 2). However, no studies have yet addressed requirements for norovirus entry into cells.

To gain access into host cells, viruses hijack cellular processes. The most commonly used endocytic pathway for virus entry is clathrin-mediated endocytosis. Viral entry can also occur via caveolin-mediated endocytosis, clathrin/caveolin-independent endocytosis, macropinocytosis, or phagocytosis (reviewed in 18). Clathrin-mediated endocytosis delivers viruses into the acidic environment of early endosomes while caveolin-mediated endocytosis can traffic virus into neutral caveosomes or acidic endosomes (5, 15, 21). Feline calicivirus (FCV) is the only calicivirus whose entry has been studied to date. FCV-F9 strain enters cells by clathrin-mediated endocytosis in a pH-dependent manner (14, 29). As a part of entry, viruses must deliver their viral genome into the host cytoplasm. This critical event during the virus life cycle, termed uncoating, is often triggered by the acidic environment of endosomes and/or by binding to cellular receptors (reviewed in 32)

3.3 Materials and Methods

Cell culture and mice. RAW 264.7 cells and SRDCs were purchased from ATCC (Manassas, VA) and maintained as previously described (84). Swiss Webster mice were purchased from Charles River. Bone marrow-derived macrophages (BMDMs) and bone marrow derived primary dendritic cells (BMDCs) were isolated as previously described (84).

Virus stocks. The plaque-purified MNV-1 clone (GV/MNV1/2002/USA) MNV-1.CW3 was used at passage 6 for all experiments (74).

Growth curves. RAW 264.7 cells or BMDMs were plated at 2 x 10^5 cells/ml in 12-well plates and allowed to attach overnight. Cells were then incubated with the indicated concentrations of chloroquine (chloro) (Sigma-Aldrich, MO) in dimethyl sulfoxide (DMSO), bafliomycin A (Baf. A), or vehicle control for 30 min. Cells were infected with MNV-1 or VSV at the indicated MOI in the presence of drugs or vehicle control for 60 min on ice. The cells were washed and fresh media containing inhibitor added. Infection was allowed to proceed until the indicated time point, when the cells were freeze-thawed twice, and viral titers were determined by plaque assay as previously described (84).

Immunofluorescence assay. RAW 264.7 cells, SRDCs, BMDMs, or BMDCs were plated at 2 x 10^5 cells/ml in 6-well plates containing sterile glass coverslips (Fisher Scientific) and allowed to attach overnight. Cells were then incubated with the indicated concentrations of chloroquine (chloro) (Sigma-Aldrich, MO) in dimethyl sulfoxide (DMSO), bafliomycin A (Baf. A) in DMSO or vehicle control (DMSO) for 60 min. Cells were infected with MNV-1 or VSV at the indicated MOI in the presence of inhibitor or vehicle control for 60 min on ice. Cells were washed and fresh media containing inhibitor added. Infection proceeded until the indicated time point when the cells were fixed with 4% paraformaldehyde in phosphate-buffered saline (PBS) for 10 min, washed once with PBS, and stained for the viral nonstructural protein VPg (81) or VSV matrix (38), and/or CD11c as previously described (54). Briefly, cells were incubated with a monoclonal mouse antibody raised against MNV-1 VPg (81) diluted 1:5,000 or VSV matrix (38) diluted 1:10,000 in wash buffer (PBS, 1% bovine serum, 1% goat serum, 0.1%

Triton X-100) for 1 h. Cells were then washed three times with wash buffer before incubation with an Alexa 594-conjugated goat anti-mouse antibody diluted 1:5,000 (Invitrogen, CA) for 1 h. Cells were washed three times as described above and mounted using Prolong Gold Antifade with DAPI (4', 6-diaminidino-2-phenylindole) (Invitrogen, CA). A total of 500 DAPI-stained cells were examined using the Olympus IX70 inverted microscope at the Center for Live Cell Imaging at the University of Michigan. Cells that had an average fluorescence intensity of at least three times the average background fluorescence intensity as determined by the Metamorph Premier version 6.3 image analysis software (Molecular Devices, Downington, PA) were counted as infected cells. The number of infected cells was then normalized to the no-treatment control.

WST-1 cell viability assay. RAW 264.7 cells, SRDCs, BMDMs, and BMDCs were plated at 2 x 10^5 cells/ml in a 96-well plate. Cells were pretreated with chloroquine, bafliomycin, (all purchased from Sigma-Aldrich, MO), or vehicle control for 30 min. Cells were then treated in the presence of inhibitor or vehicle control for the length of time indicated. At that time, media were removed, and media containing 10% WST-1 reagent (Roche) were added to cells. Cell viability was determined following the manufacturer's recommendations at 120 min after addition of reagent.

Statistics. Error bars in the figures represent the standard error between independent experiments. Statistical analysis was performed using Prism

software version 5.01 (GraphPad Software, CA). The two-tailed Student *t* test was used to determine statistical significance.

3.4 Results

To begin to elucidate how a norovirus enters cells, we studied the role of pH during MNV-1 entry into permissive macrophages and DCs. MNV is routinely propagated in RAW 264.7 cells, a murine macrophage cell line. Therefore, we first focused on the role of pH during MNV-1 infection in cultured and primary murine macrophages. Primary bone marrow-derived macrophages (BMDMs) were prepared from seronegative male Swiss Webster mice (Charles River) as previously described (35). RAW 264.7 cells and BMDMs were pretreated for 30 min with chloroquine (200 μM or 100 μM), a lysosomotropic agent that raises intracellular pH, or bafilomycin A1 (250 μM), a specific inhibitor of vacuolar ATPases. For all experiments, concentrations were chosen after performing dose-response studies that maintained at least 80% cell viability compared to untreated control cells while at the same time showing a significant effect on vesicular stomatitis virus (VSV), our positive control for a pH-dependent virus (). Cells were infected with MNV-1 or VSV in the presence or absence of these inhibitors at a multiplicity of infection (MOI) of 5 for 1 h on ice and then washed three times in phosphate buffered saline (PBS). To maintain cell viability, media containing inhibitor was added for 4 h and then replaced with fresh media without

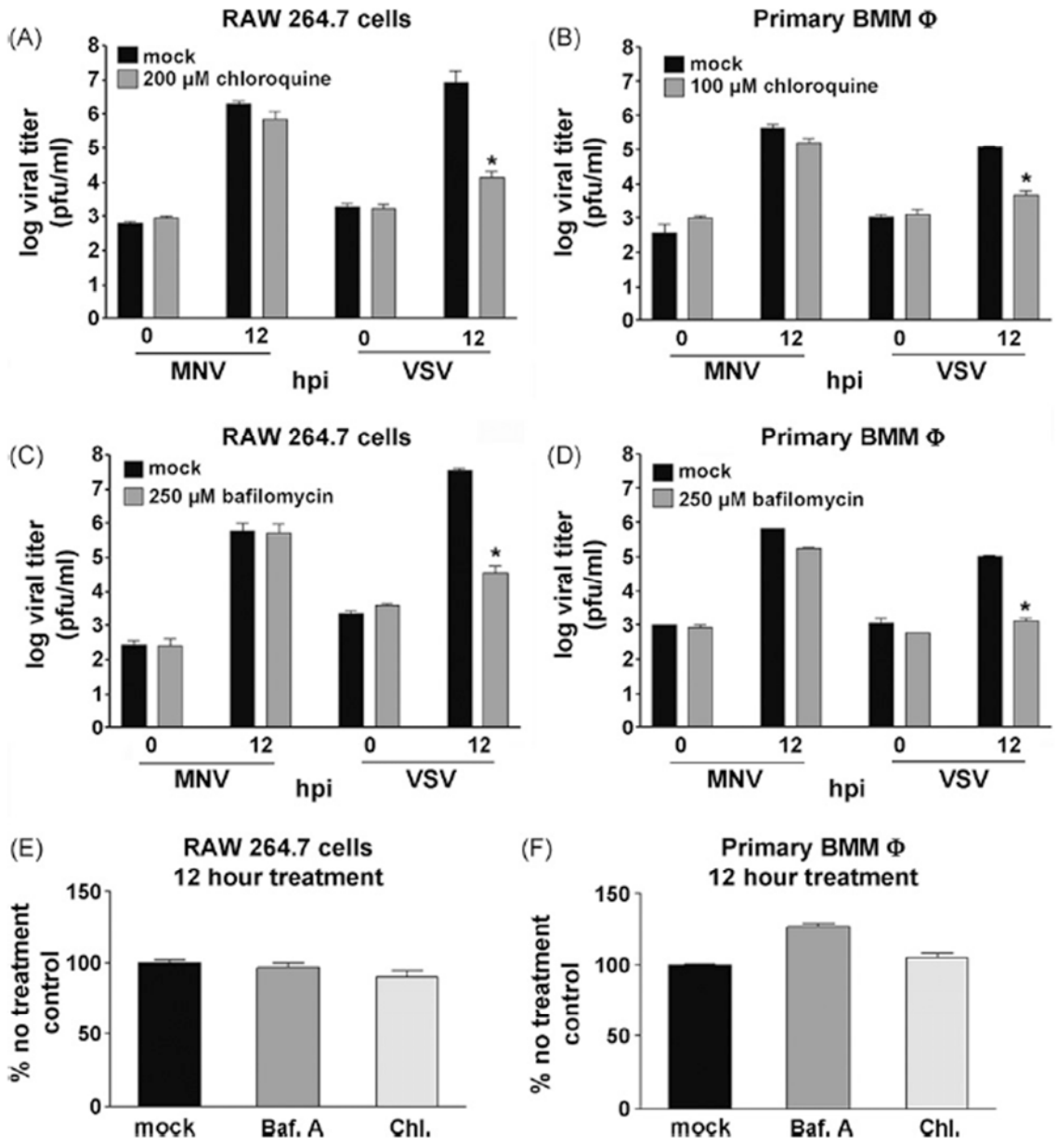

Figure 3.1. MNV-1 infection is pH-independent in murine macrophages. RAW 264.7 cells (A and C) and primary bone marrow-derived (BMMΦ) macrophages (B and D) were infected with murine norovirus 1 (MNV-1) or vesicular stomatitis virus (VSV) in the absence (mock) or presence of chloroquine (Chl.) or bafilomycin A1 (Baf. A) at a multiplicity of infection (MOI) of 5 for 1 h on ice. Viral titers were determined by plaque assay. (E and F) Viability of uninfected cells undergoing drug treatment for 12 h using WST-1 (Roche). (A–F) Results represent means±SE from three independent experiments. Statistical analysis was performed using the paired *t*-test (GraphPad Prism). *$P < 0.05$.

inhibitor. At 0, 8, 10 and 12 h post-infection (hpi), cells and media were frozen together at −80 °C. After two freeze/thaw cycles, MNV-1 and VSV viral titers were determined by plaque assay on RAW 264.7 cells as previously described (35) (Fig. 3.1 and data not shown). Experiments repeated with each virus at an MOI of 0.5 and 0.05 showed similar results (data not shown). For all experiments, cellular respiration, specifically mitochondrial dehydrogenase activity, as a measure of cell viability was monitored by WST-1 reagent (Roche) following the manufacturer's recommendations. Viability throughout the experiment remained above 80% for all conditions (Fig. 3.1E and F). VSV viral titers were significantly reduced 8, 10, 12 hpi in both bafilomycin A1- and chloroquine-treated murine macrophages as expected for a pH-dependent entry of VSV (Fig. 3.1 A–D, data not shown). However, no changes in MNV-1 titers between untreated and treated cells were seen at these timepoints (Fig. 3.1 A–D, data not shown). This indicated that MNV-1 infection may be pH-independent in cultured and primary murine macrophages.

These data suggested that endosome acidification is not required for MNV-1 entry. Since toxicity of the inhibitors required their removal after 4 h, it is unclear whether the ablation of endosome acidification lasted throughout the experiment. To ensure that removal of the drugs did not alter the experimental outcome, viral gene expression was examined at 6 hpi by immunofluorescence assay in the continued presence of the drugs. Infections were performed as described above with the following modifications. To maintain cell viability above

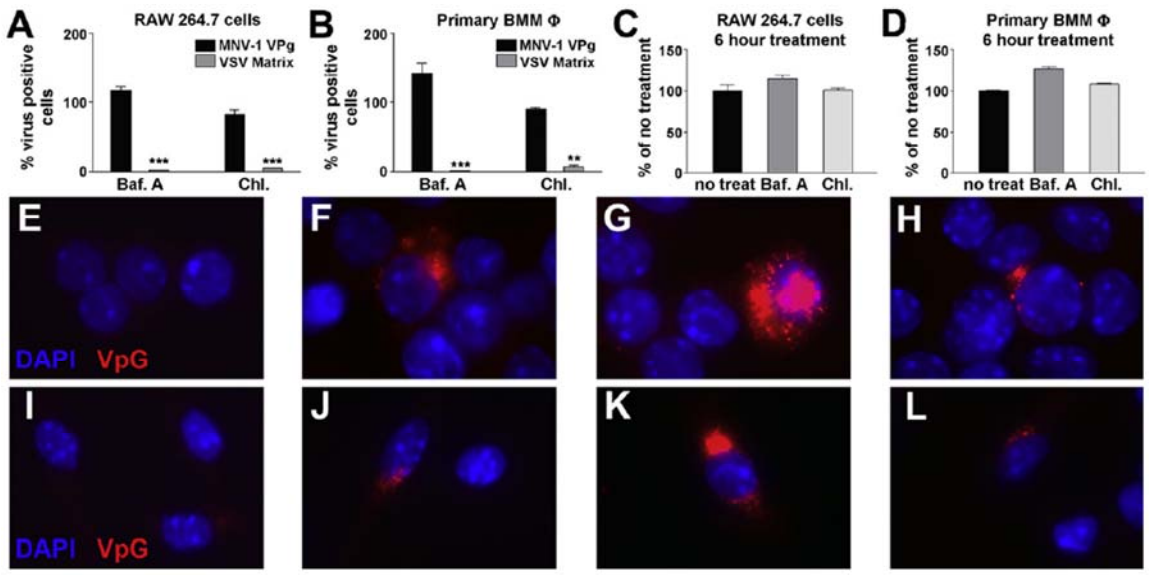

Figure 3.2. Expression of MNV-1 VPg is pH-independent in murine macrophages. RAW 264.7 cells (A) and primary bone marrow-derived macrophages (B) were infected with MNV-1 and VSV at a MOI of 10 for 1 h on ice in the absence (no treat) or presence of 250 μM bafilomycin A1 (Baf. A) or 50 μM chloroquine (Chl.). The percentage of cells showing viral gene expression 6 hpi was determined by immunofluorescence assay and normalized to a no treatment control set at 100%. (C and D) Viability of uninfected cells undergoing drug treatment for 6 h using WST-1 (Roche). (A–D) Results represent means±SE from three independent experiments. Statistical analysis was performed using the paired *t*-test (GraphPad Prism). Representative immunofluorescence images are shown for RAW264.7 cells (E–H) and primary bone marrow-derived macrophages (I–L) infected with MNV-1 and stained with DAPI (blue) and amonoclonal antibody against VPg (red) at 0 (E and I) or 6 hpi (F–H, J–L). Images were collected with Metamorph Premier v6.3 image analysis software (Molecular Devices, Downingtown, PA) and compiled using Adobe Photoshop v9.0 (Adobe Systems, Mountain View, CA). ***$P < 0.001$; **$P < 0.01$; VPg = viral protein, genome-linked.

80% as determined by WST-1 (Fig. 3.2C and D), the concentration of chloroquine was reduced to 50 μM. RAW 264.7 cells and BMDMs were infected at an MOI of 10 to increase the percentage of infected cells per field of view. The immunofluorescence assay was performed as previously described (27) with the following modifications. Macrophages were seeded on coverslips at 1×10^6 cells/ml and allowed to attach overnight. After fixing and permeabilization, cells were blocked with 10% bovine serum in PBS. A solution of 1% bovine serum and 1% goat serum in PBS was used for diluting primary described above with the following modifications. RAW 264.7 cells and BMDMs were infected at an MOI of 10 to increase the percentage of infected cells per field of view. The immunofluorescence assay was performed as previously described (27) with the following modifications. Macrophages were seeded on coverslips at 1×10^6 cells/ml and allowed to attach overnight. After fixing and permeabilization, cells were blocked with 10% bovine serum in PBS. A solution of 1% bovine serum and 1% goat serum in PBS was used for diluting primary (1:10,000) and secondary (1:5000) antibodies and was also used for washes. To stain nuclei, DAPI was added to the secondary antibody dilution. Fluorescently labeled cells were examined using the Olympus IX70 inverted microscope at the Center for Live Cell Imaging at the University of Michigan. To identify infected cells, MNV-1 expression of genes encoding non-structural proteins was followed using a monoclonal antibody to MNV-1 VPg (viral protein, genome-linked) (34). VSV viral gene expression was scored using the monoclonal antibody 23H12 against matrix protein (17). 700 cells as indicated by DAPI staining were counted per

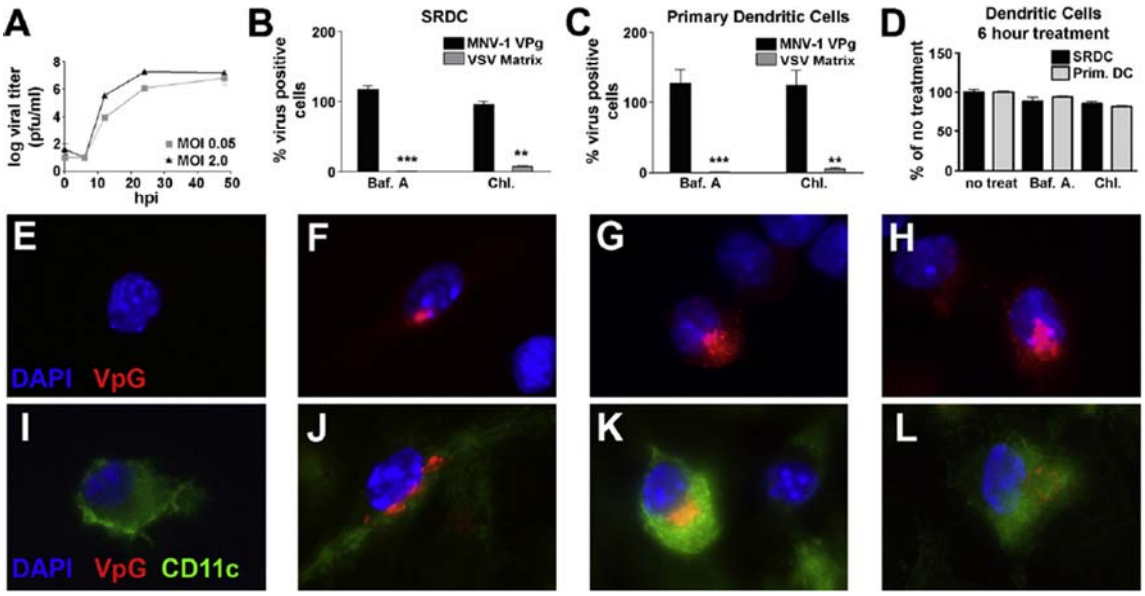

Figure 3.3. Expression of MNV-1 VPg is pH-independent in murine dendritic cells. (A) Splenic derived-dendritic cells (SRDC) were infected with MNV-1 at MOI of 0.05 and 2 and viral titers determined at various time points after infection via plaque assay. Immunofluorescence analysis of VPg gene expression 6 hpi in SRDC (B) and primary bone marrow-derived dendritic cells (C) infected with MNV-1 or VSV at a MOI of 10 in the absence (no treat) or presence of 250 μM bafilomycin A1 (Baf. A) or 50 μM chloroquine (Chl.). The no treatment control was set at 100%. (D) Viability of uninfected cells undergoing drug treatment for 6 h usingWST-1 (Roche). (A–D) Results represent means±SE from three independent experiments. Statistical analysis was performed using the paired *t*-test (GraphPad Prism). Representative immunofluorescence images are shown for SRDCs (E–H) and primary bone marrow-derived DCs (I–L) infected with MNV-1 and stained with DAPI (blue) and a monoclonal antibody against VPg (red) at 0 (E and I) or 6 hpi (F–H, J–L). Primary dendritic cells were also stained with a CD11c (green). Images were collected with Metamorph Premier v6.3 image analysis software (Molecular Devices, Downingtown, PA) and compiled using Adobe Photoshop v9.0 (Adobe Systems, Mountain View, CA). ***P < 0.001; **P < 0.01; VPg = viral protein, genome-linked.

condition and scored for MNV-1 or VSV gene expression. No VPg signal was observed at 0 hpi in untreated or treated macrophages (Fig. 3.2E and I, data not shown). Approximately 10% of cells stained positive for VPg at 6 hpi and increased over time. A cell was scored as infected if the average fluorescent intensity was three times that of the uninfected controls using the Metamorph Premier v6.3 image analysis software (Molecular Devices, Downingtown, PA) (Fig. 3.2 F–H, G–L). Their percentage was normalized to the no treatment control. No significant differences were observed in the number of cells expressing MNV-1 VPg in the presence or absence of inhibitor in either primary or cultured murine macrophages (Fig. 3.2A and B, F–H, G–L). Interestingly, the level of fluorescence was increased in the majority of bafilomycin A1-treated macrophages. In contrast to MNV-1 infected cells, the diffuse cytoplasmic staining of the VSV matrix protein indicative of VSV viral gene expression was significantly decreased by both inhibitors (Fig. 3.2A and B and data not shown). These results are consistent with viral growth data (see Fig. 3.1A–D) and demonstrated that in murine macrophages MNV-1 entry is pH-independent while VSV entry is pH-dependent.

In addition to murine macrophages, MNV-1 also shows a tropism for murine DCs (). To test whether the pH-independent entry mechanism observed in macrophages also occurred in DCs, we performed immunofluorescence assays as described above with the following modifications. As a source of DCs, we used both primary bone marrow-derived DCs and a DC-like cell line. Ruiz et

al. generated an immortalized DC cell line, termed SRDCs, that have a phenotype, morphology and activity similar to CD4− CD8α+ CD205+ CD11b− DCs purified *ex vivo*. SRDCs were cultivated as described (24). MNV-1 infection of SRDCs resulted in titers similar to MNV-1 infection of RAW 264.7 cells (Fig. 3.3A) (31). Primary bone marrow-derived murine DCs were generated from seronegative Swiss Webster mice (Charles River) as previously described (35). The adherent SRDCs were plated at 1×10^6 cells/ml on coverslips overnight. To promote adherence of primary DCs to coverslips, sterile coverslips were first coated overnight at 4 °C with rat tail collagen type 1 (2 mg/ml in 60% ethanol) before seeding primary DCs (5×10^5 cells/ml) onto coated coverslips overnight. Immunofluorescence assays were performed as described above. For primary DCs, inhibitors and virus were added directly to cells without media change, and viral gene expression was scored only in cells that co-stained with CD11c (1:2000 dilution, BD Pharmingen), a DC marker. SRDC and primary DC cell viability remained above 80% throughout the experiment as determined by WST-1 (Fig. 3.3D). No VPg signal was observed at 0 hpi in untreated or treated DCs (Fig. 3.3E and I, data not shown). Infected cells were scored as described above. No significant difference was observed in the number of MNV-1-infected DCs expressing VPg with or without inhibitors (Fig. 3.3B, C, F–H, G–L). In contrast, the number of cells expressing VSV matrix protein was significantly decreased by both inhibitors (Fig. 3.3B and C). These data demonstrated that MNV-1 viral gene expression is also independent of pH in primary and cultured DCs, suggesting MNV-1 entry into DCs does not require low pH.

Taken together, our data demonstrate that MNV-1 infection and viral gene expression in murine macrophages and DCs occur in a pH-independent manner. This is consistent with a pH-independent entry mechanism for MNV-1 into productively infected cell types.

3.4 Discussion

Due to the absence of an efficient cell culture system for HuNoV and the recent discovery of a MNV-1 culture system, no studies have addressed the cell biology of norovirus entry in tissue culture. Here, we have used MNV-1 to elucidate the role of pH during entry into murine macrophages and DCs. We have shown that MNV-1 infection at 12 hpi and viral gene expression at 6 hpi were not inhibited by bafilomycin A1 or chloroquine, two known endosome acidification inhibitors. These findings suggest that a low intracellular pH does not trigger MNV-1 uncoating.

FCV has been used extensively as a surrogate for noroviruses, because it is a member of the calicivirus family and grows in tissue culture. A recent study using the FCV-F9 strain showed that treatment of Crandell-Rees feline kidney cells with either bafilomycin A1 or chloroquine during the first hour of infection dramatically decreases the number of FCV-infected cells as determined by immunofluorescence analysis (29). The sensitivity of FCV to low pH is explained by its uptake mechanism via clathrin-mediated endocytosis and entry into Rab-5 positive early endosomes (29). The different effect of low pH on MNV-1 and FCV

may suggest a clathrin-independent entry route for MNV-1 infection of macrophages and DCs or cell type specific differences.

MNV-1 is an enteric virus that infects its host by the oral route and replicates in lamina propria cells of the small intestine (20). Thus to reach the site of replication MNV must travel through the acidic pH of the stomach. A previous study demonstrated that extracellular low pH, including a pH of 2, does not affect MNV-1 infectivity, while the same treatments significantly decreased infectivity of FCV-F9 (4). Together with our data indicating no role for intraendosomal pH during MNV-1 infection, this suggests that low pH does not trigger conformational changes in the capsid that are required for uncoating. Similarly, other enteric viruses that infect the host via the gastrointestinal tract also enter cells by pH-independent mechanisms (18). This insensitivity to extracellular low pH among enteric viruses may be a feature of their route of infection. Encountering the low pH of the stomach would needlessly activate a pH-sensitive virus, making it fusogenic in a location of the host that lacks cells used for virus replication. Consistent with this idea is the observation that norwalk virus retains infectivity at pH 2.7 for 3 h but (8) FCV-F9, a respiratory virus, is pH-sensitive (4).

Further investigations into the cellular mechanisms of MNV-1 entry and uncoating are important to understand MNV biology. In addition, the findings reported here also contribute to the discovery of common themes in enteric virus infections and may lead to the elucidation of potential antiviral targets.

3.5 References

1. **Baert L., Wobus C.E., Van Coillie E., Thackray L.B., Debevere J. and Uyttendaele M.** 2008. Detection of murine norovirus 1 by using plaque assay, transfection assay, and real-time reverse transcription-PCR before and after heat exposure. *Appl. Environ. Microbiol.*, 742 pp. 543–546.
2. **Belliot G., Lavaux A., Souihel D., Agnello D. and Pothier P.** 2008. Use of murine norovirus as a surrogate to evaluate resistance of human norovirus to disinfectants. *Appl. Environ. Microbiol.*, 74 10, pp. 3315–3318.
3. **Brandenburg B., Lee L.Y., Lakadamyali M., Rust M.J., Zhuang X. and Hogle J.M.** 2007. Imaging poliovirus entry in live cells. *PLoS Biol.*, 5 7 (2007), p. e183.
4. **Cannon J. L., Papafragkou E., Park G.W., Osborne J., Jaykus L.A. and Vinje J.** 2006.Surrogates for the study of norovirus stability and inactivation in the environment: a comparison of murine norovirus and feline calicivirus. *J. Food Protect.*, 69 11, pp. 2761–2765.
5. **Cantin C., Holguera J., Ferreira L., Villar E. and Munoz-Barroso I.** 2007 Newcastle disease virus may enter cells by caveolae-mediated endocytosis. *J. Gen. Virol.*, 88 Pt 2, pp. 559–569.
6. **Chaudhry Y., Nayak A., Bordeleau M.E., Tanaka J., Pelletier J., Belsham G.J., Roberts L.O. and Goodfellow I.G.** 2006 Caliciviruses differ in their functional requirements for eIF4F components. *J. Biol. Chem.*, 281 35, pp. 25315–25325.
7. **Daughenbaugh K.F., Wobus C.E. and Hardy M.E.** 2006. VPg of murine norovirus binds translation initiation factors in infected cells. *Virol. J.*, 3, p. 33.
8. **Dolin R., Blacklow N.R., DuPont H., Buscho R.F., Wyatt R.G., Kasel J.A., Hornick R. and Chanock R.M.** 1972. *Proc. Soc Exp Biol. Med.*, 140 2, pp. 578–583.
9. **Duizer E., Schwab K.J., Neill F.H., Atmar R.L., Koopmans M.P. and Estes M.K.** 2004. Laboratory efforts to cultivate noroviruses. *J. Gen. Virol.*, 85 Pt 1, pp. 79–87.
10. **Golden J.W., Bahe J.A., Lucas W.T., Nibert M.L. and Schiff L.A.** 2004. Cathepsin S supports acid-independent infection by some reoviruses. *J. Biol. Chem.*, 279 10, pp. 8547–8557.
11. **Golden J.W., and Schiff L.A.** 2005. Neutrophil elastase, an acid-independent serine protease, facilitates reovirus uncoating and infection in U937 promonocyte cells. *Virol. J.*, 2, p. 48.
12. **Green K.Y., Caliciviridae, Knipe P.M.H.D.M.,** Editor. 2007. *Fields Virology*, vols. 1, 2 (5 ed.), Lippincott Williams & Wilkins, Philadelphia, pp. 949–980.
13. **Hsu C.C., Wobus C.E., Steffen E.K., Riley L.K. and Livingston R.S.** 2005. Development of a microsphere-based serologic multiplexed fluorescent immunoassay and a reverse transcriptase PCR assay to

detect murine norovirus 1 infection in mice. *Clin. Diagn. Lab. Immunol.*, 12 10, pp. 1145–1151.

14. **Kreutz L.C. and Seal B.S.** 1995. The pathway of feline calicivirus entry. *Virus Res.*, 35 1, pp. 63–70.
15. **Liebl D., Difato F., Hornikova L., Mannova P., Stokrova J. and Forstova J.** 2006. Mouse polyomavirus enters early endosomes, requires their acidic pH for productive infection, and meets transferrin cargo in Rab11-positive endosomes. *J. Virol.*, 80 9, pp. 4610–4622.
16. **Lopez S. and Arias C.F.** 2006. Early steps in rotavirus cell entry. *Curr. Top. Microbiol. Immunol.*, 309, pp. 39–66.
17. **Lyles D.S., Puddington L. and McCreedy B.J.** 1988 Vesicular stomatitis virus M protein in the nuclei of infected cells. *J. Virol.*, 62 11, pp. 4387–4392.
18. **Marsh M. and Helenius A.** 2006. Virus entry: open sesame. *Cell*, 124 4, pp. 729–740.
19. **Muller B., Klemm U., Mas Marques A. and Schreier E.** 2007. Genetic diversity and recombination of murine noroviruses in immunocompromised mice. *Arch. Virol.*, 152 9, pp. 1709–1719.
20. **Mumphrey S.M., Changotra H., Moore T.N., Heimann-Nichols E.R., Wobus C.E., Reilly M.J., Moghadamfalahi M., Shukla D. and Karst S.M.** 2007. Murine norovirus 1 infection is associated with histopathological changes in immunocompetent hosts, but clinical disease is prevented by STAT1-dependent interferon responses. *J. Virol.*, 81 7, pp. 3251–3263.
21. **Pelkmans L., Kartenbeck J. and Helenius A.** 2001. Caveolar endocytosis of simian virus 40 reveals a new two-step vesicular-transport pathway to the ER. *Nat. Cell. Biol.*, 3 5, pp. 473–483.
22. **Pietiainen V.M., Marjomaki V., Heino J. and Hyypia T.** 2005. Viral entry, lipid rafts and caveosomes. *Ann. Med.*, 37 6, pp. 394–403.
23. **Regan A.D., Shraybman R., Cohen R.D. and Whittaker G.R.** 2008. Differential role for low pH and cathepsin-mediated cleavage of the viral spike protein during entry of serotype II feline coronaviruses. *Vet. Microbiol.*
24. **Ruiz S., Beauvillain C., Mevelec M.N., Roingeard P., Breton P., Bout D. and Dimier-Poisson I.** 2005. A novel CD4-CD8alpha+CD205+CD11b- murine spleen dendritic cell line: establishment, characterization and functional analysis in a model of vaccination to toxoplasmosis. *Cell. Microbiol.*, 7 11, pp. 1659–1671.
25. **Simmonds P., Karakasiliotis I., Bailey D., Chaudhry Y., Evans D.J. and Goodfellow I.G.** 2008. Bioinformatic and functional analysis of RNA secondary structure elements among different genera of human and animal caliciviruses. *Nucleic Acids Res.*, 36 8, pp. 2530–2546.
26. **Sosnovtsev S.V., Belliot G., Chang K.O., Prikhodko V.G., Thackray L.B., Wobus C.E., Karst S.M., Virgin H.W. and Green K.Y.** 2006. Cleavage map and proteolytic processing of the murine norovirus nonstructural polyprotein in infected cells. *J. Virol.*, 80 16, pp. 7816–7831.

27. **Straight S.W., Karnak D., Borg J.P., Kamberov E., Dare H., Margolis B. and Wade J.B.** 2000. mLin-7 is localized to the basolateral surface of renal epithelia via its NH(2) terminus. *Am. J. Physiol. Renal Physiol.*, 278 3, pp. F464–F475.
28. **Straub T.M., Honer zu Bentrup K., Orosz-Coghlan P., Dohnalkova A., Mayer B.K., Bartholomew R.A., Valdez C.O., Bruckner-Lea C.J., Gerba C.P., Abbaszadegan M. and Nickerson C.A.** 2007. In vitro cell culture infectivity assay for human noroviruses. *Emerg. Infect. Dis.*, 13 3, pp. 396–403.
29. **Stuart A.D., and Brown T.D.** 2006. Entry of feline calicivirus is dependent on clathrin-mediated endocytosis and acidification in endosomes. *J. Virol.*, 80 15, pp. 7500–7509.
30. **Superti F., Seganti L., Ruggeri F.M., Tinari A., Donelli G. and Orsi N.** 1987. Entry pathway of vesicular stomatitis virus into different host cells. *J. Gen. Virol.*, 68 Pt 2, pp. 387–399.
31. **Thackray L.B., Wobus C.E., Chachu K.A., Liu B., Alegre E.R., Henderson K.S., Kelley S.T. and Virgin H.W.** 2007. Murine noroviruses comprising a single genogroup exhibit biological diversity despite limited sequence divergence. *J. Virol.*, 81 19, pp. 10460–10473.
32. **Tsai B.** 2007. Penetration of nonenveloped viruses into the cytoplasm. *Annu. Rev. Cell. Dev. Biol.*, 23, pp. 23–43.
33. **Ward J.M., Wobus C.E., Thackray L.B., Erexson C.R., Faucette L.J., Belliot G., Barron E.L., Sosnovtsev S.V. and Green K.Y.** 2006. Pathology of immunodeficient mice with naturally occurring murine norovirus infection. *Toxicol. Pathol.*, 34 6, pp. 708–715.
34. **Ward V.K., McCormick C.J., Clarke I.N., Salim O., Wobus C.E., Thackray L.B., Virgin H.W. and Lambden P.R.** 2007. Recovery of infectious murine norovirus using pol II-driven expression of full-length cDNA. *Proc. Natl. Acad. Sci. U.S.A.*, 104 26, pp. 11050–11055.
35. **Wobus C.E., Karst S.M., Thackray L.B., Chang K.O., Sosnovtsev S.V., Belliot G., Krug A., Mackenzie J.M., Green K.Y. and Virgin H.W.** 2004. Replication of norovirus in cell culture reveals a tropism for dendritic cells and macrophages. *PLoS Biol.* 2 12, p. e432.
36. **Wobus C.E., Thackray L.B. and Virgin H.W.** 2006. Murine norovirus: a model system to study norovirus biology and pathogenesis. *J. Virol.*, 80 11, pp. 5104–5112.

Chapter 4

Antiviral Activity of a Small Molecule Deubiquitinase Inhibitor Occurs via Induction of the Unfolded Protein Response.

(This chapter is a manuscript in revision with PLoS Pathogens. Jeffrey W. Perry, Mohammad Ahmed, Kyeong-Ok Chang, Nicholas J. Donato, Holis D. Showalter, and Christiane E. Wobus. Antiviral activity of a small molecule deubiquitinase inhibitor occurs via induction of the unfolded protein response. PLoS Pathogens.)

(J.W. Perry designed and performed experiments, analysed data and prepared the manuscript. M. Ahmed performed plaque assays for figure 2. K. Chang performed experiments with the Norwalk virus replicon and the Hepatitis C virus replicon. N. J. Donato provided the small WP1130 and analysed data. H.D. Showalter provided the biotinylated versions of WP1130 and the inactive analog as well as the inactive analog of the USP14 inhibitor, IUC. C. E. Wobus designed experiments, analysed data, and prepared the manuscript.)

4.1 Abstract

Ubiquitin (Ub) is a vital regulatory component in various cellular processes, including cellular responses to viral infection. As obligate intracellular pathogens, viruses have the capacity to manipulate the Ub cycle to their advantage by encoding Ub-modifying proteins including deubiquitinases (DUBs). However, how cellular DUBs modulate specific viral infections, such as norovirus, is poorly understood. To examine the role of DUBs during norovirus infection, we used WP1130, a small molecule inhibitor of a subset of cellular DUBs. Replication of murine norovirus in murine macrophages and the human norovirus Norwalk virus in a replicon system were significantly inhibited by WP1130. Chemical proteomics identified the cellular DUB USP14 as a target of WP1130 in murine macrophages, and pharmacologic inhibition or siRNA-mediated knockdown of USP14 inhibited murine norovirus infection. USP14 is a proteasome-associated DUB that also binds to the inositol-requiring enzyme 1 (IRE1), a critical mediator of the unfolded protein response (UPR). WP1130 treatment of murine macrophages did not alter proteasome activity but activated the X-box binding protein-1 (XBP-1) through an IRE1-dependent mechanism. In addition, WP1130 treatment or induction of the UPR also reduced infection of other RNA viruses including encephalomyocarditis virus, Sindbis virus, and La Crosse virus but not vesicular stomatitis virus. Pharmacologic inhibition of the IRE1 endonuclease activity partially rescued the anti-viral effect of WP1130. Our studies support a model whereby induction of the UPR through cellular DUB inhibition blocks some but not all viral infections. Our work also suggests that

cellular DUBs and the UPR represent novel targets for future development of broad spectrum antiviral therapies.

4.2 Introduction

Noroviruses are small non-enveloped viruses with positive-strand RNA genomes [1]. Human Norovirus (HuNoV) is the major cause of sporadic and epidemic non-bacterial gastroenteritis worldwide in people of all ages [2,3]. These infections result generally in high morbidity and economic costs but occasionally in mortality [4,5,6]. However, no directed antiviral treatments or vaccination strategies are currently available to prevent or control norovirus outbreaks. This is in part due to the inability to reproducibly culture HuNoV in the laboratory, which has seriously hampered studies of this pathogen [7,8,9]. Recently, a replicon system was developed by stably expressing a plasmid containing the prototypic norovirus strain, Norwalk virus, and an antibiotic resistant cassette enabling limited studies on the replication requirements of HuNoV [10,11,12]. In addition, the discovery of murine norovirus 1 (MNV-1) and identification of murine macrophages and dendritic cells as permissive cell types led to the development of the first norovirus cell culture system [13,14,15]. MNV shares many biological and molecular properties with HuNoV [15]. Like its human counterparts, MNV is an enteric virus that is infectious after oral inoculation, replicates in the intestine and is shed in the stool, resulting in fecal oral transmission [15]. MNV also shares the typical genomic organization, biophysical properties of the viral capsid, and molecular mechanisms of

translation initiation with HuNoV [15,16,17]. Therefore, MNV is increasingly being used to uncover principles of norovirus biology.

The ubiquitin (Ub) cycle is required for many cellular processes, including proteasomal degradation [18] and the unfolded protein response (UPR) (e.g.[19,20,21]), a cellular process whereby cells respond to the accumulation of unfolded proteins in the endoplasmic reticulum (ER) [22]. Ub-conjugating and Ub-deconjugating processes are precisely and tightly regulated, and dysregulation can lead to disease (*e.g.* [23,24,25,26]). Ub is a small 8 kDa protein that can be covalently linked to cellular proteins in a post-translational manner through a series of Ub-modifying enzymes [27]. Removal of Ub by deubiquitinases (DUBs) is a critical step to counterbalance Ub conjugation. DUBs are a group of cysteine proteases that process poly-Ub during protein translation, recycle partially catalyzed Ub intermediates, remove Ub from target proteins, and process free polymeric Ub chains cleaved from target proteins [28,29]. Based on common structural features, DUBs are divided into five families, including the ubiquitin C-terminal hydrolases (UCH) and the ubiquitin-specific proteases (USPs). USPs are the largest and most diverse DUB family and target proteins with Ub modifications. In addition to the well-characterized roles of DUBs in proteasomal degradation [30], DUBs are implicated in regulating other universal cellular processes such as the UPR [31]. The sensors inositol-requiring enzyme 1 (IRE1), PKR (double-stranded-RNA-dependent protein kinase)-like ER Kinase (PERK), and activating transcription factor 6 (ATG6) initiate the three arms of the UPR, which collectively upregulate ER chaperone expression, increase ER-

associate degradation (ERAD), and attenuate protein translation to reduce the amount of misfolded proteins in the ER [22]. A recent study demonstrated that USP14 interacts with the cytoplasmic region of IRE1 to inhibit ERAD under nonstress conditions [31]. While the details of USP14-IRE1 regulation remain to be determined, these studies suggest a critical role for ubiquitin and its modifying proteins in the UPR.

As obligate intracellular pathogens, many viruses manipulate the Ub cycle to their advantage by hijacking cellular Ub-modifying enzymes, including DUBs, or by encoding proteases and isopeptidases that recognize Ub-modified proteins [28]. However, how cellular DUBs function in modifying viral infections is poorly understood. One recent study showed that the cellular DUB USP11 restricts influenza A virus replication [32]. The monoubiquitinated nucleoprotein associates with the ribonucleoprotein complex during viral replication. However, USP11 can cleave monoubiquitin from the nucleoprotein, inhibiting colocalization of the nucleoprotein in ribonucleoprotein complexes and significantly inhibiting viral replication. This suggests that DUBs may function as cell-intrinsic restriction factors during virus infections, but whether DUBs are required for virus infection is unknown. Furthermore, the role of DUBs during norovirus infection has not previously been addressed.

To examine the role of DUBs during norovirus infection, we used a small molecule, WP1130, which inhibits a subset of cellular DUBs [33]. WP1130 is a cell permeable inhibitor of DUBs that induces the accumulation of ubiquitinated proteins in multiple cell lines including the MNV-permissive murine macrophage

line RAW 264.7 [33,34]. In Z138 mantle cell lymphoma cells, WP1130 inhibits USP9x, USP5, USP14, UCH37, and UCH-L1 [33,35]. In addition to its anticancer activity [36,37,38], WP1130 has anti-bacterial effects since treatment enhances killing of *Listeria monocytogenes* in murine macrophages (30). Herein, we show that WP1130 also significantly inhibited MNV-1 infection in murine macrophages and genomic replication of Norwalk virus in the replicon system. USP14, a proteasome-associated DUB [39], was subsequently identified as a target of WP1130 in murine macrophages. Inhibition of USP14 activity reduced MNV-1 infection but WP1130 did not inhibit proteasome activity in murine macrophages. Instead, WP1130 treatment activated the UPR. Pharmacologic activation of the UPR with thapsigargin, an inhibitor of the sarco/endoplasmic reticulum calcium ATPase [40], also significantly inhibited MNV-1 infection. This effect was not limited to noroviruses or murine macrophages. A similar inhibition of viral infection by WP1130 was demonstrated in African green monkey kidney (Vero) and human neuroblastoma (Be2-c) cells and with several RNA viruses including, encephalomyocarditis virus (EMCV), Sindbis virus, and La Crosse virus but not vesicular stomatitis virus (VSV). In all cases, the antiviral activity of WP1130 was partially reversed by inhibition of IRE1 endonuclease activity. Taken together, our results suggest that WP1130 restricts viral replication in part through the IRE1-dependent UPR. Thus, DUB inhibitors and UPR activators could provide a novel approach in antiviral therapy.

4.3 Materials and Methods

Cell culture and mice. RAW 264.7 cells were purchased from ATCC (Manassas, VA) and maintained as previously described [14]. Swiss Webster mice and BALB/c mice were purchased from Charles River. Bone marrow-derived macrophages (BMDMs) were isolated as previously described [14]. HG32 cells containing the Norwalk virus replicon were cultured as previously described [10]. Vero cells and Be2-(c) cells were purchased from ATCC (Manassas, VA) and maintained as suggested by ATCC.

Virus stocks. The plaque purified MNV-1 clone (GV/MNV1/2002/USA) MNV 1.CW3 was used at passage 6 for all experiments [64]. Encephalomyocarditis virus, Sindbis virus, and La Crosse virus were obtained from Dr. David Miller (University of Michigan) and propagated as previously described [65].

Small molecule inhibitors. All small molecules were dissolved in DMSO, except ribavirin (dissolved in PBS). WP1130, biotinylated WP1130, biotinylated WP1130 null probe, and the inactive USP14 inhibitor IU1C were synthesized by the Vahlteich Medicinal Chemistry Core (University of Michigan). Ribavirin, MG132, Bortezimib, and Thapsigargin were obtained from Sigma-Aldrich™. The USP14 inhibitor IU1 was obtained from OTAVA LTD™. Irestatin was purchased from Axon Medchem™.

Growth curves. RAW cells, BMDMs, Be-2c, or Vero cells were plated at 2 x 10^5 cells/ml in 12-well plates and allowed to attach overnight. Cells were then

incubated with the concentrations of inhibitors and lengths of time as indicated. Next, cells were infected with an MOI of 5 with the indicated virus for one hour on ice. Infected cells were washed three times with ice-cold PBS. Media containing the appropriate inhibitors was added back to cells and the infection was allowed to proceed until the indicated time point. The cells were freeze-thawed twice, and viral titers were determined by plaque assay as previously described on RAW cells for MNV-1 or on Vero cells for all other viruses [14].

Immunofluorescence assay. RAW cells or BMDMs were plated at 2 x 10^5 cells/ml in 6-well plates containing sterile glass coverslips (Fisher Scientific) and allowed to attach overnight. Cells were then infected as described above. Infection was allowed to proceed until the indicated time point when the cells were fixed with 4 % paraformaldehyde in PBS for ten minutes, washed once with PBS, and stained for the viral nonstructural protein VPg [66] as previously described [67].

Neutral red assay. RAW cells were plated at 1 x 10^6 cells/ml in 6-well plates and allowed to attach overnight. For pre-treatments, cells were incubated with 5 μM WP1130 or DMSO for 30 min. Cells were infected with MNV-1 at an MOI of 0.001 in the presence of 5 μM WP1130, or DMSO. After 60 min, the infection was exposed to white light and a plaque assay preformed as previously described [42]. To assess the non-specific effects of the compound (i.e. posttreatment), cells were infected for 60 minutes at an MOI of 0.001 in the

absence of inhibitor, virus particles not yet uncoated were inactivated by exposure to white light, and inhibitors added back for an equal length of time as the pre-treatments. To determine the dynamic range of the experiment, DMSO treated cells were infected at an MOI of 0.001 and illuminated 0 minutes or 60 minutes after addition of virus.

Binding Assay. RAW cells were plated at 2 x 10^5 cells/ml in 12-well plate and allowed to attach overnight. The following day, cells were treated with 5 μM WP1130 or DMSO (control) for 30 minutes. The cells were then placed on ice and media aspirated. Media containing MNV-1 at an MOI of 5 and DMSO or 5 μM WP1130, was added to the plate for 1 hour on ice. Cells were then washed three times with ice-cold PBS. After the final wash, RNA was isolated with Trizol™ (Invitrogen™) following the manufacturer's recommendations. Viral cDNA was then prepared and genome titers measured by qRT-PCR as previously described [41].

MNV-1 Replication Assay. 4 x 10^5 RAW cells were transfected with 1 μg of viral RNA obtained from TRIZOL™ extraction of viral lysate using 8 μl Lipofectamine 2000 (Invitrogen™) for 6 hours in OPTIMEM media. RNA was harvested from transfected cells after 12 hours using Trizol™ (Invitrogen™). In parallel, media from additional samples was aspirated and media containing DMSO or 5 μM WP1130 was added back to the cells for an additional 12 hours. RNA was

harvested from cells and viral genomes were quantitated as previously described [41].

HuNoV Replicon Assay. HG23 cells containing the Norwalk virus replicon plasmid under G418 selection were plated at 2 x 10_5 cells in 6-well plates and allowed to attach overnight. After 24 hours media was aspirated, and DMSO or 5 μM WP1130 was added back. Cells were incubated for an additional 24 hours, at which time RNA was isolated from cells using TRIZOL™ (Invitrogen™). Norwalk virus genomes were then quantitated by qRT-PCR as previously described [10].

Streptavidin Precipitation Assay. RAW cells were plated at 1 x 10_7 cells in T75 flasks and allowed to attach overnight. The following day, cells were treated with 5 μM biotinylated WP1130 or 5 μM of the biotinylated inactive analog of WP1130 for 30 minutes. The cells were then placed on ice and media aspirated. Media containing DMSO, 5 μM biotinylated WP1130 or 5 μM biotinylated inactive analog of WP1130 were added to the plate for 1 hour on ice. Cells were then washed three times in ice-cold PBS. After the final wash media containing the indicated inhibitor was added. The cells were incubated for an additional hour at 37°C, and then lysed in RIPA buffer on ice for ten minutes. Insoluble protein was removed by high-speed centrifugation at 16.1 RCF for 30 minutes at 4°C. Soluble protein was added to agarose beads conjugated to streptavidin (Invitrogen) and incubated with shaking at 4°C overnight. The next day, agarose beads were washed four times with PBS containing Complete Mini, EDTA-free protease

tablets (Roche), boiled in 2 x SDS PAGE sample buffer, and loaded onto SDS PAGE gels. Proteins were visualized using Sypro Ruby Red fluorescent protein stain (Invitrogen ™) according to the manufacturer's instructions. The indicated bands were then cut and sent for mass spectrometry analysis at the University of Michigan Pathology Mass Spectrometry Lab.

Deubiquitinase Labeling Assay. RAW cells were plated at 1 x 10_6 cells/ml in 6-well plates and allowed to attach overnight. The following day cells were treated with 5 μM WP1130 or DMSO for 30 minutes at 37°C. Cells were then placed on ice, media aspirated, and replaced with media containing 5 μM WP1130 or DMSO. Cells were then infected on ice with mock lysate, or MNV-1 at an MOI of 10 for 1 hour. Cells were washed three times with ice-cold PBS, and media containing WP1130 or DMSO was added back to the cells. Cells were incubated for 1 hour at 37°C, and then placed on ice and washed once with ice-cold PBS. Cells were then scraped in PBS and pelleted. The PBS was aspirated and DUB labeling buffer (50 mM Tris-HCL, pH 7.5, 0.5% NP-40, 5 mM $MgCl_2$, 150 NaCl, and complete mini EDTA-free protease inhibitor cocktail (Roche™)) was added to the cells. RAW cells were then sonicated for 3 seconds at a power of 3 using a Microson Ultrasonic Cell Disruptor XL with a microprobe tip (Misonix). Insoluble proteins were removed by centrifugation at 16.1 RCF for 30 minutes at 4°C. The concentration of the cell lysates was determined by Bradford assay. Protein samples (20 μg) were then added to 200 ng of HA-Ubiquitin Vinyl Sulfone (Boston Biochem ™) and incubated at 37°C for 90 minutes. Next, samples were

diluted in RIPA buffer on ice, and incubated with 2 µg of an anti- HA antibody (Invitrogen™) for 1 hour on ice with gentle mixing. Protein A-coated agarose beads (Invitrogen™) were added and incubated overnight with rocking at 4°C. The next day the agarose beads were washed four times with PBS containing Complete Mini, EDTA-free protease tablets (Roche™), boiled in SDS Page sample buffer, and loaded onto SDS PAGE gels. After SDS PAGE, gels were transferred to nitrocellulose membrane and an immunoblot was performed using an anti- USP14 antibody (Abcam ™) at a dilution of 1:2000 and a secondary goat anti-mouse HRP dilution of 1:5000 as described below.

Proteasome Activity Assay. RAW cells were plated at 1 x 10_6 cells/ml in 6-well plates and incubated overnight. Cells were treated with 5 µM WP1130, 50 µM MG132, 200 nM Bortezimib, or DMSO for 2 hours at 37° C. Next, cells were placed on ice, washed with PBS, and lysed in ice-cold lysis buffer (50 mM HEPES [pH7.5], 5 mM EDTA, 150 mM NaCl, and 1 % Triton X-100). Insoluble protein was removed by centrifugation as described above, and protein concentrations were determined by Bradford assay. Each sample (10 µg) was added to 100 nM fluorogenic substrate, Suc-LLVY-AMC (Boston Biochem™), which measures chymotrypsin activity including 20S proteasome activity [33]. After incubation for 60 minutes at 37°C, the fluorescent intensity of each sample was determined using a Synergy HT plate reader (Bio Tek™). Fluorescent intensities were normalized to DMSO control.

XBP-1 RT-PCR. RAW cells were plated at 1 x 10^6 cells/ml in 6-well plates and allowed to attach overnight. Next, cells were treated with 5 μM WP1130, 3 μM Thapsigargin, or DMSO for 30 minutes at 37°C. Cells were then placed on ice, media aspirated, and media containing appropriate inhibitors with mock lysate, or MNV-1 at an MOI of 10 was added back for 1 hour. Cells were washed three times with ice-cold PBS and media containing appropriate inhibitors added back. At the times indicated, RNA was isolated using the SV Total RNA Isolation Kit (Promega™), and cDNA was synthesized followed by PCR amplification using XBP-1 specific primers as previously described [50]. PCR products were run on a 3 % agarose gel and visualized with SYBR Green (Invitrogen™) on an Alpha Imager HP (Alpha Innotech™).

siRNA knockdown. RAW cells were plated at a density of 2 x 10^5 cells/ml in a 6-well plate and incubated overnight. Protein knockdown was performed as previously described [42]. Briefly, cells were washed with Accell siRNA Delivery Media (Dharmacon™), and incubated with Accell siRNA delivery media containing 1 μM of the indicated siRNA. After 72 hours, RAW cells were washed once with DMEM and incubated in DMEM overnight. Cells were then infected as described above for 12 hours. RAW cells were analyzed by immunofluorescence assay or western blot as described herein.

Western blot analysis. Whole cell lysates from 2 x10^5 RAW cells were generated by adding 2 x SDS-PAGE sample buffer to cells and boiling samples

for 5 minutes. Lysates were separated by SDS-PAGE, and immunoblots performed as previously described [42]. The following antibodies and dilutions were used: 1:2000 anti-HA (Invitrogen™), 1:2000 anti-PERK (Abcam ™), 1:2000 anti-phosphoPERK (Abcam ™), 1:2000 anti-ATF6 (Abcam ™), and 1:2000 anti-USP14 (Abcam ™). Band densities were quantitated as previously described [42].

Statistics. Error bars represent standard error between at least three independent experiments with at least two replicates per condition. Statistical analysis was performed using the Prism Software v 5.01 (GraphPad Software ™). The two-tailed student t-test was used to determine statistical significance. * $p < 0.05$, ** $p < 0.01$, and *** $p < 0.001$.

4.4 Results

The small molecule DUB inhibitor WP1130 inhibits MNV-1 replication.

The role of cellular DUBs during norovirus infection has not been investigated. Towards that end, we used WP1130, a small molecule that inhibits a subset of DUBs [33] (Fig. 4.1). Murine macrophages were treated with 5 μM WP1130 for 30 minutes prior to MNV-1.CW3 (MNV-1) infection, and viral titers were determined by plaque assay (Fig. 4.2A, B). Pretreatment with WP1130 significantly reduced viral titers in both RAW 264.7 (RAW) cells, a murine macrophage cell line (Fig. 4.2A), and primary bone marrow-derived macrophages (BMDMs) (Fig. 4.2B). Interestingly, the anti-viral effect of WP1130

was only observed during the early stages of infection. Addition of the compound post infection (1 hour after infection for RAW cells or 4 hours after infection for BMDMs) ablated WP1130 anti-viral activity (Fig. 4.2A, B). The compound's effect on cell viability was not significantly different from the DMSO control as measured by WST-1 reagent (Fig. 4.9) (Roche™). Overall, these results suggest that WP1130 inhibits MNV-1 infection of murine macrophages, but only when added to cells prior to or early during infection. These results raised the possibility that WP1130 was effective at an early step in the MNV-1 life cycle. To determine the effect of WP1130 treatment on viral attachment, the amount of viral particles bound to cells was measured using a qRT-PCR attachment assay previously described by our laboratory [41] (Fig. 4.2C). RAW cells were incubated with vehicle control (DMSO) or 5 μM WP1130 prior to infection, infected with MNV-1 on ice, washed, and cell-attached viral genomes were quantitated (Fig. 4.2C). While the genome levels on WP1130- treated were slightly decreased compared to DMSO-treated cells, this difference was not statistically significant, suggesting that MNV-1 attachment was not affected by WP1130 treatment.

We next examined the effect of WP1130 treatment on viral entry (*i.e.* attachment, internalization, and uncoating) using the neutral red assay previously adapted in our laboratory for use with MNV [42] (Fig. 4.2D). Neutral red, a photoactivated chemical, is passively incorporated into viral particles, which when exposed to white light cross-links the viral genome to the protein coat and renders the virus non-infectious [43]. This assay enables examination of MNV

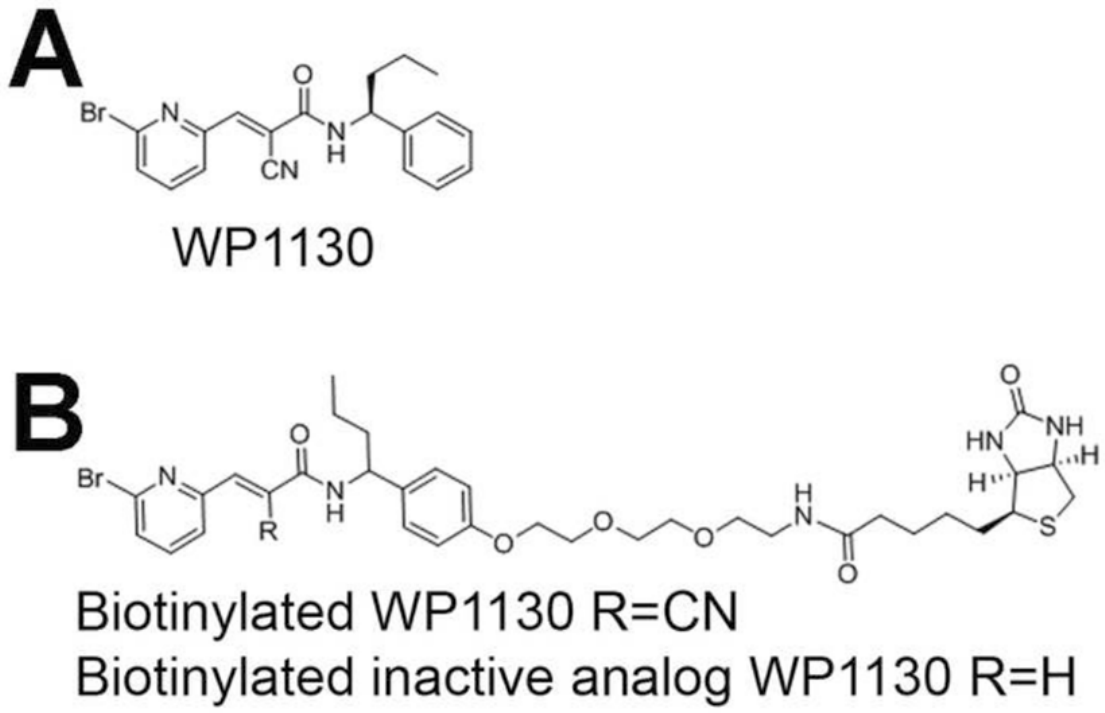

Figure 4.1 Chemical structures of WP1130 and its derivatives used herein. (A) WP1130, (B) biotinylated WP1130 and an inactive analog.

entry in the presence of inhibitor without impacting later stages of the viral life cycle. RAW cells were treated with WP1130 or DMSO prior to or after infection with neutral red-containing MNV-1 (Fig. 4.2D). To show the dynamic range of the assay, RAW cells treated with DMSO were illuminated at the same time as viral infection was initiated (Fig. 4.2D, DMSO 0 min) or after 60 minutes (Fig. 4.2D, DMSO 60 min) when MNV-1 was previously shown to become insensitive to light inhibition [42]. The number of infectious events was normalized to the DMSO control at 60 minutes of infection prior to illumination (Fig. 4.2D, DMSO 60 min). WP1130 treatment did not alter viral infectivity when RAW cells were treated with WP1130 either prior to infection (Fig. 4.2D, WP1130 pre-treatment) or after 60 minutes of infection (Fig. 4.2D, WP1130 post-treatment). Due to the short half life of WP1130 (approximately 12 hours in culture), we hypothesized that the antiviral effect did not completely inhibit viral infection and spread in this assay which lasts for 48 hours. However, a marked difference in plaque size was observed, although not statistically different from the DMSO control samples, suggesting that WP1130 may have inhibited viral infection in the early stages of plaque development, but not for the entire length of the experiment, 48 hours. This suggested that WP1130 does not inhibit attachment, internalization, or uncoating of MNV-1 in RAW cells (Fig. 4.2).

A critical next step in the viral life cycle following entry is replication. Thus, to determine whether WP1130 treatment inhibited viral replication, MNV-1 genomes were isolated from infected cell lysates and transfected into RAW cells (Fig. 4.2E). MNV-1 genomes were quantified by qRT-PCR [41] either after

transfection for 12 hours but prior to treatment (Fig. 4.2E, input) or after an additional 12 hour treatment with WP1130 or DMSO (Fig. 4.2E). WP1130 treatment significantly reduced the number of MNV-1 genomes compared to DMSO-treated cells, demonstrating that WP1130 inhibited viral replication. It is currently not possible to follow the full infectious cycle of HuNoV in a laboratory setting [7,8,9]. However, the Norwalk virus replicon system measures Norwalk virus genomic replication [10,11,12]. Thus, we next determined whether WP1130 treatment also inhibited replication of Norwalk virus (Fig. 4.2F). Replicon bearing hepatoma HG23 cells were grown in the presence of WP1130 or DMSO for 24 hours, and Norwalk virus genomes quantitated using qRT-PCR as previously described [10] (Fig. 4.2F). The number of Norwalk virus genomes was reduced approximately 50 % upon treatment with WP1130 (Fig. 4.2F). As a positive control, HG23 cells were treated with ribavirin, a nucleoside analog previously shown to reduce Norwalk virus replication [11]. Ribavirin reduced replication to approximately 20 % of the DMSO-treated cells. These results demonstrated that WP1130 also significantly inhibits Norwalk virus replication. Taken together, these findings demonstrate that WP1130 is an effective inhibitor of MNV-1 and Norwalk virus replication but does not block the earlier stages of MNV-1 infection (attachment, internalization, or uncoating). Since WP1130 is a known inhibitor of a subset of DUBs [33], these results suggest that all or some of the WP1130-responsive cellular DUBs are important for optimal norovirus replication.

WP1130 treatment inhibits the cellular deubiquitinase USP14.

Figure 4.2 WP1130 treatment inhibits norovirus replication. (A, B) WP1130 treatment inhibits MNV-1 infection in (A) RAW 264.7 (RAW) cells or (B) bone marrow-derived macrophages (BMDMs). Cells were infected with MNV-1 (MOI 5) in the presence of 5 μM WP1130 or DMSO (-). Cells were incubated with WP1130 30 min prior to infection (pre) or at the indicated times post infection. Virus titers were determined by plaque assay 8 hours (RAW) or 12 hours (BMDMs) post infection. (C) MNV-1 attachment to murine macrophages is not significantly altered by WP1130 treatment. MNV-1 (MOI 5) was incubated for 1 hour on ice with RAW cells treated with 5 μM WP1130 or DMSO. Virus attachment was quantified by qRT-PCR. (D) WP1130 does not inhibit MNV-1 entry. RAW cells were infected with neutral red-containing MNV-1 (MOI 0.001) for 60 min at room temperature and then illuminated with white light. Cells were either treated prior to infection (pre-treatment) or treated for 90 minutes after infection (post-treatment) with 5 μM WP1130 or DMSO. To show the dynamic range of the assay, cells treated with DMSO were also illuminated with white light at the same time as infection was initiated (0 min). (E) WP1130 treatment inhibits MNV-1 replication. MNV-1 genomic RNA was transfected into RAW cells and quantified either 12 hours (Input) or 24 hours later using qRT-PCR. Cell were treated with DMSO or 5 μM WP1130 for the final twelve hours. MNV-1 genome copy number was normalized to DMSO-treated samples.(F) WP1130 treatment inhibits Norwalk virus replication. Norwalk virus replicon-bearing HG23 cells were treated with DMSO, 5 μM WP1130, or 100 μg/ml Ribavirin for 24 hours and Norwalk virus genomes quantitated by qRT-PCR. HuNoV genome copy number was normalized to DMSO-treated samples. In all cases, data from at least three independent experiments with two experimental replicates per condition are presented as means +/- S.E.M. *P <0.05, **P <0.01 and *** P < 0.001, N.S. non significant.

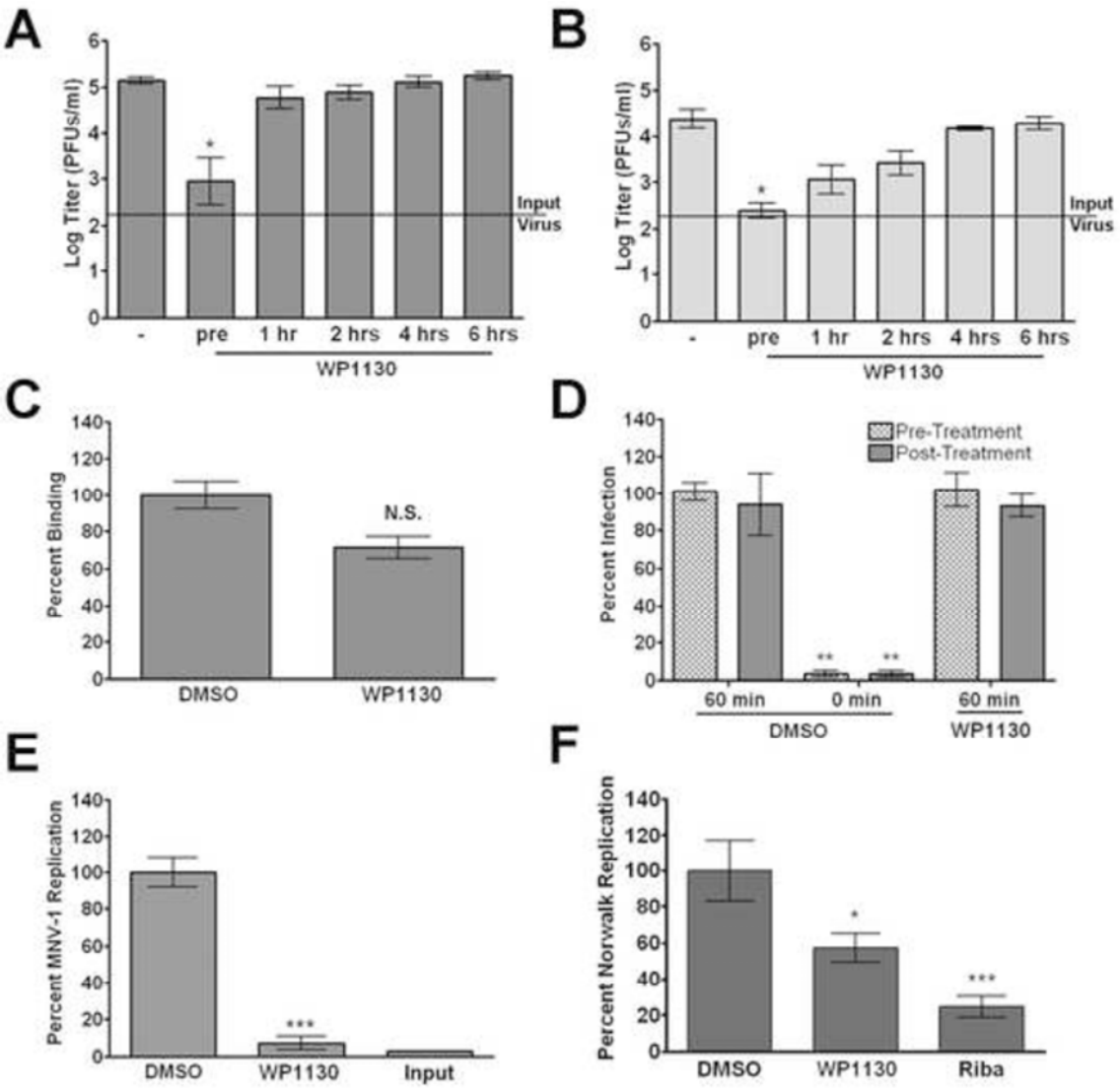
A
Log Titer (PFUs/ml)
Input Virus
-
pre
1 hr
2 hrs
4 hrs
6 hrs
WP1130
B
Log Titer (PFUs/ml)
Input Virus
-
pre
1 hr
2 hrs
4 hrs
6 hrs
WP1130
C
Percent Binding
N.S.
DMSO
WP1130
D
Percent Infection
Pre-Treatment
Post-Treatment
60 min
0 min
60 min
DMSO
WP1130
E
Percent MNV-1 Replication
DMSO
WP1130
Input
F
Percent Norwalk Replication
DMSO
WP1130
Riba

We next sought to identify macrophage-specific DUBs that may mediate antiviral activity observed during WP1130 treatment. Towards that end, we employed two different labeling strategies. First, an activity-based DUB labeling assay, and second utilizing biotinylated WP1130 to facilitate pull-down of macrophage-expressed DUBs with affinity for WP1130 (Fig. 4.3). Activity-based DUB profiling utilizes an HA-tagged Ub (HA-Ub-vinyl sulfone; HA-UbVS), which irreversibly binds to the active site of DUBs [33]. RAW cells were treated with 5 μM WP1130 or DMSO prior to infection with MNV-1 or mock lysate, washed, and media containing WP1130 or DMSO added back for one hour. RAW cells were then lysed by sonication, and HA-tagged soluble proteins were detected by immunoblotting using an anti-HA antibody. Multiple DUBs reproducibly showed greater HA labeling upon infection with MNV-1 in DMSO-treated cells (Fig. 4.3A). In addition, some of these active DUBs were inhibited by WP1130 treatment following infection (Fig. 4.3A). Of particular interest was a DUB with the approximate molecular weight for USP14, a cellular DUB previously identified as a target of WP1130 in lymphoma cells [33] (Fig. 4.3A, arrow head). To specifically address whether USP14 was indeed inhibited by WP1130 treatment, or if the band mentioned above was not USP14 but another DUB, we tested directly tested USP14 activity. To test whether the activity of USP14 was inhibited by WP1130 treatment, we labeled DUBs in mock- and MNV-1-infected RAW cells that were treated with DMSO or WP1130. Active DUBs were labeled with HAUbVS, immunoprecipitated with an anti-HA antibody and USP14 was detected by immunoblot. Four independent experiments showed that WP1130

treatment significantly reduced USP14 activity in both mock- and virally infected samples compared to DMSO (Fig. 4.3B). To test if WP1130 specifically degraded USP14, we performed immunoblots examining total USP14 in parallel experiments to the above DUB labeling experiments. We observed no change in total USP14 protein levels, suggesting that WP1130 did not cause USP14 degradation, but instead inhibited USP14 in another unknown mechanism. These results demonstrated that USP14 activity is inhibited by WP1130 treatment in RAW cells. To identify proteins that interacted with WP1130, we used a biotinylated version of WP1130 and its inactive analog for pull-down experiments (Fig. 4.1B). No significant difference between the biotinylated and non-biotinylated WP1130 was detected in their ability to inhibit MNV-1 infection and chemically inactive biotinylated version of WP1130 (Null-Biotin) did not block MNV-1 infection (Fig. 4.3C). This demonstrated biotinylation of WP1130 did not affect its antiviral activity. Hence, uninfected RAW cells were incubated with either the biotinylated WP1130 (WP) or the inactive biotinylated analog (Null), lysed, and biotinylated proteins precipitated with streptavidin agarose beads (Invitrogen™). Proteins were resolved by SDS-Page and stained with Sypro Ruby Red (Invitrogen™) as instructed by the manufacturer (Fig. 4.3D). Biotinylated WP1130, but not the inactive analog (Fig. 4.3D, asterisk), pulled down a band of similar molecular weight as identified by the activity-based DUB profiling (Fig. 4.3A). Trypsin-derived peptides from this stained gel band were subjected to mass spectrometric analysis, which identified USP14 only in samples treated with biotinylated WP1130 but not the inactive analog. These

Figure 4.3 WP1130 inhibits the host deubiquitinase USP14 in murine macrophages. (A) WP1130 treatment inhibits the activity of multiple DUBs in murine macrophages. RAW cells were treated with DMSO (D, V+D) or 5 μM WP1130 (V+WP) for 30 minutes prior to infection. Cells were then infected with MNV-1 (V+D, V+WP) or mock lysate (D), washed, and incubated for an additional hour. Cell lysates were incubated with a non-hydrolysable ubiquitin conjugated to an HA tag (HA-UbVS) before separation by SDS-PAGE and immunoblotting with an anti-HA antibody. The experiment was performed three times and a representative blot is shown. A band of the anticipated molecular weight for USP14 is indicated by the arrow head. (B) WP1130 treatment inhibits USP14 activity. RAW cells were treated with DMSO (D) or 5 μM WP1130 (WP) and then infected with MNV-1 (MOI 5) or mock lysate, washed, and incubated for an additional hour. Cell lysates were labeled with HA-UbVS and immunoprecipitated using an anti-HA antibody. Proteins were separated by SDS PAGE and immunoblots performed using an anti-USP14 antibody. A representative blot is shown. Densitometry was performed on four independent experiments, quantitated, and normalized to the mock- and DMSO-treated sample. (C) Biotinylated WP1130 inhibits MNV-1 infection in RAW cells. Cells were treated with DMSO or 5 μM of WP1130 (WP1130), biotinylated WP1130 (Biotin), inactive biotinylated WP1130 analog (Null Biotin) prior to MNV-1 infection (MOI 5). Viral titers were determined by plaque assay 8 hours post infection. Data from three independent experiments with two experimental replicates per condition are presented as means +/- S.E.M. $^{**}P < 0.01$, N.S. non significant. (D) Biotinylated WP1130 interacts with USP14. RAW cells were treated with 5 μM of biotinylated WP1130 (WP) or the inactive biotinylated WP1130 analog (Null), lysed, and lysates incubated with streptavidin beads. Precipitated proteins were separated by SDS-PAGE and visualized with Ruby Red protein stain. Peptides corresponding to USP14 were recovered from the band indicated by the asterisk (*) by mass spectrometry.

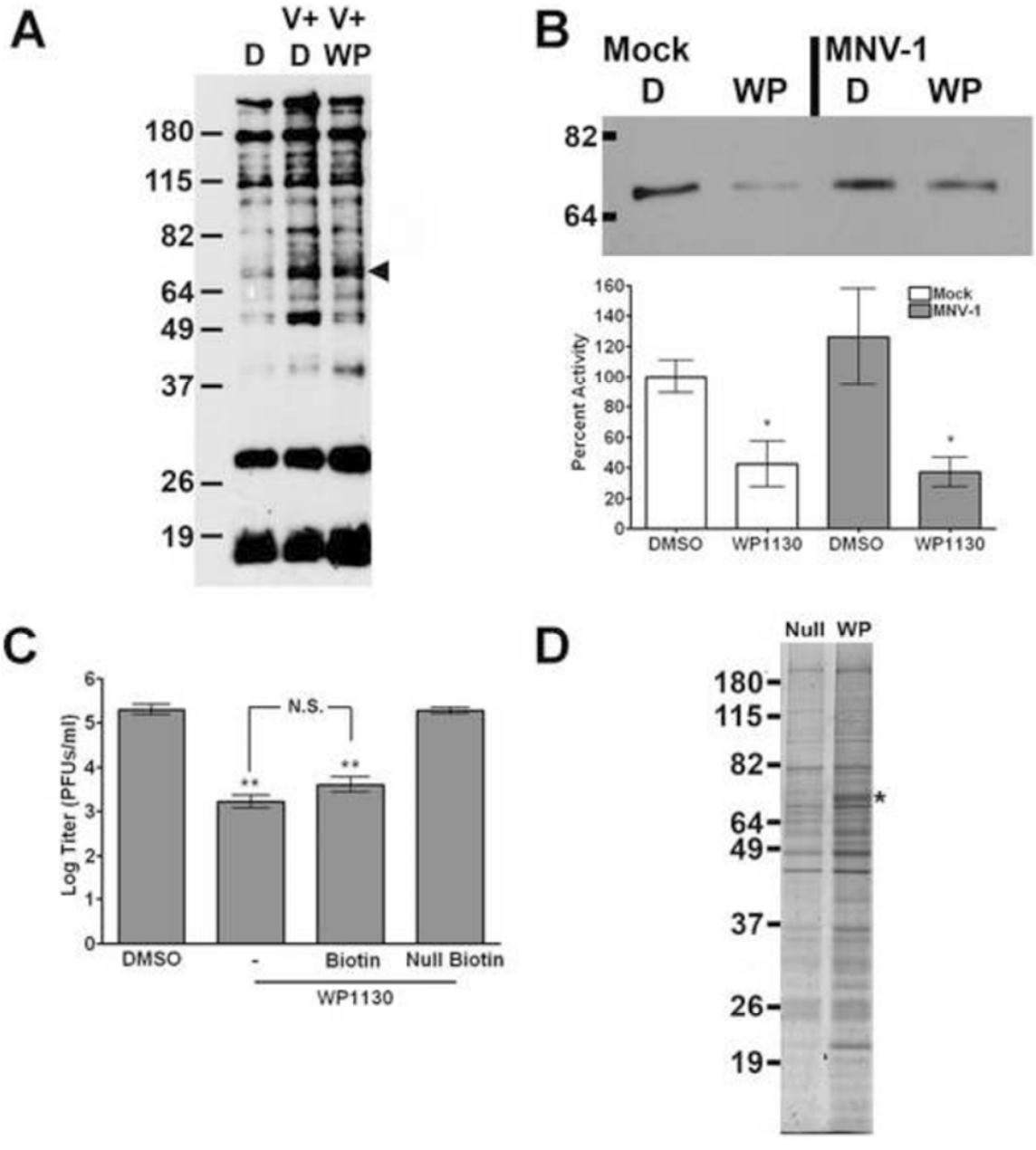
A
V+ V+
D D WP
180
115
82
64
49
37
26
19
B
Mock
MNV-1
D
WP
D
WP
82
64
Mock
MNV-1
Percent Activity
160
140
120
100
80
60
40
20
0
DMSO
WP1130
DMSO
WP1130
C
Log Titer (PFUs/ml)
6
5
4
3
2
1
0
N.S.
**
**
DMSO
-
Biotin
Null Biotin
WP1130
D
Null
WP
180
115
82
64
49
37
26
19
*

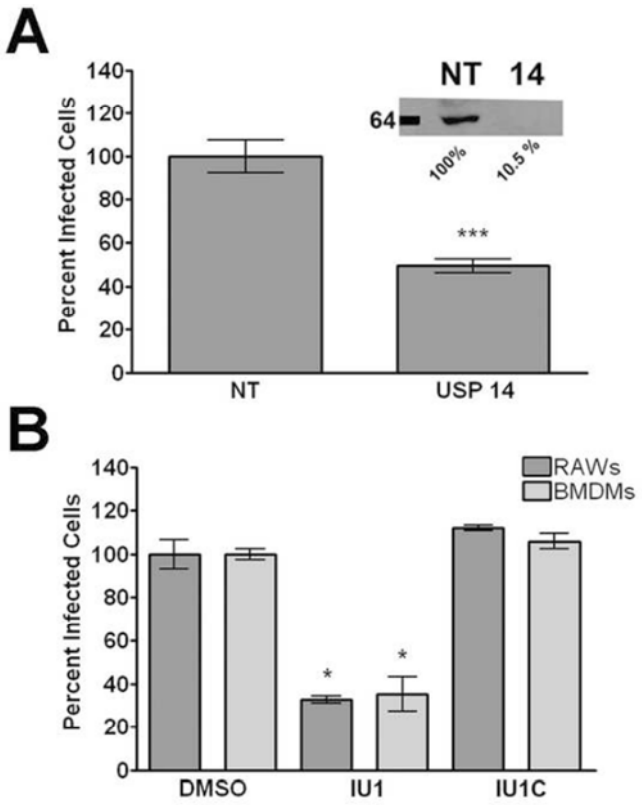

Figure 4.4 USP14 is required for optimal MNV-1 infection in murine macrophages. (A) siRNA knockdown of USP14 significantly reduces the number of MNV-1-infected RAW cells. Cells were transfected with non-targeting (NT) or USP14 targeted (USP14) Accell siRNA and infected with MNV-1 (MOI 5). Twelve hours post-infection, cells were fixed and stained with an anti-VPg antibody to quantify the number of infected cells. A representative immunoblot verifying protein knockdown in transfected cell lysates using an anti-USP14 antibody is also shown (inset). (B) The USP14 specific inhibitor IUC decreases the number of virally infected murine macrophages. RAW cells and BMDMs were treated with the USP14 inhibitor IU1 or the inactive analog IU1C for 30 min prior to infection, and the number of MNV-1 infected cells quantitated 12 hours later by immunofluorescence as in (A). In all cases, data from three independent experiments with two experimental replicates per condition are presented as means +/- S.E.M. *P <0.05, *** P < 0.001.

results demonstrated that WP1130 binds and inhibits USP14 in murine macrophages.

Inhibition or knockdown of USP14 significantly reduces MNV-1 infection.

To elucidate the role of USP14 during MNV-1 infection, we used both protein knockdown and pharmacologic inhibition of USP14. First, RAW cells were transfected with siRNA targeting USP14 or a non-targeting (NT) control siRNA as previously described [42]. USP14 siRNA knockdown reduced protein levels to 20.5 % +/- 23.1 % compared to the NT-treated RAW cells (Fig. 4.4B, inset). Transfected RAW cells were then infected with MNV-1 and the number of virally infected cells was determined by immunofluorescence staining for the MNV-1 nonstructural gene, VPg, as previously described [42]. Following USP14 knockdown, the number of cells expressing the MNV-1 nonstructural gene VPg was significantly reduced by approximately 50 % compared to the NT control (Fig. 4.4A), suggesting USP14 is required during MNV-1 infection. Although a trend of decreasing viral titers during USP14 knockdown was observed, no significant different in viral titers were detected in RAW cells 8 hours post infection as determined by plaque assay (data not shown).

To verify these results, we used a specific inhibitor of USP14, called IU1 [44], and tested its effects on MNV-1 infection (Fig. 4.4C). RAW cells or BMDMs were treated with 5 μM IU1 or IU1C, an inactive analog of IU1, prior to infection with MNV-1. The number of virally infected cells was determined as described above. Cell viability was > 80 % during these experiments as measured by

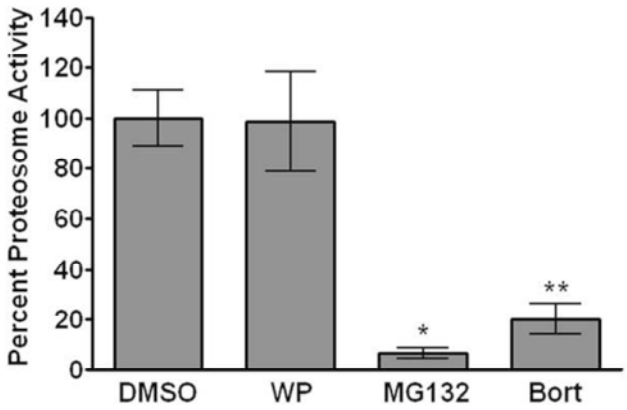

Figure 4.5 WP1130 treatment does not inhibit the proteasome. RAW cells were treated with 5 μM WP1130 (WP), 50 μM MG132, 200 nM Bortezomib (Bort), or DMSO for 2 hours at 37°C. Equal amounts of protein from each cell lysate were incubated with 100 nM of the fluorogenic substrate Suc-LLVY-AMC for 60 minutes at 37°C. The fluorescence intensity for each sample was measured and normalized to the DMSO control. Data from three independent experiments with two experimental replicates per condition are presented as means +/- S.E.M. *P <0.05, ** P < 0.01.

WST1 (ROCHE™) assay. Similar to the USP14 siRNA knockdown studies, the number of MNV-1 infected cells significantly decreased following treatment with IU1, but not the inactive analog IU1C (Fig. 4.4C). Similarly to the knockdown of USP14, IU1 treatment was unable to significantly reduce viral titers compared to control during an 8 hour infection of RAW cells (data not shown). Unfortunately, we were unable to determine the requirements of USP14 for Norwalk virus replication due to excessive cell toxicity in replicon-containing HG23 cells after a 24 hour treatment with IU1 (data not shown).

Overall, our results indicate a requirement of USP14 for efficient MNV-1 infection. Furthermore, the difference in the antiviral effect of the specific USP14 inhibitor (Fig. 4.4C) compared with the antiviral effect of WP1130 (a broader spectrum DUB inhibitor) (see Fig. 4.2A, B) suggests that additional WP1130 targeted DUBs also promote MNV-1 infection.

WP1130 does not inhibit proteasome activity.

USP14 regulates proteasome activity [45], and pharmacologic inhibition of USP14 can increase the rate of protein degradation in the cell [44]. Previous reports demonstrated that WP1130 had limited impact on 20S proteasome activity in lymphoma and leukemic cells [33]. To confirm this in murine macrophages, we determined proteasome activity in RAW cells treated with WP1130, two known proteasome inhibitors MG132 and Bortezomib [46,47], or DMSO control as described [33] (Fig. 4.5). As anticipated the proteasome

Figure 4.6 Activation of the UPR inhibits MNV-1 infection. (A) WP1130 treatment activates XBP-1. RAW cells were treated with 5 μM WP1130 (WP), 3 μM thapsigargin (T), or DMSO (D) and then mock- or MNV-1 infected (MOI 10). At 1 and 8 hours post infection, RNA was isolated and XBP-1 message amplified. Activation of XBP-1 results in a faster migrating spliced form (s) of the unspliced XBP-1 (u). As previously observed [47], a hybrid PCR product was also detected (*). Densitometry was performed on three independent experiments, quantitated, and normalized to the 1 hr thapsigargin-treated sample. (B) UPR induction by thapsigargin inhibits MNV-1 infection in RAW cells, while the antiviral activity of WP1130 is partially rescued by Irestatin, an IRE1 specific inhibitor. RAW cells were treated with DMSO, 3 μM thapsigargin (Thapsi), 5 μM WP1130, 2.5 μM Irestatin (Ires.), or both 2.5 μM Irestatin and 5 μM WP1130 (WP1130 & Ires.) for 30 min prior to MNV-1 infection (MOI 5). Viral titers were determined by plaque assay at 8 hours after infection. (C) UPR induction by thapsigargin inhibits MNV-1 infection in bone marrow derived macrophages (BMDMs), while the antiviral activity of WP1130 is partially rescued by Irestatin. The experiment was carried out as described under (B), except MNV-1 titers were determined at 12 hours postinfection. In all cases, data from three independent experiments are presented as means +/- S.E.M. ** P <0.01, and *** P < 0.001.

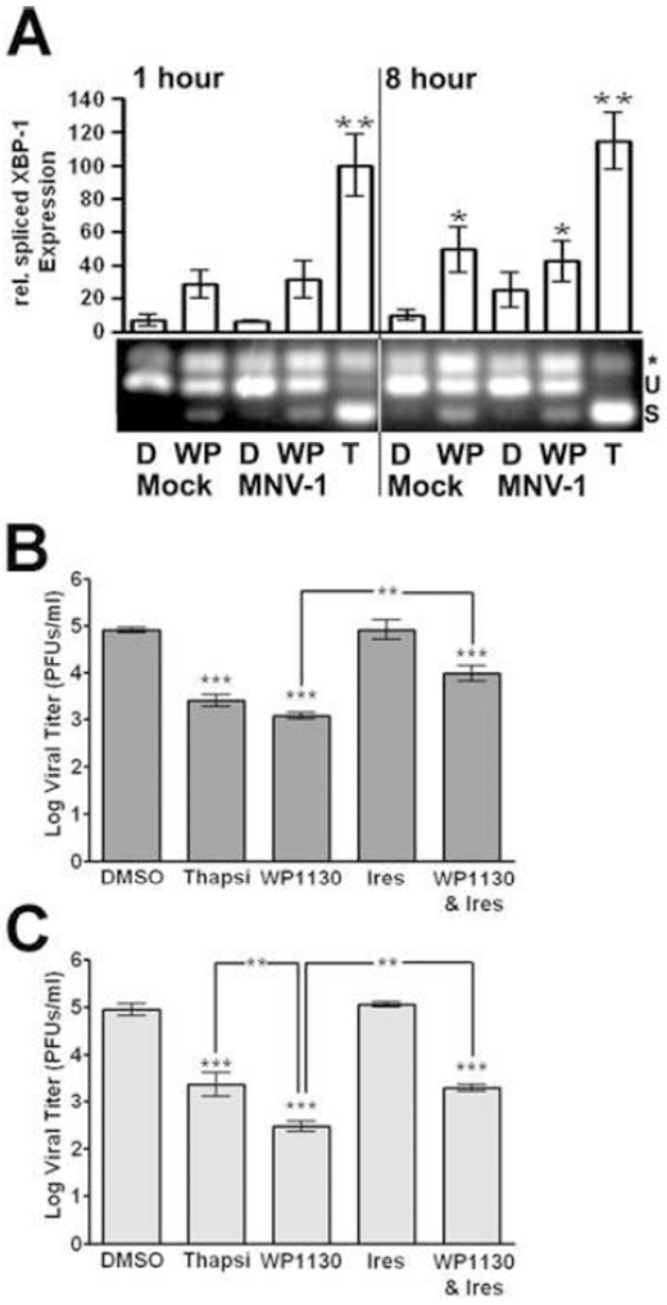

inhibitors, MG132 and Bortezomib, significantly reduced proteasome activity (Fig. 4.5), while WP1130 treatment did not. These results confirmed that WP1130's antiviral activity is not associated with 20S proteasome inhibition and suggest

that DUBs play a critical role in other cellular processes important for MNV-1 infection.

Activation of the unfolded protein response inhibits MNV-1 infection.

In addition to regulating proteasome function, USP14 regulates the UPR by associating with inactive IRE1α, although the mechanism of this regulation has not been elucidated [31]. We hypothesized that inhibition of USP14 by WP1130 would result in IRE1 activation, one of the three sensors of the UPR [48].

The active endonuclease domain of IRE1 splices the mRNA encoding XBP-1, which leads to expression of the active XBP-1 transcription factor [48]. To determine the effect of WP1130 treatment on IRE1, we measured splicing of XBP-1 mRNA (Fig. 4.6A) in RAW cells treated with WP1130 or DMSO and then infected with MNV-1 or mock lysate. RNA was harvested at 1 and 8 hours post infection. As a control, RAW cells were pretreated with 3 μM thapsigargin for 30 minutes to chemically induce the UPR and then RAW cells incubated for 1 and 8 hours. PCR was performed after cDNA synthesis using XBP-1 specific primers as previously described [49]. Three bands appeared upon XBP-1 amplification. Based on similar reports in the literature (reviewed in [50]), the top band is a hybrid PCR product (Fig. 4.6A, asterisk), while the middle and lower bands

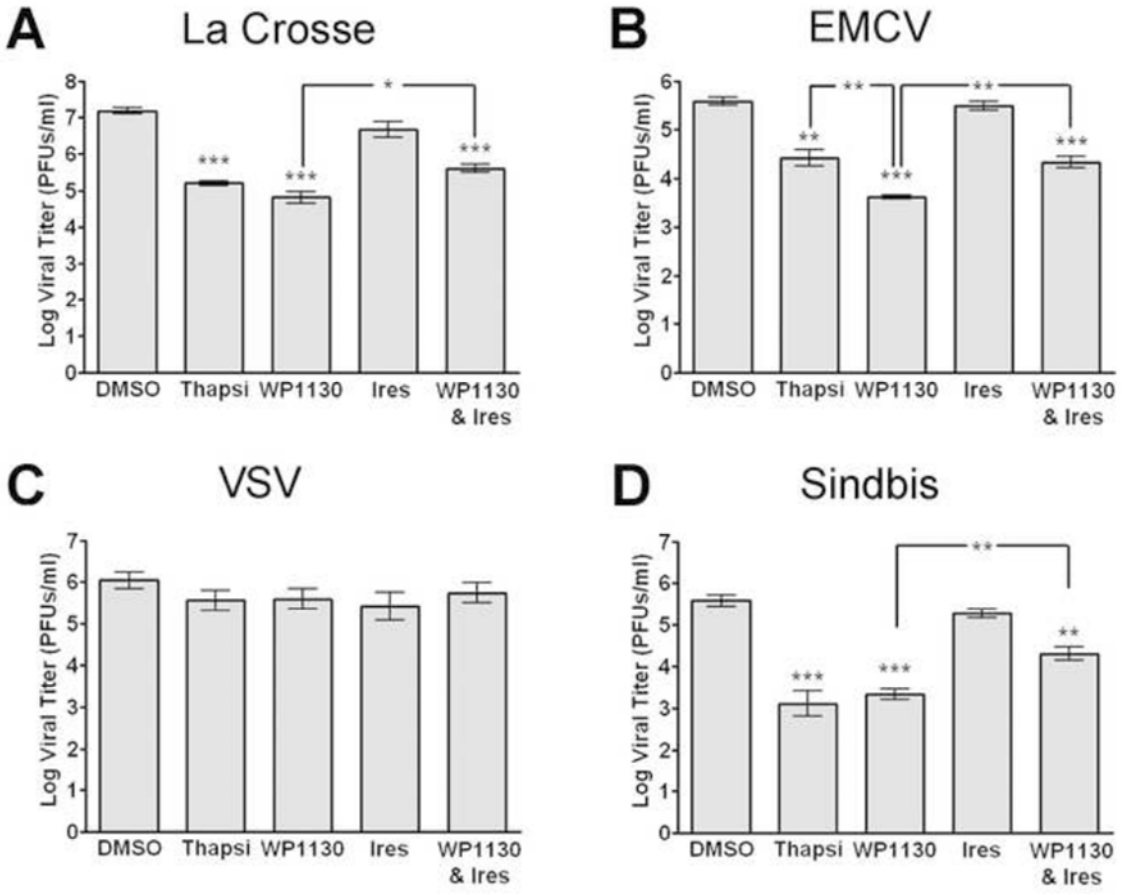

Figure 4.7 Activation of the UPR and WP1130 treatment show broad antiviral effects. (A – D) Cells were treated with DMSO, 3 μM thapsigargin (Thapsi), 5 μM WP1130, 2.5 μM Irestatin (Ires.), or both 2.5 μM Irestatin and 5 μM WP1130 (WP1130 & Ires.) prior to infection. (A) La Crosse virus infection of Be2-c cells is inhibited by WP1130 or thapsigargin. Treated Be2-c cells were infected with La Crosse virus (MOI 5) for 12 hours and viral titers determined by plaque assay on Vero cells. (B) Encephalomyocarditis virus (EMCV) infection of Vero cells is inhibited by WP1130 or thapsigargin. Treated Vero cells were infected with EMCV virus (MOI 5) for 12 hours and viral titers determined by plaque assay on Vero cells. (C) Vesicular stomatis virus (VSV) infection of Vero cells is not inhibited by WP1130 or thapsigargin. Treated Vero cells were infected with VSV virus (MOI 5) for 12 hours and viral titers determined by plaque assay on Vero cells. (D) Sindbis virus infection of Vero cells is inhibited by WP1130 or thapsigargin. Treated Vero cells were infected with Sindbis virus (MOI 5) for 12 hours, and viral titers determined by plaque assay on Vero cells. In all cases, data from at least three independent experiments with two experimental replicates per condition are presented as means +/- S.E.M. *P <0.05, **P <0.01, and *** P < 0.001.

correspond to the unspliced (U) inactive and spliced (S) active forms of XBP-1, respectively (Fig. 4.6A). Quantitation of activate XBP-1, spliced (s), was also performed from three independent experiments, although this quantification did not result in significant differences due to experimental variablity. WP1130 treatment induced XBP-1 activation as early as 1 hour after infection with MNV-1 or mock lysate, although not as robustly as the positive control thapsigargin (Fig. 4.6A). No difference in XBP-1 activation was observed between mock-infected and MNV-1-infected RAW cells at 1 hour post infection. However, at 8 hours post infection there was a faint but reproducible XBP-1 signal in infected cells, suggesting that MNV-1 infection activated the UPR at later stages of the infectious cycle. Our findings demonstrated that WP1130 treatment results in XBP-1 activation irrespective of MNV-1 infection and suggested WP1130 activates the IRE1-dependent arm of the UPR.

Since UPR activation can inhibit viral infections [51], we investigated the effect of UPR activation on MNV-1 infection (Fig. 4.6B, C). RAW cells (Fig. 4.6B) or BMDMs (Fig. 4.6C) were treated with thapsigargin prior to infection and viral titers determined by plaque assay. MNV-1 titers were significantly reduced in murine macrophages treated with thapsigargin (Fig. 4.6B, C). This reduction was not significantly different to the antiviral effect observed with WP1130 treatment in RAW cells, while in BMDMs WP1130 treatment further inhibited MNV-1 infection. Since the IRE1-dependent arm of the UPR was induced upon WP1130 treatment, we tested whether inhibition of IRE1 with Irestatin, a specific inhibitor of the IRE1 endonuclease activity, could rescue the WP1130-induced block in

MNV-1 infection. We first tested Irestatin to determine if it could inhibit IRE1 endonuclease activity by treating RAW cells with 3 μM Thapsigargin, 2.5 μM Irestatin, or a combination of both inhibitors. Irestatin was able to inhibit most of the XBP1 activation, but a faint spliced band still remained (Fig. 4.11). We next tested if Irestatin could rescue viral infection during WP1130 treatment. Murine macrophages were pre-treated with WP1130 or Irestatin alone or combined prior to MNV-1 infection and viral titers were measured by plaque assay (Fig. 4.6B, C). RAW cells and BMDMs treated with both compounds produced significantly (~ 50%) more viral progeny than WP1130 alone, while Irestatin treatment alone had no significant effect on MNV-1 titers. These results demonstrate that Irestatin can partly inhibit the antiviral effect of WP1130 and allow limited rescue of MNV-1 infection, suggesting that the anti-MNV-1 activity of WP1130 is, in part, mediated by IRE1. Interestingly, the antiviral activity of thapsigargin was completely reversed by Irestatin treatment (Fig. 4.12). These findings suggest that thapsigargin's antiviral effects are completely dependent on IRE1 endonuclease activity, but WP1130's antiviral effects must be augmented by other mechanisms independent of the IRE1 dependent UPR.

Taken together, these data showed that WP1130 treatment activated XBP-1 and that the IRE1 endonuclease activity was partly responsible for the anti-MNV-1 activity of WP1130. Furthermore, pharmacologic activation of the UPR significantly inhibits MNV-1 infection in primary and cultured murine macrophages, identifying new targets for the development of anti-norovirus therapies.

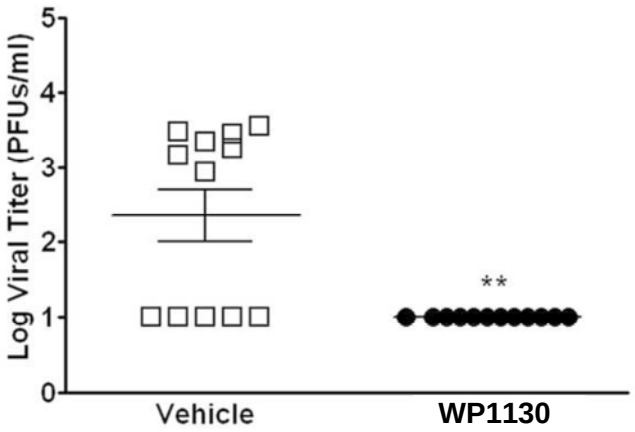

Figure 4.8 WP1130 inhibits MNV-1 infection in mice. Balb/c mice were administered 30 mg/kg of WP1130 dissolved in 20 % DMSO and 80 % PEG200 or vehicle control once daily via oral gavage. Mice were infected orally with 1 x 10^6 PFUs of MNV-1 four hours after the first dose. After 72 hours post infection, tissues were harvested along the gastrointestinal tract and viral titers determined by plaque assay. Shown are viral titers in the jejunum/duodenum of mice treated with WP1130 (empty box) or vehicle control (filled circle). Each symbol represents one animal. Data are from three independent experiments with 4 mice per condition and are presented as means +/- S.E.M. ***P* <0.01.

Activation of the UPR has broad antiviral effects.

Targeting host-specific functions and pathways such as the UPR may have broad-spectrum anti-viral efficacy. Thus, we tested the effect of WP1130 and induction of the UPR on additional viruses with positive- and negative-sense RNA genomes and enveloped or non-enveloped capsids. Be2-c cells (Fig. 4.7A) or Vero cells (Fig. 4.7B - D) were treated with thapsigargin, WP1130, Irestatin, WP1130 and Irestatin, or DMSO prior to infection. Cells were then infected with La Crosse virus, an enveloped negative-strand virus (Fig. 4.7A), EMCV, a nonenveloped positive-strand RNA virus (Fig. 4.7B), VSV, an enveloped negativestrand RNA virus (Fig. 4.7C), or Sindbis virus, an enveloped positive-strand RNA virus (Fig. 4.7D) at an MOI of 5. Both WP1130 and thapsigargin treatment significantly reduced La Crosse virus, EMCV, and Sindbis virus progeny production, suggesting that activation of the UPR can inhibit select virus infections. Similar to findings with MNV-1, cells treated with Irestatin and WP1130, but not Irestatin alone, showed a small (~50%) but significant rescue of La Crosse virus, EMCV, and Sindbis virus infections compared to WP1130 treatment alone (Fig. 4.7A, B, D). We did not observe a significant inhibition of infection with any of the treatments during VSV infection (Fig. 4.7C). Taken together, these data demonstrate that UPR activation is inhibitory to many but not all RNA viruses, and that the anti-viral activity of WP1130 is dependent in part on the IRE1-dependent arm of the UPR.

WP1130 inhibits MNV-1 infection of Mice.

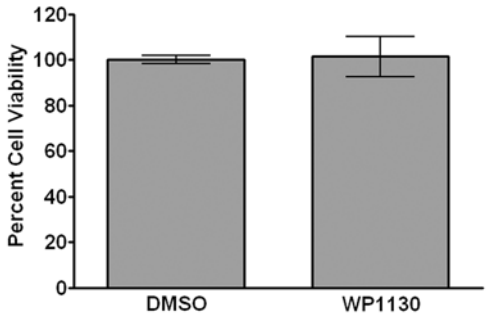

Figure 4.9 WP1130 does not affect cell viability. RAW cells were treated with DMSO (DMSO), or 5 μM WP1130 (WP1130) for 30 min prior to incubation on ice for one hour, three washes with ice cold PBS, and incubation at 37^{o}C in the presence of the compound for 8 hours. At 8 hours of treatment, RAW cells were washed once with PBS, and WST-1 reagent diluted 1 to 10 in media. OD_{420} was determined 90 minutes after addition of WST-1 and normalized to the DMSO treated cells.

To test the effectiveness of WP1130 in a mouse model, 12 6 – 8 week old Balb/c mice were administered 30 mg/kg of WP1130 dissolved in 20 % DMSO and 80 % PEG200 or vehicle control. Mice were allowed to recover for four hours before infection per oral with 1 x 10^6 PFUs of MNV-1. 24 and 48 hours after infection, mice were administered an equal dose of WP1130 or vehicle control. 72 hours after infection, mice were harvested and viral titers determined for the entire gastrointestinal tract as previously described (13). A significant decrease in viral titers was observed in the jejunum/duodenum of mice treated with WP1130 compared to vehicle control treated mice. However, no other significant differences were observed in the gastrointestinal tract. We hypothesize that these results suggest that the poor solubility and bioavailability of WP1130 could be limiting its effect to the location of the drug delivery, where the drug is at its highest concentration. Dilution of the drug through the gastrointestinal tract most likely reduces its ability to inhibit viral infection. Further modification of WP1130 to increase its solubility and bioavailability, are essential to properly develop this compound into a more suitable candidate for animal studies, as well as future clinical trials.

4.5 Discussion

The roles of DUBs required for virus replication are poorly understood, and there are currently no DUBs reported to regulate norovirus replication. Using a small molecule inhibitor of a subset of cellular DUBs, WP1130, we demonstrated that MNV requires DUBs during viral replication. Specifically,

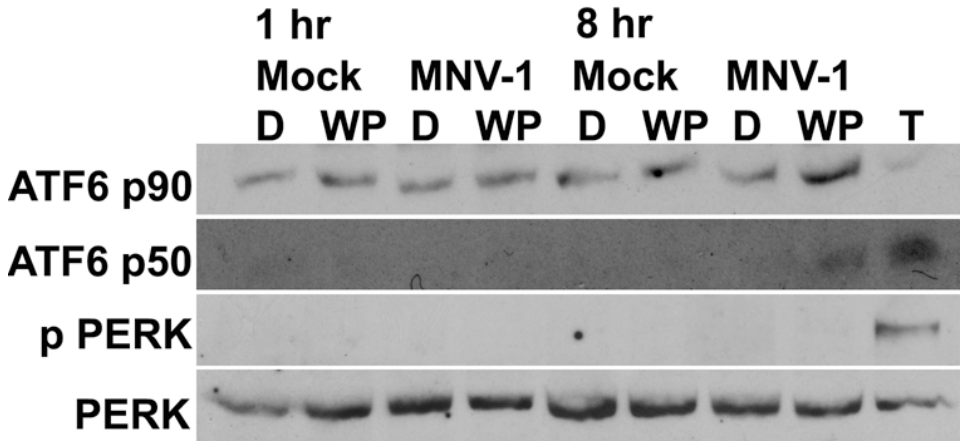

Figure 4.10 WP1130 treatment or MNV-1 infection do not activate PERK or ATF6 in RAW cells. RAW cells were treated with DMSO (D), 5 μM WP1130 (WP), or 3 μM thapsigargin (T) for 30 min prior to MNV-1 infection (MNV-1) or mock (Mock) infection for one hour on ice. Inoculums were washed off and media containing DMSO, 5 μM WP1130, or 3 μM thapsigargin added back to cells. Cells were lysed in SDS Page sample buffer 1 and 8 hours post-infection and separated on a 10% SDS-PAGE gel. Immunoblots were performed to determine phosho-PERK levels (pPERK), total PERK levels (PERK) or cleavage of ATF6 (ATF6 p90, ATF6 p50). Images are a representation of two experiments.

USP14 was identified as a direct target of WP1130 in murine macrophages. Of the two known functions of USP14, *i.e.* regulation of proteasomal degradation or modulation of the UPR, changes in proteasome activity were not detected during WP1130 treatment. Instead, activation of the UPR as indicated by XBP-1 splicing was induced by WP1130. The anti-MNV-1 activity of WP1130 was in part mediated by the UPR sensor IRE1 as treatment with Irestatin, a specific inhibitor of the IRE1 endonuclease activity, partially rescued MNV-1 infection in the presence of WP1130. Similar findings were made with other RNA viruses including, La Crosse virus, EMCV, and Sindbis virus. In addition, activation of the UPR with thapsigargin, a widely used UPR activator, also exhibited broad spectrum anti-viral activity. These data are consistent with a model whereby induction of the UPR through inhibition of cellular DUBs blocks infection. The activity of cellular DUBs during norovirus infection has not been addressed previously. Our work demonstrates for the first time that a cellular DUB, the proteasome- associated USP14, is required for optimal MNV-1 infection of murine macrophages. The mechanism by which USP14 inhibits MNV-1 infection remains to be defined. We hypothesize that one mechanism involves its interaction with IRE1 and activation of downstream UPR targets. Alternatively, USP14 interactions with viral or host proteins essential during norovirus infection may also play a role. Additional DUBs remain to be identified as antiviral effectors since specific inhibition or knockdown of USP14 was unable to recapitulate the entire anti-MNV-1 activity of WP1130 (see Fig. 4.2 and 4.4). To date, we have tested two previously identified targets of WP1130, USP5 and

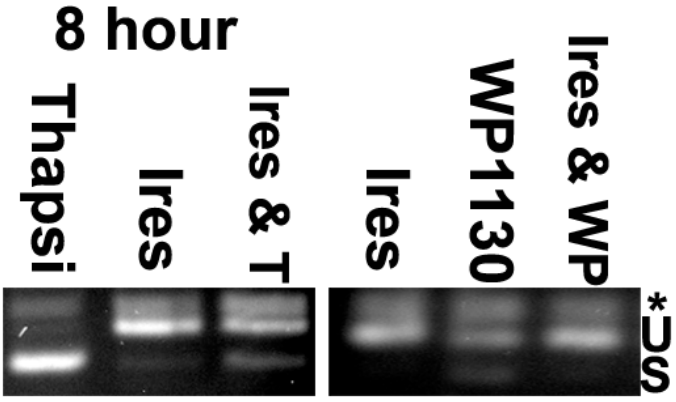

Figure 4.11 Irestatin inhibits XBP1 splicing in RAW cells. RAW cells were treated for eight hours with 3 μM thapsigargin (Thapsi), 2.5 μM Irestatin (Ires), and both 2.5 μM Irestatin and 5 μM WP1130 (Ires & T), or 2.5 μM Irestatin (Ires), 5 μM WP1130 (WP1130), or both (Ires & WP). RNA was isolated and XBP-1 message amplified. Activation of XBP-1 results in a faster migrating spliced form (s) of the unspliced XBP-1 (u). As previously observed [47], a hybrid PCR product was also detected (*).

USP9x [33], using siRNA knockdown. However, no changes in MNV-1 titers were observed (data not shown). This suggested only some of the DUBs targeted by WP1130 exhibit antiviral activity, enabling the development of more specific small molecule DUB inhibitors with anti-norovirus activity.

Our work also demonstrates that induction of the UPR with thapsigargin or WP1130 inhibits MNV-1 infection in murine macrophages (see Fig. 4.6). The antiviral effect of WP1130 was partially reversed by inhibition of the IRE1 endonuclease activity through Irestatin. This suggests that the IRE1/XBP-1 arm of the UPR can limit MNV-1 infection. To examine the role of the other two arms of the UPR response, PERK and ATF6, immunoblots were performed to determine activation of PERK, by examining phosphorylation of PERK, and ATF6, examining the cleavage of ATF6 into an activate p50 protein from the inactivate p90 precursor. Immunobloting with a phospho specific PERK antibody showed that PERK was not activated during virus infection or WP1130 treatment up to 8 hours post infection, but was activate during thapsigargin treatment. Cleavage of inactivate ATF6 (ATF6 p90) into the active subunit (ATF6 p50) was not observed during WP1130 treatment or viral infection. However, WP1130 treatment and MNV-1 infection had a small activation of ATF6, while thapsigargin had a robust activation of ATF6 (Fig. 4.10). Furthermore, the downstream effectors of the UPR that mediate viral inhibition remain to be defined. One attractive hypothesis is the link between the UPR and lipid metabolism, whereby ER stress results in the XBP-1-dependent activation of phospholipid biosynthesis pathways [52]. The recruitment of host membranes to viral replication sites or

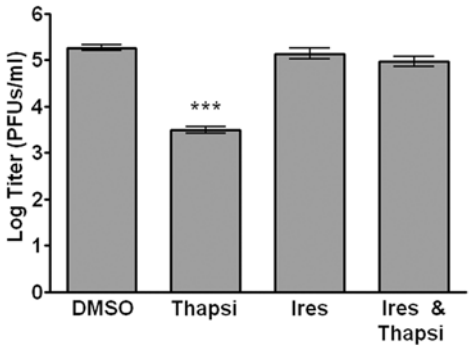

Figure 4.12 Irestatin inhibits thapsigargin's anti-MNV-1 effect in RAW cells. RAW cells were treated with DMSO (DMSO), 3 μM thapsigargin (Thapsi), 2.5 μM Irestatin (Ires), or a combination of both inhibitors (Ires & Thapsi) for 30 min prior to MNV-1 infection for one hour on ice. Inoculums were washed off with 3 washes of ice cold PBS, and media containing inhibitors added back to cells for 8 hours. Viral titers were determined by plaque assay. Data from three independent experiments with two experimental replicates per condition are presented as means +/- S.E.M. *** $P < 0.001$.

virus factories is a common requirement for positive strand RNA viruses, such as MNV-1 and EMCV [53]. Therefore, we speculate that activation of the UPR prior to MNV-1 infection might limit the amount of membrane available for the virus to recruit to its replication sites. Interestingly, a slight activation of XBP-1 splicing is observed later during MNV-1 infection. This suggests that timing of UPR induction may be critical during infection, whereby UPR induction prior to or early during MNV-1 infection inhibits infection while UPR induction late in the viral life cycle has no effect or promotes infection. Indeed, WP1130 post-treatment of murine macrophages does not inhibit MNV-1 infection (see Fig. 4.2). This is similar to findings with infection by West Nile virus, strain Kunjun, which is also sensitive to thapsigargin treatment early but not late in infection [54]. Interestingly, inhibition of Norwalk virus replication by WP1130 was not as strong as MNV-1 replication (see Fig. 4.2). This may suggest differences in the ability of both viruses to directly modulate the UPR. Another explanation may be that in the replicon system the virus has already established replication factories and may need less membrane synthesis. It is further conceivable that inhibition of membrane synthesis may not be the only mechanism by which WP1130 inhibits norovirus infections and that signaling from other branches of the UPR, or signaling through other IRE1 adaptors, such as JNK [55], play a role. Further characterizing the role of the UPR during norovirus infection could lead to novel insights into norovirus biology and identification of new anti-noroviral drug targets.

In addition to MNV-1, induction of the UPR also had anti-viral effects against the RNA viruses ECMV, La Crosse virus, and Sindbis virus, but not VSV (see Fig. 4.7). Protein synthesis during viral infection in general is thought to induce the UPR, and experimental evidence demonstrates Sindbis virus and VSV infections induce ER stress [56,57]. However, the consequences of UPR induction for individual virus infections are less well understood. For other RNA viruses such as HCV or rotavirus, induction of the UPR can lead to inhibition of viral infection, while modulation of the UPR by viral proteins can facilitate infection [58,59,60,61,62,63]. For HCV, the IRE1/XBP-1 arm of the UPR is suppressed in HCV replicon-containing cells resulting in decreased ER associated protein degradation [58]. Since WP1130 inhibits viral infection in part in an IRE1-dependent manner, active suppression of this pathway by HCV would make HCV insensitive to WP1130. Consistent with our hypothesis, we observed no inhibition of HCV replication by WP1130 in HCV replicon-containing cells (data not shown). We speculate that viruses would only be sensitive to WP1130 treatment if activation of the UPR inhibits viral replication.

The mechanism by which UPR activation or DUB inhibition could inhibit enveloped virus infection remains unclear. Induction of the degradative capacity of the UPR could reduce the stability of viral glycoproteins that are required for virion formation, since these proteins traffic through the ER. Degradation of HCV glycoproteins via the UPR has been observed in infected cells [59]. Other mechanisms of inhibition may be mediated through modulation of membrane synthesis [52], since virus budding and viral replication factories rely on cellular

membranes. Investigations into the role of the UPR and DUBs during Sindbis and La Crosse virus infections will help elucidate these cell-intrinsic anti-viral mechanisms.

In summary, we demonstrate that blocking DUB activities and induction of UPR has inhibitory effects on infection with the non-enveloped viruses MNV-1 and EMCV, and the enveloped viruses Sindbis virus and La Crosse virus. Therefore, targeting DUBs and/or the UPR with small molecules may provide a unique pathway for broad spectrum antiviral therapies.

4.6 References

1. **Green KY** (2007) Caliciviridae. In: D. M. Knipe PMH, editor. Fields Virology. 5 ed. Philadelphia: Lippincott Williams & Wilkins. pp. 949-980.
2. **Atmar RL** (2010) Noroviruses - State of the Art. Food Environ Virol 2: 117-126.
3. **Koopmans M** (2008) Progress in understanding norovirus epidemiology. Curr Opin Infect Dis 21: 544-552.
4. **van Asten L, Siebenga J, van den Wijngaard C, Verheij R, van Vliet H, et al.** (2011) Unspecified gastroenteritis illness and deaths in the elderly associated with norovirus epidemics. Epidemiology 22: 336-343.
5. **van den Brandhof WE, De Wit GA, de Wit MA, van Duynhoven YT** (2004) Costs of gastroenteritis in The Netherlands. Epidemiol Infect 132: 211-221.
6. **Lee BY, McGlone SM, Bailey RR, Wettstein ZS, Umscheid CA, et al.** (2011) Economic impact of outbreaks of norovirus infection in hospitals. Infect Control Hosp Epidemiol 32: 191-193.
7. **Duizer E, Schwab KJ, Neill FH, Atmar RL, Koopmans MP, et al.** (2004) Laboratory efforts to cultivate noroviruses. J Gen Virol 85: 79-87.
8. **Guix S, Asanaka M, Katayama K, Crawford SE, Neill FH, et al.** (2007) Norwalk virus RNA is infectious in mammalian cells. J Virol 81: 12238-12248.
9. **Lay MK, Atmar RL, Guix S, Bharadwaj U, He H, et al.** (2010) Norwalk virus does not replicate in human macrophages or dendritic cells derived from the peripheral blood of susceptible humans. Virology.
10. **Chang KO, Sosnovtsev SV, Belliot G, King AD, Green KY** (2006) Stable expression of a Norwalk virus RNA replicon in a human hepatoma cell line.Virology 353: 463-473.
11. **Chang KO, George DW** (2007) Interferons and ribavirin effectively inhibit Norwalk virus replication in replicon-bearing cells. J Virol 81: 12111-12118.
12. **Chang KO** (2009) Role of cholesterol pathways in norovirus replication. J Virol 83: 8587-8595.
13. **Karst SM, Wobus CE, Lay M, Davidson J, Virgin IV HW** (2003) STAT1-dependent innate immunity to a Norwalk-like virus. Science 299: 1575-1578.
14. **Wobus CE, Karst SM, Thackray LB, Chang KO, Sosnovtsev SV, et al.** (2004) Replication of Norovirus in cell culture reveals a tropism for dendritic cells and macrophages. PLoS Biol 2: e432.
15. **Wobus CE, Thackray LB, Virgin IV HW** (2006) Murine norovirus: a model system to study norovirus biology and pathogenesis. J Virol 80: 5104-5112.
16. **Daughenbaugh KF, Fraser CS, Hershey JW, Hardy ME** (2003) The genome linked protein VPg of the Norwalk virus binds eIF3, suggesting its role in translation initiation complex recruitment. EMBO J 22: 2852-2859.
17. **Daughenbaugh KF, Wobus CE, Hardy ME** (2006) VPg of murine norovirus binds translation initiation factors in infected cells. Virol J 3: 33.
18. **Glickman MH, Ciechanover A** (2002) The ubiquitin-proteasome proteolytic pathway: destruction for the sake of construction. Physiol Rev 82: 373-428.
19. **Rong J, Chen L, Toth JI, Tcherpakov M, Petroski MD, et al.** (2011)

Bifunctional apoptosis regulator (BAR), an endoplasmic reticulum (ER)-associated E3 ubiquitin ligase, modulates BI-1 protein stability and function in ER Stress. J Biol Chem 286: 1453-1463.

20. **Gao B, Lee SM, Chen A, Zhang J, Zhang DD, et al.** (2008) Synoviolin promotes IRE1 ubiquitination and degradation in synovial fibroblasts from mice with collagen-induced arthritis. EMBO Rep 9: 480-485.
21. **Kaneko M, Ishiguro M, Niinuma Y, Uesugi M, Nomura Y** (2002) Human HRD1 protects against ER stress-induced apoptosis through ER associated degradation. FEBS Lett 532: 147-152.
22. **Diehl JA, Fuchs SY, Koumenis C** (2011) The cell biology of the unfolded protein response. Gastroenterology 141: 38-41, 41 e31-32.
23. **Lehman NL** (2009) The ubiquitin proteasome system in neuropathology. Acta Neuropathol 118: 329-347.
24. **Hussain S, Zhang Y, Galardy PJ** (2009) DUBs and cancer: the role of deubiquitinating enzymes as oncogenes, non-oncogenes and tumor suppressors. Cell Cycle 8: 1688-1697.
25. **Shackelford J, Pagano JS** (2004) Tumor viruses and cell signaling pathways: deubiquitination versus ubiquitination. Mol Cell Biol 24: 5089-5093.
26. **Rytkonen A, Holden DW** (2007) Bacterial interference of ubiquitination and deubiquitination. Cell Host Microbe 1: 13-22.
27. **Finley D** (2009) Recognition and processing of ubiquitin-protein conjugates by the proteasome. Annu Rev Biochem 78: 477-513.
28. **Isaacson MK, Ploegh HL** (2009) Ubiquitination, ubiquitin-like modifiers, and deubiquitination in viral infection. Cell Host Microbe 5: 559-570.
29. **Petroski MD** (2008) The ubiquitin system, disease, and drug discovery. BMC Biochem 9 Suppl 1: S7.
30. **Lee MJ, Lee BH, Hanna J, King RW, Finley D** (2011) Trimming of ubiquitin chains by proteasome-associated deubiquitinating enzymes. Mol Cell Proteomics 10: R110 003871.
31. **Nagai A, Kadowaki H, Maruyama T, Takeda K, Nishitoh H, et al.** (2009) USP14 inhibits ER-associated degradation via interaction with IRE1alpha. Biochem Biophys Res Commun 379: 995-1000.
32. **Liao TL, Wu CY, Su WC, Jeng KS, Lai MM** (2010) Ubiquitination and deubiquitination of NP protein regulates influenza A virus RNA replication. Embo J 29: 3879-3890.
33. **Kapuria V, Peterson LF, Fang D, Bornmann WG, Talpaz M, et al.** (2010) Deubiquitinase Inhibition by Small-Molecule WP1130 Triggers Aggresome Formation and Tumor Cell Apoptosis. Cancer Res.
34. **Burkholder KM, Perry JW, Wobus CE, Donato NJ, Showalter HD, et al.** (2011) A small molecule deubiquitinase inhibitor increases localization of iNOS to the macrophage phagosome and enhances bacterial killing. Infect & Immunity.
35. **Sun H, Kapuria V, Peterson LF, Fang D, Bornmann WG, et al. (**2011) Bcr-Abl ubiquitination and Usp9x inhibition block kinase signaling and promote CML cell apoptosis. Blood.
36. **Bartholomeusz G, Talpaz M, Bornmann W, Kong LY, Donato NJ** (2007) Degrasyn activates proteasomal-dependent degradation of c-Myc. Cancer

Res 67: 3912-3918.
37. **Bartholomeusz GA, Talpaz M, Kapuria V, Kong LY, Wang S, et al.** (2007) Activation of a novel Bcr/Abl destruction pathway by WP1130 induces apoptosis of chronic myelogenous leukemia cells. Blood 109: 3470-3478.
38. **Kapuria V, Peterson LF, Fang D, Bornmann WG, Talpaz M, et al.** (2010) Deubiquitinase Inhibition by Small-Molecule WP1130 Triggers Aggresome Formation and Tumor Cell Apoptosis. Cancer Res 70: 9265-9276.
39. **Borodovsky A, Kessler BM, Casagrande R, Overkleeft HS, Wilkinson KD, et al**. (2001) A novel active site-directed probe specific for deubiquitylating enzymes reveals proteasome association of USP14. Embo J 20: 5187-5196.
40. **Thastrup O, Cullen PJ, Drobak BK, Hanley MR, Dawson AP** (1990) Thapsigargin, a tumor promoter, discharges intracellular Ca2+ stores by specific inhibition of the endoplasmic reticulum Ca2(+)-ATPase. Proc Natl Acad Sci U S A 87: 2466-2470.
41. **Taube S, Perry JW, Yetming K, Patel SP, Auble H, et al.** (2009) Ganglioside linked terminal sialic acid moieties on murine macrophages function as attachment receptors for murine noroviruses. J Virol 83: 4092-4101.
42. **Perry JW, Wobus CE** (2010) Endocytosis of murine norovirus 1 into murine macrophages is dependent on dynamin II and cholesterol. J Virol 84:6163-6176.
43. **Brandenburg B, Lee LY, Lakadamyali M, Rust MJ, Zhuang X, et al.** (2007) Imaging Poliovirus Entry in Live Cells. PLoS Biol 5: e183.
44. **Lee BH, Lee MJ, Park S, Oh DC, Elsasser S, et al.** (2010) Enhancement of proteasome activity by a small-molecule inhibitor of USP14. Nature 467: 179-184.
45. **Hu H, Li L, Kao RY, Kou B, Wang Z, et al.** (2005) Screening and identification of linear B-cell epitopes and entry-blocking peptide of severe acute respiratory syndrome (SARS)-associated coronavirus using synthetic overlapping peptide library. J Comb Chem 7: 648-656.
46. **Rock KL, Gramm C, Rothstein L, Clark K, Stein R, et al.** (1994) Inhibitors of the proteasome block the degradation of most cell proteins and the generation of peptides presented on MHC class I molecules. Cell 78: 761-771.
47. **Teicher BA, Ara G, Herbst R, Palombella VJ, Adams J** (1999) The proteasome inhibitor PS-341 in cancer therapy. Clin Cancer Res 5: 2638-2645.
48. **Yoshida H, Okada T, Haze K, Yanagi H, Yura T, et al.** (2001) Endoplasmic reticulum stress-induced formation of transcription factor complex ERSF including NF-Y (CBF) and activating transcription factors 6alpha and 6beta that activates the mammalian unfolded protein response. Mol Cell Biol 21:1239-1248.
49. **Samali A, Fitzgerald U, Deegan S, Gupta S** (2010) Methods for monitoring endoplasmic reticulum stress and the unfolded protein response. Int J Cell Biol 2010: 830307.
50. **Hiramatsu N, Joseph VT, Lin JH** (2011) Monitoring and manipulating mammalian unfolded protein response. Methods Enzymol 491: 183-198.

51. **He B** (2006) Viruses, endoplasmic reticulum stress, and interferon responses.Cell Death Differ 13: 393-403.
52. **Lee JI, Sollars PJ, Baver SB, Pickard GE, Leelawong M, et al.** (2009) A herpesvirus encoded deubiquitinase is a novel neuroinvasive determinant. PLoS Pathog 5: e1000387.
53. **Hyde JL, Sosnovtsev SV, Green KY, Wobus C, Virgin HW, et al.** (2009) Mouse norovirus replication is associated with virus-induced vesicle clusters originating from membranes derived from the secretory pathway. J Virol 83: 9709-9719.
54. **Ambrose RL, Mackenzie JM** (2011) West Nile virus differentially modulates the unfolded protein response to facilitate replication and immune evasion. J Virol 85: 2723-2732.
55. **Urano F, Wang X, Bertolotti A, Zhang Y, Chung P, et al.** (2000) Coupling of stress in the ER to activation of JNK protein kinases by transmembrane protein kinase IRE1. Science 287: 664-666.
56. **Nivitchanyong T, Tsai YC, Betenbaugh MJ, Oyler GA** (2009) An improved in vitro and in vivo Sindbis virus expression system through host and virus engineering. Virus Res 141: 1-12.
57. **Liu J, HuangFu WC, Kumar KG, Qian J, Casey JP, et al**. (2009) Virus induced unfolded protein response attenuates antiviral defenses via phosphorylation-dependent degradation of the type I interferon receptor. Cell Host Microbe 5: 72-83.
58. **Tardif KD, Mori K, Kaufman RJ, Siddiqui A** (2004) Hepatitis C virus suppresses the IRE1-XBP1 pathway of the unfolded protein response. J Biol Chem 279: 17158-17164.
59. **Chan SW, Egan PA** (2009) Effects of hepatitis C virus envelope glycoprotein unfolded protein response activation on translation and transcription. Arch Virol 154: 1631-1640.
60. **Ke PY, Chen SS** (2011) Activation of the unfolded protein response and autophagy after hepatitis C virus infection suppresses innate antiviral immunity in vitro. J Clin Invest 121: 37-56.
61. **Li S, Ye L, Yu X, Xu B, Li K, et al.** (2009) Hepatitis C virus NS4B induces unfolded protein response and endoplasmic reticulum overload response dependent NF-kappaB activation. Virology 391: 257-264.
62. **Zambrano J, Ettayebi K, Maaty W, Faunce N, Bothner B, et al.** (2011) Rotavirus infection activates the UPR but modulates its activity. Virol J 8: 359.
63. **Trujillo-Alonso V, Maruri-Avidal L, Arias CF, López S** (2011) Rotavirus Infection Induces the Unfolded Protein Response of the Cell and Controls It through the Nonstructural Protein NSP3. J Virol 85: 12594-12604.
64. **Thackray LB, Wobus CE, Chachu KA, Liu B, Alegre ER, et al.** (2007) Murine noroviruses comprising a single genogroup exhibit biological diversity despite limited sequence divergence. J Virol 81: 10460-10473.
65. **Peltier DC, Simms A, Farmer JR, Miller DJ** (2010) Human neuronal cells possess functional cytoplasmic and TLR-mediated innate immune pathways influenced by phosphatidylinositol-3 kinase signaling. J Immunol

184: 7010-7021.
66. **Ward VK, McCormick CJ, Clarke IN, Salim O, Wobus CE, et al.** (2007) Recovery of infectious murine norovirus using pol II-driven expression of full-length cDNA. Proc Natl Acad Sci U S A 104: 11050-11055.
67. **Perry JW, Taube S, Wobus CE** (2009) Murine norovirus-1 entry into permissive macrophages and dendritic cells is pH-independent. Virus Res 143: 125-12.

Chapter 5:

Discussion and Future Directions

5.1 Overview

The main focus of this thesis was to elucidate the entry mechanism of murine norovirus (MNV) into permissive cells. By transfecting MNV genome directly into non-permissive cells, virus progeny is produced as observed by increased viral titers determined by viral plaque assay (unpublished data). This evidence suggests that the entry process, the only steps of the viral life cycle circumvented during the transfection, dictates permissiveness to MNV. Interestingly, human norovirus (HuNoV) genomes transfected into non-permissive cells can also produce virus progeny, although their infectivity has not been tested (20). Therefore, the entry process of noroviruses determines cell infectability. Chapter 2 describes efforts to characterize the internalization of MNV into murine macrophages (Macs). The role of endosome acidification during MNV infection of both murine dendritic cells (DCs) and Macs is examined in Chapter 3. MNV must travel to the proper place and time within the cell to initiate infection, or else the virus is rendered non-infectious. By determining how MNV makes it to this place and time, we may gain insight into how this virus is restricted to infection of Macs and DCs. Using this insight, we can develop

strategies that intervene during virus trafficking in the cell to prevent it from getting to the right place and time for productive infection. This knowledge may allow for understanding of how HuNoV infects cells, and possibly aid in the development of a HuNoV culture system and antiviral therapies.

Another focus of this thesis work was to characterize the mechanism by which the small molecule WP1130 inhibits viral infection. The broad spectrum antiviral capabilities of WP1130 suggested that a conserved cellular function was being modulated during treatment with the compound. In Chapter 4, the characterization of WP1130 involving both modulation of the ubiquitin (Ub) cycle and the unfolded protein response (UPR) is outlined. Further investigation into how WP1130 affects cells and viral infection may lead to more effective derivatives and possibly a new antiviral compound to be tested clinically.

5.2 Endocytosis of murine norovirus 1 into murine macrophages is dependent on dynamin II and cholesterol

A critical first step of viral infection is the entry step. For noroviruses, this step is the determinant of host cell tropism, i.e. whether a cell can be infected or not (unpublished data, (20)). To determine the mechanism of internalization by MNV into murine Macs, I used various pharmacological inhibitors, dominant negative constructs, siRNA knockdown, and embryonic genetic knockouts. In addition to these traditional experiments to determine viral entry, I developed an assay that specifically addressed viral uncoating adapted from a published protocol for poliovirus (4). Using the small vital dye neutral red, a virus that was

light-sensitive, but only until the virus uncoated, was generated. Using the inhibitors of the various endocytic processes, we were able to determine their requirement in MNV uncoating, and therefore productive infection (Chapter 2, Figure 2). I demonstrated that MNV requires both host dynamin II and cholesterol to productively infect murine Macs (Chapter 2, Figure 4 & 7). This entry process was independent of clathrin, caveolin, flotillin, GRAF1, phagocytosis and macropinocytosis (Chapter 2, Figure 5, 6 & 8). In addition, I determined that MNV attaches to, internalizes into, and uncoats Macs with a half life of 33 minutes (Chapter 2, Figure 2). This rapid infection process is logical for a RNA genome virus that causes an acute infection, because it allows the virus to start protein translation immediately upon infection. Newly translated proteins may then alter the immune response of the infected cell possibly through inactivation of cytosolic immune surveillance pathways and allow progeny production more quickly. In unpublished data, I have also examined additional requirements of MNV infection in murine Macs, including the requirement of the GTPases rab-protein (Rab) 5 and 7. Rab 5 facilitates the fusion of endosomes to early endosomes, while Rab 7 facilitates the fusion of early to late endosomes (reviewed in (36)). Neither Rab 5 nor 7 dominant negative constructs inhibited MNV infection of murine Macs (unpublished data). This suggests that MNV internalizes into Macs quickly, and uncoats before trafficking of the newly formed endosome to the early or late endosome occurs. This rapid entry may highlight the race the virus must win against the immune system to complete the infection and produce progeny.

MNV infects murine Macs and DCs, two professional phagocytes, raising the question whether phagocytosis is hijacked by the virus to infect these cells. However, under conditions that inhibit phagocytosis, we observed a significant increase in the ability of the virus to infect Macs. This suggests that MNV is degraded by phagocytosis, or that inhibition of phagocytosis possibly up-regulates an endocytic process that is beneficial for MNV infection. Since phagocytosis is not a productive route of infection, my thesis work suggests that the phagocytic nature of these cells is not the shared critical characteristic that allows MNV to infect phagocytes. I have demonstrated that MNV requires a protein on the cell surface required for infection of Macs, by inhibiting MNV infection with protease K treatment (unpublished data). This suggests that permissiveness is determined by a specific surface protein, and not the process of phagocytosis.

The characterization of dynamin II- and cholesterol-dependent endocytosis is still in its infancy. Many poorly characterized endocytic pathways requiring these two components may be broadly categorized as dynamin II- and cholesterol-dependent endocytosis, but may be independent processes (reviewed in (40)). Two mechanisms of endocytosis, requiring flotillin 1 (2, 18, 32) and GRAF1 (13, 30), may be categorized into dynamin II- and cholesterol-dependent endocytosis although the requirement of dynamin II in these processes have not been directly tested. To determine the role of flotillin 1 and GRAF1 during MNV infection, I used siRNA knockdowns of these proteins and measured MNV nonstructural gene expression by immunofluorescence

microscopy. We observed no significant reduction in MNV infection with knockdown of flotillin 1 or GRAF1 compared to the non-targeting control. These results suggest that flotillin 1 and GRAF1 do not play a major role in MNV infection. Further characterization of dynamin II- and cholesterol-dependent endocytosis may reveal separate processes including proper cellular markers to differentiate the various processes.

In addition to MNV, several other viruses enter cells using dynamin II- and cholesterol-dependent endocytosis. Feline infectious peritonitis virus (FIPV) infects monocytes, a Mac progenitor cell, in a dynamin II- and cholesterol-dependent manner (44). Since the cell types infected by FIPV and MNV are from the same lineage, these viruses may use a conserved mechanism for infection of Macs and monocytes. In addition to FIPV, Group B coxsackievirus 3 infection of HeLa cells (37), and rotavirus infection of MA104 cells (41) occurs in a dynamin II- and cholesterol-dependent manner. Recently, the dynamin II- and cholesterol-dependent entry of herpes simplex virus type 1 (HSV-1) into keratinocytes (38) or Chinese hamster ovarian cells and HEK 293Ts over-expressing alpha V beta 3 integrin, an entry receptor for HSV-1 (16, 17), has also been documented. The mounting evidence including the number of viruses entering a variety of cell types by dynamin II- and cholesterol-dependent endocytosis suggests that this process may be more common than previously believed. However, whether these viruses enter cells by the same conserved mechanism remains to be elucidated. Using these viruses, including MNV, as tools to probe the cell may

elucidate unique endocytic processes vital in other cellular functions and contribute to a greater understanding of cell biology.

Some viruses can enter cells by more than one endocytic mechanism including infuenza A (10) and SV40 (12). We determined the requirements of various endocytic processes on minor routes of productive infection for MNV using combinations of pharmacological inhibitors in the context of the neutral red assay (Chapter 2 Figure 9). No combination of inhibitors revealed other minor productive routes of entry for MNV. This suggests that MNV does not productively infect cells by phagocytosis, clathrin-, or caveolin-mediated endocytosis even as a minor entry route. However, inhibition of cholesterol-dependent mechanisms and clathrin-mediated endocytosis significantly increased MNV infection, even when combinations of inhibitors significantly decreased cell viability to about 60% of untreated controls (Chapter 2 Table 1 & Figure 9). Why the loss of clathrin-mediated and cholesterol-dependent endocytosis in Macs increased the ability of MNV to infect these cells is still an unanswered question. Did this combination of inhibitors up-regulate a productive pathway for MNV infection, or is this observation due to an off-target effect? Further characterization of the entry mechanism of MNV will help solve this puzzle.

The future direction of this project is to further characterize the mechanism of entry by MNV. Recent attempts at using siRNA libraries as an approach to systematically test all the host proteins required for viral infection have been promising. Using this approach, a novel requirement for actin remodeling has

been shown for Hepatitis C virus (HCV) (11). I have developed a high-throughput screen of MNV infection using an automated fluorescent microscope and labeling infected Macs with an antibody raised against the MNV nonstructural gene, VPg. In combination with a siRNA library, this assay could determine host requirements of MNV infection. However, as this assay tests for nonstructural gene expression and not entry directly, any potential requirements for infection would need to be further tested in the neutral red assay to determine its role in viral entry. In addition, low transfection efficiencies in Macs could result in a technically challenging screen, although fluorescently-labeled transfected cells would be one approach at overcoming this issue. Another approach would be to identify the entry receptor of MNV, and use that receptor as a tool to determine the trafficking of MNV. Based on the observation that protease K treatment inhibits MNV infection, our laboratory is now trying to elucidate the identity of this viral receptor. Once the receptor has been identified, it will provide further insight into the mechanism of MNV entry. Determining cellular markers of dynamin II- and cholesterol-dependent endocytosis may help to elucidate not only how MNV enters Macs, but also unravel a unique mechanism for endocytosis into the cell.

5.3 Murine Norovirus 1 entry into permissive macrophages and dendritic cells is pH-independent.

After internalization of a virus particle into the cell, the virus must traffic to the current site to begin the uncoating process. A crucial step in the uncoating process is for the virus particle to react to a cue in the environment that signifies

to the virus that it is in the proper time and place to infect its host. This signal may be a combination of factors such as interaction with an entry receptor, acidification, and/or proteolytic cleavage. I determined the role of endosome acidification during MNV infection of murine Macs and DCs. Using endosome acidification inhibitors; I demonstrated that viral infection does not require endosome acidification to occur in murine Macs (Chapter 3, Figure 1 & 2) or DCs (Chapter 3, Figure 3).

MNV is not the only virus to infect cells by a pH-independent mechanism. In fact, most enteric viruses do not rely on acidification of endosomes alone. This is most likely due to the route of infection of these viruses. Since enteric viruses travel through the gastrointestinal tract, including the extremely acidic stomach, particles reacting with a low pH environment, would improperly trigger the virus to uncoat in the stomach. Both MNV and HuNoV are extremely stable at very low pH for extended amounts of time (5, 14). Other enteric viruses, including reoviruses, rotaviruses, and coronaviruses, indirectly use the acidification of endosomes as a trigger for viral uncoating, but only in the context of host proteases activated by acidic pH. Using host proteases, these viruses distinguish between an intracellular acidic environment from an extracellular acidic environment of the stomach (19, 29, 39).

MNV uncoating is triggered in a pH-independent manner. This leaves two other known triggers for uncoating, cleavage by a protease, for instance cathepsins, or direct receptor-virus interactions. For example, cathepsin S cleavage of reovirus is required for viral infection (19). To date, there is no

evidence suggesting the MNV capsid is cleaved by a protease, including cathepsins. I have performed MNV infections of murine Macs with several pharmacologic inhibitors of host proteases, including the broad cathepsin inhibitor, E64, and caspase inhibitors targeting caspase 3, 7, and 9, without successfully showing a decrease in viral infection (unpublished data). In addition, I have performed immunoblots for MNV capsid during infection of murine Macs and not detected a cleaved capsid protein (unpublished data). Although, this evidence is not definitive proof that the MNV capsid does not become cleaved, it supports the hypothesis that MNV may require direct interactions with the entry receptor as a trigger for uncoating. Another calicivirus, feline calicivirus (FCV) interacts with its receptor the feline junctional adhesion molecule 1 (fJAM 1) to facilitate conformational changes in the capsid that have been observed using cryo-electron microscopy (3). In addition, poliovirus, a closely related non-enveloped virus with a positive-strand RNA genome, requires direct interactions of the poliovirus receptor (PVR) to initiate non-reversible conformational changes in the virus particle (15). Studies looking at direct virus-receptor interactions would help to determine the process of MNV uncoating. Unfortunately, the identity of the entry receptor has yet to be elucidated, making such studies not yet possible.

5.4 Antiviral activity of a small molecule deubiquitinase inhibitor occurs via induction of the unfolded protein response.

Once the virus has internalized and uncoated within a permissive cell, the virus genome traffics to the site of viral replication. Whether the cell provides the proper place and time for the virus to infect is controlled by many cellular regulatory mechanisms. I discovered the antiviral effect of the small molecule, WP1130, which significantly inhibits MNV infection of murine Macs, and also the HuNoV replicon system, through a mechanism that involves the Ub cycle (Chapter 4, Figure 2). WP1130 can directly interact with and inhibit a subset of cysteine proteases that specifically cleave Ub from poly-Ub target proteins, called deubiquitinases (DUBs). Using biotinylated WP1130, I identified the host DUB Ub-specific protease (USP) 14 as one protein that bound to the compound (Chapter 5, Figure 3). Next, I determined that USP14 knockdown significantly inhibited MNV infection of murine Macs (Chapter 5, Figure 4). USP14 has two characterized functions in the cell: regulation of the proteasome (21), and regulation of the UPR through interactions with IRE1 alpha (34). Although WP1130 treatment did not modulate proteasome activity (Chapter 5, Figure 5), it did activate the UPR (Chapter 5, Figure 6). Specifically, I was able to show that the antiviral effect of WP1130 was partially dependent on the endonuclease activity of IRE1, and inhibition of this part of the IRE1 pathway with irestatin, rescued part of the viral infection (Chapter 5, Figure 7). I also demonstrated that induction of the UPR by other pharmacologic triggers (i.e. thapsigargin, tunicamycin) inhibited MNV infection as well (Chapter 5, Figure 7 & unpublished data). Interestingly, I repeated these observations in several cell types (i.e. primary bone marrow-derived Macs, green monkey kidney epithelial cells (Vero

cells), and neuronal progenitor cells (Be2-c cells)), and with several viruses (i.e. encephalomyocarditis virus, La Crosse virus, and Sindbis virus) (Chapter 5, Figure 8). The inhibition of viral infection was not universal as vesicular stomatitis virus could productively infect cells during WP1130 treatment or an active UPR (Chapter 5, Figure 8). These results suggest that WP1130 can be developed into a broad spectrum antiviral compound.

The requirement of cellular Ub-modifying proteins including DUBs during viral infection is poorly understood for RNA viruses. USP 11 is an antagonist for influenza A infection. It facilitates the removal of a monoubiquitin from the viral nucleoprotein (N) protein, thereby inhibiting N's interaction with influenza's replication machinery (27). This suggests that DUBs can function as a restriction factor in cells during RNA virus infection. In contrast, my work has shown that DUBs can also promote RNA virus infection. In fact, the requirement of USP14 for optimal infection of MNV is the first evidence that RNA viruses can require host DUBs for infection. Further characterization of the Ub cycle during viral infection will determine novel interactions between viruses and the host and may identify novel antiviral targets.

The mechanism by which USP14 regulates MNV infection is not understood. One study has suggested that USP14 can inhibit the activation of the UPR by interacting with IRE1 (34). Therefore, loss of USP14 by siRNA, or loss of USP14 activity by WP1130 treatment, may activate the UPR. A working model to explain these observations includes that the UPR inhibits MNV infection, that the antiviral activity of WP1130 is dependent in part on the

IRE1UPR pathway, and that WP1130 inhibition of USP14 activates the IRE1-dependent arm of the UPR pathway. This model clarifies the role of USP14 during MNV inhibition by WP1130, how WP1130 establishes an antiviral environment in the cell, and, lastly, gives a broad mechanism for the inhibition of other viruses through activation of the UPR. However, direct involvement of USP14 during WP1130 treatment and activation of the UPR still needs to be elucidated. USP14 may also have other roles in the life cycle of MNV, and could directly interact with viral proteins, including the viral protease. We observed activation of the UPR late in viral infection in the absence of WP1130 (Chapter 5, Figure 7). One mechanism to explain activation of the UPR could be through removal of USP14 by viral protease cleavage. Indeed, norovirus proteases have been shown to cleave host proteins (24), and loss of USP14 has been shown to activate the UPR (34). Another mechanism by which MNV could activate the UPR involves the recruitment of ER membrane to the membranous web, which would reduce the ER's capacity to properly fold proteins, thereby activating the UPR. Further investigation into whether viral proteins interact with USP14 directly or indirectly may reveal how USP14 promotes MNV infection.

We have also identified additional host DUBs that bind to WP1130 in a similar method used to identify USP14 (Chapter 4, Figure 3). Using mass spectrometry analysis, we have identified USP5, USP13, USP17, USP30, USP47, and OTUD1. We have used siRNA to knock down each individual DUB, and determined the level of MNV infection in these Macs. Although USP5, USP13, USP47, and OTUD1 did not alter viral titers, USP17 and USP30 both

significantly inhibited MNV infection in RAW cells, by 90 % or 50 % of controls, respectively. USP17 may play a role in regulating RIG I signaling through removing Ub from RIG I and inhibiting its activation (8). How this interaction of antiviral signaling would support MNV infection is unclear at this point, but may be facilitated by undefined functions of USP17. Less is known about USP30 as it is a transmembrane protein located on the outer membrane of the mitochondria, the only mitochondrial-targeted DUB known currently (35). Since innate antiviral signaling, including RIG I signaling, is mediated by signaling complexes anchored to the mitochondria (reviewed in (28)), further investigation into USP30 may lead to a novel regulation of innate immune signaling. By characterization of USP17 and USP30 during MNV infection of Macs, we may elucidate mechanisms by which MNV can modulate the innate immune response and elucidate mechanisms by which DUBs promote noroviral infections.

The role of the UPR during viral infection is currently a topic of great interest. A role of the UPR during viral infection has been documented for Hepatitis B virus (9, 25), HCV (6, 7, 26, 41, 46), West Nile virus (1, 31), influenza A (13), several herpesviruses (33, 42) and rotavirus (43, 45). In general, the activation of the UPR before or early during infection is detrimental to enveloped virus infection. This could be due to the inhibition of protein translation by PERK, or an increase in endoplasmic reticulum- associated degradation (ERAD) that can degrade viral glycoproteins (reviewed in (23)). Clearly, viruses have evolved mechanisms to supress the UPR to ensure virus replication and progeny production. Further investigation into encephalomyocarditis virus, La Crosse

virus, and Sindbis virus infections may elucidate mechanisms by which the UPR regulates enveloped virus infections.

The mechanism of inhibition of non-enveloped viruses by the UPR is not currently understood. Since the non-enveloped viruses tested do not traffic through the ER , we hypothesize that the requirement of these viruses for host membranes, including ER, links viral infection to the regulation of ER synthesis by the UPR. Specifically, UPR-induced ER synthesis could inhibit or sequester ER membrane from the membranous web required for viral replication. For MNV, ER-derived membranes are trafficked to sites of viral replication (22) and provide a potential explanation on how induction of the UPR inhibits MNV infection. One explanation of how UPR- induced ER synthesis inhibits MNV replication may be that MNV actively recruits host membranes, including ER, to sites of replication with different affinities. By increasing the amount of ER in the host cell, MNV may no longer recruit the sufficient membranes required for replication. Another potential mechanism by which the UPR can inhibit non-enveloped virus infection includes activation of PERK and inhibition of host translation. However, I observed no activation of PERK during WP1130 treatment (Chapter 4, Figure 11), suggesting that at least in case of MNV UPR-mediated inhibition of infection is independent of PERK. Further elucidation into the role of the UPR during the life cycle of non-enveloped viruses in general, and MNV in particular, may reveal how the host inhibits viral infection.

Currently, there is no therapeutics available to treat HuNoV infections, and only strict hygienic measures can restrict the spread of outbreaks. There is also a

need for broader spectrum antiviral compounds that can inhibit multiple human pathogens, including noroviruses. In addition, my thesis work on WP1130 has shown one avenue to develop a broad-spectrum antiviral that also targets noroviruses. Specifically, I have demonstrated that WP1130 treatment inhibits MNV infection in culture (Chapter 4, Figure 2), in mice (Chapter 4, Figure 9) and HuNoV replication in a replicon system (Chapter 4, Figure 2). Furthermore, WP1130 treatment has antiviral capabilities in several RNA virus infections (Chapter 4, Figure 8). Although the compounds efficacy was restricted spatially to the site of inoculation in a mouse model of infection, WP1130 significantly reduced MNV infection in the jejunum and duodenum. Chemical modifications of WP1130 have yielded derivatives that are more soluble and less cytotoxic, at least in culture. Using these derivatives in the future, we will be able to add higher concentrations of compound to increase antiviral efficacy in a mouse model of viral infection. Hopefully, these derivatives will exhibit better inhibition of MNV infection and in regions of the intestine more distal to the administration site. In the future, additional research and development could help determine whether or not derivatives of WP1130 would make effective antiviral drugs.

5.5 Conclusion

The entry process of a virus into the cell is an early preventable step of a viral infection. To disrupt this process, one must know how a virus enters a cell. Thus, understanding the mechanism of norovirus entry is essential in development of antiviral compounds. This work has shown for the first time that

MNV enters cells by a dynamin II- and cholesterol-dependent mechanism. This process is independent of clathrin, caveolin, flotillin, GRAF1, phagocytosis, macropinocytosis, and endosome acidification. Although further characterization is necessary to specifically inhibit the MNV entry process, this thesis work provides an important scaffold to build upon with additional discoveries. Additionally, I have determined that the UPR can significantly inhibit a diverse set of RNA viruses, including MNV, encephalomyocarditis virus, La Crosse virus, and Sindbis virus. Further investigation into how the UPR regulates viral infection could bring greater insight into how these viruses modulate the UPR. Further investigation into MNV entry and the role of the UPR during viral infections may reveal chinks in their armor necessary to developing antiviral therapies.

5.6 Future Directions

- **Identification of cellular markers associated with MNV entry**
- **Characterization of the mechanism by which the UPR can inhibit non-enveloped and/or enveloped virus infection**
- **Elucidation of host DUBs that are activated during or required for MNV infection**
- **Identification of the mechanisms by which USP14 regulates MNV infection**
- **Determination of the DUBs activated or inactivated during MNV infection of murine Macs**

5.7 References

1. **Ambrose, R. L., and J. M. Mackenzie.** 2011. West Nile Virus Differentially Modulates the Unfolded Protein Response To Facilitate Replication and Immune Evasion. The Journal of Virology 85:2723-2732.
2. **Babuke, T., and R. Tikkanen.** 2007. Dissecting the molecular function of reggie/flotillin proteins. European Journal of Cell Biology 86:525-532.
3. **Bhella, D., and I. G. Goodfellow.** 2011. The Cryo-Electron Microscopy Structure of Feline Calicivirus Bound to Junctional Adhesion Molecule A at 9-Angstrom Resolution Reveals Receptor-Induced Flexibility and Two Distinct Conformational Changes in the Capsid Protein VP1. J Virol 85:11381-11390.
4. **Brandenburg, B., L. Y. Lee, M. Lakadamyali, M. J. Rust, X. Zhuang, and J. M. Hogle.** 2007. Imaging Poliovirus Entry in Live Cells. PLoS Biol 5:e183.
5. **Cannon, J. L., E. Papafragkou, G. W. Park, J. Osborne, L. A. Jaykus, and J. Vinje.** 2006. Surrogates for the study of norovirus stability and inactivation in the environment: aA comparison of murine norovirus and feline calicivirus. J Food Prot 69:2761-5.
6. **Chan, S.-W., and P. Egan.** 2009. Effects of hepatitis C virus envelope glycoprotein unfolded protein response activation on translation and transcription. Arch Virol 154:1631-1640.
7. **Chan, S.-W., and P. A. Egan.** 2005. Hepatitis C virus envelope proteins regulate CHOP via induction of the unfolded protein response. The FASEB Journal.
8. **Chen, R., L. Zhang, B. Zhong, B. Tan, Y. Liu, and H.-B. Shu.** 2010. The ubiquitin-specific protease 17 is involved in virus-triggered type I IFN signaling. Cell Res 20:802-811.
9. **Cho, H. K., K. J. Cheong, H. Y. Kim, and J. Cheong. 2011.** Endoplasmic reticulum stress induced by hepatitis B virus X protein enhances cyclo-oxygenase 2 expression via activating transcription factor 4. Biochemical Journal 435:431-439.
10. **Coburn, B., B. Wagner, and S. Blower.** 2009. Modeling influenza epidemics and pandemics: insights into the future of swine flu (H1N1). BMC Medicine 7:30.
11. **Coller, K. E., K. L. Berger, N. S. Heaton, J. D. Cooper, R. Yoon, and G. Randall.** 2009. RNA Interference and Single Particle Tracking Analysis of Hepatitis C Virus Endocytosis. PLoS Pathog 5:e1000702.
12. **Dietz, V. J.** 1994. Potential impact on vaccination coverage levels by administering vaccines simultaneously and reducing dropout rates. Archives of pediatrics & adolescent medicine 148:943-9.
13. **Doherty, G. J., M. K. Åhlund, M. T. Howes, B. Morén, R. G. Parton, H. T. McMahon, and R. Lundmark.** 2011. The endocytic protein GRAF1 is directed to cell-matrix adhesion sites and regulates cell spreading. Mol Biol Cell 22:4380-4389.
14. **Dolin, R., N. R. Blacklow, H. DuPont, S. Formal, R. F. Buscho, J. A. Kasel, R. P. Chames, R. Hornick, and R. M. Chanock.** 1971. Transmission of acute infectious nonbacterial gastroenteritis to volunteers by oral administration of stool filtrates. J Infect Dis 123:307-12.
15. **Fricks, C. E., and J. M. Hogle.** 1990. Cell-induced conformational change in

poliovirus: externalization of the amino terminus of VP1 is responsible for liposome binding. J Virol 64:1934-1945.
16. **Gianni, T., and G. Campadelli-Fiume.** 2012. αVβ3-Integrin Relocalizes nectin1 and Routes Herpes Simplex Virus to Lipid Rafts. J Virol 86:2850-2855.
17. **Gianni, T., V. Gatta, and G. Campadelli-Fiume.** 2010. αVβ3-integrin routes herpes simplex virus to an entry pathway dependent on cholesterol-rich lipid rafts and dynamin2. Proceedings of the National Academy of Sciences 107:22260-22265.
18. **Glebov, O. O., N. A. Bright, and B. J. Nichols.** 2006. Flotillin-1 defines a clathrin-independent endocytic pathway in mammalian cells. Nat Cell Biol 8:46-54.
19. **Golden, J. W., J. A. Bahe, W. T. Lucas, M. L. Nibert, and L. A. Schiff.** 2004. Cathepsin S supports acid-independent infection by some reoviruses. J Biol Chem 279:8547-57.
20. **Guix, S., M. Asanaka, K. Katayama, S. E. Crawford, F. H. Neill, R. L. Atmar, and M. K. Estes.** 2007. Norwalk virus RNA is infectious in mammalian cells. J Virol 81:12238-48.
21. **Hu, M., P. Li, L. Song, P. D. Jeffrey, T. A. Chernova, K. D. Wilkinson, R. E. Cohen, and Y. Shi.** 2005. Structure and mechanisms of the proteasome-associated deubiquitinating enzyme USP14. Embo J 24:3747-3756.
22. **Hyde, J. L., S. V. Sosnovtsev, K. Y. Green, C. Wobus, H. W. Virgin, and J. M. Mackenzie.** 2009. Mouse Norovirus Replication Is Associated with Virus-Induced Vesicle Clusters Originating from Membranes Derived from the Secretory Pathway. The Journal of Virology 83:9709-9719.
23. **Kaufman, R. J., S. H. Back, B. Song, J. Han, and J. Hassler.** 2010. The unfolded protein response is required to maintain the integrity of the endoplasmic reticulum, prevent oxidative stress and preserve differentiation in β-cells. Diabetes, Obesity and Metabolism 12:99-107.
24. **Kuyumcu-Martinez, M., G. Belliot, S. V. Sosnovtsev, K.-O. Chang, K. Y. Green, and R. E. Lloyd.** 2004. Calicivirus 3C-Like Proteinase Inhibits Cellular Translation by Cleavage of Poly(A)-Binding Protein. J Virol 78:8172-8182.
25. **Li, B., B. Gao, L. Ye, X. Han, W. Wang, L. Kong, X. Fang, Y. Zeng, H. Zheng, S. Li, Z. Wu, and L. Ye.** 2007. Hepatitis B virus X protein (HBx) activates ATF6 and IRE1-XBP1 pathways of unfolded protein response. Virus Res 124:44-49.
26. **Li, S., L. Ye, X. Yu, B. Xu, K. Li, X. Zhu, H. Liu, X. Wu, and L. Kong.** 2009. Hepatitis C virus NS4B induces unfolded protein response and endoplasmic reticulum overload response-dependent NF-[kappa]B activation. Virology 391:257-264.
27. **Liao, T.-L., C.-Y. Wu, W.-C. Su, K.-S. Jeng, and M. M. C. Lai.** 2010. Ubiquitination and deubiquitination of NP protein regulates influenza A virus RNA replication. Embo J 29:3879-3890.
28. **Loo, Y.-M., and M. Gale Jr. 2011.** Immune Signaling by RIG-I-like Receptors. Immunity 34:680-692.
29. **Lopez, S., and C. F. Arias.** 2006. Early steps in rotavirus cell entry. Curr Top Microbiol Immunol 309:39-66.

30. **Lundmark, R., G. J. Doherty, M. T. Howes, K. Cortese, Y. Vallis, R. G. Parton, and H. T. McMahon.** 2008. The GTPase-Activating Protein GRAF1 Regulates the CLIC/GEEC Endocytic Pathway. Current Biology 18:1802-1808.
31. **Medigeshi, G. R., A. M. Lancaster, A. J. Hirsch, T. Briese, W. I. Lipkin, V. DeFilippis, K. Fruh, P. W. Mason, J. Nikolich-Zugich, and J. A. Nelson.** 2007. West Nile Virus Infection Activates the Unfolded Protein Response, Leading to CHOP Induction and Apoptosis. The Journal of Virology 81:10849-10860.
32. **Morrow, I. C., S. Rea, S. Martin, I. A. Prior, R. Prohaska, J. F. Hancock, D. E. James, and R. G. Parton.** 2002. Flotillin-1/Reggie-2 Traffics to Surface Raft Domains via a Novel Golgi-independent Pathway. Journal of Biological Chemistry 277:48834-48841.
33. **Mulvey, M., C. Arias, and I. Mohr.** 2007. Maintenance of Endoplasmic Reticulum (ER) Homeostasis in Herpes Simplex Virus Type 1-Infected Cells through the Association of a Viral Glycoprotein with PERK, a Cellular ER Stress Sensor. J Virol 81:3377-3390.
34. **Nagai, A., H. Kadowaki, T. Maruyama, K. Takeda, H. Nishitoh, and H. Ichijo.** 2009. USP14 inhibits ER-associated degradation via interaction with IRE1[alpha]. Biochem Biophys Res Commun 379:995-1000.
35. **Nakamura, N., and S. Hirose.** 2008. Regulation of Mitochondrial Morphology by USP30, a Deubiquitinating Enzyme Present in the Mitochondrial Outer Membrane. Mol Biol Cell 19:1903-1911.
36. **Ng, E. L., and B. L. Tang.** 2008. Rab GTPases and their roles in brain neurons and glia. Brain Research Reviews 58:236-246.
37. **Patel, K. P., C. B. Coyne, and J. M. Bergelson.** 2009. Dynamin- and Lipid Raft-Dependent Entry of Decay-Accelerating Factor (DAF)- Binding and Non-DAF-Binding Coxsackieviruses into Nonpolarized Cells. Journal of Virology 83:11064-11077.
38. **Rahn, E., P. Petermann, M.-J. Hsu, F. J. Rixon, and D. Knebel-Mörsdorf.** 2011. Entry Pathways of Herpes Simplex Virus Type 1 into Human Keratinocytes Are Dynamin- and Cholesterol-Dependent. PLoS ONE 6:e25464.
39. **Regan, A. D., R. Shraybman, R. D. Cohen, and G. R. Whittaker.** 2008. Differential role for low pH and cathepsin-mediated cleavage of the viral spike protein during entry of serotype II feline coronaviruses. Vet Microbiol.
40. **Sandvig, K., S. Pust, T. Skotland, and B. van Deurs.** 2011. Clathrin-independent endocytosis: mechanisms and function. Curr Opin Cell Biol 23:413-420.
41. **Tardif, K. D., K. Mori, R. J. Kaufman, and A. Siddiqui.** 2004. Hepatitis C Virus Suppresses the IRE1-XBP1 Pathway of the Unfolded Protein Response. Journal of Biological Chemistry 279:17158-17164.
42. **Tirosh, B., N. N. Iwakoshi, B. N. Lilley, A.-H. Lee, L. H. Glimcher, and H. L. Ploegh.** 2005. Human Cytomegalovirus Protein US11 Provokes an Unfolded Protein Response That May Facilitate the Degradation of Class I Major Histocompatibility Complex Products. J Virol 79:2768-2779.
43. **Trujillo-Alonso, V., L. Maruri-Avidal, C. F. Arias, and S. López.** 2011. Rotavirus Infection Induces the Unfolded Protein Response of the Cell and

Controls It through the Nonstructural Protein NSP3. J Virol 85:12594-12604.
44. **Van Hamme, E., H. L. Dewerchin, E. Cornelissen, B. Verhasselt, and H. J. Nauwynck.** 2008. Clathrin- and caveolae-independent entry of feline infectious peritonitis virus in monocytes depends on dynamin. Journal of General Virology 89:2147-2156.
45. **Zambrano, J., K. Ettayebi, W. Maaty, N. Faunce, B. Bothner, and M. Hardy.** 2011. Rotavirus infection activates the UPR but modulates its activity. Virol J 8:359.
46. **Zheng, Y.** 2005. Hepatitis C virus non-structural protein NS4B can modulate an unfolded protein response. The journal of microbiology 43:529-36.